Exploring the roles of the sex determinant Doublesex in the adult gut of *Drosophila melanogaster*

Laura Martin-Coll

Thesis is submitted for the degree of

Doctor of Philosophy

Institute of Clinical Sciences

Faculty of Medicine

Imperial College London

Science is about the gorgeous feeling of teetering into the unknown

Inspired by “Travel is about the gorgeous feeling of teetering into the unknown” from Anthony Bourdain

Personal Declaration

I, Laura Martin-Coll, declare that the work in this thesis is entirely my own work. It is otherwise clearly indicated by reference or acknowledgment when it is from other sources or external contributions. I carried out all the work in the Gut Signalling and Metabolism group, led by Professor Irene Miguel-Aliaga, at the Medical Research Council London Institute of Medical Sciences (MRC-LMS). Thanks to the funding granted to me by the MRC, I could work on my PhD thesis from October 2017 until October 2021. At the time of submission, no part of the thesis has been submitted for any publication. The main text is type size 12, with 1.5 line spacing, and does not exceed the permitted 100.000-word limit.

Copyright Declaration

Acknowledgements

I am enormously grateful to every single person who helped me, both scientifically and personally, to make it through this big adventure and life challenge called PhD.

First and foremost, I would like to deeply thank Prof. Irene Miguel-Aliaga for her support and scientific freedom. Four years ago, she granted me the opportunity to join as a student in her group. Without her, none of the work would have been possible. Throughout all those years, I have been privileged to be part of her team and I have increased my scientific knowledge and skills by her side. I will always be inspired by her sincere curiosity and "outside the box" thinking.

I would like to mention that this project stems from Bruno Hudry's excellent work and I thank him for his advice during my PhD. I am grateful to all the lab members, past and present, who have helped me and created a wonderful team throughout the four years (Ale, Alex, Alvaro, Bruno, Chris A., Chris S., Chryssa, Dafni, Emily, Eva, George, Gigi, Hannah, Kitty, Laura, Oceane, Pedro, Siamak, Tatiana, Tomo). Particularly, I would like to acknowledge Alessandro Mineo. From the beginning (and unselfishly) he has mentored me, taught me everything I know about flies and transmitted me his love for *Drosophila*. He has been a crucial support throughout all these years and has brought me up in the hard moments. I am very lucky I could learn from him, grow professionally and personally by his side, and share time together in the fly room. Also, Chris Amourda's immense technical skills, magic hands and patience have been key for my molecular work. Thanks for sharing your optimism and research passion with me, I am very grateful for our discussions about science and research lifestyle. Thanks to Chris and Pedro for keeping the lab running and well organised, to the Greek mammas Dafni and Alex for their encouragement and enormous support; and special mention to Mary O'Sullivan, who is the best fly food chef and a crucial piece in the lab. I would like to thank the fly community in the institute, the labs of Susumu Hirabayashi and Helena Cocheme, for all the help, reagents and fun time in the fly room. Finally, to all the world-wide fly community for their enormous will in sharing and advising.

At the core facilities of MRC, I am extremely grateful to Ivan Andrew and Laurence Game (Genomics) for the technical assistance in the RNA-sequencing. Also, to Yi-Fang Wang (Bioinformatics) for analysing the sequencing data and providing endless support and guidance

despite her busy agenda. Lastly, to Dirk Dormann and Chad Whilding at the microscopy facility.

Alongside my scientific bubble, there are many people who made this possible. My friends in London (Lucie, Cecília, George, Julia, Aubin, Jean-François, Ifi, Eleni, Vlad, Tatiana, Pedro, Nevena, James, Piotr, Luke, Benji, Joel), Copenhagen (Lisa, Tesa, Verena, Valentin, Giulio, Carla, Lucía, Àgata), Barcelona (Paula, Marina, Marta, Manu, Adri, Albert, Laura Valls, Laura Rubió, Carlota, Rubén) and Girona (Laura Carreras, Martí, Sílvia, Pitu, Dolors, Irene) have continuously been a great pillar during this journey. Even from many kilometres apart, I have always felt encouraged and comprehended. My Oakworth Road family (Lucie, Bethany, Holly) made me feel at home; and Manuel Torregrosa, who enlightened me with his wisdom and taught me to begin to understand myself better. Ultimately, to Amer Dzankic, who has been unconditional since we met and filled me with his "rational" positivity. Thanks for being patient by myside and for reminding me that I am more than a PhD student.

I genuinely thank my family. All of this is the result of their support during my career, and I am left wordless to describe their encouragement, warmth and love ("Moltes gràcies mama, papa i Eloi").

To my grandparents, who I wish could have seen the result of these past four years away from home and who I miss enormously.

Abstract

Molecular and cellular sexual dimorphisms contribute to the establishment of sex differences in various aspects of physiology. There is an increasing realization that the incidence and/or prognosis of many disorders differs between sexes, with incomplete understanding of the underlying mechanisms. In *Drosophila melanogaster*, the molecular pathway determining sexual traits is well studied, particularly in the reproductive and nervous systems. Previous work from our lab and others have characterised the expression of the last effector in the sex determination pathway, Doublesex, in somatic tissues such as the intestine. In this thesis I have validated that Dsx has a sex- and cell type-specific expression in the midgut, being only detected in male enterocytes. The fly intestine is an excellent system to study physiology, mostly because of its metabolic roles and adaptability towards internal/external environmental changes; and sexual dimorphism in anatomy, proliferation, immunity and metabolism. I have investigated contributions of the intrinsic sexual fate of enterocytes by exploring the roles of Dsx. To start characterizing its functions, I have downregulated *dsx* in adult enterocytes and sought to identify downstream targets using transcriptomics. I have begun to describe its effects on the expression of lipid genes, for example on the female enriched *CG17192* lipase, and assessed the changes in intestinal lipid droplets and whole-body fat. Finally, I have unravelled a novel function of the oncogene Myc in adult enterocytes in regulating lipid processes. Myc expression is higher in female midguts, and its knock-down in enterocytes impacts lipid metabolism and, extrinsically, stem cell proliferation. My work opens up the possibility that Dsx controls lipid metabolism in a sexually dimorphic manner via the indirect/direct control of *Myc*, warranting further examination. This thesis reveals a new concept of Dsx and Myc establishing sexual dimorphism of lipids from the enterocytes, potentially affecting proliferation, disease incidence and reproductive success.

Keywords:

Drosophila, lipid metabolism, intestine, midgut, enterocytes, Doublesex, sexual dimorphism, Myc, CG17192, lipid droplets, triacylglycerol

Table of Contents

List of Figures and Tables

List of Abbreviations

20HE	20-hydroxyecdysone
Abd-B	Abdominal B
ACC	Acetyl-CoA carboxylase
Acsl	Acyl-CoA synthetase long-chain
Akh	Adipokinetic hormone
Akt	Protein kinase B
Apc1	Adenomatous polyposis coli 1
ATGL	Adipose triglyceride lipase
ATP	Adenosine triphosphate
Bab1/2	Bric-a-brac
BL	Bloomington
Bmm	Brummer
BP	Biological process
CD	Control diet
CD36	Cluster of differentiation 36
CNS	Central nervous system
CYP	Cytochrome P450 enzyme
DAG	Diacylglycerol
DAGT	Diacylglycerol acyltransferases
DesatF	Desaturase F
Dilps or Ilps	*Drosophila* insulin-like peptides
Dl	Delta
Dmrt	Doublesex/mab-3 related
DSS	Dextran sulfate sodium
Dsx	Doublesex
EB	Enteroblast
Ec	Ecdysone
EC	Enterocyte
EEC	Enteroendocrine cell
eGFP	Enhanced green fluorescent protein
Egfr	Epidermal growth factor receptor
Esg	Escargot
FA	Formaldehyde
FA	Fatty acid
FABP	Fatty acid-binding protein
FASN	Fatty acid synthase
FATP	Fatty acid transport protein
FBE	Fat body enhancer
Fit	Female-specific independent of transformer
FLP	Site-specific recombination flippase
Fmo-2	Flavin-containing monooxygenase-2
FoxO	Forkhead box class O
FRT	Flippase recognition target sequence
Fru	Fruitless
G3P	Glycerol-3-phosphate

GO	Gene ontology
GPAT	Glycerol-3-phosphate acyltransferases
Her	Hermaphrodite
Hr96	Hormone receptor-like in 96
HRP	Horseradish peroxidase
HSD	High sugar diet
Hsl	Hormone-sensitive lipase
IIS	Insulin/insulin-like growth factor signalling
Ilp	Insulin-like peptide
IPC	Insulin producing cell
ISC	Intestinal stem cell
Ix	Intersex
JH	Juvenile hormone
KEGG	Kyoto encyclopaedia of genes and genomes
Krn	Keren
LD	Lipid droplet
LPA	Lypophosphatidic acid
LPAAAT or AGPAT	Lypophosphatidic acid acyltransferase
Lpp	Lipophorin
Lsd1/2	Lipid storage droplet 1/2
LTP	Lipid transfer particle
MAG	Monoacylglycerol
Mag	Magro
MARCM	Mosaic analysis with a repressive cell marker
MBOAT	Membrane bound o-acyl transferase
Mdy	Midway
Mex1	Midgut expression 1
MF	Molecular function
MGAT	Monoacyglycerol acyltransferases
Mino	Minotaur
miRNA	microRNA
Msl-2	Male-specific lethal-2
Myo1A	Myosin 1
Npc1/2	Niemann-Pick C1/2
Nplp2	Neuropeptide-like precursor 2
Opbp	Odorant-/pheromone-binding protein
PA	Phosphatidic acid
PBS	Phosphate-buffered saline
PBST	Phosphate-buffered saline triton
PBSTN	Phosphate-buffered saline triton with 4% normal horse serum
PCA	Principal component analysis
Pdm1	POU domain protein 1
PFA	Paraformaldehyde
Plin1/2	Perilipin1/2
PM	Peritrophic matrix
Pros	Prospero
qPCR	Quantitative polymerase chain reaction
RFP	Red fluorescent protein

Rheb	Ras homologue enriched in brain
RNAi	RNA of interference
RT	Room temperature
SEM	Standard error of the mean
Spi	Spitz
SR-BI	Scavenger receptor class B type I
SREBP	Sterol regulatory element-binding protein
Sxe1/2	Sex-specific enzyme 1/2
Sxl	Sex lethal
TAG	Triacylglycerol
TCA	Tricarboxylic acid cycle
TLC	Thin Layer Chromatography
TOR	Target of rapamycin
Transformer	Tra
TRiP	Transgenic RNAi project
Tse	Turn-on sex-specificity
UAS	Upstream activation sequences
VDRC	Vienna *Drosophila* resource centre
Vn	Vein
VNC	Ventral nerve cord
WT	Wild type
XSE	X-chromosome signal elements
Yp	Yolk protein

CHAPTER 1

Introduction

1.1 Sex determination in *Drosophila melanogaster*

1.1.1 Sexual dimorphism in the animal kingdom

A wide range of anatomical, physiological and behavioural traits are sexually dimorphic within the animal kingdom. Even though particularly apparent in the gonads and genitalia, sex differences between male and female organisms are observed in a wide variety of organs and tissues (Karp, Mason et al. 2017 and reviewed in Mori, Mazza et al. 2017, Clegg and Mauvais-Jarvis 2018).

Sex determination is established during early stages as a choice between the male or female developmental programs. Across the animal kingdom, the factors that trigger sexual fates can vary broadly, from environmental to genetic mechanisms (reviewed in Manolakou, Lavranos et al. 2006, Gamble and Zarkower 2012, Bachtrog, Mank et al. 2014). In mammals, the sex determination pathway is a non-cell autonomous process influenced by systemic hormones and cell-cell interactions (reviewed in Gilbert 2000, She and Yang 2014). Increasing realization that the incidence of many human diseases is sex biased has revived the study of the molecular and cellular underpinnings of sex differences, and how they impact normal physiology and its dysregulation (reviewed in Cook, Dawsey et al. 2009, Mauvais-Jarvis 2015, Clegg and Mauvais-Jarvis 2018).

1.1.2 The fruit fly as a model organism

The fruit (or vinegar) fly *Drosophila melanogaster* (order Diptera, family Drosophilidae) is a model organism broadly used in the laboratory for over a century. Research benefits from its easy, inexpensive and quick rearing conditions (females can lay hundreds of eggs). *Drosophila melanogaster* has a short life cycle, which takes approximately 10 days at 25°C: from embryo (~24h) to 1st instar larva (~24h), followed by 2nd instar (~24h) and 3rd instar larva (~2-3d), prior to pupa (~5d) and finally adult. Their life cycle is slower at low temperatures, and faster at high temperatures (reviewed in Hales, Korey et al. 2015).

Many resources are available for the research community, including fly stocks, datasets (e.g. genomic and transcriptomic) and databases (reviewed in Mohr, Hu et al. 2014). Its genome is fully sequenced and annotated (Adams, Celniker et al. 2000). *Drosophila* recapitulates some aspects of human physiology, and more than 70% of human disease-related genes have homologues in flies (Reiter, Potocki et al. 2001, Pandey and Nichols 2011). Most importantly,

the fruit fly is an amenable genetic model organism with a powerful genetic toolkit (reviewed in Bier 2005). Taken together, the abovementioned numerous advantages make *Drosophila melanogaster* a widespread and excellent model organism to work with.

Since its early times, the fruit fly has proven to be a very useful tool to understand the sex determination pathway. The first studies carefully described differences in its sexual anatomy and behaviour, which provided the foundations for the molecular examination of the sexual dimorphism. For many years, *Drosophila melanogaster*'s sex determination has been defined as a cell-autonomous process in which every cell decides their sex according to the number of X chromosomes, proceeded by a cascade of alternative splicing events (reviewed in Salz and Erickson 2010). This cell-autonomous determination view is supported by the findings of gynandromorphs within *Drosophila*, which contain both male and female cells. However, the molecular members of the sex determination cascade are not ubiquitously detected in all cells of the body (reviewed in Camara, Whitworth et al. 2008). Despite the vast numbers of cells following the deterministic program, in the recent years, non-autonomous sex determination has been described in cell types that integrate signals from the neighbouring cells. Non-autonomous sex determination is observed in the gonad (in independent cell types such as male-specific somatic gonadal precursors, pigment cell precursors and germ cells), in the genital disc and in the muscle of Lawrence (reviewed in Camara, Whitworth et al. 2008). Additionally, the sex of specific neurons (Sawala and Gould 2017, Sawala and Gould 2018) and the sex of the fat body (fly tissue akin to the mammalian adipose tissue) (Rideout, Narsaiya et al. 2015) control body growth in a non-cell autonomous manner. Therefore, sex determination mechanisms should be studied an interpreted both non-cell autonomously and according to each cell type.

1.1.2.1 Genetic tools in *Drosophila melanogaster*

The genetic tools available in the fruit fly are broad and diverse (reviewed in Hales, Korey et al. 2015). Here I briefly summarise the tools utilised in this thesis, which primarily focus on the overexpression or inactivation of genes in a cell- and time-specific manner.

The Gal4-UAS system

The Gal4-UAS binary expression system, which was adapted from *Saccharomyces cerevisiae* in 1993 (Brand and Perrimon 1993) and refined ever since, is an excellent system to control ectopic expression temporally and spatially (Southall, Elliott et al. 2008). The Gal4 DNA sequence (consisting of a DNA binding domain and an activation domain) is fused to the

enhancer of a gene. The enhancer and Gal4 construct can be inserted in many genomic landing sites. When the Gal4 sequence is inserted into the endogenous gene locus, it is called an enhancer trap. Under temporal and spatial control from the enhancer, the Gal4 is transcribed and translated, and binds to the upstream activation sequences (UAS) in other sites of the genome. The Gal4 drives expression of the downstream sequences of the UAS, usually RNA interference (RNAi), overexpression of genes, cell markers or fluorescent reporter lines. From a simple fly cross, in the progeny, the Gal4 drives the expression of UAS sequences in a tissue-specific manner (Fig. 1.1). In the fly community, there are large resources such as libraries of UAS-fused constructs and Gal4 drivers.

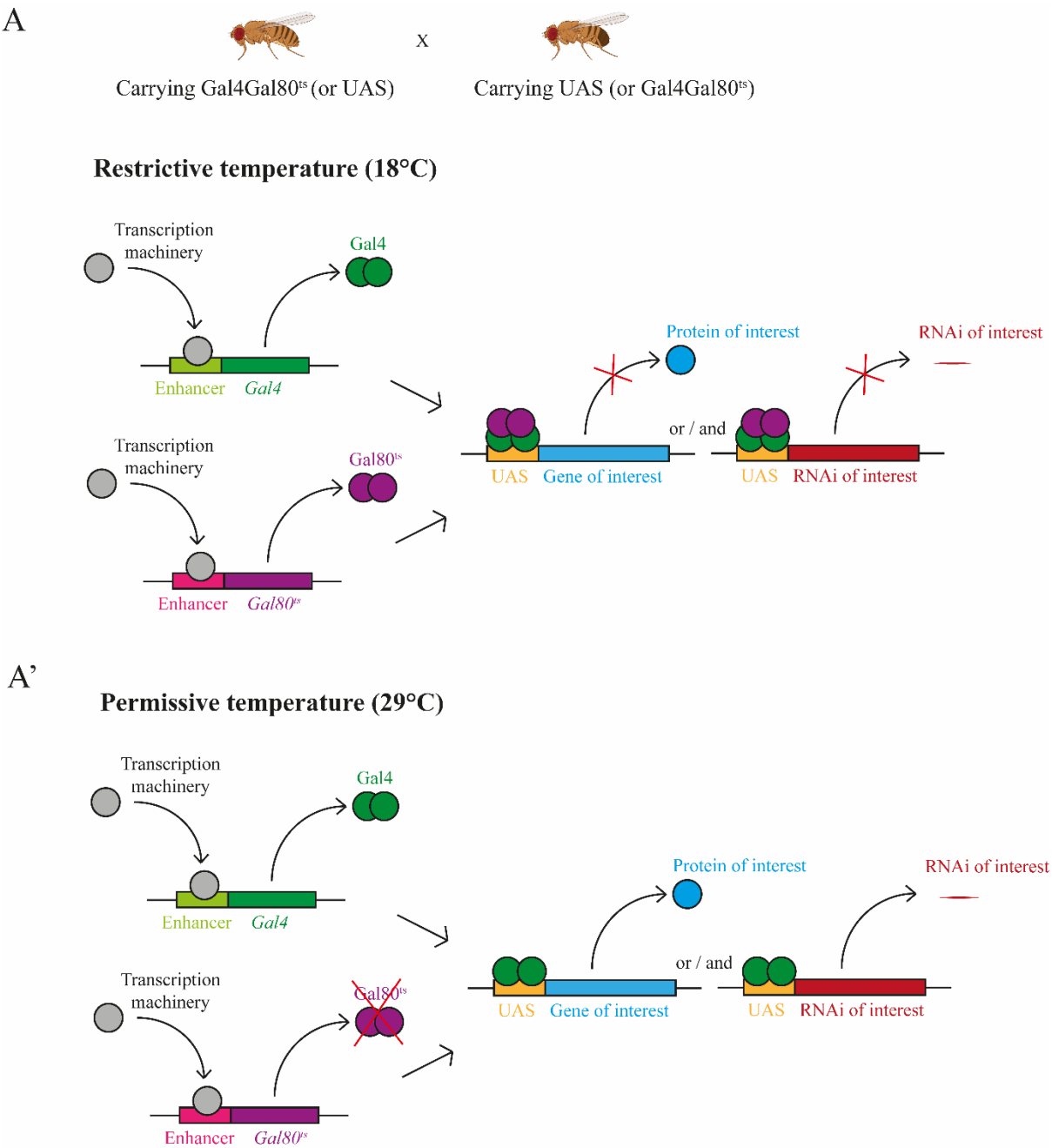

Figure 1.1: Schematic representation of the Gal4-UAS system in the presence of Gal80^{ts}

(A) From a simple genetic cross, the progeny F1 includes the Gal4Gal80^{ts} system (inherited from a progenitor) and the UAS system (from the other progenitor). At the restrictive temperature (18°C), at the tissue where the enhancers are activated, both the Gal4 and the Gal80^{ts} are transcribed and translated. The Gal80^{ts} inactivates the Gal4 by binding the activation domain, and consequently, the expression of the UAS downstream sequence is blocked. (A') The same progeny at the permissive temperature (29°C) express the protein and/or the RNAi of interest downstream of the UAS. At 29°C, the Gal80^{ts} is degraded and cannot inactivate the Gal4, therefore the Gal4 binds at the UAS and induces expression. This system allows fine-tuned spatial and temporal transcriptional control.

The Gal4-UAS binary system benefits from the intersection with Gal80, which inactivates the Gal4 activation domain (Lue, Chasman et al. 1987). The Gal80 is inserted also fused to an enhancer, and thus expressed in a tissue-specific and temporal manner (Fig. 1.1). Interestingly, the Gal80 can be temporally controlled by the usage of a temperature sensitive Gal80, Gal80^{ts} (McGuire, Le et al. 2003). It is usually fused to the promoter of a ubiquitous gene (e.g. tubulin) and combined to the Gal4-UAS system to inactivate Gal4 expression throughout development until a shift in temperature. At 18°C, Gal80^{ts} is repressive, whilst at 29°C is degraded and thus non-functional (Fig. 1.1). The Gal4Gal80^{ts}-UAS system has been extensively used throughout this thesis to facilitate temporal and spatial up/downregulation of genes.

The FLP-FRT-mediated recombination

Derived from *S. cerevisiae*, the site-specific recombinase flippase (FLP) recognises its target sequence (Flippase recognition target sequence, FRT). FLP induces mitotic recombination that excises the DNA sequence flanked by the two homotypic FRT sites (Golic and Lindquist 1989). Additionally, FLP under the control of *heat shock protein 70* promoter (*hsp70p*), catalyses recombination in a heat-induced manner: FLP is not expressed at 18°C, but is highly expressed above 30°C. Thus, a heat-shock to the flies activates the FLP/FRT system. To gain control of the spatial regulation, the system makes use of a defined promoter upstream of the FLP coding sequence, equivalent to the Gal4-UAS system. Interestingly, in a whole-body induced FLP, the frequency of recombination and the clone induction can be controlled by manipulating the duration of the heat-shock or the stage of development (clones from development grow large; clones in the adult result in small clones) (reviewed in Germani, Bergantinos et al. 2018).

Clones using the FLP-out Gal4 system

Mosaicism occurs in nature in all multicellular organisms, normally by a mutation within a single cell which generates another genotype. In *Drosophila*, it is a well-established research tool. Among its diverse benefits, it helps to distinguish between the cell-autonomous and non-autonomous gene functions.

There are different mosaic systems which allow tracing cell lineages and manipulating gene expression in the same cells inside an otherwise wild-type tissue (reviewed in Germani, Bergantinos et al. 2018). I briefly explain the methodology behind the clones generated for this thesis, which combine the Gal4-UAS and FLP-FRT systems (Ito, Awano et al. 1997). One of the genotypes of the experimental flies used in this thesis is *yw,hs-flp;UAS-dsxRNAi/Act>y>Gal4UAS-RFP* (Fig. 1.2). All cells have FLP under the heat shock promoter, two UAS constructs (RNAi against *doublesex*, and the red fluorescent protein, RFP), and one sequence containing the *yellow* gene which is flanked by two FRT sites. This sequence separates the *Actin* ubiquitous promoter from the *Gal4* coding sequence. Thus, the Gal4 is inactive and only a FLP-FRT cis-recombination would remove the flanked sites and activate it. Under fine-tuned heat-shock conditions, a FLP recombination excises the FRT-flanked sequence in some cells. In these cells, the active Gal4 binds to both UAS constructs and transcribes *RFP* and *dsxRNAi*. This FLP-out event is heritable, therefore each of the cell's progeny also expresses *RFP* and *dsxRNAi*. The recombinant clones are visually distinct by the expression of RFP, and have a cell-autonomous downregulation of *dsx* in a wild-type tissue.

All these genetic tools, together with all the previously mentioned advantages, make *Drosophila melanogaster* an exceptional model organism.

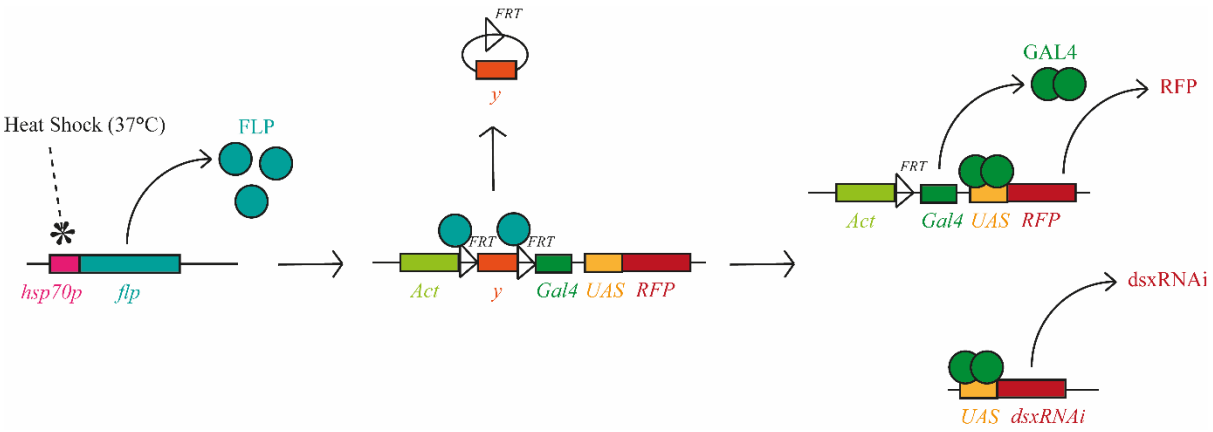

Figure 1.2: Schematic representation of the FLP-out Gal4 system

Under specific heat-shock conditions (10min at 37°C), the heat-shock sensitive promoter (*hsp70p*) induces expression of *flp* in few cells. FLP causes recombination between FRT sequences and excision of the *yellow* cassette (*y*). Consequently, the ubiquitously expressed *Actin* promoter (*Act*) induces *Gal4* expression. Gal4 binds to the UAS sequences driving the transcription of both *RFP* and *dsxRNAi*. This technique generates clones of cells downregulating *dsx* that are marked by RFP.

1.1.3 Hierarchy of the sex determination cascade in *Drosophila melanogaster*

In *Drosophila melanogaster*, sexual fate is established by the number of X chromosomes (X) (reviewed in Salz and Erickson 2010). 1X:2A cells display male fate, whilst 2X:2A individuals are female (Bridges 1921).

The sex determination pathway is a text-book model of alternative splicing events (Fig. 1.3). 2X:2A animals have two sets of X-chromosome signal elements (XSE), which activate the master switch *Sex lethal* (*Sxl*). Sxl is maintained via an autoregulatory loop, and female development begins (reviewed in Salz and Erickson 2010). On the one hand, Sxl controls splicing of *transformer* (*tra*) gene (Sosnowski, Belote et al. 1989, Inoue, Hoshijima et al. 1990). On the other hand, Sxl represses translation of the Male-specific lethal 2 (Msl-2) protein, which functions in males to increase transcription rate from the single X chromosome for dosage compensation (Gorman and Baker 1994, Bashaw and Baker 1997, Kelley, Wang et al. 1997). The binding of Sxl at the *tra* pre-mRNA overcomes a stop codon, resulting in a functional Tra protein in females. In males, there is the default splicing of *tra* pre-mRNA which retains the early stop codon (Boggs, Gregor et al. 1987). *transformer 2* (*tra2*) is ubiquitously expressed in both sexes (Mattox, Palmer et al. 1990). The binding of Tra with Tra2 (Amrein, Gorman et al. 1988, Goralski, Edstrom et al. 1989) regulates the sex-specific splicing of the downstream transcription factors *doublesex* (*dsx*) and *fruitless* (*fru*) (Baker and Wolfner 1988, Nagoshi, McKeown et al. 1988, Burtis and Baker 1989, Hoshijima, Inoue et al. 1991).

In female flies, Tra and Tra2 bind to the weak acceptor site of the pre-mRNA *doublesex*, which is spliced out as the female transcript encoding for DsxF. Also, Tra and Tra2 generate female-specific splicing of *fru* mRNA transcribed from the promoter P1, which results in a non-translated protein due to a stop codon (Ito, Fujitani et al. 1996, Ryner, Goodwin et al. 1996 and reviewed in Sato, Goto et al. 2019). In males, since Sxl is not produced, Tra is absent and *doublesex* is spliced in the default mode resulting in *dsxM*. In males, *fruitless* also undergoes default splicing from promoter P1, generating functional FruM (Nagoshi, McKeown et al. 1988, Burtis and Baker 1989, Inoue, Hoshijima et al. 1992, Heinrichs, Ryner et al. 1998). In general terms, FruM controls the neuronal sexual dimorphisms contributing to male courtship behaviour, as well as the male-female differences apparent in the muscle of Lawrence (a muscle found in the fifth abdominal region exclusively in males). Doublesex, in addition to establishing dimorphisms at the CNS level, controls the somatic differences in tissues such as

the genitalia, the gonads and the abdomen (see Introduction 1.2) (reviewed in Christiansen, Keisman et al. 2002).

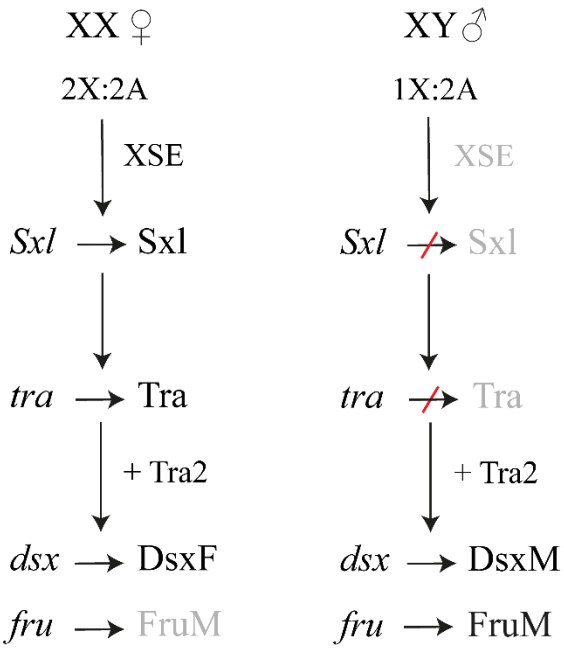

Figure 1.3: Schematic representation of the sex determination pathway in female and male flies

Female flies (2X:2A), with two sets of X-chromosome signal elements (XSE), transcribe and maintain by an autoregulatory loop the expression of *Sxl*. Sxl binding overcomes the stop codon in the pre-mRNA of *tra* and this results in a functional Tra protein. Together with Tra2, Tra splices in a female manner *dsx*, generating *dsxF*. In females, FruM is absent. Male flies (1X:2A) lack Sxl, which results in default *tra* splicing with a stop codon that impedes its translation. FruM and DsxM are produced in males.

1.2 Doublesex: the last effector in the fly sex determination pathway

1.2.1 Dsx molecular description: female and male isoforms

The *doublesex* gene (*CG11094*) is encoded in the right arm of the 3rd chromosome (3R), with exact location 7,924,323..7,967,408 [-]. It encodes six different transcripts. The three male-specific transcripts are *dsx-RD* (FBtr0330073 and NM_001275423), *dsx-RA* (FBtr0081759 and NM_169202) and *dsx-RE* (FBtr0330074 and NM_001275424). The female-specific are *dsx-RC* (FBtr0081761 and NM_079548), *dsx-RF* (FBtr0339710 and NM_001300291) and *dsx-RB* (FBtr0081760 and NM_169203).

The 1st, 2nd and 3rd exons of *dsx* are common for both sexes, whereas the 4th is female-specific (located in a male intron) and the 5th and the 6th are male-specific (Fig. 1.4A).

The three female-specific transcripts share the same three coding exons (exon 2-4) but differ in the 5' and 3' untranslated regions (UTRs). The transcripts *dsx-RF* and *dsx-RB* have the same 5'UTR (1263nt) which is a longer sequence also common for the male-specific transcripts *dsx-RA* and *dsx-RE*, but different from the 5'UTR of *dsx-RC* (874nt). The 3'UTR is mutual for *dsx-RC* and *dsx-RB* (1080nt); however, *dsx-RF* has the same sequence but lengthened (4394nt). The main female transcript is *dsx-RC* and encodes for DsxF isoform: 3238nt, 427aa and 44.8kD (predicted) (Fig. 1.4B, C).

The three male-specific transcripts have longer sequences. Exon 5 is the codifying male-specific exon. The UTRs are transcript-specific: 5'UTR is shared between *dsx-RA* and *dsx-RE* (as mentioned, same as *dsx-RF* and *dsx-RB*, 1293nt), but different from the 5'UTR of *dsx-RD* (874nt, female *dsx-RC* and male *dsx-RD* share the same 5'UTR). *dsx-RD* and *dsx-RA* have the same 3'UTR, which is shortened in *dsx-RE* (1097nt *vs* 1028nt). The main male transcript is *dsx-RD* and encodes for DsxM isoform 3621nt, 549aa and 57.4kD (predicted) (Fig. 1.4B, C). Interestingly, *dsx-RE* has a predicted longer male-specific exon, which codifies a putative longer protein of 4010nt and 572 aa, but with a stop-codon suppression (UAG) postulated.

The N-terminal domain (397aa) of DsxF and DsxM is identical, encoded by the common exons 2 and 3 (Burtis and Baker 1989). Doublesex is a zinc finger transcription factor, and the capacity of DNA binding relies within the N-terminal motif known as DM domain (Dsx/Mab-3 domain) (Erdman and Burtis 1993, Narendra, Zhu et al. 2002) (Fig. 1.4C). In addition to the DNA binding domain (DBD), the DM domain has a protein:protein oligomerization domain (OD1). Although Dsx can be detected as tetramer and oligomer (in high concentrations), only the dimeric form can bind to the DNA (Erdman and Burtis 1993, An, Cho et al. 1996, Erdman, Chen et al. 1996, Cho and Wensink 1997). Both DsxM and DsxF bind to DNA regulatory sites with the same affinity *in vitro*, suggesting that the sex-specific regulatory functions are unrelated to DNA binding (Cho and Wensink 1997). The consensus DNA binding sequence for Dsx transcription factor has been described in several papers and it has been refined according to the accuracy of the method (D'Souza 2019). The first biochemical studies identified a 13bp palindromic sequence (G/A)nnAC(A/T)A(T/A)GTnn(C/T) with the bases decisive for the binding located at the core of the sequence (Erdman, Chen et al. 1996). However, this Dsx-binding sequence is found randomly at every 2kb in the *Drosophila melanogaster* genome. Therefore, *in vivo* studies employing DamID profiling (a method that uses DNA methylation as a fingerprint as where and whether Dsx is bound to the genome)

gained greater details of the Dsx binding sites and Dsx targets (Luo, Shi et al. 2011, Clough, Jimenez et al. 2014).

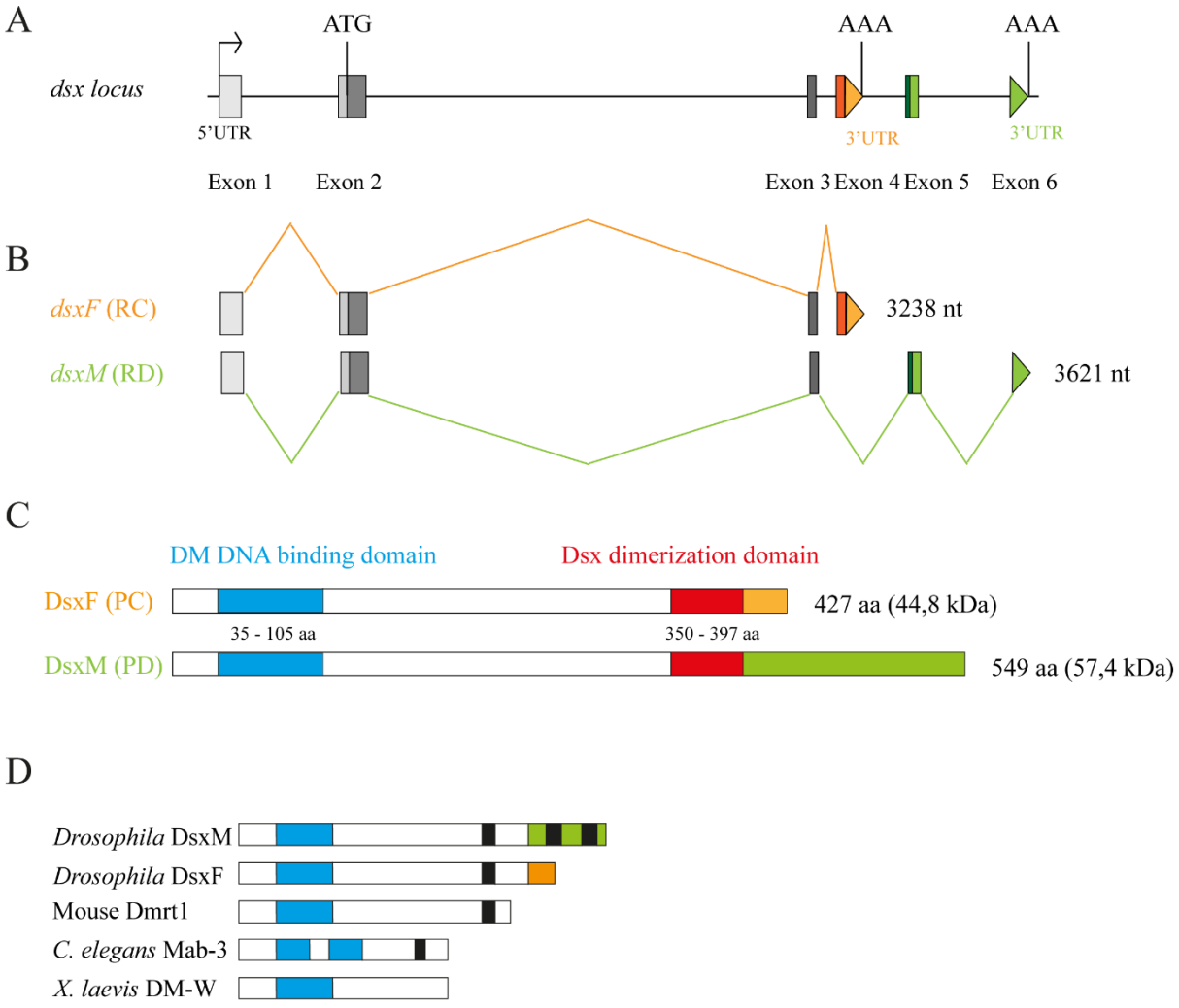

Figure 1.4: Schematic representation of *dsx* locus, female and male *dsx* transcripts, DsxF and DsxM domains and Dmrt homology across species

(A) *doublesex* locus. Exon 1 is the non-coding 5'UTR (identical in male *dsx-RD* and female *dsx-RC*). Exon 2 and exon 3 are common for both sexes. Exon 4 is female-specific, and exon 5 and exon 6 are male-specific. (B) Main female (*dsxF-RC*) and male (*dsxM-RD*) transcripts with the respective nucleotide length. (C) DsxF and DsxM protein domains. DM DNA binding domain (35-105aa) and Dsx dimerization domain (350-397aa) are common in both isoforms. The C-terminus is sex-specific (DsxF=427aa, DsxM=549aa). Adapted from Yang, Zhang et al. 2008. (D) Homology within the Dmrt family: DsxM, DsxF, Dmrt1 (mouse), Mab-3 (*C.elegans*) and DM-W (*X.laevis*) share the DM DNA binding domain. Adapted from Kopp 2012. Light grey, light orange and light green depict non-coding sequences. Orange, female. Green, male. Grey, common in both sexes. Blue, DM DNA binding domain. Red, Dsx dimerization domain. Black, proline/serine-rich domains.

Dsx proteins vary at the sex-specific C-terminus: DsxM with 152aa and DsxF with 30aa (An, Cho et al. 1996, Cho and Wensink 1997) (Fig. 1.4C). The oligomerization domain OD2 gathers a common non-sex-specific domain (of 102aa) and the sex-specific C-terminus (Burtis and Baker 1989, Erdman and Burtis 1993, Erdman, Chen et al. 1996). It is involved in the

dimerization of Dsx (three times stronger DsxM over DsxF dimerization) (Cho and Wensink 1998). Interestingly, combined expression of DsxM and DsxF results in a phenotype like the null mutant (Nagoshi and Baker 1990). This finding might be explained because of opposing roles or/and heterodimer formation. Intersex phenotypes are observed in mutants with either DM domain or dimerization domains affected (Burtis 1993, Erdman and Burtis 1993, Erdman, Chen et al. 1996, Narendra, Zhu et al. 2002). Noteworthy, DsxF and DsxM have the capacity to heterodimerize, as observed *in vitro*, yeast (two hybrid experiments) and *Drosophila* S2 cells, producing unfunctional complex (An, Cho et al. 1996, Erdman, Chen et al. 1996).

The C-terminus is the sex-specific domain that interacts with the cofactors (Burtis and Baker 1989). In females, Intersex (Ix) is an essential cofactor binding at the C-terminus of DsxF, thus unable to bind to DsxM (Waterbury, Jackson et al. 1999, Garrett-Engele, Siegal et al. 2002). *ix* mutation does not explain all the phenotypes that differ between DsxM and DsxF, and it is transcribed in males as well, suggesting the presence of other unknown cofactors. In females, DsxF can function together with Hermaphrodite (Her), which is a zinc finger protein (Li and Baker 1998). Dual action of Dsx and Her varies according to the tissue, therefore Her can also be independent of DsxF (Li and Baker 1998). Both *ix* and *her* are expressed non-sex-specifically (reviewed in Christiansen, Keisman et al. 2002).

1.2.1.1 Homology to Dmrt family members

In 1998, the *male abnormal 3* (*mab-3*), a homologue of *dsx*, was found encoded in the *Caenorhabditis elegans* genome. Also, it showed homology with a chromosomal region from the human genome associated with sex reversal (Raymond, Shamu et al. 1998). Since then, *dsx* structural and functional conservation has been observed throughout metazoans (reviewed in Matson and Zarkower 2012). These transcription factors are enclosed within the *doublesex/mab-3 related* (*Dmrt*) family. Little homology is observed except for the highly conserved DNA binding domain (DM domain, named after Dsx/Mab-3) (Fig. 1.4D).

In all animals studied, *Dmrt* genes induce either the male or the female sexual determination program, after having integrated specific spatial, temporal and sexual information. Their functions have been extensively studied in the gonad development, as well as somatic sexual dimorphism (reviewed in Hong, Park et al. 2007, Kopp 2012, Matson and Zarkower 2012). As for *dsx*, *Dmrt* expression has also been detected in non-gonadal tissues (reviewed in Hong, Park et al. 2007).

In *C.elegans*, the *Dmrt* member Mab-3 establishes male structures and inhibits female-specific genes: it is required in males to inhibit the synthesis of yolk protein and to ensure correct development of the genitalia (Shen and Hodgkin 1988). Mab-3 resembles DsxM functions to such degree that, in *C. elegans*, ectopic DsxM (not DsxF) substitutes Mab-3 functions *in vivo* (Raymond, Shamu et al. 1998).

Like *Drosophila* Dsx, Dmrt1 is capable of binding as a home- and heterodimer *in vitro* (with Dmrt3 and Dmrt5) (An, Cho et al. 1996, Erdman, Chen et al. 1996, Murphy, Zarkower et al. 2007). Efforts have been made to further investigate the similitudes within the *Dmrt* downstream targets among the family homologues. Surprisingly, a large number of Dsx targets in *Drosophila* show overlap with Dmrt1 targets in mouse (Murphy, Zarkower et al. 2007, Clough, Jimenez et al. 2014).

1.2.2 Dsx tissue expression

In *Drosophila*, Doublesex is expressed in several tissues across the body, both during development and in adult flies, specifying sexual somatic differences. Despite all cells "knowing the X chromosome number" and thus expressing Sxl accordingly (Bopp, Bell et al. 1991), *doublesex* and *fruitless* are not detected ubiquitously: their expression is time- and tissue-dependent, generating a mosaic of *dsx* (or *fru*)-expressing cells which is tightly regulated (e.g. by Hox genes) (reviewed in Camara, Whitworth et al. 2008). This suggests that Sxl is not sufficient and additional context-dependent inputs are required to drive Dsx/FruM expression.

fru expression from the most distal promoter (*fru-P1*) is restricted to the nervous system and was described as the major regulator of sexual behaviour for many years. However, Dsx has also been detected in the CNS, where it establishes sex-specific differences in the neural circuitry and consequently, in the fly behaviour. In the CNS, DsxM and FruM are co-expressed in subsets of neurons (Dsx is required for the development of the $dsx^{+}fru^{+}$ neurons) and both contribute to the courtship song behaviour in males (Rideout, Billeter et al. 2007, Rideout, Dornan et al. 2010). Dsx (and *dsx*) expression in the CNS of larvae, pupae and adults has been described and is cell, time and sex dependent (Lee, Hall et al. 2002). Interestingly, in the ventral nerve cord (VNC), a cluster of cells undergoes female-specific death in a DsxF-dependent manner. In the brain, a cluster of cells increases proliferation in a male-specific manner (Sanders and Arbeitman 2008). A non-ubiquitous Dsx expression pattern is also observed in the gonads: DsxM is specifically expressed in subsets of somatic gonad cells in the males (Hempel and Oliver 2007).

Larvae, pupae and adults are mosaics of cells with or without Dsx (and FruM). The generation of two *dsx*-Gal4 reporter lines by Rideout et al. and Robinett et al. allowed the characterization of *dsx* expression with great insight (Rideout, Dornan et al. 2010, Robinett, Vaughan et al. 2010). In the adult flies, *dsx* is mostly, but not exclusively, expressed in tissues that developmentally transcribed *dsx*. It is in the fat body (which resembles the mammalian adipose tissue) and oenocytes (which are large secretory cells underlying the abdomen), in the genitalia, in the muscles and epidermal cells within the genitalia, in a variety of muscles (from leg muscles to abdominal ones), in the trachea, in the salivary glands, in the Malpighian tubules (excretory organ) and in the digestive system (Fig. 1.5). Within the digestive system, *dsx* is detected in the proventriculus, midgut, rectum and crop, as well as visceral muscles (see Introduction 1.3) (Fig. 1.5). Its expression in the digestive tract varies according to the region and cell type: large absorptive enterocytes from the midgut express *dsx*, unlike intestinal stem cells and hormone-producing enteroendocrine cells. Both studies also characterised the expression at the central and peripheral nervous systems from adult cells (see Rideout, Dornan et al. 2010 and Robinett, Vaughan et al. 2010 for further details).

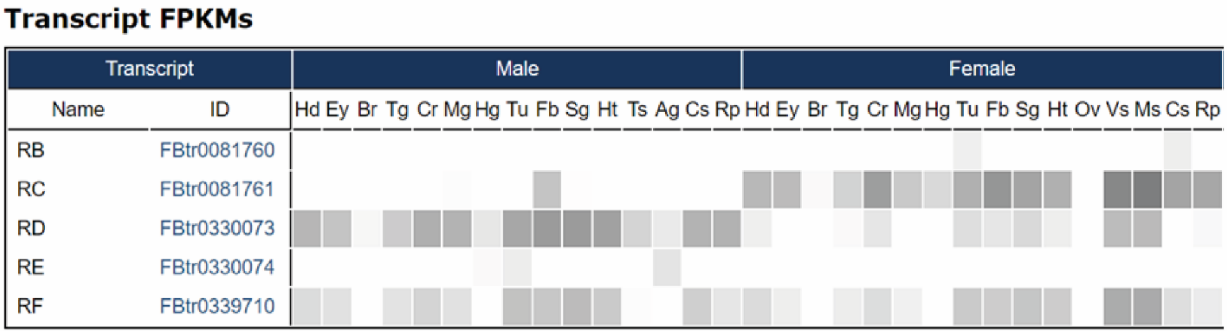

Figure 1.5: FlyAtlas expression of *dsx* transcripts in tissues of adult male and female flies

Expression of the different *dsx* transcripts (left column. RC mostly in females, RD in males) in male (central column) and female (right column) tissues. Hd = head, Ey = eye, Br = brain/CNS, Tg = thoracicoabdominal ganglion, Cr = crop, Mg = midgut, Hg = hindgut, Tu = Malpighian tubules, Fb = fat body, Sg = salivary glands, Ht = heart, Ts = testis, Ag = accessory glands, Ov = ovary, Vs = virgin spermatheca, Ms = mated spermatheca, Cs = carcass, Rp = rectal pad. Grey intensity represents level of expression (dark grey is high transcription level). FPKM = Fragments Per Kilobase of transcript per Million mapped reads. Adapted from FlyAtlas2.

1.2.3 Dsx targets, biological functions and regulation

Doublesex first spontaneous mutant was described in 1965 by Hildreth: “The most interesting feature of the mutant is that it transforms males as well as females into intersexes; both types are sterile and have extremely similar characteristics. Since both sexes are transformed and also each resulting intersex has both male and female features, the mutant has been designated “doublesex” (dsx)” and also “The third chromosome recessive gene dsx, when in homozygous

condition, causes both XX and XY individuals to develop as intersexes" (Hildreth 1965). Hildreth meticulously described the phenotypical effects of *doublesex* mutation. He characterised with great depth the changes in the abdomen, the external and internal genitalia (with variability within flies) and the foreleg, with special attention to the bristles (Hildreth 1965).

Although Dsx has been investigated for more than 50 years, the number of well-known downstream targets remains modest. Efforts to decipher the role of *dsx* have been set in tissues with visible or expected sexual dimorphisms: gonads (ovaries *vs* testis), genital disc, abdomen, fat body, sex combs (which are the sensory bristles of the legs used to grasp the female before copulation), brain and others (reviewed in Camara, Whitworth et al. 2008). Considering the importance of the role of *doublesex* as the last effector in the sex determination cascade and the increasing realization of its versatile functions, a growing number of studies have begun to unravel the direct (and indirect) targets, as well as the regulatory mechanisms behind.

Arbeitman et al. performed a microarray using one-third of the *Drosophila* genes in wild type, mutants without germline and mutants without sex-determination genes. They found 63 sex-differentially expressed genes in the soma, indirectly hinting the contribution of Dsx (Arbeitman, Fleming et al. 2004). Following up, Goldman and Arbeitman realised a microarray specifically for the adult head and CNS of males and females. They detected 54 genes downstream of Dsx; for example, one of them is the novel target gene *CG4979* (predicted as a sex-specific lipid metabolism enzyme) which is repressed by DsxF in females and activated by DsxM in males (Goldman and Arbeitman 2007). Noteworthy, and complemented by a follow-up study, the authors state that Dsx targets genes, as well as the mode of regulation, are different in the adult head of somatic tissues depending on which *Drosophila* control strain is being analysed (Goldman and Arbeitman 2007, Arbeitman, New et al. 2016). Curiously, a vast majority of genes regulated by Dsx are localised in the fourth chromosome (which has been shown to have evolved from a sex chromosome) (Arbeitman, New et al. 2016).

From the data gathered throughout these studies, they propose seven modes of Dsx-gene regulation (with supporting examples of *in vivo* data). Those are: 1) male-specific repressor, 2) female-specific repressor, 3) male-specific activator, 4) female-specific activator, 5) repressor in both sexes, 6) activator in both sexes, 7) opposing effects (Fig. 1.6) (Arbeitman, Fleming et al. 2004, Goldman and Arbeitman 2007, Arbeitman, New et al. 2016). The most frequent male-regulatory mode is female-specific repression. In females, it is strain-dependent: either male-

specific repression or female-biased expression; suggesting regulatory flexibility (Arbeitman, New et al. 2016).

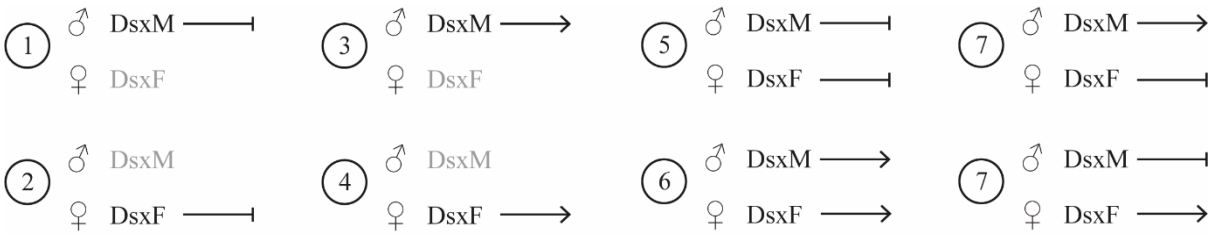

Figure 1.6: Schematics of the seven proposed modes of Dsx-gene regulation in male and female

Doublesex acts as a repressor in male (1) or female (2) only. Doublesex as an activator solely in male (3) or female (4). Doublesex regulates negatively (5) or positively (6) in both sexes. Doublesex with sex-specific opposing roles in males and females (7). From the 1st to the 4th category, Dsx is either an activator or repressor exclusively in one sex. In the 5th and the 6th category, Dsx is either a repressor or an activator, consistently in both sexes. In the 7th category, Dsx has opposing roles for the two sexes. Grey colour indicates lack of activity or absence of Dsx. Adapted from Arbeitman, New et al. 2016.

Furthermore, Chatterjee et al. identified sex-specifically expressed genes downstream of *dsx* which drive the sexually dimorphic development of the genitalia during morphogenesis. Through a genome-wide transcriptional profiling of the genital disc, the authors determined 23 genes with sex differential transcript levels (13 of them transcription factors) (Chatterjee, Uppendahl et al. 2011). In the same year, Luo et al. described around 650 potential direct DsxF target genes by the DamID method. From these targets genes, a subset of 23 are evolutionary conserved, which increases the likelihood of them being direct Dsx targets (Luo, Shi et al. 2011). One of the most extensive studies, using DamID complemented by ChIP, analysed the male (DsxM) and female (DsxF) Dsx targets in sexually dimorphic tissues (fat body and ovaries) as well as S2 cells. The main conclusion is that Dsx occupancy is sex- and tissue-dependent (Clough, Jimenez et al. 2014). Following the same approach, unpublished data corroborates these observations in heads and brains (D'Souza 2019).

From the aforementioned studies, the community has gained knowledge about Dsx target genes, their tissue-specificity, their strain-specificity and the complexity of the transcription factor Dsx regulatory mode.

Up to date, the *bona fide* direct targets of Dsx are *Yolk proteins* (*Yp1* and *Yp2*) in the fat body (Burtis, Coschigano et al. 1991, Coschigano and Wensink 1993, An and Wensink 1995, An and Wensink 1995); *bric-a-brac* (*bab1/2*) in the gonad (Camara, Whitworth et al. 2019) and in the abdomen (Williams, Selegue et al. 2008); *desaturase F* (*desatF*), a female-specific transmembrane fatty acid desaturase required for courtship pheromone production in the

oenocytes (Jallon, Lauge et al. 1988, Shirangi, Dufour et al. 2009); and *Flavin-containing monooxygenase-2* (*Fmo-2*), involved in oxidation-reduction metabolism, in specialised areas of the digestive tract and in the fat body cells of the spermatheca (female tissue to store male sperm) (Luo and Baker 2015).

Yp1, *bab1/2*, *Fmo-2* and *desatF* are expressed at higher levels in females, and their Dsx-regulatory mode varies. Since *dsx* mutants in both sexes show intermediate levels for *Yp1*, *bab1/2* and *Fmo-2*, this suggests that the mode of regulation follows the 7th category of opposing effects: DsxF activates and DsxM represses (Coschigano and Wensink 1993, Williams, Selegue et al. 2008, Luo and Baker 2015). On the contrary, *desatF* is included in the 4th category: activated by DsxF and unaffected by DsxM (Shirangi, Dufour et al. 2009).

Yolk protein genes (*Yp1* and *Yp2*) in the fat body are the most studied Dsx direct target genes. DsxM and DsxF bind to the fat body enhancer (FBE) *in vivo* and *in vitro* by their identical DNA-binding domain, to regulate *Yp1/2* expression. The sex-specific C-terminal domain leads to sex-specific protein-protein interactions with the appropriate cofactors. Whilst DsxM represses FBE, DsxF interacts with Ix as a cofactor and activates *Yp1/2* expression from the FBE (Waterbury, Jackson et al. 1999, Garrett-Engele, Siegal et al. 2002).

Another example of a Dsx direct target is *bric-a-brac1/2* (*bab1/2*) in the abdomen, genitalia and sex combs. In the adult flies, the first legs are sexually dimorphic regarding the presence of bristles. Males have increased number of dark and thicker bristles, oriented longitudinally, used as mechanosensors to grab the female's abdomen before/during copulation. These sex combs structures are lost in females, which instead have a thinner transversally increased number of bristles. The homeotic gene *Sex combs reduced* (*Scr*) is sexually dimorphic, detected in the male sex comb region. In late larvae, *Scr* activates *dsx* expression, which in turn, modulates *Scr* in the pupae: downregulation of *Scr* reduces *dsx* expression, and DsxM upregulates *Scr* while DsxF represses it (Tanaka, Barmina et al. 2011 and reviewed in Kopp 2011). However, the lack of sex combs in *Scr*-expressing females indicates that further factors contribute to its regulation. *bric-a-brac* (*bab1/2*), a BTB zinc finger transcription factor, is a negative regulator of sex comb formation (reviewed in Camara, Whitworth et al. 2008).

The role of *bab1/2*, under *dsx* (and Hox gene *Abdominal-B*) effect, is best understood at the abdominal pigmentation. In males, the abdominal segments A5 and A6 are fully pigmented. *Dsx* null mutants have pigmentation at the A6 segment. This indicates the roles of DsxF in repressing pigmentation in females, and DsxM in promoting full A5 pigmentation. *bab1/2*

levels are sexually dimorphic: Bab1/2 is detected in A2-A6 of females and in A2-A4 of males. The absence of *bab1/2* in males at A5 and A6 correlates with dark pigmentation. Abd-B induces pigmentation: it is highly expressed in A5 and A6 of males, where it represses *bab1/2*. In short, DsxM together with Abd-B represses *bab1/2* only in the male A5 and A6. In females, DsxF restores *bab1/2* expression in A5 and A6 by counteracting the repression of *bab1/2* by Abd-B. In both the sex comb formation and abdominal pigmentation, *bab1/2* is repressing the male program in females (reviewed in Christiansen, Keisman et al. 2002, Camara, Whitworth et al. 2008).

Furthermore, Dsx contributes to the genitalia sexual dimorphism via cell-autonomous and non-autonomous mechanisms: either by regulating how cells respond to a signal or by controlling the expression of the signal (reviewed in Christiansen, Keisman et al. 2002, Camara, Whitworth et al. 2008, Verhulst and van de Zande 2015).

Finally, even though Dsx contributes to the somatic morphological sex differences, it is also detected in the nervous system (Lee, Hall et al. 2002). Males have more *dsx*-expressing neurons than females (Rideout, Dornan et al. 2010, Pavlou, Lin et al. 2016). In males, silencing of *dsx*-expressing neurons eliminates the courtship song (a wing vibration produced by the males during the courtship) and male courtship is decreased (Rideout, Dornan et al. 2010). In females, targeted activation of *dsx*-expressing neurons produces male-like courtship behaviors towards either males or females (Rezaval, Pattnaik et al. 2016). Additionally, in females, *dsx*-expressing neurons in the brain controls receptive behavior (Zhou, Pan et al. 2014) and DsxF (together with Adb-B) regulates cell-death in the CNS during metamorphosis (Ghosh, Bakshi et al. 2019). Furthermore, the expression of *dsx* determines abdominal neuroblast commitment to a male or female fate during development (Taylor and Truman 1992).

Despite *doublesex* and *fruitless* being known for many years as the two independent last effectors downstream of *transformer*, new discoveries are still being made. Two recent studies identify *tra*-dependent but *dsx*-/*fru*-independent branches that regulate sexual identity (Rideout, Narsaiya et al. 2015, Hudry, Khadayate et al. 2016). Moreover, recent work has shown that Dsx regulates *fru* in the gonad stem cell niche, promoting sexual dimorphism. In the male, FruM is detected in the niche to develop and maintain sperm. Unlike the Tra-dependent *fru* expression, in this scenario, *fru* seems to be regulated in a Tra-independent, Dsx-dependent manner (Zhou, Whitworth et al. 2021).

The prior examples illustrate how Dsx contributes to the establishment of sexual dimorphism. Due to restrictions of space and the scope of the thesis, further information can be found in the following reviews: Christiansen, Keisman et al. 2002, Camara, Whitworth et al. 2008, Kopp 2012, Verhulst and van de Zande 2015, Hopkins and Kopp 2021.

Throughout this section of introduction, I have provided a brief molecular description of the last effector of the sex determination pathway Doublesex, and its male-female isoforms. Additionally, I presented an overview of its sex-specific expression, targets and biological functions. Since it is discovery, its role in sexually dimorphic tissues has been characterised, but recently, new data showed its expression in other tissues such as the digestive tract, which were, until recently, assumed to be equivalent between sexes (Robinett, Vaughan et al. 2010, Hudry, Khadayate et al. 2016).

1.3 The digestive tract of *Drosophila melanogaster*

1.3.1 The midgut of *Drosophila* at the anatomical and cellular level

The adult fruit fly digestive system is generated almost entirely *de novo* during metamorphosis. It is also an adaptive and regionalised system, which consists of several portions that differ in their developmental origin and function. Over the years, the digestive system has proven to be a more complex system than initially thought. The functions of the *Drosophila* gut are versatile and are subject to tight regulation. They include regulation of energy homeostasis through ingestion, digestion, absorption, storage and excretion of macronutrients from the food. The system engages in interorgan communication, as well as acting as a barrier against the external environment by guarding against pathogens (reviewed in Miguel-Aliaga, Jasper et al. 2018). Like in mammals, the *Drosophila* digestive tract shows fast epithelial turnover that accounts for its plasticity. Indicating its complexity, Chintapalli et al. via the FlyAtlas, and Buchon et al. via a microarray, showed that more than half of *Drosophila* genes are expressed in the adult midgut (from the approx. 750 transcription factors encoded in the genome, 460 were detected) (Chintapalli, Wang et al. 2007, Buchon, Osman et al. 2013). This vast complexity allows the gut to respond to both environmental changes (such as nutritional cues reducing the number of proliferative cells upon starvation) (reviewed in Shim, Gururaja-Rao et al. 2013) and internal variations (by female guts increasing the size after mating) (Reiff, Jacobson et al. 2015, Hudry, Khadayate et al. 2016). The similarities between the fruit fly and the human digestive system

(Fig. 1.7), at both the anatomical and cellular level, makes *Drosophila* an amenable model to further understand the digestive tract in humans.

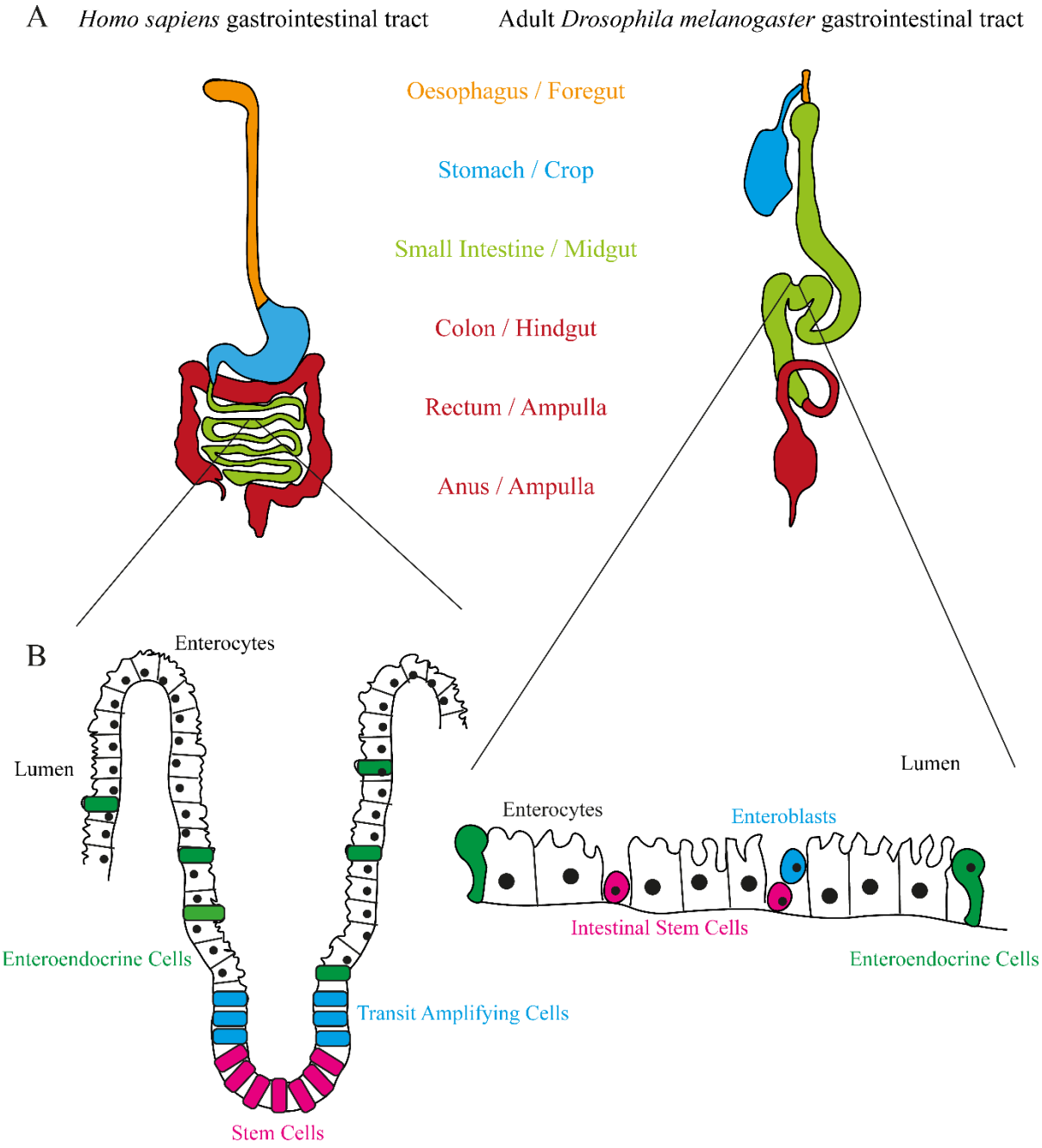

Figure 1.7: Schematic representation of the human and *Drosophila* intestine at the anatomical and cellular level

(A) Similarities between adult *Homo sapiens* and *Drosophila melanogaster* gastrointestinal digestive systems. From anterior to posterior: the oesophagus in humans and foregut in flies (orange), the stomach in humans and crop in flies (blue), the small intestine in humans and midgut in flies (green), the colon, rectum and anus in humans; the hindgut and ampulla in flies (red). (B) The intestinal epithelial in humans is made up of crypt-resident stem cells (pink) and transit amplifying cells (blue), and of villus-resident hormone-secreting enteroendocrine cells (green) and digestive enterocytes (white) (additional cell-types are not depicted for simplicity reasons). Similar cell types are detected in the fly epithelium: intestinal stem cells (pink), enteroblasts (blue), enteroendocrine cells (green) and enterocytes (white).

At the anatomical scale, the *Drosophila* digestive tract is divided into foregut, midgut and hindgut (Fig. 1.8) (reviewed in Lemaitre and Miguel-Aliaga 2013, Miguel-Aliaga, Jasper et al. 2018). The foregut is formed by the oesophagus, the crop, and the cardia (also known as proventriculus): the crop is described as a storage organ in Diptera insects (Stoffolano and Haselton 2013), the cardia (at the junction between the foregut and midgut) segregates a chitinous and glycoprotein layer called the peritrophic matrix (PM) that produces antimicrobial peptides and covers all of the midgut luminal side (King 1988); and both consist of valves that control food entry. The midgut, one of the largest organs in the fruit fly, mediates absorption and digestion. It is divided into anterior, middle and posterior portions, and is further regionalised into six major regions (R0 to R5) separated by anatomically constricted epithelial boundaries that allow the arrangement of the gut within the abdominal cavity, as well as the contractile movements promoting food transit. The midgut is further subdivided into 10-14 regions based on features including pH (being neutral at the anterior midgut, acidic at the R3 copper cell region, and mid alkaline at the posterior), proliferation rate, morphology, histology and gene expression (the final transcriptional pattern is established two days post-eclosion) (Buchon, Osman et al. 2013, Marianes and Spradling 2013). At the boundary between the midgut and the hindgut, there are the right and left Malpighian tubules, the major excretory organ. The hindgut consists of the pylorus, the ileum and the rectum (ampulla), which control water/ions exchange and excretion, and resemble the human large intestine in osmotic regulation (reviewed in Miguel-Aliaga, Jasper et al. 2018).

At the cellular scale, the midgut epithelium is composed of intestinal stem cells (ISCs), enteroblasts (EBs), enterocytes (ECs) and enteroendocrine cells (EECs) (Fig. 1.7, 1.8B-C). The most prevalent cell type is the EC: a columnar epithelial cell with microvilli on the apical site that increase the surface area (Holtof, Lenaerts et al. 2019). The epithelium is surrounded by both longitudinal and circular striated visceral muscles cells encompassing contractile movements, as well as branched trachea from the respiratory system sensing oxygen levels and the organ metabolic activity. The lumen of the gut is covered by secreted mucus. Furthermore, the gut epithelium is innervated, mostly at the anterior and posterior part. Given the close interorgan communication between the gut and the adipose tissue, a ring of fat tissue is observed with spatial proximity to the posterior gut (reviewed in Miguel-Aliaga, Jasper et al. 2018).

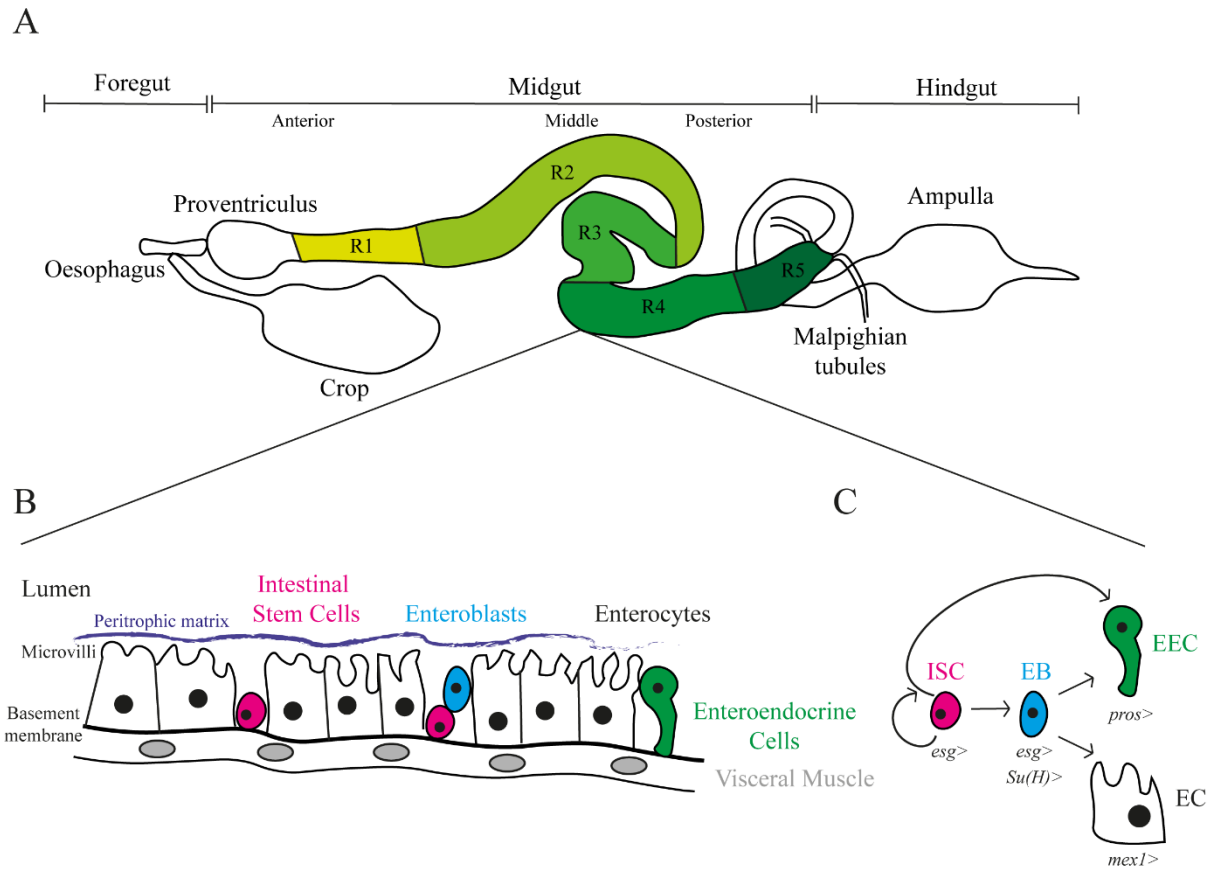

Figure 1.8: Schematic representation of the regional divisions and cell types of the fly gut

(A) The fly gastrointestinal digestive system is divided into the foregut, the midgut and the hindgut (from anterior to posterior). The foregut comprises the crop, the oesophagus and the proventriculus. The midgut is subdivided into the anterior, middle and posterior midgut, which are also regionalised in five different regions depicted in green shades (R1-R5). The hindgut is mainly represented by the ampulla. (B) Higher magnification view of the cellular composition of the midgut. Above the visceral muscle, there is the basement membrane of the epithelial cells, the microvilli of which are exposed towards the lumen of the gut tube. The peritrophic matrix covers the luminal side of the cells. There are four types of epithelial cells: the intestinal stem cells (ISCs), the enteroblasts (EBs), the enterocytes (ECs) and the enteroendocrine cells (EECs). (C) ISCs divide either symmetrically or asymmetrically, giving rise to one EB or EEC. The EB is a progenitor cell which further differentiates into either EEC or EC. The molecular hallmark of ISCs is their expression of *esg*, which is also expressed in EBs. *Su(H)* is detected in EBs only. EECs are characterised by the transcription of *pros*, and ECs are *mex1*$^{+}$ cells.

The multipotent intestinal stem cells, which are highly mitotic and express *Delta* (*Dl*) and *escargot* (*esg*), are a heterogeneous population able to replenish the specific region they belong to: under homeostatic conditions, ISCs renew the epithelium within one or two weeks (Micchelli and Perrimon 2006, Ohlstein and Spradling 2006). Symmetric divisions produce two ISCs, whereas asymmetric divisions generate an ISC (*Dl*$^{+}$ *esg*$^{+}$) and a postmitotic EB (upregulation of *Notch* and *esg*$^{+}$) or EEC (*prospero*$^{+}$ (*pros*$^{+}$)). The EB further differentiates into either a large polyploid digestive and absorptive EC (expressing *POU domain protein 1* (*Pdm1*$^{+}$), *Myosin* (*Myo1A*$^{+}$) and *midgut expression 1* (*mex1*$^{+}$)) or a hormone-secreting EEC (*pros*$^{+}$) (reviewed in Lemaitre and Miguel-Aliaga 2013, Gervais and Bardin 2017).

The cellular regionality of the midgut is also observed at the level of the enterocyte population. Depending on the region and subregion, the ECs are different in size, shape, membrane invaginations, internal structures, content particles and gene expression. The ECs compartmentalisation is in harmony with the region-specific functions of the organ (Fig. 1.8). The midgut of *Drosophila melanogaster* shows a striking diversity of enzymes (349 based on bioinformatic predictions) involved in carbohydrate (52 predicted carbohydrase), protein (the most abundant category with 234 endo/exopeptidases) and lipid metabolism (63 lipases and esterases) (reviewed in Lemaitre and Miguel-Aliaga 2013). The expression of these enzymes is region-specific. In broad terms, the anterior gut (mostly R2) expresses higher levels of enzymes that degrade the macromolecules coming from the diet, the copper-cell region (R3) has low acidic pH, and the processing and absorption of small molecules occurs in the posterior gut (R4). Lipid and sterol metabolism genes, triglyceride lipases (such as *magro* and *CG2772*), sterol binding proteins (such as *Npc2c* and *Npc1b*) and cholesterol metabolism genes (such as *ACAT*) are highly detected in R4 (Buchon, Osman et al. 2013). Other lipid genes, such as *brummer* lipase, are highly expressed in R2 and R5 region (Buchon, Osman et al. 2013). Of note, enzymes can either be secreted in the lumen, retained in the EC villi or in the endo/ectoperitrophic spaces created by the PM (reviewed in Miguel-Aliaga, Jasper et al. 2018). In addition to the region-specificity, digestive enzyme expression is sex-specific: carbohydrate and sugar genes are upregulated in male midguts (Hudry, Khadayate et al. 2016).

Midgut compartmentalization applies also to lipids (Buchon, Osman et al. 2013, Marianes and Spradling 2013, Zhao and Karpac 2020). The EC population containing lipid vesicles is detected in R2 with columnar morphology (Buchon, Osman et al. 2013) or in A2, P1 and P3, detected by electron microscopy and lipid droplet staining (Marianes and Spradling 2013) (the authors used another nomenclature referring to midgut regions: they divide the anterior portion into three regions, A1-A3, followed by the middle portion, Cu-LFC-Fe, and the four posterior portions, P1-P4).

1.3.2 Lipid metabolism

In 1960, the first obese *Drosophila melanogaster* mutant was described, leading to the establishment of the fruit fly as a model system to study lipid metabolism (Doane 1960). Since then, subsequent research has focused on exploring the interorgan lipid communication, the intracellular lipidic metabolic pathways, and the molecular misregulations causing diabetic and obese flies (Burtis and Baker 1989, Schlegel and Stainier 2007, Musselman and Kuhnlein 2018,

Chatterjee and Perrimon 2021, Heier, Klishch et al. 2021). Lipid metabolism involves a series of complex processes encompassing synthesis, breakdown, storage, transport and signalling. Around 500 genes and different organs are implicated in adult lipid regulation. Several techniques such as lipidomics, proteomics, transcriptomics and screens are combined in order to achieve a better understanding on lipid homeostasis (reviewed in Toprak, Hegedus et al. 2020). Conveniently and among other tools, thin layer chromatography (TLC) is used to measure lipids in fly homogenates (extracted lipids). At the cellular level, the neutral dye LipidTox (among other neutral dyes) helps to visualise and quantify the number and size of the lipid droplets (LDs) (Beller, Bulankina et al. 2010, Bi, Xiang et al. 2012, Wat, Chao et al. 2020 and reviewed in Musselman and Kuhnlein 2018, Heier, Klishch et al. 2021).

Lipids are biomolecules required for a diverse range of biological processes: membrane fusion/fission, signalling (both extracellular to other tissues and subcellular traffic), hormone and pheromone production, cellular compartmentalization, storage of the excess of carbon units (to prevent their accumulation as toxic metabolic intermediates) etc. A basic function of lipids is long-term energy storage within the cell, as specialised particles called lipid droplets (LDs): organelles broadly conserved from bacteria to humans. LDs are considered dynamic structures which play a role in the synthesis, movement and degradation of lipids. LDs have a hydrophobic core of triacylglycerol (TAG, a glycerol ester linked to three fatty acids (FA) which represents the 90% of the LD) and sterol esters. The core is covered by a phospholipid monolayer with proteins that regulate LDs deposition, breakdown and trafficking. In long-lasting energy demand periods, stored TAGs are slowly catabolised, resulting in a greater source of chemical energy than glycogen (accumulation of carbohydrates) (reviewed in Kuhnlein 2011, Kuhnlein 2012, Ohsaki, Suzuki et al. 2014, Musselman and Kuhnlein 2018, Toprak, Hegedus et al. 2020, Chatterjee and Perrimon 2021, Heier, Klishch et al. 2021). The complete oxidation of carbohydrates and proteins yields around 4kcal/g, compared to 9kcal/g of fatty acids (Klowden 2013).

Fat metabolism in *Drosophila* is a balance between two antagonistic processes: the catalytic lipolysis, in which fat is mobilised and broken down to obtain chemical energy, mostly in the form of adenosine triphosphate (ATP); and the anabolic lipogenesis, which results from either dietary lipid absorption or synthesis *de novo* (reviewed in Kuhnlein 2011, Kuhnlein 2012, Musselman and Kuhnlein 2018). An increasing number of studies are exploring mechanisms of lipid metabolism regulation (mainly by hormones, transcription factors, secondary messengers such as calcium and/or post-transcriptional modifications), as well as the

coordination, mobilization and traffic across tissues (reviewed in Toprak, Hegedus et al. 2020, Chatterjee and Perrimon 2021, Heier, Klishch et al. 2021). Like many other insects, *Drosophila* cannot synthetise cholesterol *de novo*, therefore relying exclusively on its dietary source. Sterols are essential for the synthesis of crucial fly hormones such as ecdysone (Lavrynenko, Rodenfels et al. 2015). Since LDs also store sterols, lipid traffic is tightly associated to sterol mobilization.

1.3.2.1 Lipid metabolism in the fat body and the midgut of *Drosophila*

Lipid homeostasis is key during fly development and physiology (e.g. reproduction). At the beginning of the *Drosophila* life cycle, the mother provides essential TAGs to the embryo ensuring sufficient energy fuel for the initial stages of its development. Once the larval stage has been reached, high quantities of lipids are acquired through the diet and stored to overcome metamorphosis (reviewed in Heier and Kühnlein 2018, Heier, Klishch et al. 2021). In the adult fly, there are several organ systems involved in TAG homeostasis: fat body, oenocytes, intestinal tract, skeletal muscle and heart, and the nervous system (reviewed in Musselman and Kuhnlein 2018, Toprak, Hegedus et al. 2020, Chatterjee and Perrimon 2021, Heier, Klishch et al. 2021).

The fat body is akin to the adipose tissue, liver and immune system of humans and is the master tissue in fat storage. The adipocytes compose the majority of the fat body. The origin of almost the whole-body TAG load comes from dietary lipids processed in the gut (90%), with the remainder synthetised *de novo* from carbohydrates (Lilián E Canavoso, Zeina E Jouni et al. 2001, Palm, Sampaio et al. 2012). Furthermore, the fat body stores abundant cholesterol esters and glycogen. It is considered a nutrient sensor, and several of its main functions are lipogenesis, lipolysis and synthesis of proteins which are transported to other organs via the haemolymph. The synthetised proteins are vitellogenins and lipoproteins, which are important for lipid packaging and traffic exiting in the midgut (reviewed in Toprak, Hegedus et al. 2020).

The oenocytes, which resemble human hepatocytes, also regulate lipid metabolism. During larval starvation, the fat body-derived *Drosophila* insulin-like peptide 6 (Dilp6 or Ilp6) induces oenocytes to accumulate large numbers of LDs and deplete stored lipids from the fat body (Gutierrez, Wiggins et al. 2007, Chatterjee, Katewa et al. 2014). Under homeostatic conditions, they synthetise very long chain FAs, producing cuticular hydrocarbons acting as pheromones, and avoiding desiccation (Wicker-Thomas, Garrido et al. 2015).

The midgut is a key organ in lipid metabolism. Together with the fat body, the two organs selectively provide energy to other organs such as the brain or muscles via the haemolymph, which is the open circulatory system of the fly (reviewed in Heier and Kühnlein 2018, Heier, Klishch et al. 2021). In short, there are six processes in the midgut which contribute to fat homeostasis: digestion, absorption, lipogenesis and *de novo* synthesis, lipolysis and transport to other organs (Fig. 1.9).

Lipid digestion

Dietary lipids are hydrolysed by lipases, phospholipases and cholesterol esterases secreted in the lumen by the ECs. Triacylglycerol (TAG), diacylglycerol (DAG), monoacylglycerol (MAG) and phospholipids are mainly broken down into free FAs and other end products such as glycerol, non-esterified cholesterol and phospholipid derivatives, which are subsequently absorbed by the ECs (reviewed in Heier and Kühnlein 2018). Lipid metabolism in the gut appears to occur in a regional manner, with hydrolysis happening in the anterior gut, whilst synthesis and storage of LDs occur at the posterior side (Buchon, Osman et al. 2013, Marianes and Spradling 2013, Hung, Hu et al. 2020 and reviewed in Holtof, Lenaerts et al. 2019).

The *Drosophila* midgut contains approximately a dozen predicted digestive lipases, many of which are still uncharacterised, such as *CG6277* or *CG6283* (Horne, Haritos et al. 2009, Sieber and Thummel 2009). The most well-studied lipase is *magro* (*mag*): it is expressed in the proventriculus and midgut, and encodes a protein with dual lipase and cholesterol esterase function. *mag* mutants decrease TAG lipase activity and dietary lipid assimilation, causing a lean phenotype (whole-body TAG levels are impaired) (Sieber and Thummel 2012).

Lipid absorption

The end products of the dietary lipid hydrolysis need to be absorbed by the ECs. The mechanisms behind lipid absorption are still rudimentary. FAs can diffuse across the plasma membrane, which can be facilitated by emulsification (reviewed in Miguel-Aliaga, Jasper et al. 2018). The uptake of FAs in the gut is enhanced by its conversion to acyl-coenzyme A (CoA). Furthermore, fatty acid-binding proteins (FABP) facilitate the diffusion of hydrophobic lipid digestion products across membranes in the midgut and other tissues. Additionally, fatty acid transport proteins (FATP) may contribute to the active transport of dietary FAs (long chain FAs) (reviewed in Holtof, Lenaerts et al. 2019, Toprak, Hegedus et al. 2020).

The midgut expresses 12 homologues of the Cluster of Differentiation 36 (CD36)/Scavenger Receptor Class B type I (SR-BI) mammalian family. Thus, it is possible that like in mammals, these membrane proteins mediate the transport of FAs and lipoproteins in flies (Herboso, Talamillo et al. 2011). Moreover, *Drosophila* expresses homologues of the transmembrane Niemann-Pick C1 (Npc1) mammalian family: whilst Npc1a and Npc2a are involved in intracellular sterol trafficking (Huang, Warren et al. 2007), Npc1b in the midgut is required for sterol absorption (Voght, Fluegel et al. 2007).

Lipogenesis and synthesis *de novo*

FAs are the elementary units for DAG and TAG anabolism. In addition to being absorbed from the diet, FAs are also synthetised *de novo*, primarily in the adipocytes, but also in the ECs and other lipid-containing tissues (reviewed in Heier and Kühnlein 2018, Heier, Klishch et al. 2021). In *de novo* FAs synthesis, the enzyme acetyl-CoA carboxylase (ACC) first converts acetyl-CoA into malonyl-CoA, which is subsequently condensed with acetyl-CoA to produce long-chain FAs by the enzyme FA Synthase (FASN). ACC highest levels are detected in the fat body, midgut and oenocytes (reviewed in Heier, Klishch et al. 2021).

Enterocytes, as well as in other lipogenic cell-types such as the adipocytes in the fat body, are capable of synthesise TAGs from FAs (Song, Veenstra et al. 2014 and reviewed in Kuhnlein 2012, Heier and Kühnlein 2018, Lian, Wu et al. 2018, Toprak, Hegedus et al. 2020, Zhou, Ding et al. 2020). The enzyme acyl-CoA synthetase long-chain (Acsl) activates the FAs to FA-CoA to begin the glycerol-3-phosphate (G3P) pathway. FA-CoA are esterified with G3P (derived from sugars) by glycerol-3-phosphate acyltransferases (GPAT enzymes, detected in both midgut and fat body, codified by *minotaur* (*mino*), *CG15450*, *Gpat4*/*CG3209*) to lypophosphatidic acid (LPA). The enzyme LPA acyltransferase (LPAAT or AGPAT, codified by *Agpat1*/*CG3812*, *Agpat2*/*fu12*, *Agpat3*/*CG4729* and *Agpat4*/*CG4753*) esterifies these LPA to phosphatidic acid (PA), which is dephosphorylated by Lipin (Mg^{+2}-dependent PA phosphatase (PAP1) enzyme) to DAG. Expression of *CG4753*, *CG4729*, and *fu12* is high in the fat body and midgut (reviewed in Kuhnlein 2012). Mutation of *Lipin* results in reduced TAGs and LDs size (Ugrankar, Liu et al. 2011). The DAGs are esterified to TAGs by the DAG acyltransferases (DGAT), and TAGs are finally stored in the LDs. The enzymes catalysing the reaction are codified by two different families: membrane bound o-acyl transferase (MBOAT) family (mostly *midway* (*DGAT1* or *mdy*) and *DGAT2* (*CG1941*, *CG1942*/*Dgat2* and *CG1946*)) (reviewed in Kuhnlein 2012, Heier and Kühnlein 2018, Toprak, Hegedus et al. 2020, Heier,

Klishch et al. 2021). Loss of *midway* reduces whole-body TAG level (Tschapalda, Zhang et al. 2016).

Besides the G3P pathway, DAGs can be generated through the monoacyglycerol acyltransferases (MGAT) pathway: dietary MAGs are esterified to DAGs by the MGAT enzyme (reviewed in Kuhnlein 2012, Heier and Kühnlein 2018, Toprak, Hegedus et al. 2020).

Lipolysis

Most *in vivo* studies have thus far focussed on the fat body because it functions as a metabolic sensor controlling whole-body nutritional homeostasis. However, research suggests that the same catabolic pathways are shared by the midgut TAGs (Palm, Sampaio et al. 2012), as observed by both transcript and protein expression (reviewed in Gronke, Muller et al. 2007, Kuhnlein 2011, Kuhnlein 2012, Heier and Kühnlein 2018).

Brummer (*bmm*) is a TAG hydrolase (adipose triglyceride lipase (ATGL) orthologue in flies) that breaks down TAG into DAG. Downregulation of *bmm* causes starvation-sensitivity (i.e. reduced lipid breakdown) and obesity, which can also be observed by the excessive TAGs in peripheral tissues such as the midgut (Gronke, Mildner et al. 2005, Palm, Sampaio et al. 2012). On the contrary, *bmm* gain of function in the fat body results in fat storage depletion and reduced LD size (Gronke, Mildner et al. 2005). Bmm is located at the surface of the LDs (Gronke, Muller et al. 2007), where there is also the Hormone-sensitive lipase (Hsl), which breaks down TAG to DAG and FA (Bi, Xiang et al. 2012). Both Hsl and Bmm interact with Perilipin1(Plin1)/Lipid storage droplet 1 (Lsd1) and Plin2/Lsd2 at the surface of LDs, respectively (Bi, Xiang et al. 2012). Perilipins are the most studied LD-associated proteins: they regulate LD structure and catabolism by limiting the accessibility and activity of the lipases. On the one hand, Hsl controls stimulated lipolysis under acute food deprivation conditions (rapid changes in lipid demands) (Beller, Bulankina et al. 2010, Bi, Xiang et al. 2012). On the other hand, Bmm ensures basal lipolysis, defined as the low rate lipolytic phase to maintain metabolic baseline, as well as participating in the acute mobilization of storage-fat (Gronke, Mildner et al. 2005, Gronke, Muller et al. 2007). Other TAG lipases are *Lipase 1-4*, *CG6295* or *CG2772* (Palanker, Tennessen et al. 2009).

The elementary product resulting from lipolysis are free FAs. These can be used for fatty acid elongation or for chemical energy. Free FAs undergo β-oxidation in the mitochondria or peroxisomes to obtain acetyl-CoA (also resulting from the glycolysis-derived pyruvate), which

can be utilised in the tricarboxylic acid cycle (TCA) in the mitochondria for further ATP production (Palanker, Tennessen et al. 2009).

Lipid transport

In ECs, the dietary absorbed FAs are firstly converted into diacylglycerol (DAG: two linked FAs fused to a glycerol ester) and loaded to carrier lipoproteins derived from the fat body. Since the midgut is incapable of synthesizing lipoproteins, it recruits high density lipophorin (Lpp) (HDLp) and lipid transfer particle (LTP), apoB-family members assembled in the fat body. Lpp is recruited in an LTP-dependent manner, and it is packed with dietary sterols and newly originated DAG in the ECs. Then, these low density Lpp (LDLp) are sent from the gut to the haemolymph and then to other tissues, also facilitating the diffusion process of absorbing dietary products (Palm, Sampaio et al. 2012). In addition to Lpp and LTP, recent work has shown that Neuropeptide-like precursor 2 (Nplp2) plays a role as an exchangeable apolipoprotein under stress heat-derived conditions (Rommelaere, Boquete et al. 2019).

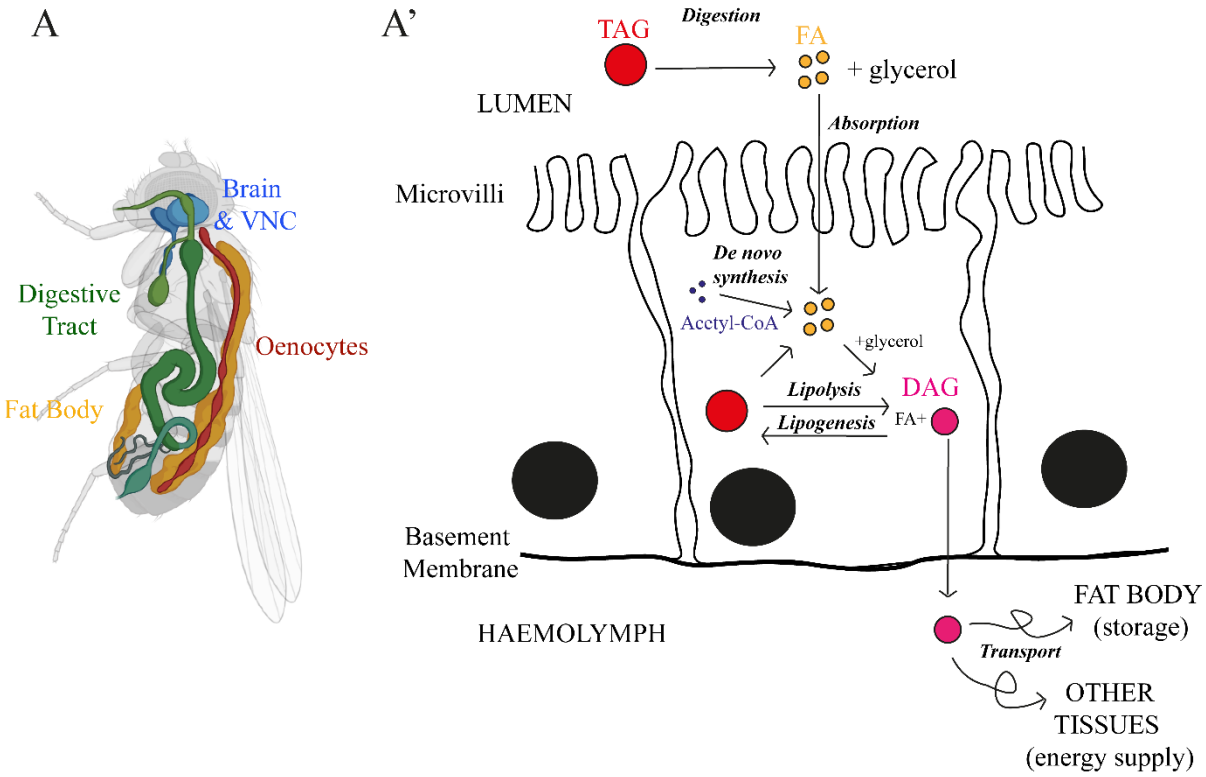

Figure 1.9: Schematics of fat metabolism in *Drosophila* enterocytes

(A) Cartoon of the fruit fly indicating different organs: the brain and the ventral nerve cord (VNC), in blue; the digestive tract, in green; the oenocytes, in red; and the fat body, in yellow. (A') Lipid metabolism in the ECs of the midgut. In the lumen, ingested TAGs are digested into FAs and glycerols. FAs are absorbed in the apical surface of ECs. The polyploid ECs are metabolic cells capable of fussing FAs to glycerol, to generate DAG which can be subsequently transported via the hemolymph. DAGs are sent to the fat body for storage, or to other tissues for energy supply. The ECs have the potential to *de novo* synthesise FAs from acetyl-CoA. In addition to lipolysis,

ECs produce TAG (from DAG and FAs) in a lipogenic process, which can be stored as chemical energy. TAG in red, DAG in pink, FA in yellow and acetyl-CoA in blue. Adapted from Heier and Kühnlein 2018.

Lipid homeostasis regulation

Fat metabolism is tightly controlled by a diverse set of mechanisms. For example, the expression of lipid genes is regulated by a variety of transcription factors, such as the sterol regulatory element-binding protein (SREBP), or Forkhead box class O (FoxO). Additionally, lipid homeostasis is controlled by complex endocrine regulation. Hormones influence the lipid metabolism and traffic via enzymes, scaffolding/regulatory proteins and transporters (reviewed in Toprak, Hegedus et al. 2020, Chatterjee and Perrimon 2021, Heier, Klishch et al. 2021).

In feeding conditions, lipoanabolic pathways are active (reviewed in Heier and Kühnlein 2018, Musselman and Kuhnlein 2018, Chatterjee and Perrimon 2021, Heier, Klishch et al. 2021). The insulin producing cells (IPCs) secrete *Drosophila* insulin-like peptides (Dilps or Ilps) that bind to the Insulin receptor and activate the signalling cascade through Protein kinase B (Akt). Akt phosphorylates FoxO and recruits it from the nucleus in the cytoplasm. In starvation conditions, unphosphorylated active FoxO ensures the transcription of lipases for lipid breakdown such as *magro*, *bmm* and *Hsl*. In fasting conditions, lipocatabolic mechanisms are active (reviewed in Heier and Kühnlein 2018, Musselman and Kuhnlein 2018, Chatterjee and Perrimon 2021, Heier, Klishch et al. 2021). In response to starvation, the neuroendocrine cells in the corpora cardiaca (CC) produce the glucagon-like adipokinetic hormone (Akh, glucagon like peptide). Akh overexpression reduces TAG levels, whereas Akh mutants are obese and show impeded lipid mobilization from the storages under starvation (Galikova, Diesner et al. 2015). In a more systemic manner, tachykinin (Tk), which is a hormone secreted from the EECs to the ECs, represses lipogenesis under starvation (Song, Veenstra et al. 2014).

The enterocytes are the *bona fide* absorptive and digestive cells of the midgut. Their metabolic functions are essential for the organism and the digestive tract physiology. At the cellular level, the ECs are in homeostasis with their environment and the rest of the cell types of the midgut. There is intercellular communication between ECs and ISCs (e.g. paracrine signals). For example, ECs are able to increase ISCs proliferation via changes in mitochondrial pyruvate metabolism that results in Unpaired3 (Upd3) signalling through Dome (JAK/STAT) in the ISCs (Wisidagama and Thummel 2019).

1.3.3 Links between lipid metabolism and intestinal stem cell proliferation

Intestinal stem cells of *Drosophila melanogaster* provide an excellent model to study stem cell homeostasis and regeneration (reviewed in Jiang and Edgar 2011, Jiang, Tian et al. 2016). ISC division promotes growth and regeneration after injury; and reduced ISC proliferation impairs the responses to damage (reviewed in Miguel-Aliaga, Jasper et al. 2018). To ensure proper homeostasis, ISCs orchestrate both external and internal cues (reviewed in Miguel-Aliaga, Jasper et al. 2018). The ISC population adapts to the changes brought by the mating process: the proliferative rate is boosted in females after mating, and within three days the midgut is dramatically remodelled with increased size and ECs number (Reiff, Jacobson et al. 2015). ISC proliferation and differentiation are also orchestrated by paracrine and local cues emitted by several midgut cell types. For example, the epidermal growth factor (EGF) pathway in ISCs, which leads to cellular division, is activated by the EGFR ligands Vein (Vn) (secreted by the visceral muscle), Keren (Krn) (secreted by EBs and ECs), and Spitz (Spi) (secreted by the EBs), in response to stressors such as pathogens or dietary toxins (Pasco, Loudhaief et al. 2015).

The distinct populations of ISCs show variations in their self-renewal rate: more quiescent at the copper-cell region R3 and more proliferative at the posterior R4 midgut (reviewed in Miguel-Aliaga, Jasper et al. 2018). The rate of ISC proliferation is in tight correlation to the incidence of intestinal tumours, more prone to occur in the posterior P1 region, followed by posterior P3 and anterior A2 (the authors used an alternative nomenclature to classify the different portions of the midgut: the anterior section is divided into three regions, A1-A3, and the posterior section into four regions, P1-P4) (Marianes and Spradling 2013). Interestingly, in these regions there is increased lipid uptake from the dietary digested nutrients observed in the ECs and ISCs (Marianes and Spradling 2013), which might indicate that lipids fuel division and tumorigenesis.

Lipolysis is key in sustaining adult ISC populations (Singh, Zeng et al. 2016). Under low lipid and sterol conditions (due to the diet or genetic defects), although ISCs continue to proliferate, the differentiation of daughter cells is affected. Through an increased Dl and Notch signalling, there is an increase of ECs relative to EECs in the posterior midgut (Obniski, Sieber et al. 2018). Furthermore, both feeding and starvation impact ISC proliferation. The onset of feeding induces ISC division (O'Brien, Soliman et al. 2011), and starvation triggers loss of ISCs/EBs

in the midgut (McLeod, Wang et al. 2010). Additionally, the young ECs (4n polyploid) experience amitosis, a process known to reduce the ploidy of a cell, to generate new ISCs under starvation (Lucchetta and Ohlstein 2017). Moreover, the EEC-secreted hormone tachykinin (Tk), which represses lipogenesis under starvation (Song, Veenstra et al. 2014), is also modulating ISC proliferation (Amcheslavsky, Song et al. 2014).

1.3.3.1 Myc role in the midgut

There are many intrinsic and extrinsic niche signals involved in regulating ISC differentiation, proliferation and self-renewal (reviewed in Jiang, Tian et al. 2016, Miguel-Aliaga, Jasper et al. 2018). One of the key players in progenitor cells is the oncogene Myc. Its role was first described in controlling cell growth in development (Johnston, Prober et al. 1999, Johnston and Gallant 2002, Wu and Johnston 2010), and its functions in cell competition and cancer are well defined (de la Cova, Abril et al. 2004, Johnston 2009, de Beco, Ziosi et al. 2012, Johnston 2014 and reviewed in de la Cova and Johnston 2006, Bellosta and Gallant 2010).

Following tissue damage, by either dextran sulfate sodium (DSS) or bleomycin feeding (Amcheslavsky, Jiang et al. 2009), Myc expression in the progenitors is upregulated to stimulate proliferation, and thus regenerate the tissue. The increase in transcription is triggered by multiple signalling pathways, involving the Hpo, JAK-STAT and/or EGFR pathways. Furthermore, a basal level of Myc is detected in homeostatic conditions (Ren, Shi et al. 2013). Regenerative midguts, as well as aging intestines, require Myc (and Wingless from the EBs) for ISC hyperproliferation (Cordero, Stefanatos et al. 2012).

Loss of *adenomatous polyposis coli 1* (*Apc1*) results in intestinal hyperplasia in the intestine. Upon loss of *Apc1*, Myc (and its binding partner Max) start and maintain ISC hyperproliferation. This mechanism comprises a non-autonomous crosstalk between the ECs and ISCs via Myc. In ISCs, Myc induces Spi ligand that binds to EGFR in ECs, generating interleukin-like ligand Upd3, which in turn stimulates ISCs proliferation via JAK-STAT signalling (Cordero, Stefanatos et al. 2012). Furthermore, cell competition mechanisms promote the growth of intestinal adenomas caused by the loss of *Apc1*: non-autonomous JNK activation and higher Yorkie activity in tumour cells induce apoptosis of surrounding wild-type cells (Suijkerbuijk, Kolahgar et al. 2016).

Overall, and in addition to proliferation, Myc (as a downstream of target of rapamycin (TOR)) in progenitor and ISCs regulates longevity, stress resistance and metabolism (Strilbytska, Semaniuk et al. 2017). Overexpression of the TOR-Myc axis (via the Ras homologue enriched

in brain (Rheb)) in ISCs and EBs (by *esg-Gal4* as a driver) decreases lifespan, starvation resistance and other metabolic traits (Strilbytska, Semaniuk et al. 2017). There was a reduction of food consumption and fecundity, and an increase in glucose, glycogen and TAGs. Interestingly, although several metabolic genes were affected, *bmm* expression did not change (Strilbytska, Semaniuk et al. 2017).

Research on intestinal Myc has been focusing on its functions in intestinal stem cells, thus the expression and role of Myc in the enterocytes has not been investigated.

1.4 Sex differences beyond sexual traits

Recent research on sex discrepancies in behaviour, development and physiology (metabolism) has increased interest in further understanding the sexual dimorphism in (a priori) less obvious sexually dimorphic organs.

At the whole-organism level, body size is highly distinctive: female flies are 30% larger than males (Fairbairn 1997).

At the organ level, the length and width of the midgut are smaller in males (Hudry, Khadayate et al. 2016). Transcriptome analyses reveal sex differences in many organs, including the midgut (Hudry, Khadayate et al. 2016, Hung, Hu et al. 2020 and unpublished RNA-seq by Tomotsune Ameku in the lab). The expression of carbohydrate and redox genes is upregulated in virgin males, whilst proliferative genes are highly expressed in virgin females (Hudry, Khadayate et al. 2016). In males, higher expression of carbohydrate metabolism genes results in increased food intake and promotes sperm maturation via the production of enterocyte-derived citrate (Hudry, de Goeij et al. 2019).

At the cellular level, in the female midgut there is elevated ISC proliferation (Reiff, Jacobson et al. 2015, Hudry, Khadayate et al. 2016, Regan, Khericha et al. 2016). Sexual differences in ISC turnover remain during aging, pathogenic bacteria and chemical insults. Females show increased tumorigenesis, exacerbated age-related dysplasia and intestinal barrier breakdown (Hudry, Khadayate et al. 2016, Regan, Khericha et al. 2016, Duneau, Kondolf et al. 2017). In addition to the biological sex influencing ISC proliferation, mating increases female ISC divisions and gut size to optimise high nutrient absorption for reproduction (Reiff, Jacobson et al. 2015). In mated females, these changes are induced by juvenile hormone (JH), which also induces changes in lipid metabolism of ECs (Reiff, Jacobson et al. 2015). Another key hormone which regulates sexual dimorphism in ISC proliferation is ecdysone (Ec) (Ahmed, Maldera et

al. 2020, Zipper, Jassmann et al. 2020). In brief, Ec is a steroid hormone mastering reproductive development and sex physiology, circulating as its active metabolite 20-hydroxyecdysone (20HE) (Riddiford, Cherbas et al. 2000). Since Ec levels are higher in females than males, Ahmed and colleagues observed an increase in ISC proliferation (and gut length) in males fed with 20HE, resembling a female gut (Ahmed, Maldera et al. 2020). Moreover, the increase of Ec in female flies promotes higher TAG and glycogen storage than in males (Sieber and Spradling 2015).

At the metabolic level, the fat signature is sexually dimorphic. In the midgut, the lipid profile changes between mated females and males: for example, males have higher saturated FAs and females more polyunsaturated cholesterol esters. Noteworthily, very few changes are observed after gonadal removal, suggesting that the gonads contribute minorly to the sex-specific lipid profile (Parisi, Li et al. 2011). Furthermore, a recent study showed that after one week on a high fat diet, there is a sex-biased effect in the transcriptomic profile of both head and body. In females, the high fat diet led to an increase of lipid metabolism transcriptional changes (Stobdan, Sahoo et al. 2019).

In many species, including mammals and insects like *Drosophila melanogaster*, females store more body fat that males (Jackson, Stanforth et al. 2002, Lease and Wolf 2011). In the fruit fly, females have higher TAG levels 5 days after eclosion; this is independent of the gonadal lipids and not caused by a lower female energetical demand (Wat, Chao et al. 2020). Interestingly, there is an anti-correlation between TAG levels and *brummer* lipase expression: low TAG levels in males are linked to high *bmm* expression that exacerbates lipolysis. Loss of *bmm* abolishes the sex differences in TAG storage and breakdown. The fat body, which expresses high levels of *bmm*, is not the only contributor to fat dimorphism, as the authors detect *bmm* and lipids in the testis and neurons. Surprisingly, the midgut, as well as the muscles and glia, despite their *bmm* expression, are not shown to establish TAG sexual dimorphism (Wat, Chao et al. 2020).

Aside from the aforementioned lipid variations, male and female flies have other sex-specific physiologic and metabolic processes such as sleep, food intake and food preferences. For example, female flies feed less under high sugar diets, their lifespan shortens more quickly and they cope better under starvation (Chandegra, Tang et al. 2017).

In addition to the contribution of hormones such as Ec and JH in determining sexual dimorphic features, the members of the sex determination pathway also establish sexual traits in a cell autonomous manner.

1.4.1 The role of the sex determinants in the physiologic sexual dimorphism

Although our knowledge is still rudimentary in understanding the role of the sex determination cascade in the metabolic and physiologic sexual dimorphism, recent studies have begun to explore and lay the foundations for this area of research.

At the whole-organism level, several studies have been deciphering the mechanisms behind the sexual dimorphic body size. Rideout and colleagues demonstrated that the control of size is Tra-dependent: loss of Tra in female flies reduces pupal size, while expression of Tra in males increases their size (Rideout, Narsaiya et al. 2015). Because the reduction of *tra* is insufficient to achieve male size, further, currently unknown, mechanisms must be involved in establishing body dimorphism. In a Tra-dependent manner, there is secretion of insulin-like peptides from the brain which regulates size (Rideout, Narsaiya et al. 2015). Females with inhibition of insulin/insulin-like growth factor signalling pathway (IIS) are smaller, whilst males with increased IIS are bigger (Millington, Brownrigg et al. 2021). Recently, in a protein-rich diet, Millington et al. elucidated the molecular regulation behind the IIS and Tra-dependent body size, which is Dsx- and FruM-independent. It involves Tra-dependent *spargel* (*srl*) regulation, which is a coactivator of *stunted* (*sun*) transcription, and results in IIS activity and increased body size in females (Millington, Brownrigg et al. 2021, Millington, Brownrigg et al. 2021). Furthermore, upon neuronal loss of Sxl, female flies are as small as male-sized flies (Sawala and Gould 2018). Moreover, Mathews and colleagues identified an additional factor that contributes to the regulation of growth sexual dimorphism: the X-chromosomal gene *Myc*. Females with reduced *Myc* dosage and lack of Tra are nearly comparable in size to XY males. The growth-promoting gene *Myc* participates in two developmental critical points that establish female size: first, in the embryo stage, Myc is a X-chromosomal element that helps activating Sxl (which starts the sex determination cascade); second, in the larval stage, Myc promotes growth. Since *Myc* escapes dosage compensation, it has a twofold increase in females *vs* males (Mathews, Cavegn et al. 2017).

At the cellular level, ISC proliferation is increased and cell-division genes are more highly expressed in females. Female ISCs have Tra-dependent cell cycle duration. This intrinsic mechanism is independent of Dsx and FruM. Interestingly, it involves a new non-canonical Tra-dependent branch with *Imaginal disc growth factor* (*Idgf1*), *Serpin 88Eb* (*Spn88Eb*) and *reduced ocelli* (*rdo*) (Hudry, Khadayate et al. 2016).

Transformer regulates the sexual dimorphism in whole-body size by both cell autonomous and non-autonomous mechanisms. In a non-cell autonomous manner, and independent of Dsx and FruM, Tra stimulates Ilp secretion from the brain which increases fat body size. Additionally, Tra increases the cell size of mitotic (wing cells) and endoreplicative cells (fat body cells). Importantly, the cell autonomous effects of Tra in the fat body might be mediated by Dsx: downregulation of *dsx* in a group of cells reduced male and female fat cell size (Rideout, Narsaiya et al. 2015). Along these lines, Mikoluk et al. revealed the role of Tra2 in regulating lipid content in the adult fat body. Downregulation of *tra2* increases TAGs in the female fat body. This upregulation is not linked to an increase of food intake since the ingestion levels remain the same. Tra2 regulates the splicing of *carnitine o-palmitoyltransferase* (*CPT1*), involved in FA degradation, which could partially explain the increase in TAGs. Additionally, it is proposed that Tra2 might be regulating the splicing of other lipid genes such as *FAS*, *ACC* or *bmm* (Mikoluk, Nagengast et al. 2018).

In the *Drosophila* head, there is a sexual dimorphism observed in the transcriptional profile of fat cells around the brain. On the one hand, females express *CG17820* (unknown function), named by the authors as *female-specific independent of transformer* (*fit*). On the other hand, males express an *odorant-/pheromone-binding protein* (*opbp*; *CG7592*) named *turn-on sex-specificity* (*tse*), a *cytochrome P450 enzyme* (*CYPs*; *cyp4d21*) called *sex-specific enzyme 1* (*sxe1*), and a *phospholipase* (*CG4979*) named as *sex-specific enzyme 2* (*sxe2*). Remarkably, the three male-specific genes are dependent on *dsx* (Fujii and Amrein 2002). Consequently, this study hints towards the idea that *dsx* is involved in lipid metabolism in a sexually dimorphic manner.

Recently, Wat et al. described how, via the adipokinetic hormone (Akh) in neurons, Tra regulates sex variability in fat storage. In males, high Akh limits TAG accumulation (Wat, Chowdhury et al. 2021). Fat accumulation is crucial for reproductive purposes: extra TAGs in males reduces fertility (Wat, Chao et al. 2020), and fecundity is reduced in slimmer females (Sieber and Spradling 2015). Noteworthily, overexpression of Tra in the male ECs

(*mex1>traF*) reduces starvation resistance (but was not reproduced using another ECs specific driver called *myo*) (Wat, Chowdhury et al. 2021).

In summary, there has been an increasing realisation of sexual dimorphism beyond the initially studied reproductive traits, which affect physiology and metabolism. The molecular members of the sex determination pathway, including Dsx, are often establishing the differences between a diverse range of cell-types in the male and female.

1.5 Aims of this thesis

Elucidating the sex-specific molecular mechanisms behind metabolism and physiology will help us to better comprehend the sexual dimorphism in disease susceptibility.

In this thesis, I use *Drosophila melanogaster* to investigate the role of the last effector of the sex determination pathway, the transcription factor Doublesex. I have studied its functions in the intestine: an adult somatic organ that responds to external and internal changes, and plays key metabolic roles.

The aims of the thesis are:

i. To investigate the role of Dsx in the enterocytes of the adult midgut of female and male flies (at first using a transcriptional approach).
ii. To explore the consequences of the molecular and cellular *dsx*-dependent changes in enterocytes and at the whole-organism level, with a focus on its contributions to sex differences in physiology.
iii. To increase the knowledge of the sex-specific metabolic profile between male and female flies.

To address these objectives, I follow the summarised approach:

i. In the first chapter of Results, after confirming the sex- and cell-specific expression of Dsx, I describe the transcriptomic changes in male and female virgin midguts upon *dsx*-downregulation in adult ECs.
ii. In the second chapter, I investigate the role of Dsx in lipid metabolism at the physiological level by quantifying the amount of intestinal and peripheral fat upon *dsx* knock-down (and overexpression) in ECs. Furthermore, to unravel the Dsx-dependent molecular mechanisms involved in fat homeostasis, I begin to explore the contributions of the sexually dimorphic lipase CG17192.

iii. In the third chapter, I assess the functions of the oncogene Myc in the adult ECs, which is also sexually dimorphic in the midgut. First, I characterise Myc expression in the ECs and start to unravel the epistasis between Dsx and Myc at the mRNA and protein levels. Second, I examine effects on stem cell proliferation following *Myc* downregulation in ECs. Third, I study its involvement in lipid metabolism in the gut and the whole fly.

In the last decade, research has shed light on the contributions of the sex determination cascade to the establishment and maintenance of sex differences in the physiology and metabolism of the fly intestine. I have used this framework to explore the roles of Dsx in enterocytes and their consequences at the whole-body level in both males and females. I also discovered a previously unrecognised sex difference in Myc expression in enterocytes and begun to investigate its relevance in the context of lipid metabolism.

Finally, I consider the wider relevance of these findings in mammalian systems, in light of the similarities between fly and human intestines, as well as the expression of Myc and the Dsx-homologue Dmrt.

CHAPTER 2

Materials & Methods

2.1 Fly husbandry

2.1.1 General maintenance

Experimental and control flies were kept in vials with filter paper in incubators (Percival DR-36VL) with 65% humidity, on a 12h light/dark cycle at the required temperature (either 18°C, 25°C or 29°C). Vials were changed approximately every 3 days.

Genetic crosses were set up at the appropriate temperature (either at 18°C for the temperature-sensitive experiments or at 25°C for the rest) to obtain experimental and control adult flies. Groups of 5 females and 5 males were mated in vials and flipped every 1-2 days to control for progeny density. Yeast sprinkles with water were added in the vials to avoid desiccation and maximise larval survival. Virgin flies with the appropriate genotype were collected and kept in separate vials (maximum of 20 flies per vial) prior to utilization.

Gal4Gal80^{ts} virgin flies were raised and aged at 18°C for 4-6d to allow for gut remodelling (O'Brien, Soliman et al. 2011), prior to being shifted to 29°C to induce transgene expression. For *dsx*, *Myc* and *CG17192* manipulations (*mex1^{ts}>dsxRNAi*, *mex1^{ts}>dsxF, mex1^{ts}>dsxM, mex1^{ts}>MycRNAi*, *mex1^{ts}>Myc* and *mex1^{ts}>CG17192RNAi*) and the appropriated controls (*mex1^{ts}>GFP*, *mex1^{ts}>Ilp4RNAi*, *mex1^{ts}>Ilp7RNAi*, *mex1^{ts}>GD*, *mex1^{ts}>+* and *+>Myc*), flies were experimentally used after 4-5d at 29°C (permissive temperature) unless otherwise stated. For *tra* knock-down, flies were kept at 29°C for 10d. The experimental flies with clones generated using the FLP-out Gal4 system were reared at 25°C, activated by heat-shock at 37°C (either for 15min for *dsxRNAi* clones or for 7-8min for *traRNAi* clones), and later transferred at 29°C for RNAi induction (4-5d for both *dsxRNAi* and *traRNAi* clones).

Non-temperature sensitive, as well as wild-type flies, were raised from crosses of 5 females and 5 males at 25°C. They were aged as virgin adults for ~4d at 25°C prior to utilization.

2.1.2 Dietary regimes

Flies were reared and aged on standard high yeast cornmeal diet, also referred as control diet (CD), unless otherwise specified. It contains 6.65% cornmeal, 7.15% dextrose, 5% yeast, 0.66% agar supplemented with 2.2% nipagin and 3.4mL/L propionic acid, to avoid fungal and bacterial contamination (prepared in a Systec MP30 mediaclave).

In the high sugar diet (HSD) experiment, *mex1*^{ts}>*dsxRNAi* and *mex1*^{ts}>*GFP* flies were aged an additional 4d at 29°C with a dietary change from CD to HSD. This 1M sucrose diet was kindly provided by the lab of Susumu Hirabayashi and for 500mL it contains: agar (5g), brewer's yeast (40g), yeast extract (10g), peptone (10g), sucrose (175g), 1M $MgSO_4x6H_2O$ stock solution (0.2%), 1M $CaCL_2x2H_2O$ stock solution (0.34%), propionic acid (0.6%) and mold inhibitor (10% p-hydroxy-benzoic acid methyl ester in 95% ethanol) (1%).

For the pH3 quantifications under dextran sulfate sodium (DSS) conditions, flies were aged an additional 3d at 29°C in an empty vial with a 3.75 cm × 2.5cm filter paper soaked with 500mL of either experimental DSS solution (3 dextran sulfate sodium diluted in 4% sucrose) or control 4% sucrose. Flies were placed in new vials with fresh feeding paper every day for 3d prior to dissection.

For the blue food assay, 1% FCF blue dye (also known as E133 or brilliant blue FCF, Sigma 807171) was added to the CD standard cornmeal/agar food. The food used for the FlyPAD experiment varied in recipe and cooking methodology (pot-cooked), and it was helpfully provided by the lab of Helena Coheme. The ingredients for 500mL are: agar (7.5g), yeast (50g), sugar (25g), nipagin (15mL), propionic acid (1.5mL) and distilled water (350mL). The food was stored at room temperature (RT) and prior to usage, it was liquefied in the microwave and solidified in a petri-dish. Pipet-tip round circles of food were placed inside each FlyPAD arena.

2.1.3 Fly stocks

Wild-type flies are Oregon R.

(BL = Bloomington, VDRC = Vienna *Drosophila* Resource Centre)

DRIVER LINES			
Name	**Origin**	**Stock number**	**Notes**
mex1-Gal4	(Phillips and Thomas 2006)		Genotype: w[*];P{w[+mC]=mex1-GAL4.2.1}10.8/CyO;P{w[+mC]=tubP-GAL80[ts]}ncd[GAL80ts-7]/TM6B
tub-Gal80^{ts}	(McGuire, Le et al. 2003)		
tub-Gal4	(Diao, Ironfield et al. 2015)		Genotype: w[*];P{Tub-GAL4DBD.D}2/CyO,P{w[+mC]=ActGFP}JMR1

REPORTER LINES			
Name	**Origin**	**Stock number**	**Notes**
Dsx::eGFP	Generated by Bruno Hudry in the lab	Derived from BL#36182	eGFP sequence is inserted in the second intron of *dsx* (3rd chromosome).
Myc::eGFP	Generated by the lab of Jean-Paul Vincent (Poernbacher, Crossman et al. 2019)		eGFP sequence is inserted before the stop codon in the intrinsic *Myc* locus (X chromosome).
CG17192-GFP	Generated by Bruno Hudry in the lab		The GFP-tagged clone (#CBGtg9060H041D) is from the library TransgeneOme Resource (Source Bioscience (Sarov, Barz et al. 2016)). The transgenic line was done through ΦC-31 integrase mediated transformation (Bestgene). The attP site used was attP40 (BDSC: 36304).
FUNCTIONAL MANIPULATIONS			
Name	**Origin**	**Stock number**	**Notes**
UAS-*dsxF*	(Lee, Hall et al. 2002)	BL#44223	Genotype: y[1] w[*]; P{w[+mC]=UAS-dsx.F}24-3
UAS-*dsxM*	(Lee, Hall et al. 2002) Kindly provided by Elizabeth J. Rideout	BL#44224	Genotype: y[1] w[*]; P{w[+mC]=UAS-dsx.M}2/CyO
UAS-*GFP*.VALIUM10		BL#35786	Suggested control for VALIUM10 and 20. Genotype: y[1] v[1]; P{y[+t7.7] v[+t1.8]=UAS-GFP.VALIUM10}attP2
UAS-*Ilp4RNAi*	(Perkins, Holderbaum et al. 2015)	BL#43288	Genotype: y[1] sc[*] v[1] sev[21]; P{y[+t7.7]v[+t1.8]=TRiP.HMS02660}attP40

UAS-*Ilp7RNAi*	(Perkins, Holderbaum et al. 2015)	BL#32862	Genotype: y[1] sc[*] v[1] sev[21]; P{y[+t7.7]v[+t1.8]=TRiP.HMS00649}attP2
UAS-*Myc*	(Johnston, Prober et al. 1999)	BL#9674	Genotype: w[1118]; P{w[+mC]=UAS-Myc.Z}132
UAS-*GD*		VDRC#60000	VDRC control. Isogenic host strain for the RNAi library.
UAS-*traRNAi*	Combined with Dicer 2 by Bruno Hudry (Dietzl, Chen et al. 2007, Perkins, Holderbaum et al. 2015)	BL#28512	Contains Dicer 2 in the X chromosome. Genotype: w[*], P{w[+mC]=UAS-Dcr-2.D}1;; P{y[+t7.7] v[+t1.8]=TRiP.JF03132}attP2 tra/TM6B, P{w[+mC]=Dfd-EYFP}, Sb[1],Tb[1], ca[1]
UAS-*CG17192RNAi*	(Perkins, Holderbaum et al. 2015)	BL#56042	Genotype: y[1] sc[*] v[1] sev[21]; P{y[+t7.7]v[+t1.8]=TRiP.HMC04350}attP40
yw,hs-flp; Act>y>Gal4UAS-CD8RFP			Clonal FLP-out Gal4 system.
yw,hs-flp; Act>y>Gal4UAS-lacZ			Clonal FLP-out Gal4 system.
***dsxRNAi* LINES**			
Name	**Origin**	**Stock number**	**Notes**
P{UAS-dsx.IR}4, P{UAS-dsx.IR}10	Created by Bruce Baker (Robinett, Vaughan et al. 2010)	BL#66709	Two constructs of dsRNA targeting exon 2 (721nt).
TRiP.JF02256 VALIUM 10 (soma)	(Perkins, Holderbaum et al. 2015)	BL#26716	Long hairpin (493nt). Targets 5'UTR/CDS of the 6 isoforms.
TRiP.HMC03795 VALIUM 20 (soma and germline)	(Perkins, Holderbaum et al. 2015)	BL#55646	Short hairpin (21nt). Targets CDS of the 6 isoforms.

			Genotype: y[1] sc[*] v[1] sev[21]; P{y[+t7.7]v[+t1.8]=TRiP.HMC03795}attP40
TRiP.GL01294 VALIUM 22 (germline)	(Perkins, Holderbaum et al. 2015)	BL#41864	Short hairpin (21nt). Targets 5'UTR of the 6 isoforms.
P{KK111266}	(Dietzl, Chen et al. 2007)	VDRC#110306	Long hairpin (356nt). Targets CDS of the 6 isoforms.
P{GD1424}	(Dietzl, Chen et al. 2007)	VDRC#11096	Long hairpin (258nt). Targets CDS of the 6 isoforms.
***MycRNAi* LINES**			
Name	**Origin**	**Stock number**	**Notes**
TRiP.HMS01538 VALIUM 20	(Perkins, Holderbaum et al. 2015)	BL#36123	dsRNA for RNAi of *Myc*. 3rd chromosome.
TRiP HMC03189 VALIUM 20	(Perkins, Holderbaum et al. 2015)	BL#51454	dsRNA for RNAi of *Myc*. 2nd chromosome.
TRiP GL01314 VALIUM 22	(Perkins, Holderbaum et al. 2015)	BL#43962	dsRNA for RNAi of *Myc*. 2nd chromosome.
P{GD1419}	(Dietzl, Chen et al. 2007)	VDRC#2947	Long hairpin (295nt). 2nd chromosome.

Table 2.1: Table of fly stocks

Fly lines used in this study classified as driver and reporter lines, functional manipulations (including the clonal FLP-out Gal4 system) and both *dsxRNAi* and *MycRNAi* stocks. Columns indicate the genetic name of the fly line, the origin, the commercial number and source, as well as additional notes.

2.2 Tissue dissections

Adult flies and larvae were immobilised on ice and sacrificed by submerging them into 100% ethanol. Dissections were performed at RT, under the stereoscope (Leica M80 stereomicroscope) and using forceps on a flat silicone elastomer (Sylgard 182).

For immunostaining (antibody and dye) purposes, flies were dissected in 1X Phosphate-Buffered Saline (PBS, by diluting 10x PBS in Milli-Q water); tissues were subsequently transferred on to poly-lysine glass slides.

For RNA extraction experiments (RNA-seq and qPCR), dissections were done in RNAse-free conditions with the equipment and surfaces wiped with RNAzap. Flies were dissected in RNA-Later, and midguts were transferred to Eppendorfs containing either RNA-Later and RLT buffer (from QIAGEN RNeasy Mini Kit, 74134) (for qPCR) or Trizol (for RNA-seq).

2.3 Antibody and dye staining

Poly-lysine glass slides were coated with 0.88g/L polylysine hydrobromide and 2.5µL/mL PhotoFlo in Milli-Q water. Once dipped in the coating solution (15min), they were dried at 55°C (15min); a process which was repeated 3 times. After 1h air-dried, edges were determined by a silicon ring for liquid retention. Slides were stored at 4°C.

Dissected tissues were transferred to the poly-lysine coated slides for antibody or dye staining.

2.3.1 Antibody staining

Tissues attached to the poly-lysine glass slide were fixed for 30min at RT using 4% paraformaldehyde (PFA) or 4% formaldehyde (FA). After, samples were washed with 1X PBS (3 times) and PBS with 0.2% Triton X-100 (PBST) (3 times). They were incubated with the primary antibody overnight (or up to 48h) at 4°C inside a humid chamber. Primary antibodies were diluted in 4% horse serum PBST (PBTN; stored at 4°C for maximum of 14d) at the right concentration (Table 2.2). Later, samples with bound primary antibodies were washed with PBST (3 times every 15min during 1h) at RT to remove the unbound antibodies. Tissues were incubated with the fluorescent secondary antibodies for 1.5-2h at RT (Table 2.2). After PBST washes (3 times every 15min for 1h at RT), they were finally washed once with PBS before being mounted. The silicon ring was removed and samples were mounted in 2-3 drops of Vectashield with DAPI (Vecta Labs #H-1200). A coverslip was placed on top with plasticine on the corners to avoid squashing of the samples. Prior to storage in dark conditions at 4°C, coverslips were sealed with nail varnish.

PRIMARY ANTIBODIES		
Species	**Dilution**	**Source**
Chicken anti-β galactosidase	1:500	Abcam
Chicken anti-GFP	1:1000	Abcam
Goat anti-GFP	1:1000	Abcam

Guinea Pig anti-Myc	1:100 (pre-absorption)	Kindly provided by Prof. Gines Morata
Mouse anti-Prospero	1:20	Developmental Studies Hybridoma Bank
Rabbit anti-pH3	1:1000	Cell Signaling
Rat anti-Dsx	1:2000	Kindly provided by Dr. Rohit Joshi
SECONDARY ANTIBODIES		
Species	**Dilution**	**Source**
Chicken Cy5	1:300	Jackson Immunoresearch
Chicken FITC	1:200	Jackson Immunoresearch
Goat FITC	1:200	Jackson Immunoresearch
Goat-HRP TRITC	1:300	Jackson Immunoresearch
Guinea pig FITC	1:200	Jackson Immunoresearch
Mouse Cy3	1:200	Jackson Immunoresearch
Rabbit Cy3	1:200	Jackson Immunoresearch
Rat Cy3	1:200	Jackson Immunoresearch

Table 2.2: List of primary and secondary antibodies

Primary and secondary antibodies used in this study. Species (left column), dilution (middle column) and source (right column) are stated.

2.3.2 Dye staining

Tissues were dissected and transferred to the poly-lysine glass slides. Fixation for 30min with 4% PFA was followed by 3 washes with PBS. LipidTox (ThermoFisher Scientific -H34477-HCS Deep Red Neutral Lipid Stain) stains the neutral lipid droplets. It was firstly diluted 1:100 in PBS before added to the slides. After 30min of incubation, and subsequent PBS washes (3 times), samples were mounted in Vectashield DAPI and sealed with nail polish. Slides were stored in the dark at 4°C but rapidly imaged to avoid dye decay.

2.4 Image acquisition, processing and quantification

2.4.1 Brightfield microscopy

Images of the genitalia and abdomen were obtained using Leica MZ16F stereomicroscope fitted with a Leica DFC420 C camera.

2.4.2 Confocal microscopy

Confocal images from dye- and antibody-stained samples were taken with a Leica SP5 II confocal microscope and Leica Application Suite Advanced Fluorescence (LAS AF) software (Leica Microsystems).

Samples that required comparison or quantification were placed on the same slide and the imaging settings (lens magnification, zoom magnification, laser power, pinhole size, gain and scanning settings) were maintained consistent across samples. The confocal Z-stack measurement was of 1.5µm. For quantification purposes (to increase the sample size), samples from different independent replicates were imaged. Although for each independent replicate, control and experimental samples were imaged from the same slide with the same settings, independent replicates (different slides) did not share the same imaging settings. Thus, data were normalised appropriately.

Images were analysed using ImageJ (Schneider, Rasband et al. 2012) and Fiji software (Schindelin, Arganda-Carreras et al. 2012); and Adobe Photoshop and Illustrator software were utilised for visualization purposes.

2.4.3 Quantifications

2.4.3.1 LipidTox quantifications

Regional quantifications

First, midguts of control and experimental flies were stained with LipidTox and mounted in Vectashield DAPI in the same slide. Second, using the same settings at the confocal microscope, the anterior (R2) and posterior (R4) midgut regions were imaged at 40X. The regionality of the midgut was assessed anatomically and morphologically. In each region, the 40X panel with higher LDs was selected, and only half of the circular midgut was imaged (focussing on the LDs in the epithelium) using ultraviolet (DAPI) and far-red (LipidTox) channels. Third, using Fiji and ImageJ for the image analysis, only one Z-stack of 1.5µm was carefully chosen from the epithelium (higher number of LDs). After the maximum Z-stack projection, a median filter (process-median filter) of one was applied before quantification. I quantified the LDs using the following commands: image-adjust-threshold (maximum entropy), process-binary-make binary, process-binary-convert to mask, and analyse-analyse particles (0-1 circularity). I chose to quantify particles with areas from 2µm^2 to infinity, in order

to avoid food residuals and background noise, and used the "count" value as a proxy for the number of LDs.

Throughout the thesis, the number of LD particles are plotted in relative percentages. Per each independent replicate, the experimental and control absolute LDs numbers were made relative by normalising the values against the mean of the LD number of the controls. Thus, the independent replicates could be plotted and statistically treated altogether.

Clonal quantifications

The number of LDs ($2.5\mu m^2$) inside and outside the control and experimental clones was measured in one Z-stack (1.5µm) of the epithelium of the R4 region. Unicellular and multicellular clones were measured undistinguishably. To quantify the LDs inside the clone, a silhouette around the RFP^+ clonal cells was drawn prior to the measurement. To calculate the LDs outside the clone, the same silhouette was enlarged 20µm, and the previously measured LDs inside the clone were eliminated, thus only the external particles were quantified.

LDs quantification using Fiji and ImageJ was performed as aforementioned. Each clone did not correlate with one independent midgut. Results are plotted as the percentage of LD number (either inside or outside the clone) divided by the area (either the area of the clone or outside the clone).

2.4.3.2 Proliferative phospho-Histone H3 cells (pH3)

Mitotic indices were quantified by manually counting phospho-Histone H3-positive cells using a Nikon Eclipse 50i clinical microscope. $pH3^+$ cells were quantified along the whole midgut and were counted as two once cell division was achieved. Absolute numbers are plotted.

2.4.3.3 GFP signal quantification in Imaris

Experimental homozygous Myc::eGFP virgin female midguts were collected from two independent experiments and thus placed in two independent slides. All four dietary variations (i.e. DSS, HY, sucrose, H_2O) had representative midguts in each slide. Imaging settings were kept consistent across the different midguts and independent experiments. Dapi, GFP (FITC) and HRP (TRITC) signals were imaged in the R4 region. Only one circular half of the midgut was imaged in 40X. The image processing was done with Imaris 9.5 (Oxford Instruments). With the 3D plotted midgut, a randomised group of small HRP^+ cells *vs* big HRP^-cells were manually selected. Later, the GFP intensity of each cell was extracted to finally calculate the mean (a minimum of 10 cells per midgut) for the two groups (HRP *vs* EC). Finally, the

measurements were repeated for all the imaged midguts (7 to 13) and plotted altogether without normalisation.

2.5 Metabolic assays

2.5.1 Thin Layer Chromatography (TLC)

Lipid extraction is required prior to TLC. First, groups of 4 females and 5 males (either cold-anesthetised or kept at -80°C to increase the replicate size) were weighted using the precision balance (Mettler-Toledo XS105) and total body weight was annotated per each group. Second, these predetermined groups of flies were dissected, by either removing the gonads or the midgut (according to the experiment), and each group placed in an independent Eppendorf. Third, 60µL of H_2O, followed by 150µL of methanol and 75µL of chloroform were added together with a steel bead to mechanically grind the tissues by using the QIAGEN TissueLyser II for 1min at 30Hz. Fourth, Eppendorfs were left for 1h at 37°C in a heat block. Fifth, 75µL of KCL flowed by 75µL of chloroform were added, and tubes were centrifuged for 2min at 3000rpm. Sixth, 100µL of the lower phase were collected and transferred to new 0.5mL Eppendorfs. After air dry for ~3h, the extracted lipids were resuspended in 16µL of 1:1 chloroform:methanol, and dissolved in heat block for 10min at 37°C. Samples were either stored at -20°C or subsequently loaded for TLC.

The TLC plate (TLC Silica gel 60W, Merk 116487) was firstly cut in a 10cm square, and a horizontal line was drawn 1cm from the bottom, with dots in every 1cm for sample loading. The glass chamber was first covered up to ~0.5cm with the mobile phase, which contains 70% hexane, 30% diethyl ether and 1% acetic acid. Few pieces of filter paper were soaked to maintain a moist atmosphere inside the chamber. Subsequently, the samples and the standard (lipid standard, mono-, di-, and triglyceride mix, 1787-1AMP Sigma, dissolved in 1:1 chloroform:methanol) were loaded in the TLC plate by adding 3µL in the previously marked dots. The TLC plate was carefully added inside the lid-closed glass chamber, and when the mobile phase reached ~1cm from the top by capillarity, the TLC plate was removed and air-dried. After, the TLC plate was dipped in CAM stain (cerium-ammonium-molybdate in 10% sulphuric acid) and placed at 80°C in the oven during 25min for the CAM stain to develop. The TLC plate, which had replicates of control and experimental samples, was scanned and quantified by using Fiji and ImageJ. The intensity of the TAG band was quantified and normalised against one control sample from the plate.

2.5.2 Feeding assays

2.5.2.1 Blue food intake

Groups of ~20 virgin flies were fed on blue food for 1h30min at 29°C (permissive temperature for the Gal4Gal80^{ts} genotypes).

Flies were separated in 2mL Eppendorf tubes in groups of three and frozen (possibly kept at -80°C for replicate collection). After addition of a metal bead with 500µL H_2O, flies were homogenised by QIAGEN TissueLyser II for 2min at 30Hz. Eppendorfs were centrifuged (for 10min at 11000rpm, and 200µL of supernatant was transferred in to separate wells of a 96 well plate (Nunclon Delta Surface MicroWell 96-Well Microplates, 167008 Thermo Scientific). Using the BMG Labtech FLUOstar Omega plate reader, the intensity of the blue dye was measured by reading 630nm absorbance. For each sex, all replicates were in the same plate, thus, the absorbance readings were plotted altogether without normalization.

2.5.2.2 FlyPAD

The FlyPAD is a system of monitoring food behaviour with multiple single fly arenas connected to a central field programmable gate array, which is connected to a laptop via USB. FlyPAD uses capacitance-based measurements to quantify physical interactions between flies and food. We follow an adaptation of the published protocol (Itskov, Moreira et al. 2014).

At first and for each arena, a small circumference of food was placed gently at the centre of the electrode. After, a single fly was mouth-pipetted per arena, and control (*mex1^{ts}>GFP*) and experimental (*mex1^{ts}>dsxRNAi*) groups of flies were separated accordingly. Data was collected for 1h30min feeding in four independent experiments done at the same time of the day. Capacitance data was acquired using the software Bonsai and the 'flyPAD library'package. Data was analysed by a Matlab (Mathworks) package which assesses several parameters, including the number of sips. Per each of the replicates, the number of sips was normalised to the mean of the control and the data of the four replicates was plotted together.

2.6 Molecular biology

2.6.1 Quantitative Real-Time Polymerase Chain Reaction (qPCR)

2.6.1.1 RNA extraction and cDNA synthesis

Dissected midguts were transferred into RNALater (10µL) and RLT buffer (90µL) solution and mechanically disaggregated using a pestle. Total RNA was extracted as instructed in QIAGEN RNeasy Mini Kit (74134). The RNA quantity was measured using a NanoDrop spectrophotometer (ThermoFisher Scientific) and varied depending on the experiment (approximately 150 to 600ng of RNA). Before cDNA synthesis, the RNA of the extracted samples was normalised to the lowest amount.

cDNA synthesis was achieved using the kit and protocol from QuantiTect Reverse Transcription Kit (Qiagen 205311). Samples were stored at -20°C or subsequently used for qPCR. cDNA samples were diluted 1:5 in most of the experiments.

2.6.1.2 qPCR and primers

Quantitative PCR were performed by mixing cDNA samples with iTag Universal SYBR Green Supermix (Bio-Rad, #172-5124) and the relevant primers in a 96-well plate. For each gene, at least three independent replicates were used, and two technical replicates were pipetted. Expression values were normalised either to *rp49* or *Vha100-4*.

The details of qPCR program in the 7900HT real-time PCR system (Applied Biosystems) were the following:

Step	Temperature	Time
Initial denaturation	94°C	2min
Denaturation (40 cycles)	94°C	15s
Annealing, extension and read fluorescence (40 cycles)	60°C	1min

Table 2.3: Details of qPCR program

Step name, temperature and time for the qPCR program used in the study.

	Forward	Reverse
bmm	GTCTCCTCTGCGATTTGCCAT	CTGAAGGGACCCAGGGAGTA
CG17192	GCAGCACTATTAGTAGCGGGT	AAATGTGCCATCCTCCTGGG
CG2772	GATATACCCTTCAAACGGCTCAA	GTCTCAACAAAATGCGATTCGG

dsx	GCCGATCTCAGTTTCCGTCA	GCTCCCAAGGATAGCGGAAT
dsxM	TATCCTTGGGAGCTGATGCC	CCACTCGAGCCTCTTCGATT
dsxF	GCGAATCGAAGAGGGCCAA	ACATTGCCGCGTTGTGTTGCG
dsxF	TATCCTTGGGAGCTGATGCC	ACGTATTGGCCCTCTTCGAT
fu12	GGAGCTGGTCTGATAGTCTTTCT	TGGAAAAAGCGCATTTCGATAGT
Lsd-1	CAGCGCATACCACTGGTCTAT	GCATTACCGATTTGCTTGACAG
Myc	TCGCAGACGACAGATAACACC	GACAGACCGTGTAGTCCAGAT
Rp49	TGTCCTTCCAGCTTCAAGATGACCATC	CTTGGGCTTGCGCCATTTGTG
Vha100-4	AAATACCAACGCCGAAACAGG	TCTCCTTGCCAGTTGTCACC

Table 2.4: List of primers

List of primers used in this study for the qPCRs. Names of the genes (first column), 5'-3' forward nucleotide sequence (middle column) and 5'-3' reverse nucleotide sequence (right column). Primers are listed alphabetically.

2.6.2 RNA-sequencing

2.6.2.1 RNA extraction and library preparation

For each sex, experimental (*mex1^{ts}>dsxRNAi*) and control (*mex1^{ts}>GFP*) midguts were collected from three independent replicates. The number of midguts varied from 16 to 28. The RNA from pooled dissected midguts was extracted using Trizol (Invitrogen).

RNA quality was assessed using the Agilent 2100 Bioanalyser RNA 6000 Nano assay. Preparation of RNA-seq libraries, library QC, and subsequent NGS sequencing was carried out by Laurence Game and Ivan Andrew of the LMS Genomics Facility. Libraries were prepared using the NEBNext Ultra II Directional RNA Library Prep Kit with NEBNext Poly(A) mRNA Magnetic Isolation Module. Library quality was evaluated on a Bioanalyser HS DNA chip and the concentrations were measured using the Qubit™ dsDNA HS Assay Kit. Libraries were pooled in equimolar quantities and sequenced on a Hiseq2500 to generate a minimum of 30 million Paired End 100bp reads per sample.

2.6.2.2 RNA-sequencing bioinformatic analyses

All RNA-seq analyses were carried out by Yi-Fang Wang in the LMS Bioinformatics facility. After demultiplexing, raw RNAseq reads were aligned against Ensembl *Drosophila* genome reference sequence assembly (dm6) using Tophat2 (Kim, Pertea et al. 2013) with argument "--library-type fr-firststrand". Reference sequence assembly and transcript annotation were obtained from Illumina iGenomes (https://support.illumina.com/sequencing/sequencing_software/igenome.html). Gene-based

read counts were obtained using featureCounts function from Rsubread Bioconductor package (Liao, Smyth et al. 2014). Normalisation and differential expression analysis were performed using DEseq2 (Love, Huber et al. 2014). Gene Ontology analysis was performed using the GOseq R package (Young, Wakefield et al. 2010).

2.7 Statistics

Statistical analysis and graphs were generated using GraphPad Prism 9 software. Error bars correspond to the Standard Error of the Mean (SEM). The specific statistical tests are annotated in each figure panel and follow the conventional form:

P-value	Summary
<0.0001	****
0.0001 to 0.001	***
0.001 to 0.01	**
0.01 to 0.05	*
≥0.05	n.s. (not significant)

CHAPTER 3

Results (I)

DOUBLESEX IN THE ADULT MIDGUT

3.1 Introduction

Doublesex is a transcription factor which generates sexual dimorphism in several tissues. Its functions have been well documented in the reproductive and nervous system, specifically in organs such as the brain, the ventral nerve cord, the genitalia, the sex combs and the abdomen (see Introduction). In addition to examining the functions in the sexually dimorphic tissues, efforts have been made to decipher the spatial and temporal regulation of *dsx* expression (see Introduction).

The role of Doublesex in the midgut has not yet been elucidated. Prior work in the field has demonstrated *dsx* expression in the adult midgut (Robinett, Vaughan et al. 2010), and the protein has been detected exclusively in the male adult enterocytes (Hudry, Khadayate et al. 2016). Previous data from our lab demonstrated that the midgut of adult flies is sexually dimorphic (Hudry, Khadayate et al. 2016). However, potential contributions of Doublesex to establishing sexual dimorphisms in the midgut remain uninvestigated.

Since the male and female fly midguts have different signatures at the gene and transcript levels (Hudry, Khadayate et al. 2016), and Dsx is observed in a male-female dimorphic pattern, I wanted to explore whether Dsx contributes to some of these transcriptional differences. Does Dsx in male ECs contribute to a male-biased transcriptional profile? Given the absence of Dsx in female midguts, would the lack of Dsx in male ECs make them more female-like? Furthermore, the function of Dsx in ECs is still unknown, and the direct and indirect target genes of Dsx remain uncharacterised.

In this chapter, I describe the expression of *dsx* transcript and Dsx protein in the midgut more comprehensively. I also begin to examine the functions of Dsx in the midgut by undertaking a transcriptional approach: I execute an RNA-sequencing from flies with *dsx* knock-down in the adult ECs.

3.2 Results

3.2.1 Doublesex is sex- and cell-specific in the adult midgut

As previously reported by Hudry et al., I corroborated the sexual dimorphism of *doublesex* (*dsx*) expression in the adult midgut, both at the transcript and at the protein level (Fig. 3.1) (Hudry, Khadayate et al. 2016).

In wild-type adult midguts, *dsx* transcript levels are sexually dimorphic: higher in males than in females (Fig. 3.1A). Despite males showing greater overall *dsx*, there is a non-statistically significant increase of male-specific spliced *dsx* (*dsxM*) in males (Fig. 3.1A'') and female-specific spliced *dsx* (*dsxF*) in females (Fig. 3.1A').

At the protein level, Dsx is also sexually dimorphic. Dsx is detected in the adult male midgut but absent in females (Fig. 3.1C-1D'''). To better visualise Dsx, I made use of an endogenous protein knock-in-reporter fly previously generated in the lab by Bruno Hudry (see Materials & Methods). As illustrated in the schematic (Fig. 3.1B), eGFP (enhanced Green Fluorescent Protein) is inserted in the long second intron. Since the second intron is shared between the two sex-spliced *dsx* forms, the reporter can be used to visualise both DsxM and DsxF (Dsx::eGFP). The reporter fly line is kept viable in homozygosis, suggesting that the presence of an eGFP tag in the protein is not altering its function. An unfertile homozygous stock would have indicated that the GFP insertion is affecting the structure/function of Dsx in determining sexual traits (see Introduction).

As well as sexually dimorphic, Dsx expression is cell-type specific. The protein is exclusive to the enterocytes (ECs). In virgin males, Dsx::eGFP does not colocalise with Prospero (Pros) and Horse Radish Peroxidase (HRP) marker, which label enteroendocrine and progenitor cells, respectively (Fig. 3.1C-C'''). To verify that the eGFP signal is real and specific to Dsx, I co-stained with anti-Dsx (Fig. 3.1E-F'''). The polyclonal antibody, kindly provided by Dr. Rohit Joshi (Ghosh, Bakshi et al. 2019), colocalised with eGFP both in the ventral nerve cord (VNC) and polyploid male ECs.

In adult virgin males, Dsx::eGFP was visualised homogeneously in ECs along the midgut, from R1 to R5 (Fig. 3.2A-A'). Although not carefully quantified, Dsx expression was occasionally absent from R3. In addition to the male midgut epithelium (Fig. 3.2C-C'), Dsx was expressed in the visceral muscle (Fig. 3.2C-C') and the gut-associated fat body (Fig. 3.2D-D'). In females, Dsx was detected in fat body, and sporadically in the visceral muscles. Intermittently, Dsx was further observed in the crop, the ampulla, the Malpighian tubules and the spermatheca (data not shown, Fig 1.4).

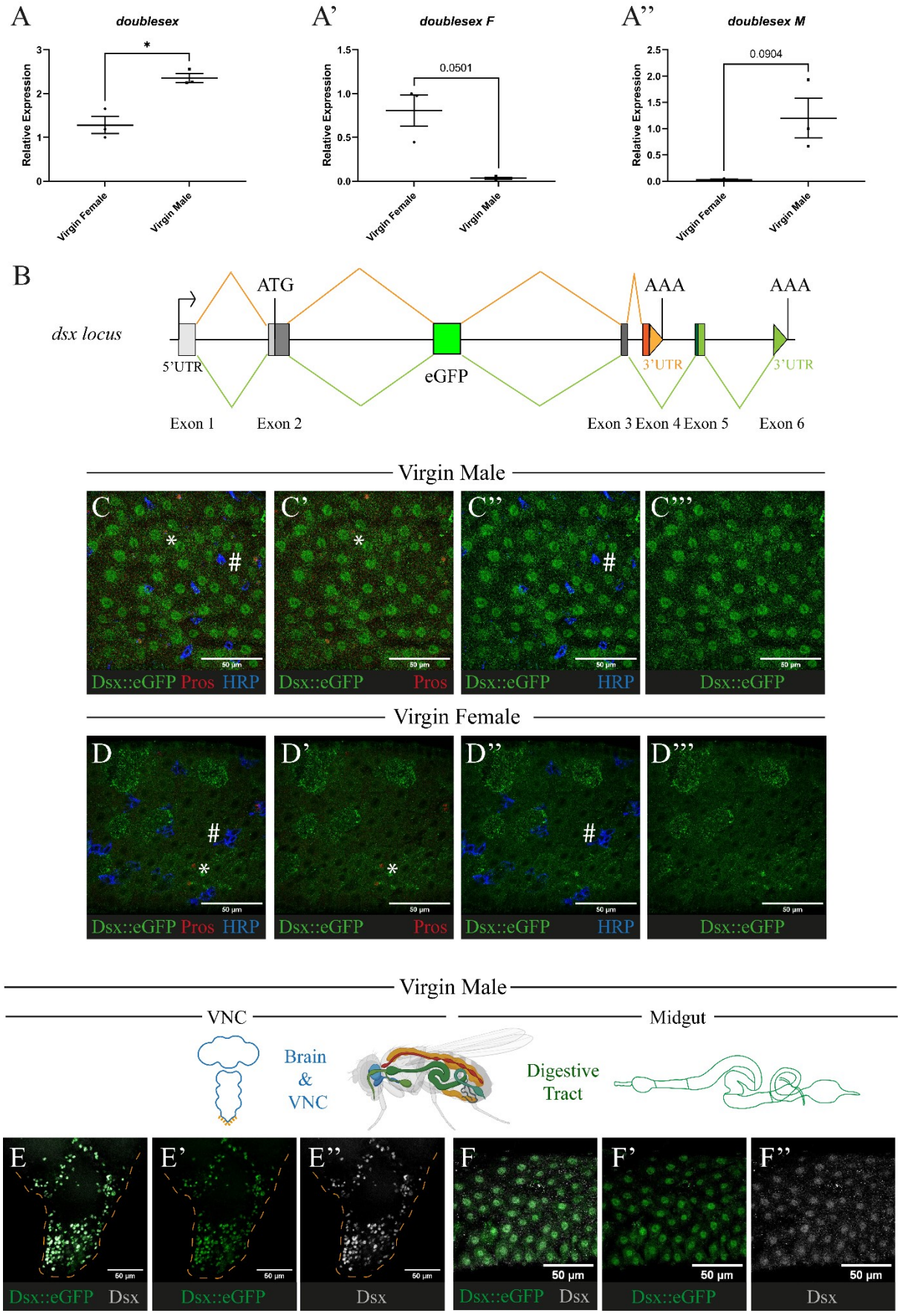

Figure 3.1: Dsx sexual dimorphism in the midgut of adult virgin males and females

Levels of *doublesex* mRNA, detected by qPCR, are sexually dimorphic in the adult midgut. (A) Virgin males show higher levels of *dsx* than virgin females. Female-specific spliced *dsx* (*dsxF*) (A') and male-specific spliced *dsx* (*dsxM*) (A'') show a non-statistically significant increase in females and males, respectively. Each data point represents 30-40 adult midguts from wild-type Oregon R flies. Samples are normalised to the housekeeping *Vha100-4*. Relative expression values are calculated against one sample control as reference. Results are shown as mean ±SEM. P-value < 0.05 with Welch's t-test. (B) Schematics of endogenous eGFP knock-in-reporter fly line (Dsx::eGFP). eGFP is inserted in the common second intron of *dsx*, spliced in both sexually dimorphic transcripts, and translated in both isoforms. (C) Dsx::eGFP adult virgin male midgut co-stained with Prospero (Pros, labelling EECs) and Horse Radish Peroxidase (HRP, labelling ISCs and EBs). (C') Dsx::eGFP is absent from enteroendocrine $Pros^{+}$ cells and progenitor HRP^{+} cells (C''). (C''') Dsx::eGFP is visualised in polyploid ECs. (D-D''') Dsx::eGFP is not detected in adult virgin female midgut. GFP is represented in green, Pros in red, HRP in blue. Example of an EEC pointed by a white asterisk, and a progenitor cell, by a white hash. (E-E'') Dsx::eGFP colocalises with polyclonal anti-Dsx in the VNC. Cartoon of the whole fly and internal organs. On the left, the brain and VNC drawn in blue, with a dashed orange line showing the tip of VNC which has been imaged in panels E-E''. On the right, the digestive tract is coloured green. (F-F'') Dsx::eGFP colocalises with anti-Dsx in the polyploid ECs in male midgut. GFP in green and anti-Dsx in grey. Scale bars (50µm) stated in each panel.

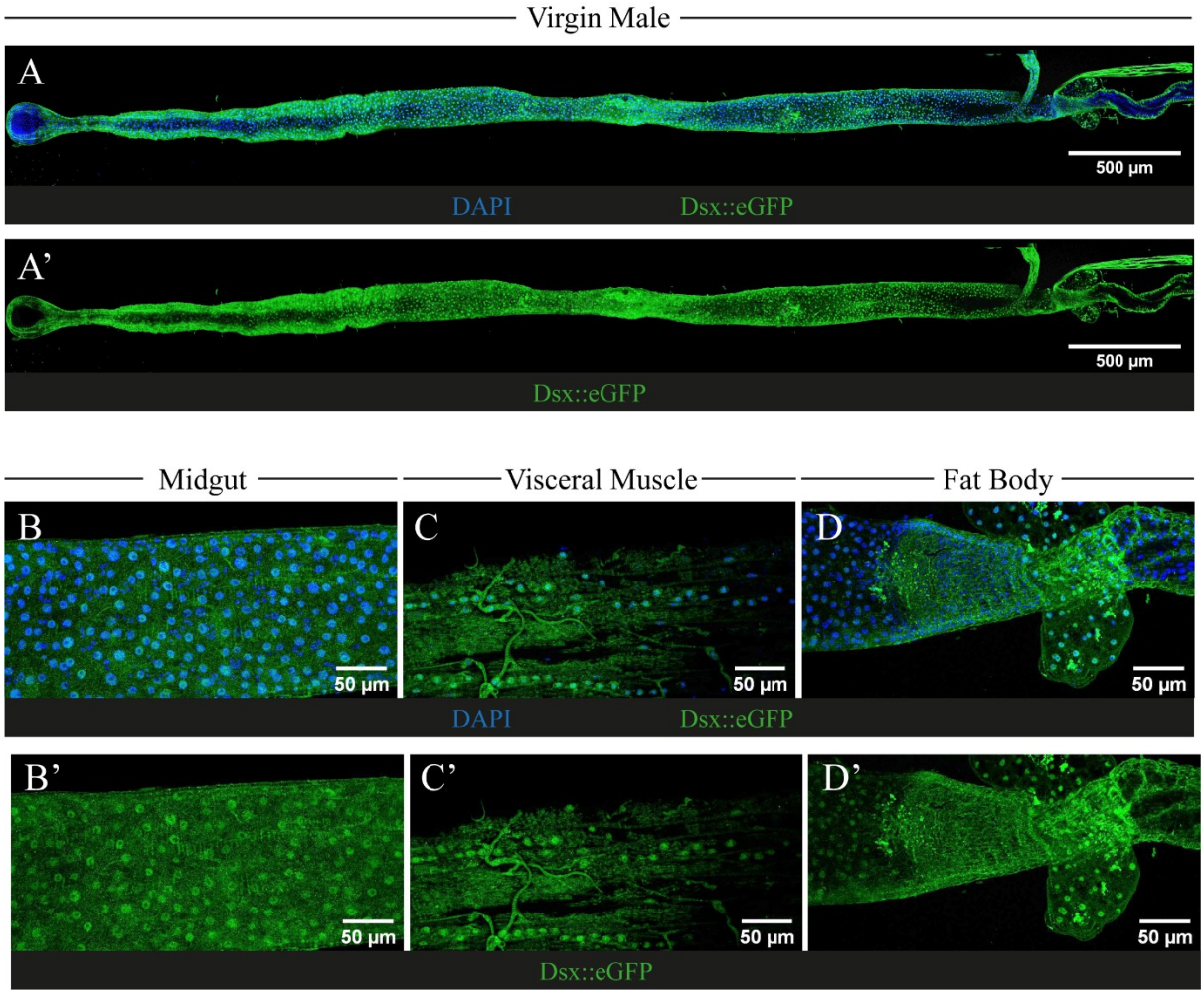

Figure 3.2: Dsx in the digestive system of a virgin male

(A-A') Dsx expression visualised along the adult male midgut using the Dsx::eGFP reporter line. Expression is observed homogeneously in the ECs of R1-R5 regions. (B-B') Close-up of the stained epithelium of males with Dsx::eGFP in ECs. Dsx in the visceral muscle of the gut (C-C') and gut-associated fat body (D-D'). DAPI represented in blue, GFP in green. Scale bars stated in each panel.

3.2.2 The role of Dsx in the adult enterocytes: transcriptional effects of *dsx* downregulation

Although the role of Dsx in other tissues has been previously described (see Introduction), its functions in the midgut had not yet been explored. To begin to investigate them, I downregulated *doublesex* specifically in the adult ECs and observed the transcriptional changes using bulk RNA-sequencing of whole midguts.

3.2.2.1 Downregulation of *dsx* in whole-body and adult enterocytes

One of the many benefits of using *Drosophila melanogaster* as a model organism is the extensive genetic toolkit that is available. In this study, I took advantage of the Gal4Gal80^{ts} system (see Introduction) to regulate gene expression in a temporal and spatial manner. Using *mex1^{ts}>dsxRNAi* flies, we were able to examine the effects of *dsx* mRNA reduced levels (due to the presence of RNAi) specifically in the enterocytes (using *mex1* as a driver) of adult flies (using the Gal4Gal80^{ts} temperature-sensitive system).

First, with the intention of finding the strongest *dsx* downregulation, I tested several *dsxRNAi* lines (see Materials & Methods). Each one targets the second exon of *doublesex* (or firstly transcribed exon), which is shared between the sex-specific transcripts (Fig. 3.3A). In order to quickly screen the best RNAi, I made use of *dsx* determining the sex combs, abdominal pigmentation and genitalia in a sexual dimorphic manner (see Introduction). The hypothesis was that knock-down of *dsx* would generate an intersex phenotype of the sexual traits, which are normally established by *dsx* during pre-pupal stages. Male flies in which *dsx* had been constitutively downregulated in all the cells (using the ubiquitous tubulin-Gal4 driver, *tub>dsxRNAi*) showed morphological changes in the sex combs. The strongest RNAi line, TRiP.HMC03795 (Bloomington line #55676), lowered both the number and thickness of the sex combs, resembling the lack of sex combs in females. The same RNAi line expressed ubiquitously in females (*tub>dsxRNAi*) generated darker pigmentation in a higher number of the lower abdominal segments, similar to a male-like pigmentation. The genitalia of those females were different from those of a wild-type female (Fig. 3.3B). From all the tested lines, only three gave morphological changes. The line TRiP.HMC03795 (Bloomington line #55676) showed the strongest phenotype when compared to the two others TRiP.GL01294 (BL#41864) and TRiP.JF02256 (BL#26716) (data not shown).

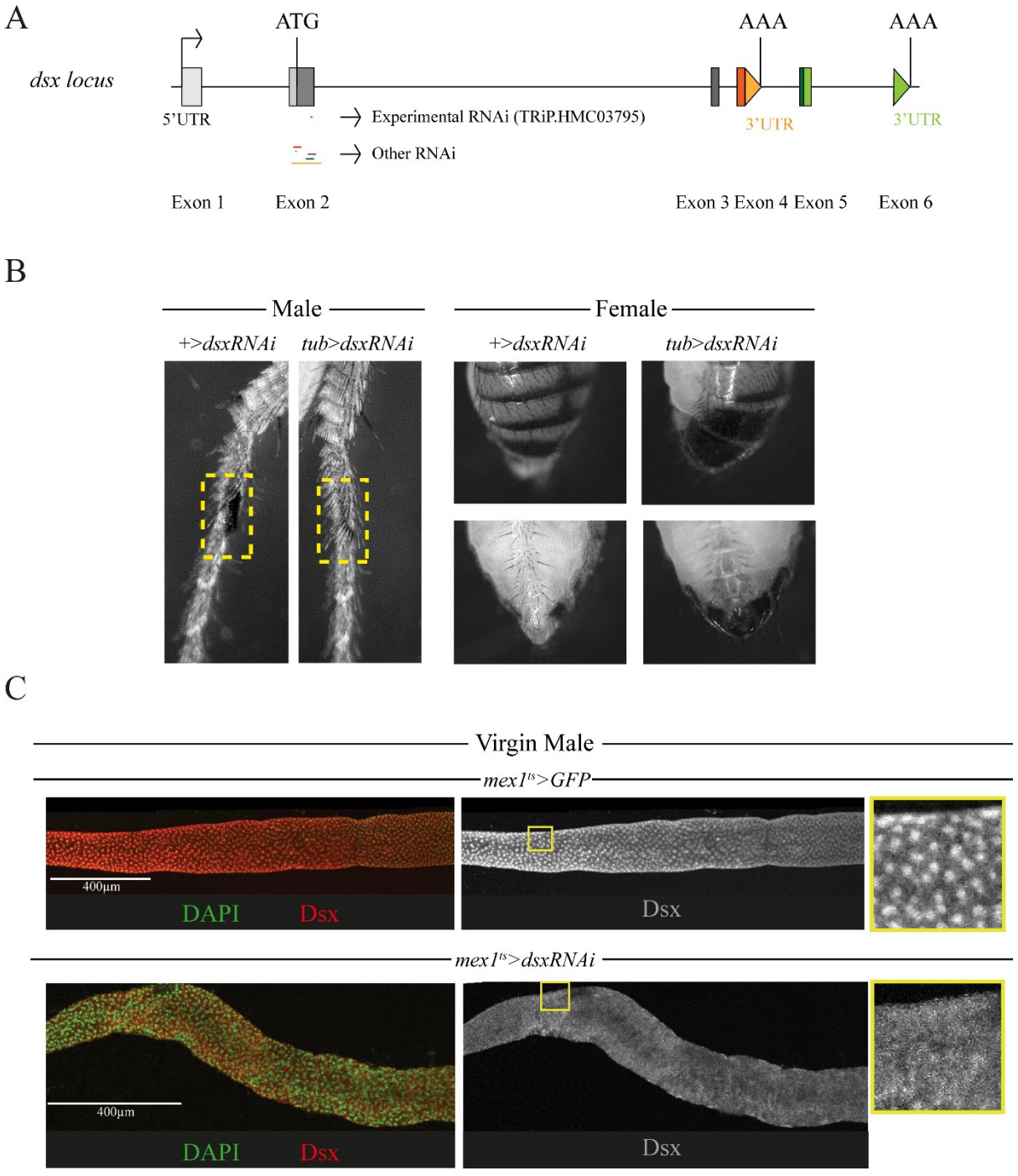

Figure 3.3: Validation of ubiquitous and enterocyte-specific *dsx* downregulation

(A) Schematics of *dsx* locus and several RNAi lines tested which target the first translated exon, common in both *dsxM* and *dsxF*. The chosen RNAi line is the Bloomington line #55646 from the TRiP collection (see Materials & Methods). (B) Sexually dimorphic phenotypic changes upon whole-body *dsx* downregulation using BL#55464. In experimental males, in which *dsx* is downregulated in all cells of the fly's body expressing tubulin (*tub>dsxRNAi*), the sex combs (dashed yellow line) are modified from the control, resembling a "female-like" sex comb. In *tub>dsxRNAi* females, the abdominal pigmentation is changed, phenocopying a "male-like" darker pigmentation. Additionally, the wild-type female vaginal plate (ovipositor) is lost, and there seems to be a gain of the wild-type male genital arch (epandrium). (C) *dsx* is downregulated in a temporal and spatial manner. *mex1^{ts}>dsxRNAi* male midgut show absence of anti-Dsx in the ECs. In the *mex1^{ts}>GFP* control males, anti-Dsx is detected along the midgut. Close-ups of the epithelium are shown inside the yellow boxes. DAPI in green, anti-Dsx in red (double-staining) or grey (single-staining). Scale bars stated in each panel.

Second, I sought to examine the efficiency of the chosen RNAi lines in downregulating *dsx* in the ECs. I crossed *mex1^{ts}* with the three RNAi candidate lines for 10 days at 29°C and performed immunostaining of the midgut. Once again, the strongest RNAi line (TRiP.HMC03795 (Bloomington line #55676)) was the only line which gave loss of Dsx in ECs (data not shown). In the interest of reducing the number of days at 29°C, instead of 10 days, I tested whether the lack of Dsx was still observed after 5 days. Dsx was absent from the ECs along the midgut in virgin males after 5 days at 29°C (detected in fat body and Malpighian tubules). Control virgin males, overexpressing GFP in the ECs instead of *dsxRNAi*, showed homogeneous Dsx expression in the midgut (Fig. 3.3C).

In conclusion, because of the alterations in the morphology of the sexual traits (i.e. sex comb, abdominal pigmentation and genitalia), and more importantly, the lack of Dsx protein in the male midgut, I settled on the TRiP.HMC03795 (Bloomington line #55676) line as a genetic tool to downregulate *dsx* in adult and cell type-specific manner for subsequent functional studies.

3.2.2.2 Transcriptional changes in adult enterocytes after *dsx* knock-down

Having verified the efficacy of the RNAi line by the lack of Dsx in adult virgin male enterocytes, I began to investigate the functions of Dsx in ECs by undertaking genome-wide transcriptional profiling analysis following *dsx* downregulation.

As summarised in Fig. 3.4A, I first collected the experimental (*mex1^{ts}>dsxRNAi*) and control (*mex1^{ts}>GFP*) flies, both virgin males and virgin females. For each of the three biological replicates, I dissected the midguts of 16-28 flies. There was a total of 12 samples, from which I checked the quality and quality of the extracted RNA by using Bioanalyser (see Materials & Methods). Second, the LMS Genomics Facility (Ivan Andrew and Laurence Game), performed the RNA sequencing (see Materials & Methods). Third, the LMS Bioinformatics Facility (Yi-Fang Wang) analysed the raw data and provided all the help, guidance and analysis needed (see Materials & Methods).

A

Experimental design

1) Fly collection

2) Midgut dissection and RNA extraction
(16-28 midguts and Trizol extraction)

3) Bioanalyser
(RNA quantity and quality)

4) RNA-seq*
(30 million reads, Hiseq 2500, Paired End 100bp)

5) Bioinformatic analysis*
(TopHat 2 Alignment)

**Performed by LMS Genomics and Bioinformatics facilities*

Samples

Control = *mex1^{ts}>GFP*

Experimental = *mex1^{ts}>dsxRNAi*

Virgin male and Virgin female
Adult flies (3-7d at 18°C + 5d at 29°C)

Biological replicates = 3

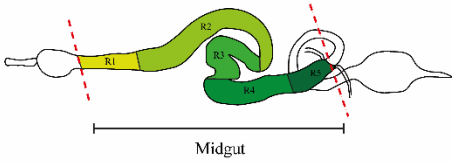

B

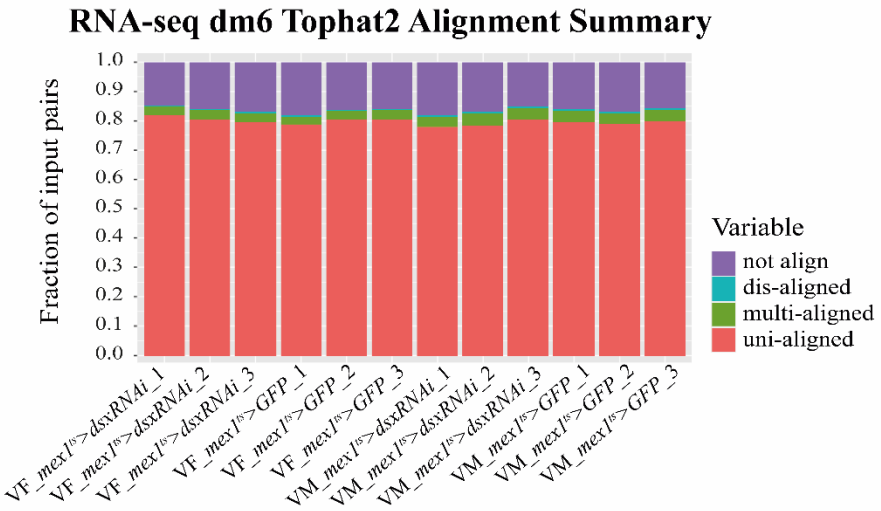

B'

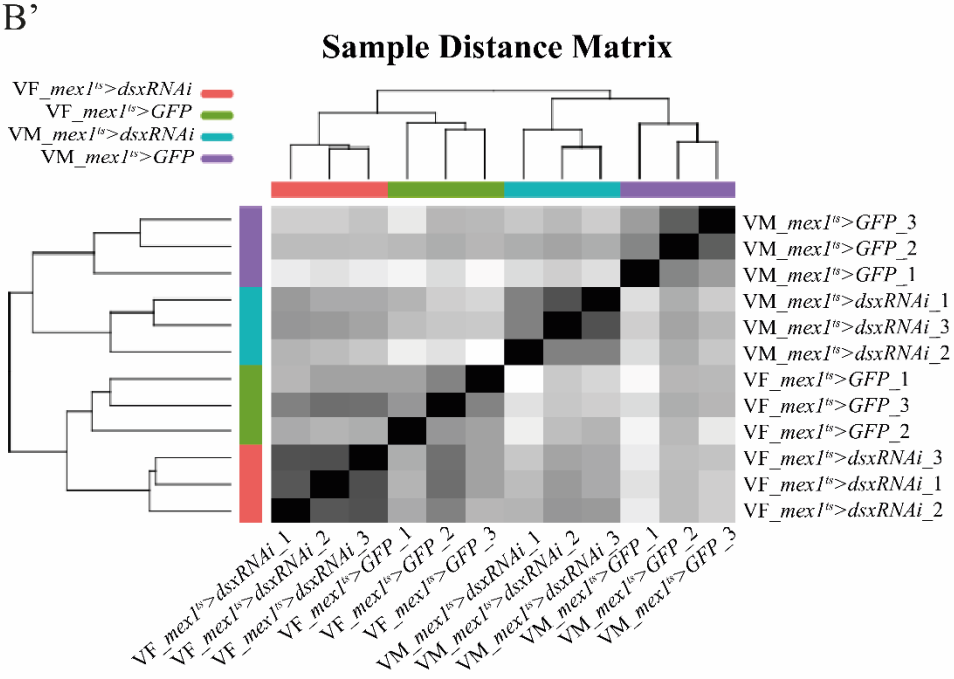

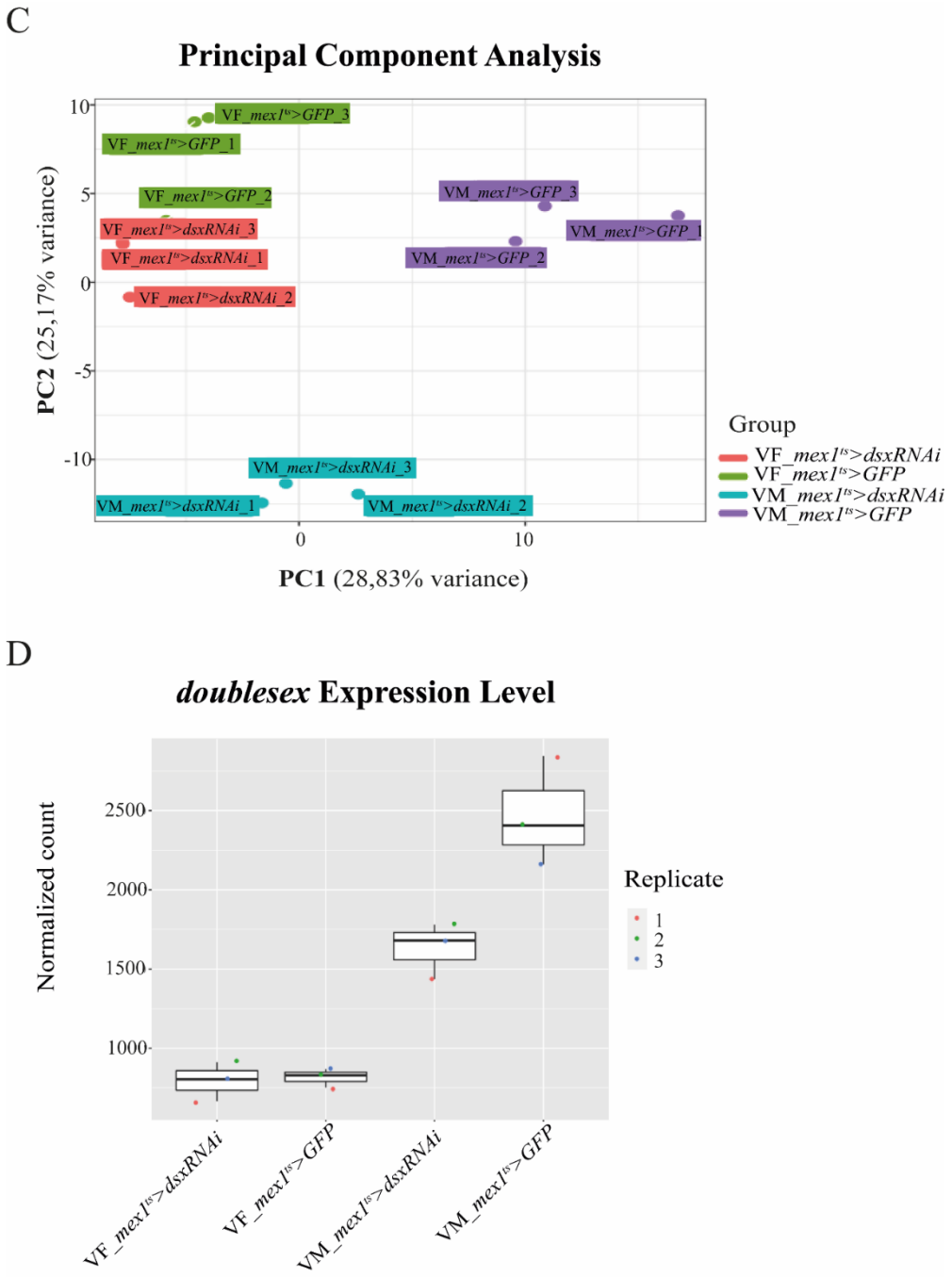

Figure 3.4: Experimental design and validation of the RNA-sequencing

(A) Summary of the experimental approach taken in this study. First, sample flies are collected. Both control (*mex1^{ts}>GFP*) and experimental (*mex1^{ts}>dsxRNAi*) virgin male and female flies are reared at 18°C. After 3-7 days at 18°C for gut remodelling, flies are transferred to 29°C for 5 days in order to activate the RNAi machinery. Three biological replicates per each condition and both sexes were used. Second, for each of the 12 samples (16-28 midguts per sample), the midguts are dissected and RNA extracted. Third, quality and quantity of RNA is evaluated by the Bioanalyser. Fourth, the LMS Genomics Facility performed the RNA-sequencing. Fifth, the LMS Bioinformatics Facility analysed the data. Cartoon of the adult gut; the regions (R1-R5) of the midgut collected for the study are depicted in green. (B) Summary of the Tophat2 alignment against *Drosophila melanogaster* 6 (*dm6*) genome as reference. For all the 12 samples, more than 80% of the input pairs is uni-aligned (in red). (B') Sample distance matrix shows high correlation (black and dark grey) of the samples which belong to the same category, (i.e. biological replicates together). Each colour represents a sample group: control female in green, control male in purple, experimental female in red, experimental male in blue. Samples cluster in grey gradient according to their transcript similarities (the strongest in black). (C) Principal component analysis (PCA) plot of

transcriptional changes in virgin male and female (n=6 per each sex) after *dsx* downregulation in adult ECs (n=3 per each condition). PCA1 and PCA2 show 28.83% and 25.17% of variance, respectively. (D) Levels of *doublesex* expression for each replicate (n=3 in different colours) in virgin females (two on the left) and virgin males (two on the right); experimental (*mex1^{ts}>dsxRNAi*) and control (*mex1^{ts}>GFP*) samples plotted next to each other. VF = virgin female, VM = virgin male.

Prior to examining the transcriptional changes, Yi-Fang evaluated the quality of the data. From the Tophat2 alignment, we observed per each sample that more than 80% of the fraction of the input pairs was uni-aligned; the approximated 20% were either not aligned, dis- or multi-aligned (Fig. 3.4B). This outcome suggested very promising and trustworthy raw data. Once she plotted the sample distance matrix, we could verify that the biological replicates were clustered together, indicating little variation in the replicates (Fig. 3.4B'). The Principal Component Analysis (PCA) plot showed the overall changes/similarities among the samples related to their transcriptional signature. The three samples of all four groups clustered together away from each other, which again, proved that the biological replicates were akin to one another. Experimental and control male were plotted the farthest away from each other, showing major changes in the transcriptional profile upon *dsx* downregulation. On the contrary, experimental and control females clustered collectively (Fig. 3.4C), suggesting little changes in the transcriptome upon *dsx* knock-down, as expected from the fact that, in females, there is no detectable Dsx protein. As further validation, we assessed the levels of *dsx* transcript across the samples. In females, no changes in *dsx* transcript levels were detected (Fig. 3.4D), consistent with the PCA plot (Fig. 3.4C), in which only slight changes between the experimental and control group were observed. On the contrary, *dsx* mRNA was reduced in males upon *dsx* knock-down (Fig. 3.4D), consistent with the pronounced changes plotted in the PCA graph (Fig. 3.4C).

In addition to documenting the changes at the overall gene expression level, Yi-Fang examined sex differences in abundance of different isoforms. Prior to focusing on the differences, the quality of the data was checked by plotting the sample distance matrix and PCA for transcripts only (Fig. 3.5A-B). The same trends as at the gene level were observed for the isoform level: samples were more similar to their biological replicates (Fig. 3.5A) and clustered according to their genotype in the PCA plot (Fig. 3.5B). At the isoform level, the lack of changes in experimental female flies was more pronounced, since the samples showed more similarities to the control in the PCA plot. In males, there was an obvious divergence between control and experimental group (Fig. 3.5B).

A

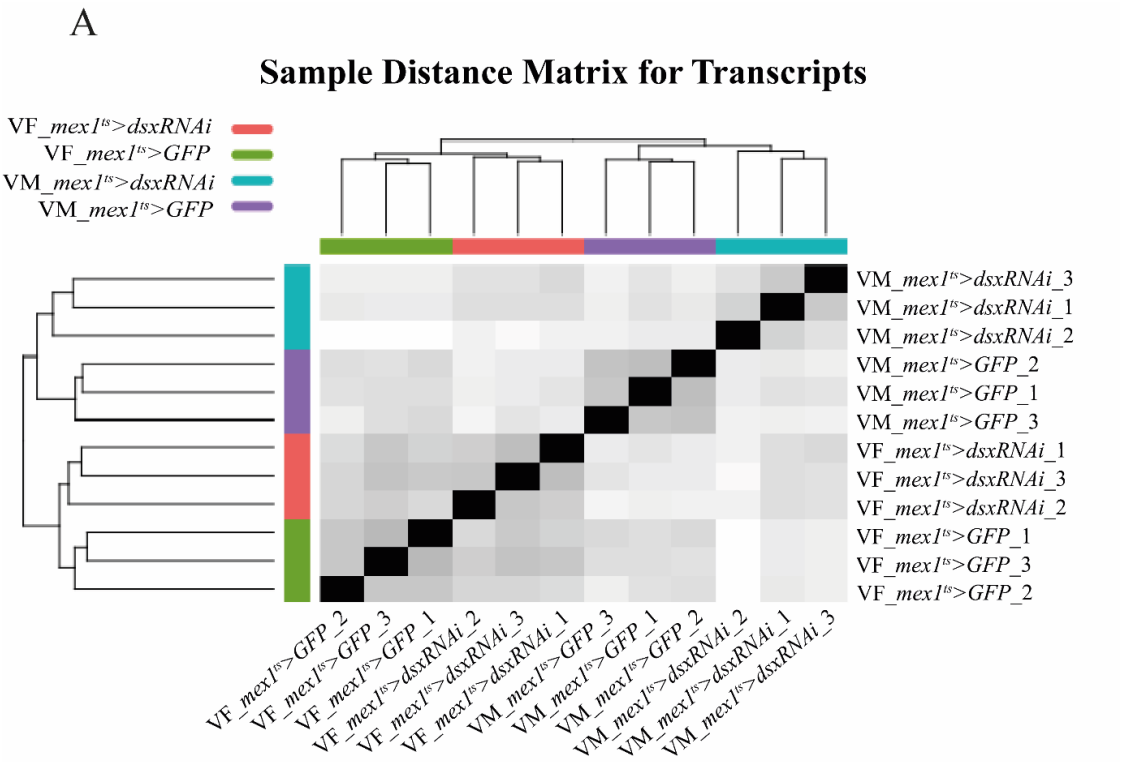
Sample Distance Matrix for Transcripts
VF_mex1ts>dsxRNAi
VF_mex1ts>GFP
VM_mex1ts>dsxRNAi
VM_mex1ts>GFP
VM_mex1ts>dsxRNAi_3
VM_mex1ts>dsxRNAi_1
VM_mex1ts>dsxRNAi_2
VM_mex1ts>GFP_2
VM_mex1ts>GFP_1
VM_mex1ts>GFP_3
VF_mex1ts>dsxRNAi_1
VF_mex1ts>dsxRNAi_3
VF_mex1ts>dsxRNAi_2
VF_mex1ts>GFP_1
VF_mex1ts>GFP_3
VF_mex1ts>GFP_2

B

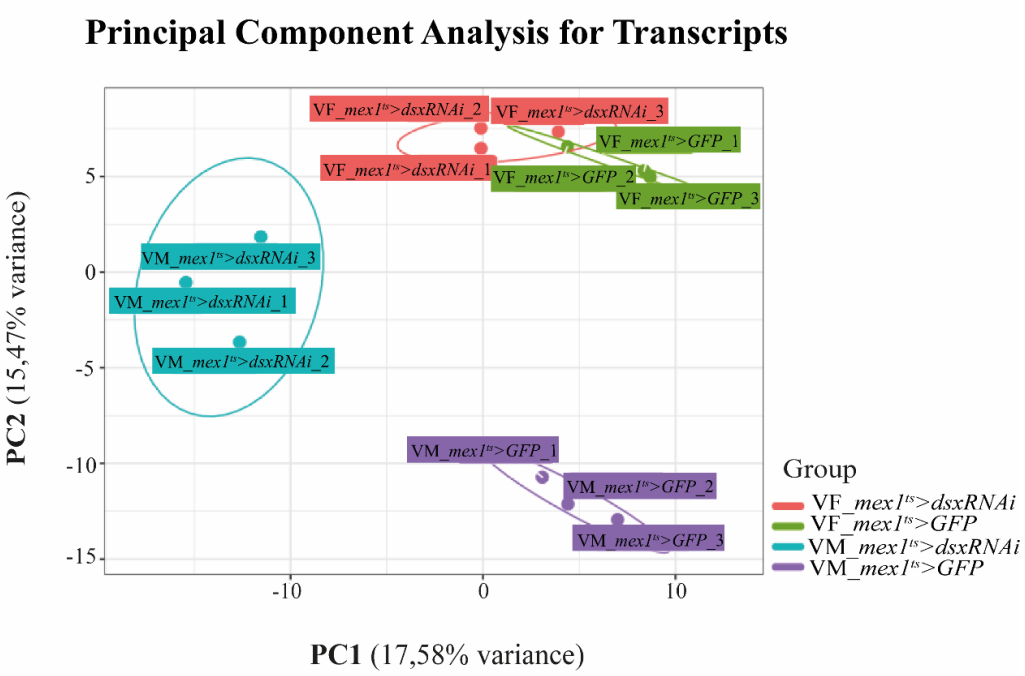
Principal Component Analysis for Transcripts
PC2 (15,47% variance)
PC1 (17,58% variance)
VF_mex1ts>dsxRNAi_2
VF_mex1ts>dsxRNAi_3
VF_mex1ts>GFP_1
VF_mex1ts>dsxRNAi_1
VF_mex1ts>GFP_2
VF_mex1ts>GFP_3
VM_mex1ts>dsxRNAi_3
VM_mex1ts>dsxRNAi_1
VM_mex1ts>dsxRNAi_2
VM_mex1ts>GFP_1
VM_mex1ts>GFP_2
VM_mex1ts>GFP_3
Group
VF_mex1ts>dsxRNAi
VF_mex1ts>GFP
VM_mex1ts>dsxRNAi
VM_mex1ts>GFP

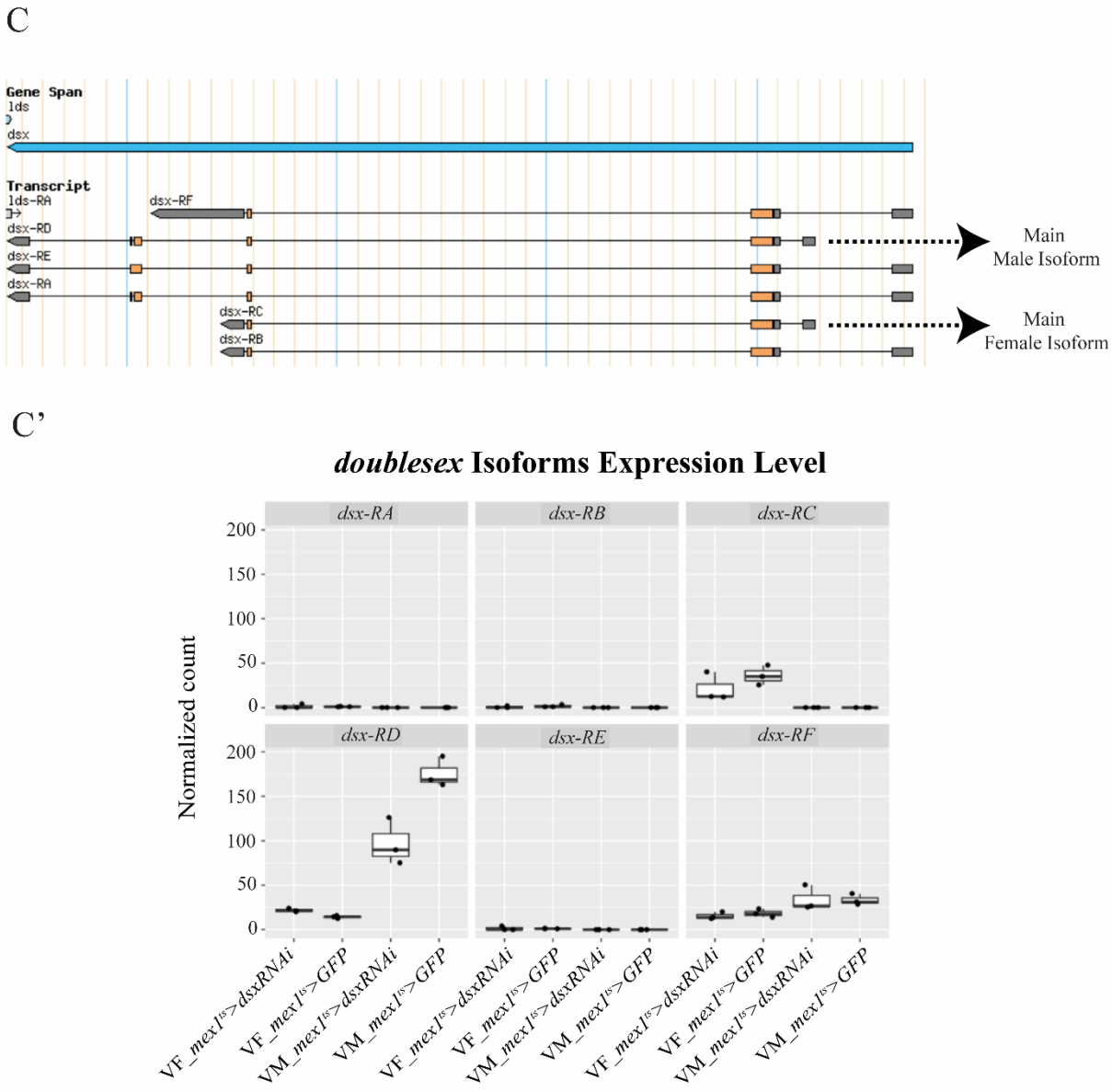

Figure 3.5: *dsx* transcript analyses of the RNA-sequencing datasets

(A) Sample distance matrix for the transcripts. Each colour represents a sample group: control female in green, control male in purple, experimental female in red, experimental male in blue. Samples cluster in grey gradient according to their transcript similarities. (B) Principal component analysis (PCA) plot of transcriptional changes in isoforms in virgin males and females (total of 12 samples). PCA1 and PCA2 show 17.58% and 15.47% of variance, respectively. Female samples do not show clear separation between control and experimental conditions. (C) Modified screenshot from the GBrowse. *dsx* locus is depicted as a blue box with an arrow indicating the direction of transcription. Sex-specific transcripts show both similarities and differences in their sequences. Exons in orange, non-coding sequences in grey. In the transcript category, *dsxRF* (female), *dsxRD* (male), *dsxRE* (male), *dsxRA* (male), *dsxRB* (female) and *dsxRA* (female). (C') Levels of the distinct *doublesex* transcripts from the RNA-seq in female and male under *dsx* downregulation (three replicates per condition). VF = virgin female, VM = virgin male.

From the *doublesex* locus, six different isoforms are transcribed, three per each sex. The three male isoforms are *dsxRD*, *dsxRE* and *dsxRA*. The three female isoforms are *dsxRF*, *dsxRC* and *dsxRB* (see Introduction and Fig. 3.5C). The main isoforms are: *dsxRD* in males, and *dsxRC* in females. Accordingly, in the RNA-sequencing data we detected higher levels of *dsxRD* and

dsxRC in females and males, respectively. In contrast to the reduction of *dsxRD* upon *dsx* downregulation, *dsxRC* was not affected by *dsx* knock-down (Fig. 3.5C'), which is consistent with the unchanged gene level (Fig. 3.4D). Interestingly, we observed expression of *dsxRD* in the female (both control and experimental conditions), suggesting the presence of *dsxM* transcript in the female midguts. These are coherent with previous analyses in the lab from the RNA-seq published in Hudry, Khadayate et al. 2016. It has been shown that in female midguts, although levels of *dsx* transcript belong mostly to the female isoform, there is a noticeable male isoform contribution. In males, purely all transcript is male isoform. These can be explained because by default, *dsx* is spliced to *dsxM*: it is only with the presence of Tra, that the female-splicing of *dsxF* can be achieved (see Introduction). Interestingly, and intriguingly, both in females and males we detected expression of *dsxRF*, although at much lower levels than the main isoforms (Fig. 3.5C').

To summarise the analyses at the global gene and transcript isoform levels, we have found that:

i. The reads from the RNA-sequencing showed excellent Tophat 2 alignment.
ii. The samples clustered according to their category, indicating a lack of substantial intra-group variation (sample matrix distance).
iii. The experimental and control male samples differed dramatically (PCA plots).
iv. The experimental and control females were little different (PCA plots).
v. *doublesex* gene and sex-specific isoform *dsxRD* were significantly reduced upon *dsx* knock-down in males.
vi. *doublesex* gene and sex-specific isoform *dsxRC* did not show reduction upon *dsx* knock-down in females.

Subsequently, we further examined the transcriptional changes with a greater focus at the number of up/downregulated genes (Fig. 3.6). To identify the differentially expressed (DE) genes, we compared the gene expression between experimental (*mex1^{ts}>dsxRNAi*) *vs* control (*mex1^{ts}>GFP*) and used padj<0.05 as a threshold. The majority of DE genes were male-specific (i.e. only changing expression levels in males) consistent with the strong *dsx* downregulation (1384 DE genes in males, 196 in females and 382 in both sexes) (Fig. 3.6A-B). In females, there were fewer genes changing in a female-specific manner (only 196 DE genes), which is consistent with the insufficient *dsx* knock-down. All the DE genes were divided in two categories: upregulated DE genes (higher in experimental samples) or downregulated (higher in control samples) DE genes. In males, there were more DE genes upregulated than

downregulated (816 *vs* 586). In females, there were marginally higher levels of downregulated DE genes (88 *vs* 126) (Fig. 3.6). In summary, *dsx* knock-down robustly and preferentially affected the male transcriptome, with a slight bias for the DE genes to be upregulated following *dsx* knock-down.

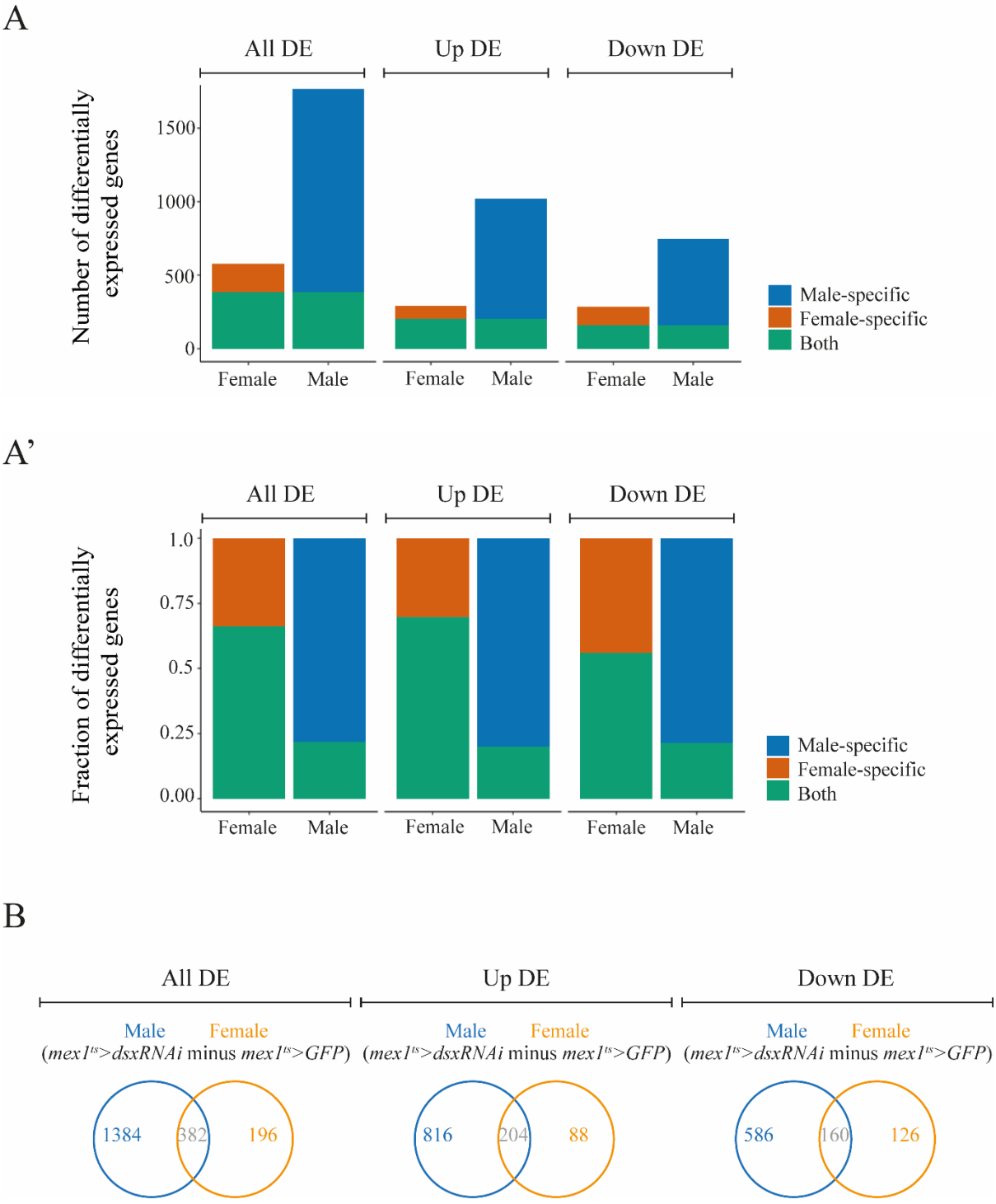

Figure 3.6: Global transcriptional changes in the number of genes of virgin male and female adult midguts upon *dsx* downregulation

(A) Number of differentially expressed (DE) genes (defined by a padj<0.05 threshold) comparing *mex1^{ts}>dsxRNAi* with *mex1^{ts}>GFP* in females and males. All DE expressed genes (two columns on the left) are further divided into upregulated DE genes (two middle columns) and downregulated DE genes (two columns on the right). DE genes only changing in male samples (male-specific) are plotted in blue. Female-specific DE genes in orange, and DE genes changing in both sexes are depicted in green. (A') Fraction of the DE genes comparing *mex1^{ts}>dsxRNAi* with *mex1^{ts}>GFP* in both female and male. Same categories and colour legend as in (A), but the data is plotted relative (instead of absolute) to the total genes per each group. (B) Three Venn diagrams representing all (left), upregulated (middle) and downregulated (right) DE genes. Per each category, number of DE genes changing transcription between experimental and control samples exclusively in male samples (male-specific) are shown in blue within blue circles: total of 1384 DE genes, which 816 are upregulated and 586 are downregulated. DE genes varying exclusively between experimental and control female samples (female-specific) are depicted in orange: 196 in total, 88 upregulated and 126 downregulated. In grey there are annotated the number of DE genes that switched expression in *mex1^{ts}>dsxRNAi* minus *mex1^{ts}>GFP* common in both sexes (382 DE genes in total, 204 upregulated and 160 downregulated).

To investigate whether the transcriptional changes induced by *dsx* downregulation in adult ECs were suggestive of specific biological functions, we examined which categories were affected in the Gene Ontology analyses (GO) and Kyoto Encyclopaedia of Genes and Genomes (KEGG). For simplicity reasons, only KEGG changes are shown (Fig. 3.7); however, we also conducted analyses to examine the significant alterations within the Biological Processes (BP) (Fig. S1) and Molecular Function (MF) (data not shown) from the GO. Because of the lack of *dsx* mRNA reduction in females upon *dsx* knock-down in ECs, we focused exclusively on the male samples.

The KEGG category with the highest number of differentially expressed genes was "metabolic pathways" (genes upregulated in *mex1^{ts}>dsxRNAi* males). This finding was expected because the midgut is a key metabolic organ. The other KEGG categories in the top three of upregulated genes were "oxidative phosphorylation" and "ribosome". Of note, "peroxisome" genes were also differentially upregulated in experimental males. The "cytochrome P450" genes were the most downregulated, with lower numbers of gene per category when compared with the upregulated genes (Fig. 3.7).

A

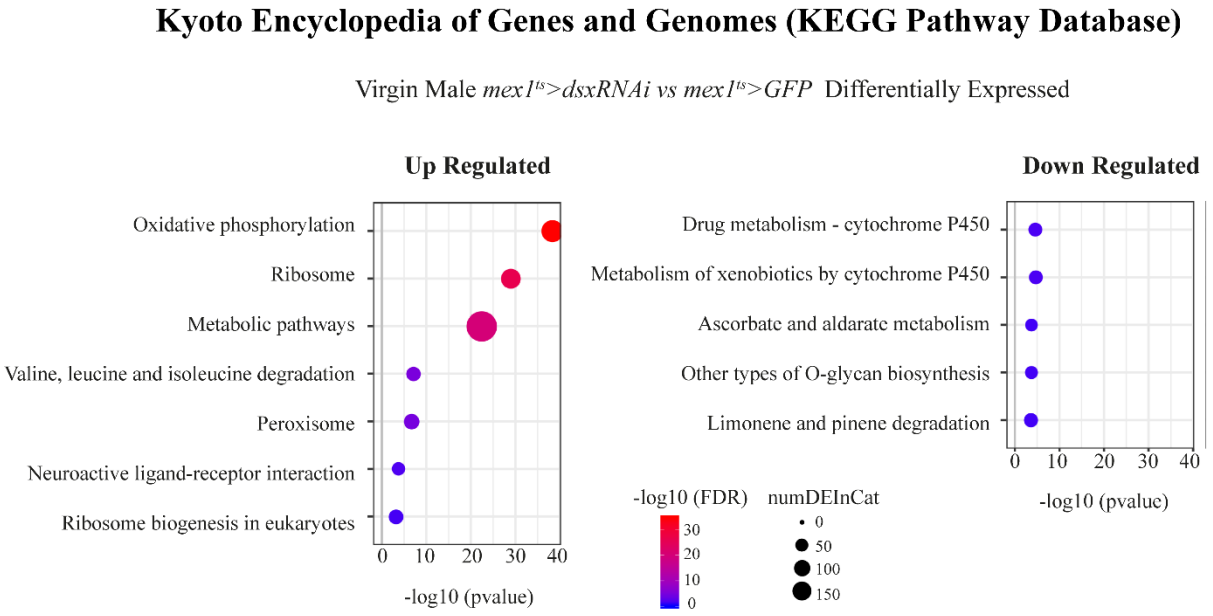

Figure 3.7: KEGG analysis from the gene changes in virgin male midguts upon *dsx* downregulation in the ECs

Changes at the level of differentially expressed genes from experimental (*mex1^{ts}>dsxRNAi*) *vs* control (*mex1^{ts}>GFP*) virgin males. KEGG categories of upregulated (left) and downregulated (right) genes. List of the gene categories in the Y axis. Value of -log10(p-value) in the X axis. The size of the circular points in the graph shows the number of differentially expressed genes in each category (from small to big, 0 to 150 genes). Colour of the circle corresponds to the -log10 of False Discovery Rate (FDR), which corrects for multiple comparisons. The lower -log10(p-value) correlates with the lower -log10(FDR).

The transcriptional variation suggestive of changes in metabolic pathways caught our attention given previous studies in the lab, which had investigated the sex differences in glucose metabolism from adult midguts (Hudry, de Goeij et al. 2019), and several other studies that had revealed sex differences in fly metabolism (see Introduction).

Excitingly, adult midguts of *mex1^{ts}>dsxRNAi* virgin males had differential expression of genes involved in lipid metabolism (Fig. 3.8A, B). Within the wide category of lipid metabolism, there were genes belonging to lipid synthesis, breakdown, absorption and digestion. Additionally, most of those genes were also sexually dimorphic in control flies (Fig. 3.8A').

Subsequently, I decided to validate a few of the candidate genes belonging to the lipid metabolism category using qPCR. One of the examples is the *CG17192* gene, coding for a lipase. This was one of the genes with the most pronounced sexually dimorphic expression (both in this RNA-seq (Fig. 3.8A') and in the RNA-seq from Hudry, Khadayate et al. 2016). Also, it was highly upregulated in experimental males, as well as in *mex1^{ts}>dsxRNAi* females (Fig. 3.8A, Fig. S2). By qPCR, although not statistically significant most likely due to the low

number of samples, I saw that upon a *dsx* decrease in *mex1^{ts}>dsxRNAi* males (Fig. 3.8C), *CG17192* expression was higher (Fig. 3.8C'), aligned with the results from the RNA-seq. In females, reduction of *CG17192* expression was observed upon "*dsx* downregulation" (0.5x fold change) (Fig. 3.8C'').

To summarise the findings of the transcriptional changes at a biological level, we have found that:

i. In males, the midgut transcriptome changed dramatically upon downregulation of *dsx* in the adult ECs. Differentially expressed genes were more often upregulated than downregulated in *mex1^{ts}>dsxRNAi* male samples.
ii. From the male GO and KEGG analyses, we observed major alterations in metabolic genes (as well as in the oxidative phosphorylation and ribosome categories).
iii. In males, a large number of lipid metabolism genes was differentially expressed upon *dsx* downregulation. These genes code for proteins involved in lipid synthesis, breakdown, transport and absorption.
iv. Many of the lipid metabolism genes were sexually dimorphic in the adult midgut.

Figure 3.8: Changes in lipid metabolism genes in the midgut of virgin adults upon *dsx* downregulation in the ECs

(A) Volcano plot of transcriptional changes of lipid metabolism genes in experimental (*mex1^{ts}>dsxRNAi*) *vs* control virgin males (*mex1^{ts}>GFP*). (A') Volcano plot of the sexual dimorphism in lipid metabolism transcript profile from control (*mex1^{ts}>GFP*) female and male. (A-A') Y axis is -log10(p-adjusted), X axis is log2(fold change). Black dots and genes written in black show no difference of expression. Orange dots and gene names are the ones which upregulate expression upon *dsx* downregulation. Turquoise dots and gene names, the ones with lowered expression in *dsx* knock-down. P-adjusted of less than 0.05 are counted as statistically significant changes. (B) Heatmap of lipid metabolism DE genes. List of genes clustered in three groups according to their expression in the four analysed sample groups (virgin males of *mex1^{ts}>GFP* and *mex1^{ts}>dsxRNAi*, as well as virgin females of *mex1^{ts}>GFP* and *mex1^{ts}>dsxRNAi*). Z-score is the gene expression value in the sample of interest, subtracting the mean expression across all samples, and divided by the standard deviation. Z-score is depicted in a yellow-to-blue colour scale. Samples are exhaustively annotated at the bottom of the heatmap and grouped as four categories at the top of the heatmap (dark orange is male control, light orange, experimental male. Dark pink is female control, light pink, experimental). (C) Relative expression of *dsx* levels in virgin male adult midguts comparing *mex1^{ts}>GFP* with *mex1^{ts}>dsxRNAi* by qPCR. Relative expression of *CG17192* levels in control and experimental male (C') and female (C'') midguts by qPCR. Sample (n=3) normalised to the housekeeping *rp49.* Relative expression values are calculated against one sample control as reference. Results are shown as mean ±SEM. P-value < 0.05 with Mann-Whitney test.

A

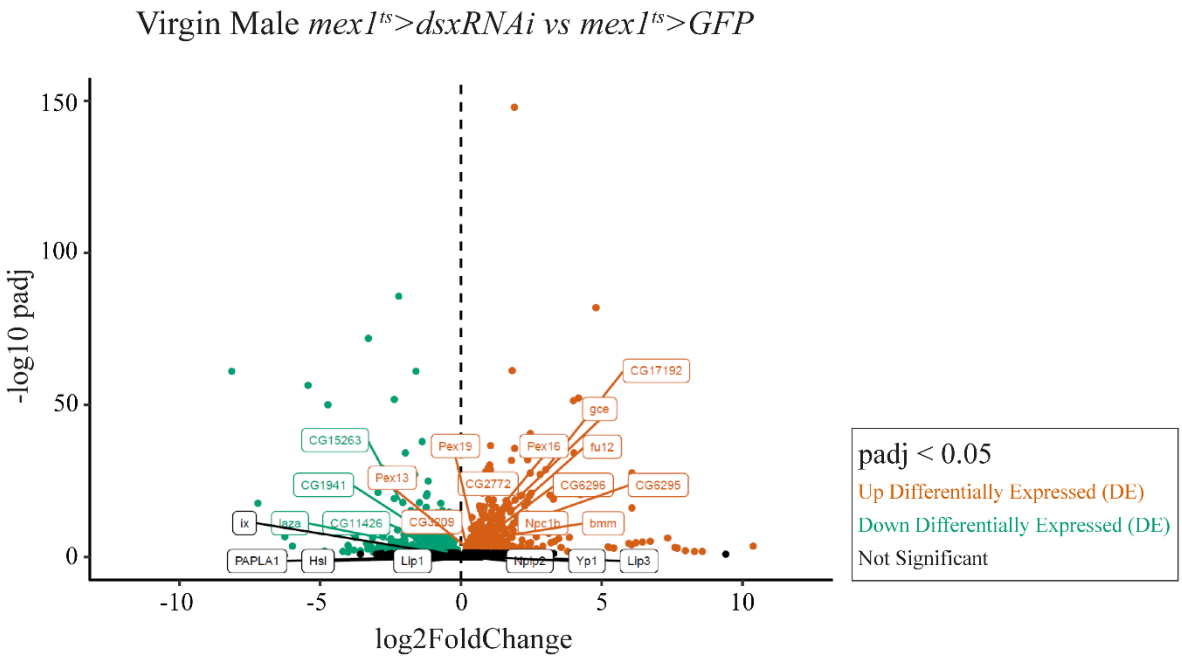
Virgin Male mex1ts>dsxRNAi vs mex1ts>GFP
-log10 padj
log2FoldChange
CG17192
gce
CG15263
Pex19
Pex16
fu12
Pex13
CG2772
CG6296
CG6295
CG1941
CG11426
CG3209
Npc1b
bmm
Ix
laza
PAPLA1
Hsl
Lip1
Nplp2
Yp1
Lip3
padj < 0.05
Up Differentially Expressed (DE)
Down Differentially Expressed (DE)
Not Significant

A'

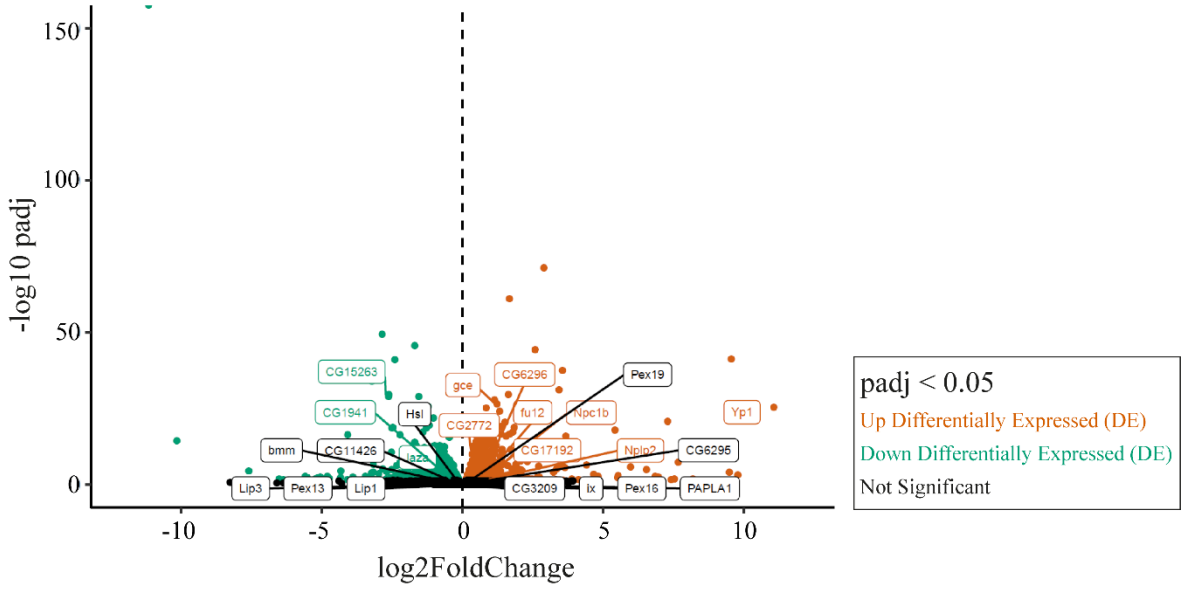
Virgin Female mex1ts>GFP vs Virgin Male mex1ts>GFP
-log10 padj
log2FoldChange
CG15263
gce
CG6296
Pex19
CG1941
Hsl
fu12
Npc1b
Yp1
CG2772
bmm
CG11426
laza
CG17192
Nplp2
CG6295
Lip3
Pex13
Lip1
CG3209
Ix
Pex16
PAPLA1
padj < 0.05
Up Differentially Expressed (DE)
Down Differentially Expressed (DE)
Not Significant

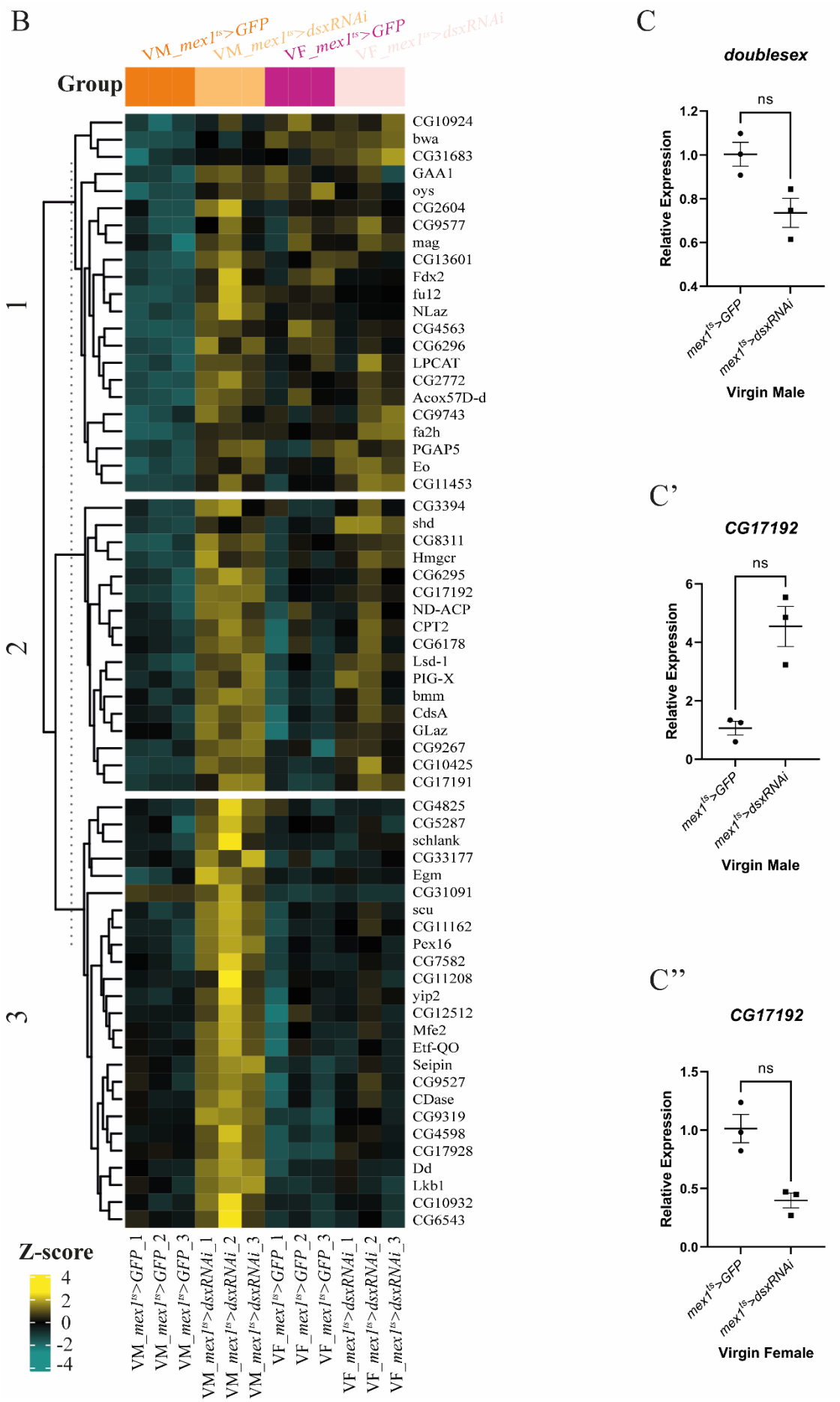
B
VM_mex1ts>GFP
VM_mex1ts>dsxRNAi
VF_mex1ts>GFP
VF_mex1ts>dsxRNAi
Group
1
2
3
CG10924
bwa
CG31683
GAA1
oys
CG2604
CG9577
mag
CG13601
Fdx2
fu12
NLaz
CG4563
CG6296
LPCAT
CG2772
Acox57D-d
CG9743
fa2h
PGAP5
Eo
CG11453
CG3394
shd
CG8311
Hmgcr
CG6295
CG17192
ND-ACP
CPT2
CG6178
Lsd-1
PIG-X
bmm
CdsA
GLaz
CG9267
CG10425
CG17191
CG4825
CG5287
schlank
CG33177
Egm
CG31091
scu
CG11162
Pex16
CG7582
CG11208
yip2
CG12512
Mfe2
Etf-QO
Seipin
CG9527
CDase
CG9319
CG4598
CG17928
Dd
Lkb1
CG10932
CG6543
VM_mex1ts>GFP_1
VM_mex1ts>GFP_2
VM_mex1ts>GFP_3
VM_mex1ts>dsxRNAi_1
VM_mex1ts>dsxRNAi_2
VM_mex1ts>dsxRNAi_3
VF_mex1ts>GFP_1
VF_mex1ts>GFP_2
VF_mex1ts>GFP_3
VF_mex1ts>dsxRNAi_1
VF_mex1ts>dsxRNAi_2
VF_mex1ts>dsxRNAi_3
Z-score
4
2
0
-2
-4
C
doublesex
ns
Relative Expression
1.2
1.0
0.8
0.6
0.4
mex1ts>GFP
mex1ts>dsxRNAi
Virgin Male
C'
CG17192
ns
Relative Expression
6
4
2
0
mex1ts>GFP
mex1ts>dsxRNAi
Virgin Male
C''
CG17192
ns
Relative Expression
1.5
1.0
0.5
0.0
mex1ts>GFP
mex1ts>dsxRNAi
Virgin Female

At this point, we decided to use a different control line for subsequent experiments. The control line used for the RNA-seq was the GFP control line recommended by the TRiP collection (UAS-GFP.VALIUM10), which is widely used in the field, as well as in previous studies in the lab (Hudry, Khadayate et al. 2016). Due to the substantial overexpression of GFP in the ECs of our samples, we were uncertain whether some differential gene expression in the *dsx* knock-down experiments was a consequence of GFP expression rather than *dsx* downregulation. We suspected that this would be the case for two reasons. Firstly, the (admittedly small) number of genes differentially expressed in female flies following *dsx* knock-down. Females do not express detectable Dsx protein and *dsx* knock-down had not resulted in significant *dsx* transcript downregulation in females. Secondly, Tomotsune Ameku compared the control samples of this study with male and female Oregon R midguts from his RNA-seq (not published). He observed 2089 genes sexually dimorphic in Oregon R samples, and 2236 genes in $mex^{ts}>GFP$ control. Only 859 genes were shared between the two datasets, and thus being sexually dimorphic in both control lines (data not shown, personal communication). For these reasons, we chose a new control line based on the following criteria: a) we wanted it to be a UAS-RNAi line, so that its generic, unspecific effects (if any) are the same as those of the *dsxRNAi* experimental line does (as opposed to those resulting from GFP protein overexpression), b) targeting a *Drosophila*-specific gene (as opposed to an exogenous protein, for the same reasons as in a)), c) targeting a gene which is not normally expressed in wild-type midguts, d) a RNAi line from the TRiP collection with the same genetic background as the *dsxRNAi* experimental line (variations in the genetic backgrounds may otherwise affect metabolic traits).

Considering all the above-mentioned requisites, we decided to use $mex1^{ts}>Ilp4RNAi$ (*Insulin-like peptide 4*) as a control line for most of the follow-up experiments. However, since the genetic background had to match the experimental RNAi line, in few experiments, the control line was changed to $mex1^{ts}>Ilp7RNAi$. Neither *Ilp4* nor *Ilp7* are expressed in the midgut, based on three independent RNA-seq datasets available in the lab and, in the case of Ilp7, confirmation by immunostaining (Miguel-Aliaga, Thor et al. 2008, Hudry, Khadayate et al. 2016 and data not shown).

3.3 Conclusion & Discussion

In this chapter, I have validated that Dsx is sex and cell-type specific in the adult midgut, detected only in male ECs. However, although *dsx* transcript is sexually dimorphic and highly

expressed in males, it is nevertheless detected in females. Even though female midguts have lower levels of *dsx* transcript, the presence of DsxF in the ECs would still be expected. The lack of DsxF is suggestive of female-specific post-transcriptional regulation, which might be midgut-specific, since DsxF was detected in other tissues such as the VNC, the fat body or the Malpighian tubules.

There are experimental arguments which point to a novel female-specific post-transcriptional regulation of *dsx* in the female midgut. First, the levels of *dsx* in females increase after mating. An unpublished RNA-seq performed by Jake Jacobson compared the transcriptomes of virgin females with mated females. In this experiment, the levels of *dsx* post-mating are increased, comparable to the levels found in the male midguts. This finding prompts us to two conclusions: a) the lack of DsxF in female midguts is not explained by immunostaining sensitivity issues because it is also absent from mated female midguts in which the levels of *dsx* resemble the amount of *dsx* mRNA in males (data not shown); and b) the increase in transcription might hint towards a putative novel function of the transcript. Second, I have preliminary observed Dsx::eGFP in a mosaic manner where Tra was knocked-down from an adult female midgut; expression was only apparent in *traRNAi* clones (Fig. 3.9). This is suggestive of DsxF being repressed in a Tra-dependent, cell-intrinsic manner (independent of external signals such as paracrine or endocrine cues) in the female enterocytes. Third, the minor effects of *dsx* downregulation observed in the female samples (RNA-seq from this study) could be in consonance with *dsx* transcript being retained and inaccessible for the RNAi machinery.

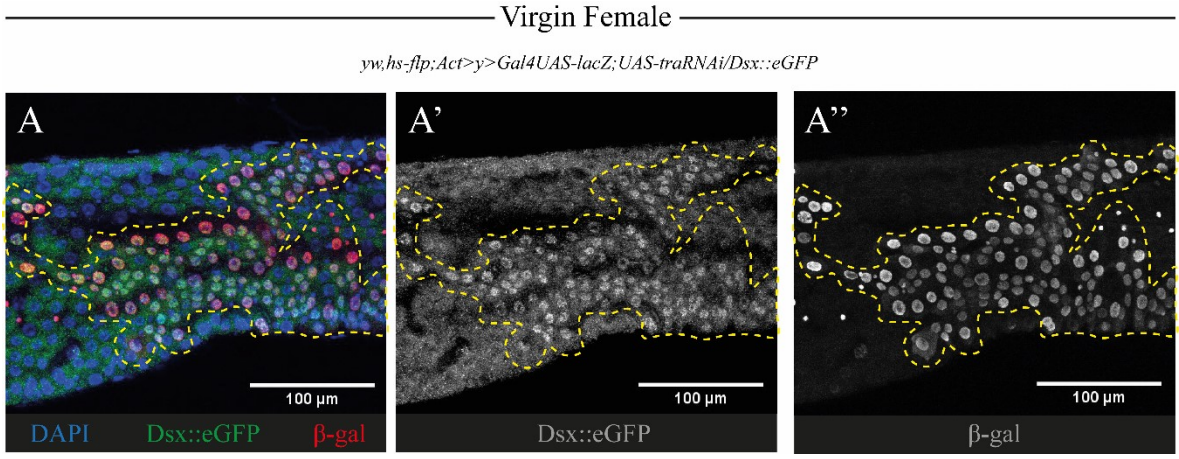

Figure 3.9: Dsx in masculinised clones in the female midgut

Confocal images showing Dsx::eGFP expression in a mosaic manner in "masculinised" female cells by *tra* downregulation (*yw.hs-flp;Act>y>ActUAS-lacZ;UAS-traRNAi/Dsx::eGFP*). In the triple staining (A), DAPI is in blue, Dsx::eGFP in green and β-galactosidase in red. In the single stainings, Dsx::eGFP is in grey (A'), as well as β-galactosidase (A''). Yellow dashed line depicts the silhouette of the experimental clone. Scale bars (100µm) stated in each panel.

Furthermore, there are examples in the literature of Dmrt family members being controlled post-transcriptionally, indicative of a common regulation among different species. For instance, DMD-4 in the brain of *Caenorhabditis elegans* is post-translationally regulated in a sex-specific manner through ubiquitin binding (Bayer, Stecky et al. 2020). Also, members of the sex determination pathway are involved in post-transcriptional regulation in *Drosophila*. For example, Sxl in females translationally controls *msl-2* mRNA to prevent dosage compensation, and it does so through the UTRs, upstream open reading frames (uORFs) and interaction sites for RNA-binding proteins (Medenbach, Seiler et al. 2011). Moreover, post-transcriptional regulation has been described in medaka fish of the *dmrt1a/dmrt1bY* gene pair (Herpin and Schartl 2011). Finally, in human tissues the relatively low correlation between mRNA and protein levels is suggestive of a great presence of post-transcriptional regulatory mechanisms in establishing the proteasome (Franks, Airoldi et al. 2017). These studies, together with the findings in this chapter, highlight the importance of elucidating sexual dimorphism at the proteomic level, along with at the transcriptomic level.

The absence of correlation between *dsx* transcript and DsxF in females is very intriguing and leads to many avenues for further research. What are the mechanisms underlying the post-transcriptional regulation? Does *dsxF* transcript have an uncharacterised function? Does female-specific regulation occur? And if so, is it specific to the female midgut or to the female *dsx* transcript?

The mechanisms behind the *dsx* female-specific post-translational regulation in the ECs are unknown and could be due to the female environment or to the female transcript. Whether intrinsic to the *dsxF* transcript, I surmise that among other mechanisms, regulation via UTRs and microRNAs (miRNAs) could possibly have an influence. *dsxM* and *dsxF* main isoforms differ at the level of UTR: despite sharing the same 5'UTR, the 3'UTR is sexually dimorphic. The 3'UTR has been demonstrated to be involved in post-transcriptional regulation (reviewed in Szostak and Gebauer 2013, Mayr 2017) and the 3'UTR of *dsxF* has several features which could explain its control (e.g. a stem loop predicted by the RegRNA2 software (Chang, Huang et al. 2013)). Furthermore, the female 3'UTR shows increased numbers of miRNA binding sites compared to the male 3'UTR (by Target Scan Fly software (Agarwal, Subtelny et al. 2018)), suggestive of miRNAs mediating post-transcriptional gene expression silencing (transcript instability and degradation) in a temporal and spatial manner (Wessels, Lebedeva et al. 2019). Alternatively, the fact that DsxF is not translated could also be caused by the female environment (i.e. specific sexually dimorphic complexes affecting overall or DsxF translation).

Experimentally, this assumption could be addressed by expressing *dsxM* exclusively in the female ECs (depleted of *dsxF* by *tra* knock-down) and check for its translation. To corroborate that the post-transcriptional regulation is specific to the female *dsxF* transcript, one could express *dsxF* in the male ECs (partially depleted of *dsxM* by *tra* overexpression) and verify its translation.

Furthermore, I speculate whether in the female midgut there are sex-specific mechanisms controlling the stability and proteolysis of DsxF. I began comparing the PEST residues (sequences targeting protein degradation) between DsxM and DsxF, and realised that DsxF has fewer PEST residues. For future exploratory experiments, it would be relevant to make use of proteasome inhibitory fly lines: is DsxF visualised in adult female ECs where protein degradation is blocked by the knock-down of the proteasome?

Interestingly, preliminary data hints towards a putative presence and role of DsxF in female midguts: the well-established Dsx target Yolk protein (Yp1::eGFP) seems to be present in the female adult midgut (my observations and Hudry, de Goeij et al. 2019). This is based on the assumption that Yp1 in the midgut is regulated by DsxF as in the fat body. Alternatively, Yp1 could have been exported from the fat body to the midgut, as observed in the oocyte (even though the majority of vitellogenin in the oocyte comes from *Yp2* translation, there is a small absorption of Yp1 secreted from the fat body to the haemolymph) (reviewed in Hoy 2019). From the expression levels of the RNA-seq generated in this thesis, I hypothesise that *Yp1* mRNA is not residual and it is transcribed in female guts. From the RNA-seq in female midguts, *Yp1* expression varies from control to experimental samples, with a -1.58 log2fold change (lower in *dsx* knock-down). However, this reduction in transcription is not statistically significant. Further research elucidating Yp1 expression and its regulation in the female midgut needs to be done prior to extrapolating DsxF contributions.

In summary, the key conclusions drawn from this chapter are:

i. *dsx* levels are higher in males than females. Dsx is specific to male ECs.
ii. Knock-down of *dsx* in adult male ECs show dramatic changes in the midgut transcriptome profile.
iii. Lipid metabolism gene expression is under the regulation of *dsx* in ECs.

Many of the lipid metabolism genes are sexually dimorphic and regulated by *dsx* in males (acquiring a female trend upon *dsxRNAi*). Therefore, this might suggest that the presence of DsxM in the male midgut sets a male-specific lipid signature (or that the lack of DsxF in the

female midgut sets a female-specific lipid signature). The lack of Dsx in males shows a "feminisation" of the lipid profile. I wonder whether the sex-specific signature of a concrete cell type in the midgut could influence lipid metabolism at the cellular, organ and whole-organism level. Thus, in the next chapter I start exploring the changes on lipid homeostasis driven by Dsx in ECs.

CHAPTER 4

Results (II)

DOUBLESEX INFLUENCES LIPID METABOLISM IN THE ADULT MIDGUT

4.1 Introduction

In the previous chapter, I have shown a link between the expression of Doublesex and that of lipid metabolism genes in the adult midgut. Preceding studies have reported male and female differences in fat homeostasis, and researchers have been describing the contributions of Tra in establishing this sexual dimorphism (see Introduction). However, whether (and how) Dsx helps to orchestrate the sexual dimorphism in lipid metabolism is currently unknown.

Several findings point towards a putative connection between the transcription factor Dsx and expression of lipid genes. One of the well-characterised direct targets of Dsx is *Yolk protein*: DsxM represses *Yp*, whereas DsxF activates it (see Introduction). Yolk protein, as well as providing the major protein source for the eggs during embryogenesis, is a triacylglycerol lipase involved in lipid catabolism. Interestingly, both Dsx and Yp are localised in the adult fat body, suggestive of Dsx controlling fat homeostasis in a sexually dimorphic manner. Additionally, a genome-wide occupancy experiment investigated the binding sites of DsxM and DsxF in the fat body of adult flies (Clough, Jimenez et al. 2014). The authors concluded that although many targets are shared between males and females, the mode of their regulation is sexually dimorphic (e.g. as observed by activation/repression of *Yp*) (see Introduction). Thus, this indicates that Dsx might participate in regulating the differences in fat homeostasis from the fat body. In particular, downregulation of *dsx* in the fat body cells reduces the cell size in both males and females (Rideout, Narsaiya et al. 2015). Additionally, a recent study carefully characterised these sex differences by exploring the contribution of fat storage and break down. This led to the finding that sex-biased expression of the lipase *brummer* plays a key role in the regulation of triacylglycerol homeostasis between the sexes, with lower amounts of TAG correlating with higher *bmm* expression (Wat, Chao et al. 2020).

Although the fat body is the master regulator of lipid homeostasis, the midgut also plays active roles at the level of digestion, absorption, transport, lipolysis and lipogenesis (see Introduction). Inspired by the Tra-dependent (but Dsx-independent) sex differences in carbohydrate metabolism and redox processes in the midgut (Hudry, Khadayate et al. 2016, Hudry, de Goeij et al. 2019), I wondered whether Dsx regulates lipid metabolism in a sexually dimorphic manner.

4.2 Results

4.2.1 Sexual dimorphism in the adult midgut of wild-type flies

The R1-R5 regions of the midgut are classified according to their anatomy and gene expression (reviewed in Miguel-Aliaga, Jasper et al. 2018). Midgut regionalization is apparent at the level of proteins involved in lipid homeostasis (see Introduction), and also seems to apply to lipid stores. Previous studies show that lipid vesicles are detected in the ECs of R2 (Buchon, Osman et al. 2013), or in A2, P1 and P3 (the authors used another nomenclature referring to midgut regions: they divide the anterior portion into three regions, A1-A3, followed by the middle portion, Cu-LFC-Fe, and the four posterior portions, P1-P4) (Marianes and Spradling 2013).

Before studying the effects of Dsx on the lipid profile of the adult midgut, I started by characterising the number of lipid droplets (LDs) stored in wild-type and control flies.

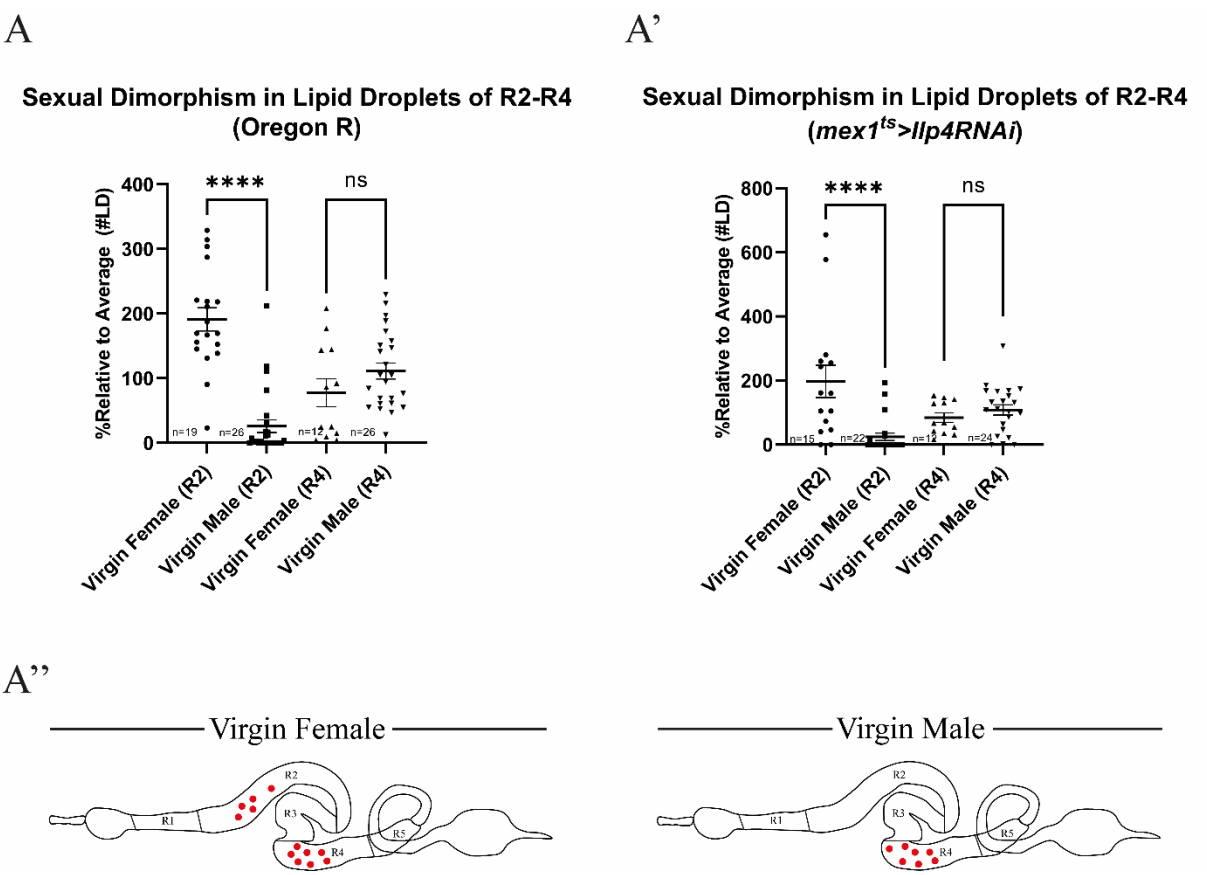

Figure 4.1: Sexual dimorphism in lipid droplets of the anterior (R2)/posterior (R4) midgut of wild-type and control virgin adult midguts

Graphs showing comparisons between the number of LDs in Oregon R wild-type (A) and *mex1^{ts}>Ilp4RNAi* (A'), in the anterior (R2) and posterior (R4) region of female and male adult midguts. Number of LDs differ between female and male R2 (both in the wild-type and control). Number of LDs in the R4 are not sexually dimorphic.

(A'') Schematics of the LD signature in virgin female and virgin male midguts. The quantity of guts analysed per category is stated in the graph (n=12-26). Values are plotted as a percentage relative to the average of LD particles in R2 (or R4) per each experimental day. The average is the sum of male and female LD quantifications divided by the number of measurements on a particular day. Results are shown as mean ±SEM. P-value < 0.05 with Mann-Whitney test.

As aforementioned, after the RNA-seq experiment, I used the control line *mex1^{ts}>Ilp4RNAi* to compare it phenotypically with *mex1^{ts}>dsxRNAi*. In both *mex1^{ts}>Ilp4RNAi* control and Oregon R wild-type flies, reared in parallel (18°C to 29°C), I have observed a sexual dimorphism in the number of LDs in the midgut (Fig. 4.1). I made use of the neutral dye LipidTox to visualise and quantify LDs, which are shown in red throughout the thesis (see Materials & Methods). Female and male midguts showed LDs in the region R4. However, there was a sexual dimorphism at the R2 region of the midgut: LDs were detected in the anterior region of the female midgut, but absent (or at much lower levels) in the R2 of males (Fig. 4.1).

Hence, in virgin flies, lipid accumulation in the midgut is regional and this regionality differs between sexes.

4.2.2 Changes in midgut lipid droplets upon *dsx* downregulation

The RNA-seq experiments pointed to a role of Dsx in lipid metabolism in adult virgin midguts (see Results I). To start characterizing the phenotypic changes of lipid homeostasis upon *dsx* downregulation, I quantified the levels of LDs in the midgut (see Materials & Methods). Since Dsx is only detected in male ECs (see Results I), and males have LD in the posterior midgut only (see above), I concentrated on analysing the amount of LD in the R4 of *mex1^{ts}>dsxRNAi* males (Fig. 4.2).

Fewer LDs were apparent in the midgut epithelium of the R4 region of males with lower levels of *dsx* in the ECs (Fig. 4.2). This reduction was noticeable when *mex1^{ts}>dsxRNAi* experimental flies were compared to two different controls: *mex1^{ts}>GFP* (from the RNA-seq) and *mex1^{ts}>Ilp4RNAi* (from the phenotypic analysis) (Fig. 4.2B). Of note, the two controls had different LD levels (Fig. 4.2B). This reduction was also consistently observed regardless of the diet: in both control diet (Fig. 4.2A-A' and Fig. 4.2C) and a high sugar diet (Fig. 4.2C'), the number of LDs in the R4 is reduced upon *dsx* downregulation in ECs.

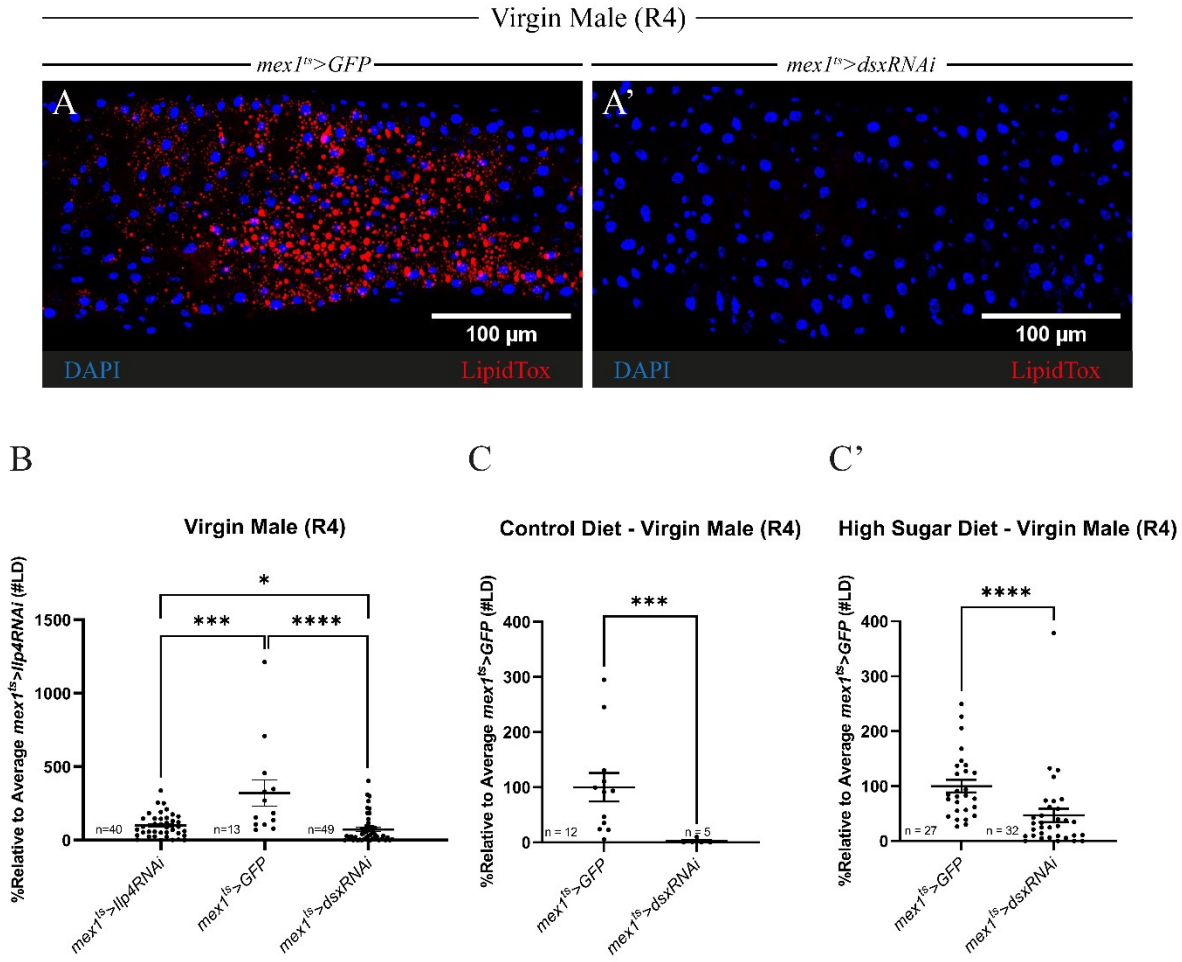

Figure 4.2: *dsx* downregulation reduces LDs in the R4 of virgin males

R4 posterior region of control *mex1*ts>GFP virgin males (A) compared to experimental *mex1ts>dsxRNAi* (A'). In red, LDs in the midgut epithelium stained with LipidTox. In blue, DAPI. Scale bars in the immunostaining images. (B) Quantification of LDs in *mex1ts>Ilp4RNAi*, *mex1ts>GFP* and *mex1ts>dsxRNAi*. Number of midguts analysed per category is stated in the graph (n=13-49). Amount of LDs in R4 of control (*mex1ts>GFP*) and experimental (*mex1ts>dsxRNAi*) virgin males under control (C) or high sugar diet (C'). Number of midguts analysed per category is stated in the graph (n=5-32). Values are plotted as a percentage relative to the average of LD particles of the *mex1ts>Ilp4RNAi* or *mex1ts>GFP* control per each experimental day. Results are shown as mean ±SEM. P-value < 0.05 with Mann-Whitney test.

Subsequently, I wanted to examine whether this reduction in LDs is systemic or cell-autonomous. To do so, I downregulated *dsx* specifically in a mosaic manner by making use of *Drosophila* clonal genetic tools (see Introduction and Materials & Methods) (Fig. 4.3).

In experimental clones, in which *dsx* was downregulated, there were fewer LDs when compared to the area outside the clone (Fig. 4.3A-A', B'). In control clones, the levels did not change inside or outside the clone (Fig. 4.3B).

This finding is consistent with the effects of downregulating *dsx* specifically in adult male ECs (*mex1ts>dsxRNAi*), which also reduced the number of LDs in the R4 region (Fig. 4.2). Hence,

in a male midgut, Dsx appears to be regulating the levels of lipid droplets in enterocytes cell autonomously.

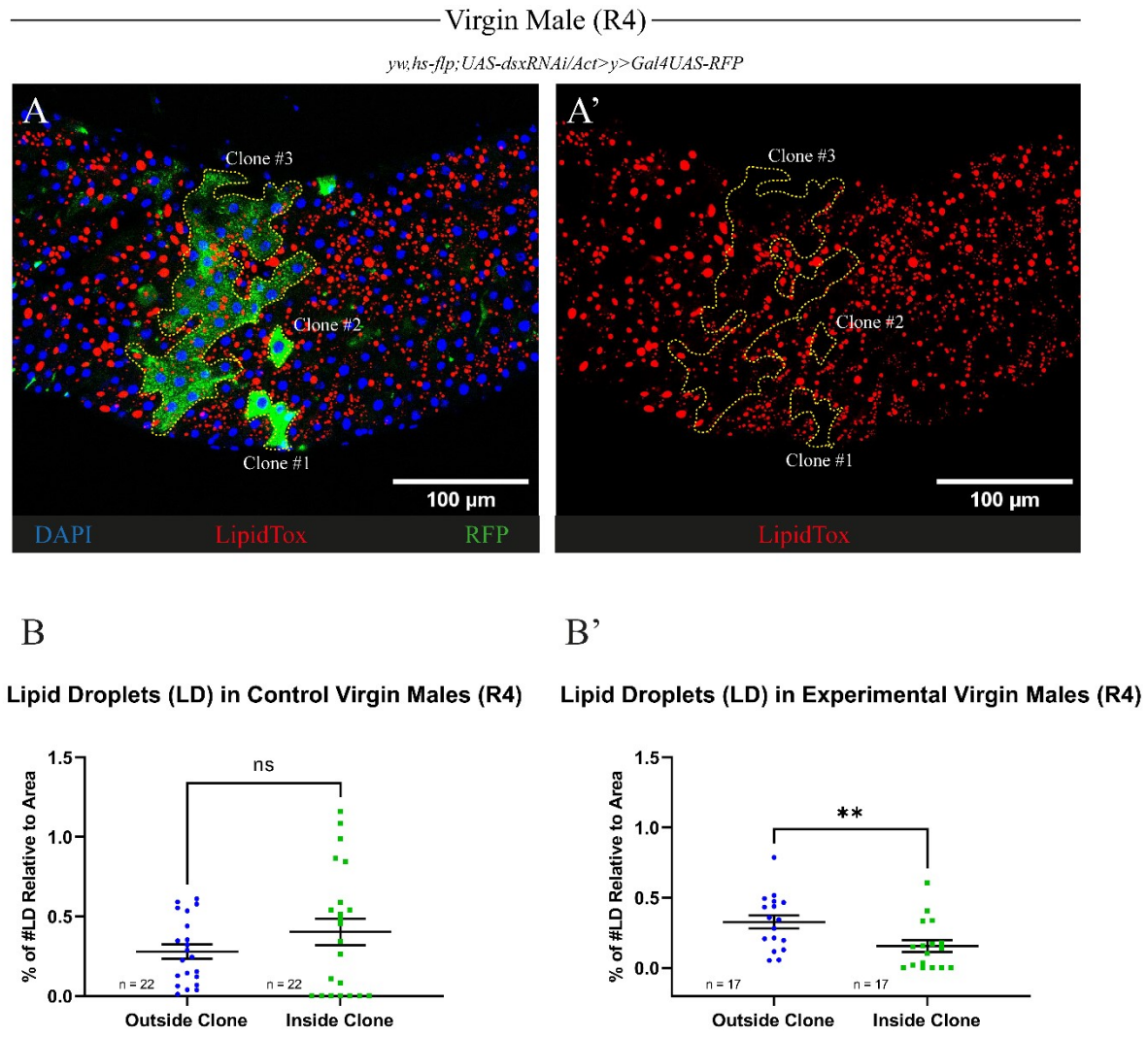

Figure 4.3: Mosaic *dsx* downregulation in a clonal manner shows reduction of LDs as cell-autonomous

Adult and mosaic-specific downregulation of *dsx* in the male R4 region reduces the number of LDs. (A) Posterior R4 midgut of an experimental virgin male. In a heat-shock manner, recombination occurs in a small subset of cells (cells from the three green clones inside the dashed yellow line), which produces the expression of Gal4. Subsequently, Gal4 turns on the expression of *dsxRNAi* and RFP (used as a control for the recombination event by marking the clones). Therefore, *dsx* is specifically downregulated in the RFP^+ clones (RFP is false coloured in green to maintain LDs in red throughout the thesis). The *yw,hs-flp;UAS-dsxRNAi/Act>y>Gal4UAS-RFP* virgin male flies were reared at 25°C and aged 4-5d to allow for post-eclosion gut growth (O'Brien, Soliman et al. 2011). Then, heat shock was induced for 15 min at 37°C. Experimental flies were transferred to 29°C for RNAi induction for 4-5 days. (A') Same experimental male R4 region with three clones (dashed yellow line), which shows fewer LDs (red) inside the clones. DAPI in blue, LDs LipidTox in red, RFP in green. Scalebars included in the images. (B) Quantification of LDs relative to the area outside (blue) *vs* inside (green) the clone in control flies. No significant changes are observed in the control clones. N=22 clones quantified. (B') Quantification of LDs relative to the area outside (blue) *vs* inside (green) the clone in experimental flies. Downregulation of *dsx* (inside clone in experimental flies) reduces the number of LDs in a cell-autonomous manner. N=17 clones quantified. Number of LDs quantified are plotted as: percentage of the number of LDs inside (or outside) the clone divided by the area of the clone (or outside the clone). Results are shown as mean ±SEM. P-value < 0.05 with Mann-Whitney test.

4.2.3 Changes in midgut lipid droplets upon *dsx* overexpression

Having assessed lipid levels upon *dsx* downregulation (both in a whole-midgut and in a mosaic manner), I investigated the effects of *dsx* overexpression on LDs.

First, I validate the genetic tools for *dsxF* and *dsxM* overexpression in the ECs. Second, I observe the changes in the amounts of LDs of virgin male midguts, as well as virgin female, upon these *dsx* genetic manipulations.

4.2.3.1 *doublesexF* and *doublesexM* overexpression in adult enterocytes

The publicly available Bloomington line #44223 has *dsxF* inserted under the UAS promoter in the 3rd chromosome. The line BL#44224 has UAS-*dsxM* in the 2nd chromosome (see Materials & Methods). Both UAS-*dsxF* and UAS-*dsxM* constructs contain the sex-specific coding sequence of *dsx*, and despite not having 5'UTR, a residual fragment of the 3'UTR was detected by sequencing (data not shown). Before addressing the changes at the phenotypical level, I first validated the overexpression in adult ECs of these two lines at the protein and transcript level.

On the one hand, I confirmed Dsx protein expression in adult midguts. In ECs of virgin males and females, I visualised Dsx (using anti-Dsx antibody) upon both *dsxF* and *dsxM* overexpression in the ECs (Fig. 4.4 A-D'). Because neither the experimental set-up nor the image acquisition settings were shared across samples, protein levels should not be compared. Experimental flies were raised and aged as adults for 4-6d at 18°C and then shifted to 29°C to induce transgene expression. Unlike in most of the experiments (see Materials & Methods), in this set of immunostainings the midguts were dissected after 7 or 10 days at 29°C (*mex1^{ts}>dsxF* males and females, as well as *mex1^{ts}>dsxM* males were dissected after 10d; whilst *mex1^{ts}>dsxM* females were dissected after 7d).

On the other hand, I checked the levels of *dsx* transcript (experimental set-up as detailed in Materials & Methods). In brief, in virgin female and male midguts, overexpression of *dsx* (either *dsxF* or *dsxM*) increased *dsx* mRNA (either with or without statistical significance), confirming the validity of these fly lines (Fig. 4.4E-E'). This was also observed when using *dsx* sex-specific primers: *dsxF* was high in *mex1^{ts}>dsxF* females, whereas *dsxM* was increased in female *mex1^{ts}>dsxM* (Fig. 4.4E''-E''').

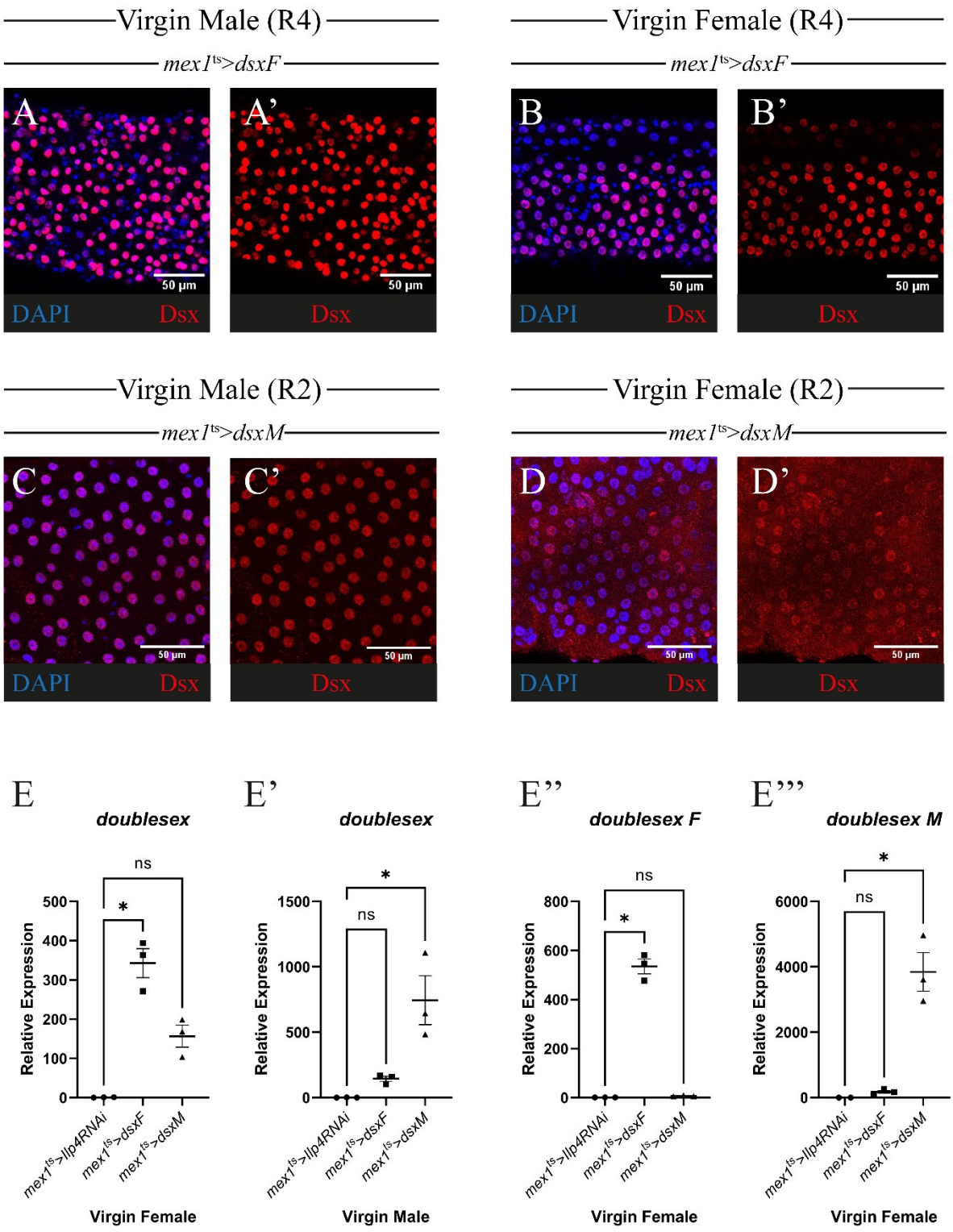

Figure 4.4: Validation of *mex1^{ts}>dsxF* and *mex1^{ts}>dsxM* experimental lines in virgin male and female adult midguts

Validation at the protein level of *dsx* overexpression in adult ECs: *mex1^{ts}>dsxF* in the R4 of virgin male (A-A') and female (B-B'), and *mex1^{ts}>dsxM* in the R2 of virgin male (C-C') and female (D-D') adult midguts. Detection of Dsx in the polyploid enterocytes. DAPI in blue, anti-Dsx in red. Scale bars stated in the immunostaining images. Of note, experimental flies were dissected after 7d (female *mex1^{ts}>dsxM*) or 10d (*mex1^{ts}>dsxF* and male *mex1^{ts}>dsxM*) at the permissive temperature (29°C). *doublesex* expression in virgin female (E) and virgin male (E') control *mex1^{ts}>Ilp4RNAi, mex1^{ts}>dsxF* and *mex1^{ts}>dsxM* adult midguts. In both sexes, *dsx* overexpression

increases *dsx* transcript when compared with the control (either statistically significant or showing an increasing trend). In females, *mex1^{ts}>dsxF* show higher levels of *dsx* than *mex1^{ts}>dsxM*. In males, *mex1^{ts}>dsxM* guts have higher amounts of *dsx* mRNA than *mex1^{ts}>dsxF*. (E'') Transcript levels of sex-specific *dsxF* isoform in virgin females upon *dsx* manipulations. *dsxF* is dramatically increased in *mex1^{ts}>dsxF* females. (E''') *dsxM* transcript increases in *mex1^{ts}>dsxM* virgin females. Sample (n=3) normalised to the housekeeping *Vha100-4*. Relative expression values are calculated against one sample control as reference. Results are shown as mean ±SEM. P-value < 0.05 with Kruskal-Wallis test.

Interestingly, *dsx* transcript expression was highest in *mex1^{ts}>dsxF* of female midguts, and *mex1^{ts}>dsxM* of male guts (Fig. 4.4E-E'). Also, the same fly line analysed in the two different sexes, showed different *dsx* levels of expression (*mex1^{ts}>dsxF* (or *dsxM*) had different levels of *dsxF* (or *dsxM*) in females than males). This might hint towards a sex-specific pre-transcriptional or post-transcriptional regulation: the optimal situation of *dsx* transcription is achieved when the sex of the transcript and the sex of the midgut correlate. Noteworthy, the overall levels of *dsx* transcript were higher in male midguts, which might be due to the wild-type presence of *dsx* in the males (Fig. 4.4E-E').

In conclusion, I confirmed that the two overexpression lines lead to expression of the two Dsx isoforms (male and female) both at transcriptional and protein levels in the enterocytes of both male and female flies.

4.2.3.2 Changes in LDs upon *dsxF* and *dsxM* overexpression in ECs

Having confirmed successful overexpression, I examined the amount of lipid droplets of both virgin male and virgin female adult midguts by LipidTox staining.

In the R4 of virgin males, *dsxM* overexpression in the ECs pointed towards a reduction of LDs: 26 out of the 33 *mex1^{ts}>dsxM* midguts showed lack of LDs (values in Y axis equal zero) (Fig. 4.5A, A'', B'). However, 2 out of the 33 samples (belonging to the same independent replicate) had very high amounts of LDs. This might explain why, when comparing the changes in LDs between the control *mex1^{ts}>Ilp4RNAi* and *mex1^{ts}>dsxM*, there was a statistically significant overall increase in lipids upon *dsxM* overexpression (~100% *vs* ~112%). Upon removal of the two samples, there was a statistically significant reduction in the R4 of *mex1^{ts}>dsxM* virgin males (~100% *vs* ~20%). To reach a clear conclusion, either more experimental replicates should be analysed or further statistical tests applied.

dsxF overexpression in the ECs seemed not to statistically change the numbers of LDs in the R4 region of virgin males (Fig. 4.5A, A', B'). However, virgin *mex1^{ts}>dsxF* males had lipids in the R2 (Fig. 4.5B). Thus, overexpression of *dsxF* in the male ECs appeared to "feminise" a

male midgut by recapitulating the female regionality of LDs (apparent in both R2 and R4) (Fig. 4.1 and Fig. 4.5B).

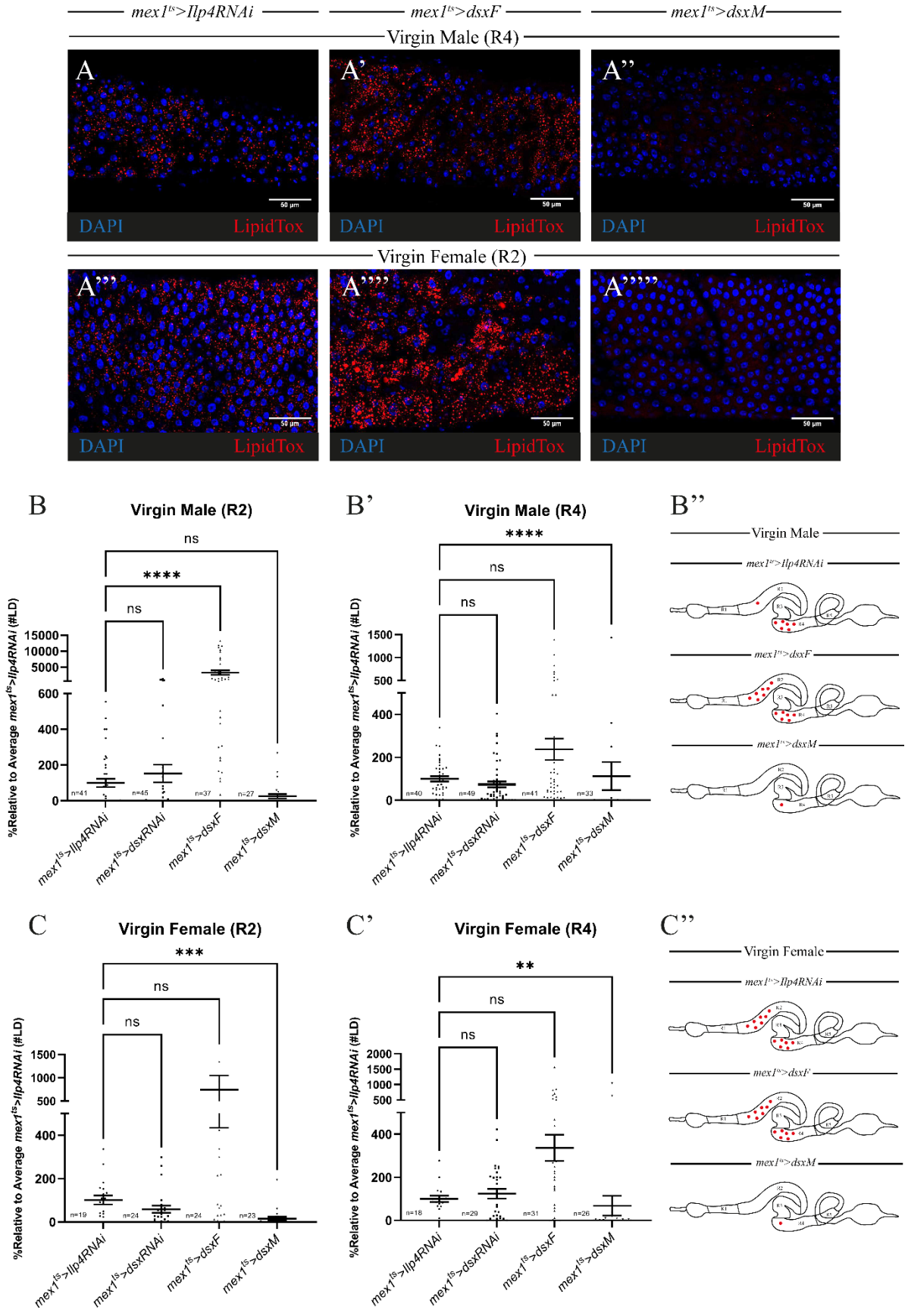

Figure 4.5: LD sexual dimorphism in the adult midgut is lost upon *dsxM* and *dsxF* overexpression in the adult ECs

LipidTox stainings of a virgin male R4 control *mex1^{ts}>Ilp4RNAi* (A), *mex1^{ts}>dsxF* (A') and *mex1^{ts}>dsxM* (A''), as well as of a virgin female R2 control *mex1^{ts}>Ilp4RNAi* (A'''), *mex1^{ts}>dsxF* (A'''') and *mex1^{ts}>dsxM* (A'''''). DAPI in blue, LipidTox in red. Scale bars stated in the immunostaining images. Quantification of LDs in the R2 (B) and R4 (B') of virgin male *mex1^{ts}>Ilp4RNAi, mex1^{ts}>dsxRNAi, mex1^{ts}>dsxF* and *mex1^{ts}>dsxM.* (B'') Cartoon illustrating the lipid profile in control males (by the presence of LDs in R4 only), in *mex1^{ts}>dsxF* males (by the gain of LDs in R2) and in *mex1^{ts}>dsxM* males (by the loss of LDs in R4). Quantification of LDs in the R2 (C) and R4 (C') of virgin female *mex1^{ts}>Ilp4RNAi, mex1^{ts}>dsxRNAi, mex1^{ts}>dsxF* and *mex1^{ts}>dsxM*. (C'') Cartoon showing LDs in control females (LDs both in R2 and R4), *mex1^{ts}>dsxF* females (both in R2 and R4) and *mex1^{ts}>dsxM* females (LDs absent from R2). Number of midguts analysed per category is stated in the graph (n=18-49). Values are plotted relative to the average of LD particles of the *mex1^{ts}>Ilp4RNAi* control per each experimental day. Results are shown as mean ±SEM. P-value < 0.05 with Kruskal-Wallis test. Lipid droplets are illustrated as red circles, and regions R1-R5 annotated within the midgut.

In the R4 of virgin females, *dsxM* overexpression showed a reduction of LDs (Fig. 4.5C'). In the R2, *mex1^{ts}>dsxM* had smaller numbers of LDs (Fig. 4.5A''', A''''', C), which resembled a wild-type male (Fig. 4.1). Thus, overexpression of *dsxM* in the female ECs seemed to "masculinise" the lipid profile by reducing the number of LDs in R2 (Fig. 4.5C).

In summary, upon *dsxM* overexpression in ECs, female midguts showed reduction of LDs in R4 and R2. Although further analyses are required, the same trend was observed in the R4 of *mex1^{ts}>dsxM* virgin males (26 out of 33 midguts). Males with *dsxF* overexpression had lipids in the R2 (Fig. 4.5B'', C''). Therefore, based on the effects on LDs in the R2 region (in which the presence of LDs is normally sexually dimorphic), I suggest that *mex1^{ts}>dsxF* might "feminise" a male midgut, and *mex1^{ts}>dsxM*, "masculinise" a female midgut.

4.2.4 Effects of *dsx* manipulations on peripheral lipid stores

In the previous sections, I have shown that the lipid accumulation in adult midguts varies according to the *dsx* manipulations in the ECs. LipidTox staining allowed me to visualise a snapshot of the LDs present in the midgut at a certain time. However, lipid homeostasis comprises a fine balance of several metabolic processes (see Introduction). Changes in the midgut LDs may result from differential food intake, lumen digestion and absorption, lipolysis, lipogenesis, transport to other organs, and/or differential rate of excretions (see Introduction). In this section, I seek to see whether midgut LDs accumulation is positively or negatively correlated with changes in peripheral fat stores. To do so, I used Thin Layer Chromatography (TLC) to quantify the level of peripheral triacylglycerol (TAG) by two different approaches (Fig. 4.6). On the one hand, I quantify the peripheral TAG of flies from which I have previously removed the gonads (Fig. 4.6A, B, C). Consequently, I can evaluate the total lipid content without any potential confounds of egg production/egg retention. On the other hand, to assess

how the changes observed in the midgut LDs relate to lipid levels in the whole fly, I measure the amount of TAG of flies from which I have discarded the midgut (Fig. 4.6A', B', C').

In virgin males, the levels of TAG did not change between *mex1^{ts}>Ilp4RNAi, mex1^{ts}>dsxRNAi, mex1^{ts}>dsxF* and *mex1^{ts}>dsxM* with only gonads removed (Fig. 4.6B). When I removed the midgut, the only effect I observed was *mex1^{ts}>dsxF* virgin males, in which peripheral TAG was reduced (Fig. 4.6B'). Since more LDs were apparent in both R2 and R4 midgut regions in these males with "feminised" ECs (Fig. 4.5B-B''), this observation suggests that lipids from the diet and/or resulting from intestinal lipogenesis maybe absorbed/produced in ECs at a higher rate than they are exported, leading to their accumulation in ECs (Fig. 4.6B').

In virgin females with only gonads removed, the levels of TAG did not change between *mex1^{ts}>Ilp4RNAi, mex1^{ts}>dsxRNAi, mex1^{ts}>dsxF* and *mex1^{ts}>dsxM* (Fig. 4.6C). Removal of the midgut revealed that peripheral TAG levels were increased in *mex1^{ts}>dsxM* flies. Since in the midgut of *mex1^{ts}>dsxM* virgin females, there was a reduction of LDs (Fig. 4.5C-C''), this points to the reverse situation to that described above for male with feminised ECs: namely, in females flies with masculinised ECs, increased lipid efflux from ECs relative to their absorption/synthesis may result in selective depletion of LDs from ECs relative to the periphery.

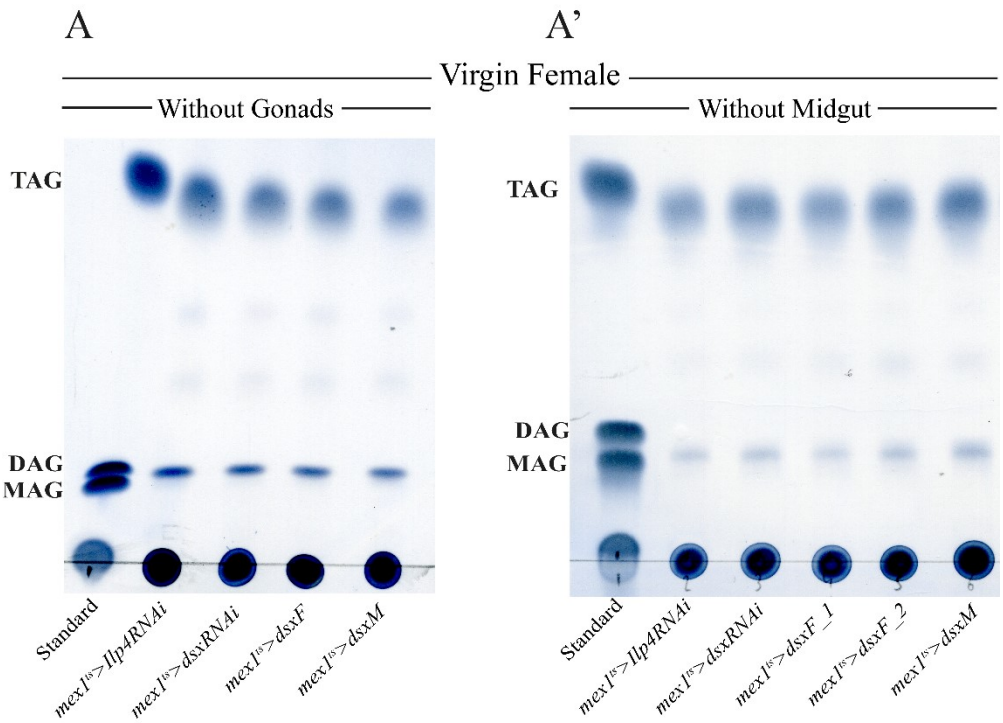

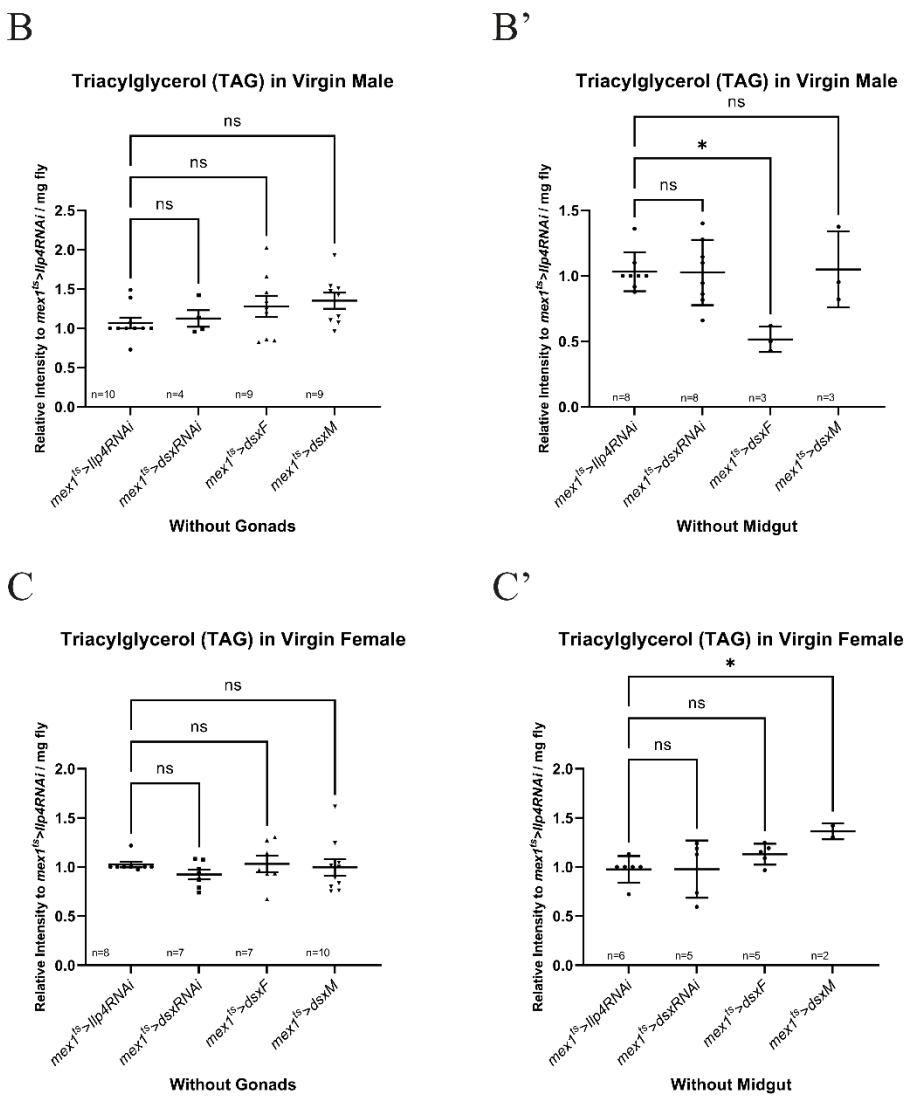

Figure 4.6: Changes in TAG in virgin male and female adult flies, without gonads or without midgut

Example of TLC of whole-fly virgin females without gonads (A) or without midgut (A'). Standard shows the migration height of monoacylglycerides (MAG), diacylglycerides (DAG) and triacylglycerides (TAG). Samples are: *mex1^{ts}>Ilp4RNAi* (control), *mex1^{ts}>dsxRNAi*, *mex1^{ts}>dsxF*, *mex1^{ts}>dsxM* (experimental). (B) Quantification of TAG in virgin males without gonads. (B') Quantification of TAG in virgin males without midgut. (C) Quantification of TAG in virgin females without gonads. (C') Quantification of TAG in virgin females without midgut. In the X axis, the control and the experimental genotypes. In the Y axis, the relative intensity to control flies normalised by the weight (see Materials & Methods). Number of samples in the graph shows the number of replicates (n=2-10), which consist of groups of 4 females or 5 males. Results are shown as mean ±SEM. P-value < 0.05 with Kruskal-Wallis test.

In summary, upon *dsxM* overexpression in the ECs, females reduced LDs in both R4 and R2, and the same trend seem to be true for the male R4 region (26 out of 33 midguts analysed had absence of LDs). The levels of TAG in males were not affected, but female flies with the midgut removed showed an increase in whole-body lipids. Upon *dsxF* overexpression in the

ECs, males gained LDs in the R2, resembling a wild-type female. This fat retention in the midgut was also observed by the TLC: *mex1*^{ts}>*dsxF* males without midgut had lower TAG.

4.2.5 Dsx regulates lipid metabolism via CG17192 lipase

In the previous chapter, my data pointed to links between Dsx and sex differences in lipid metabolism at the transcriptional level (see Results I). At the beginning of this chapter, I have validated these links at the physiological level. In this section, I focus on understanding the molecular mechanisms by which, directly or indirectly, *dsx* in ECs might contribute to sex differences in lipid metabolism. Doublesex is a zinc-finger transcription factor which might directly bind to the regulatory regions of genes coding for proteins with roles in lipid metabolism.

One such gene was *CG17192*, coding for a recently characterized extracellular midgut TAG lipase involved in lipid catabolism (Praggastis, Lam et al. 2021). I chose to investigate the role of this lipase, under the regulation of *dsx* because: a) it is one of the top genes which was particularly upregulated in *mex1*^{ts}>*dsxRNAi* males, b) it is one of the highest female-biased genes in the midgut (from both the RNA-seq of this study and the previously published RNA-seq in Hudry, Khadayate et al. 2016), c) its robust adult midgut-specific expression (FlyBase) and because d) its role in lipid digestion and catabolism (Praggastis, Lam et al. 2021).

Additionally, *CG17192* belongs to a cluster of expected lipase genes. Interestingly, this cluster in located in the *RYa-R* (receptor of neuropeptides RYamide-1 and -2) locus, which might be involved in supressing feeding behaviour (Ida, Takahashi et al. 2011). Horne and Haritos examined this highly dynamic genome section which has undergone multiple tandem duplication events. This cluster is conserved in other *Drosophila* species. The authors propose that the lipase cluster has been evolutionary dynamic to adapt to lipid changes in the diet (e.g. by changing the residues adjacent to the serine in the catalytic site of these lipases) (Horne and Haritos, 2008). Additionally, we have noticed that there seems to be temporal specificity in the expression of these lipases: a few lipases are larval-specific (e.g. CG6271) whereas others are adult-specific (cluster II lipases, such as CG17192) (FlyBase). Furthermore, CG17192 in flies is orthologous to human lipase H (LIPH), lipase I (LIPI) and phospholipase A1 member A (PLA1A) (Alliance of Genome Resources, v4.1.0, FB: FBgn0039472).

4.2.5.1 *CG17192* expression in the midgut

Prior to studying the effects of Dsx on *CG17192*, I started by characterizing the expression of *CG17192* in the adult midgut. In the previous chapter I have shown that *CG17192* is much higher in females (in both my control RNA-seq and in the RNA-seq published in Hudry, Khadayate et al. 2016) and its expression levels change upon *dsx* regulation. By RNA-seq I have observed that *CG17192* levels are upregulated in both male and female *mext1^{ts}>dsxRNAi*, and while non-statistically significant, I have observed the same trends by qPCR (Fig. 3.8C'-C''). In FlyBase, CG17192 is shown to be midgut-specific; and by the high levels of expression, we would predict that is expressed in the ECs.

I began by investigating the levels of the protein along the midgut. To do so, I made use of a fosmid line that was generated in the lab by Bruno Hudry (see Materials & Methods). This genetic fly line consists of a GFP fused to the gene, which is inserted to a specific landing site of the genome (Sarov, Barz et al. 2016). Therefore, in addition to the wild-type CG17192, there is CG17192-GFP from the non-endogenous locus. Unfortunately, I did not detect any GFP signal from the CG17192 fosmid line, neither endogenous GFP nor anti-GFP (data not shown, corroborated by Bruno Hudry, personal communication). This could be because the predicted lipase is a small peptide, and the fusion with a GFP is affecting the folding of the protein (even though it is already linked to a small GFP). Also, the addition of GFP could be affecting its secretion. Alternatively, the site of insertion of CG17192-GFP could be giving very weak expression. Overall, the fosmid line was not informative, thus failing to conclude about the CG17192 protein levels in the midgut.

As an alternative, I focussed on exploring possible regional differences at the transcriptional level and the putative *dsx*-dependent regulation.

Firstly, I characterised *CG17192* regional expression by comparing mRNA levels between the anterior (R2) and posterior (R4) midgut by qPCR. The adult female and male wild-type midguts did not show any differences between the housekeeping genes *rp49* and *Vha100-4* when comparing the anterior R2 *vs* the posterior R4 region (Fig. 4.7A-A''''). Hence, these genes were used to normalise the levels of expression of *CG17192* in R2/R4 regions (Fig. 4.7B-B'). In both Oregon R male and female adult midguts, *CG17192* showed a non-statistically significant higher expression in the anterior region R2 than R4 (Fig. 4.7B, B'). This is in agreement with the prevailing idea that lipid breakdown occurs preferentially in the anterior midgut, whereas lipid synthesis tends to be confined to the posterior midgut (see Introduction).

Furthermore, in the single-cell RNA-seq of the gut published recently (Hung, Hu et al. 2020), *CG17192* is higher in the anterior ECs, which is aligned with my qPCR findings. Secondly, I analysed the changes of *CG17192* expression in the R2 region upon *dsx* manipulations in the adult ECs of the midgut (Fig. 4.7C-C'). From the RNA-seq, *CG17192* showed upregulation in *mex1^{ts}>dsxRNAi* males and females. In the R2 of virgin males, *CG17192* did show a trend of upregulation upon *dsx* knock-down in ECs, although not statistically significant (Fig. 4.7C). This might be explained by the different sensitivity of qPCR *vs* RNA-seq, as well as low numbers of replicates and/or variation between replicates in the qPCR. Additionally, in the R2 region of males, levels of *CG17192* were unchanged upon *dsxF* overexpression in ECs (Fig. 4.7C) but showed a decreasing trend in *mex1^{ts}>dsxM* (Fig. 4.7C). To summarise, in the R2 of virgin males, *CG17192* seems to be upregulated under *dsx* knock-down, and downregulated under *dsxM* overexpression (although more replicates are required to validate the statistical significance). Thus, this might point towards Dsx negatively regulating *CG17192* expression in the midgut. In the R2 of virgin females, only *mex1^{ts}>dsxM* modified *CG17192* transcription, by reducing its levels (same as in the R2 of males) (Fig. 4.7C'). Nonetheless, these results are not to be fully trusted because the levels of the housekeeping genes (*rp49* and *Vha100-4*) changed in the R2 of *mex1^{ts}>dsxM* compared to the control *mex1^{ts}>Ilp4RNAi* in virgin females (Fig. 4.7C'').

To extend the knowledge behind the sexual dimorphism of *CG17192* regulation, I checked its levels of transcription in females with *tra* knock-down in ECs. *mex1^{ts}>traRNAi* females have "masculinised" ECs: without Tra, DsxF is not produced, and the default DsxM is expressed instead (see Introduction). In the midgut of *mex1^{ts}>traRNAi* females, I observed a non-statistically significant increase in *dsx* transcription, consistent with the wild-type scenario in males (Fig. 4.7D). Remarkably, *CG17192* mRNA levels showed a non-statistically significant downregulation in "masculinised" virgin females (Fig. 4.7D'). Thus, mimicking the sexual dimorphism in wild-type males (higher in females than in males).

To summarise, *CG17192* seemed to be region-specific in the midgut, higher in R2, and under the transcriptional control of Dsx: downregulation in ECs increased *CG17192* transcription (from the RNA-seq in this study), whilst *dsxM* overexpression decreased *CG17192* mRNA levels (trend from qPCR in Fig. 4.7C). Also, in females with Tra reduction in ECs, the levels of *CG17192* show a non-statistically significant reduction, similarly to a wild-type male. Thus, I hypothesise that Dsx is negatively regulating the expression of the lipase *CG17192* in the enterocytes, specifying its sexual dimorphism. In females, in which there is absence of Dsx,

the lipase is highly expressed. In males, because of the presence of Dsx, the *CG17192* levels are reduced.

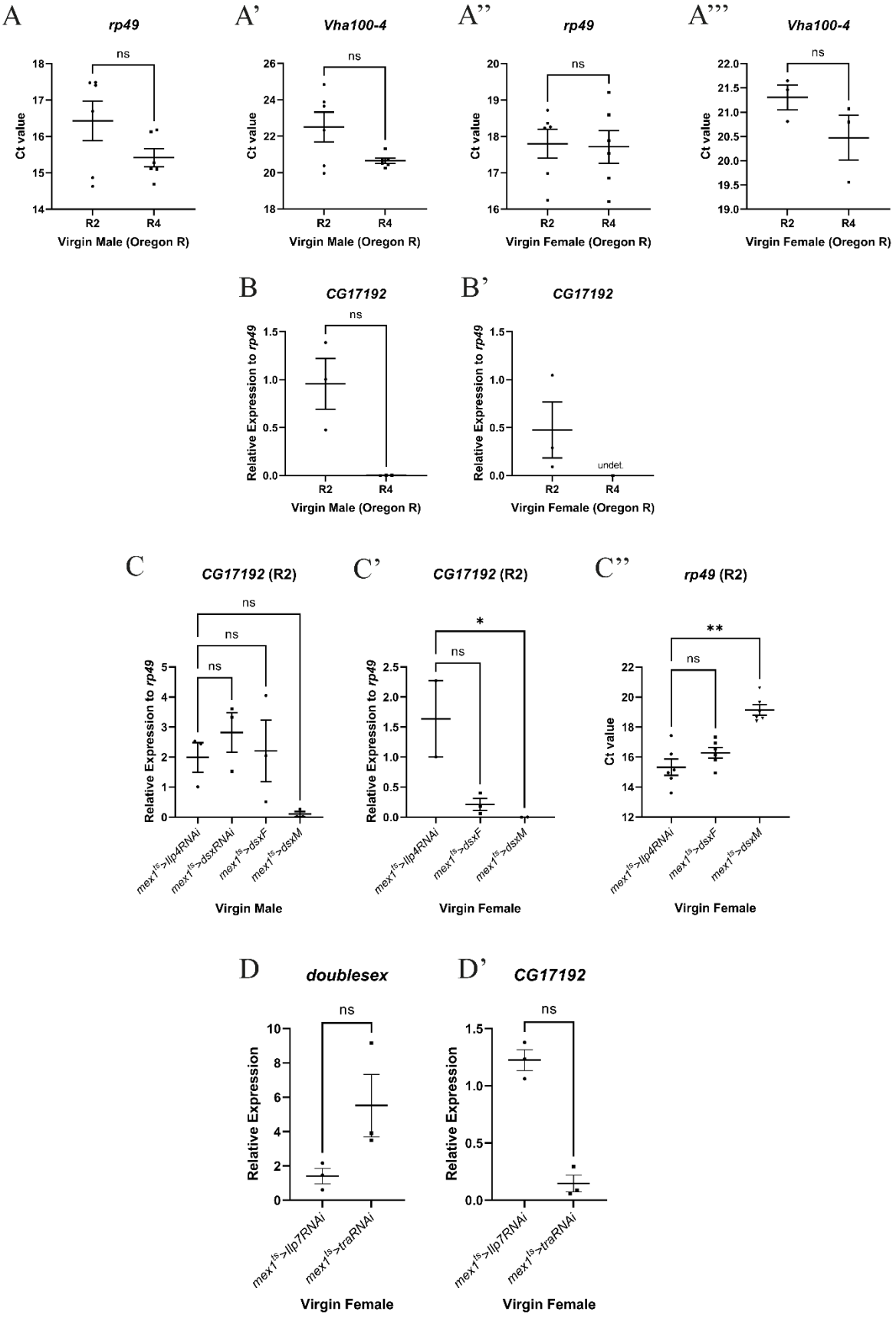

Figure 4.7: *CG17192* expression levels are region-specific in the adult midgut of male and female flies and regulated by *dsx* and *tra* manipulations in ECs

The expression level of the *rp49* housekeeping gene does not change between the anterior (R2) and posterior (R4) region of the adult midgut both in wild-type (Oregon R) males (A) and females (A''). The same is observed for the housekeeping gene *Vha100-4* in males (A') and females (A'''). *CG17192* show region-specific expression in wild-type males and females. *CG17192* mRNA seems more abundant in the anterior (R2) region of adult virgin male (B) and female (B') wild-type, although non-statistically significant. (C) Levels of *CG17192* upon *dsx* down/upregulation in the R2 of virgin males. In $mex1^{ts}$>*dsxM* there is a descending trend of *CG17192* expression in the anterior adult midgut. (C') Levels of *CG17192* (in R2) of virgin females upon *dsx* downregulation and *dsxF*/*dsxM* upregulation in adult ECs. A statistically significant reduction in *CG17192* expression is observed in the R2 of $mex1^{ts}$>*dsxM* females. There is a non-statistically significant reduction of *CG17192* in $mex1^{ts}$>*dsxF* females. Because of the high SEM of $mex1^{ts}$>*Ilp4RNAi* control samples, and the variation of housekeeping *rp49* gene expression between conditions (C''), no strong conclusion can be drawn from the female R2 samples. (D) *doublesex* increasing trend in $mex1^{ts}$>*traRNAi* virgin females. (D') *CG17192* is downregulated (although non-statistically significant) upon *tra* knock-down in the ECs of virgin females. Raw Ct values from the qPCR plotted in A-A''' for *rp49* and *Vha100-4* genes. N= 3 (two technical replicates per condition except for *Vha100-4* in virgin females). In B and B' (n=3), samples are normalised to the housekeeping gene *rp49*. Same results are obtained against *Vha100-4* (data not shown). In C-C' the normalisation is against *rp49* (n=3 samples). In C'', raw Ct values from the qPCR are plotted (n=3 and two technical replicates per condition). For both C-C', the same results are observed with *Vha100-4* (data not shown). In D-D', n=3 samples are normalised to *Vha100-4*. For all the conditions with relative expression, the values are calculated against one sample control as reference. Results are shown as mean ±SEM. P-value < 0.05 with Mann-Whitney test (A-A''', B-B', D-D') or with Kruskal-Wallis test (C-C'').

Subsequently, I investigated whether interfering with the expression of the *CG17192* lipase shows any effects on lipid homeostasis. This could shed some mechanistic light on the role of Dsx in regulating lipid homeostasis.

4.2.5.2 CG17192 regulates lipid content

CG17192 is a recently characterized midgut-specific lipase (Praggastis, Lam et al. 2021). Based on its amino acid sequence, it may be secreted to the extracellular space. Thus, it is potentially released by the enterocytes into the midgut lumen for lipid digestion, specifically in the anterior R2 midgut. In this section, I validate and further examine whether CG17192 influences lipid homeostasis. As for the approach undertaken to describe the physiological roles of *dsx* in lipid metabolism, I quantified both the LDs in the midgut and the whole-body TAG upon *CG17192* knock-down in adult ECs (Figure 4.8).

First, I validated the publicly available Bloomington *CG17192* RNAi line, by knocking-down its expression in the adult ECs by using $mex1^{ts}$ as a driver (Fig. 4.8A). I tested the experimental set-up in virgin females because the levels of *CG17192* are sexually dimorphic and higher in female midguts. I observed a strong reducing trend of its mRNA upon RNAi in ECs (Fig. 4.8A), which confirmed the utility of this reagent and further suggested that *CG17192* is expressed in the ECs.

Second, I quantified the number of LDs in the R2 and R4 region of females (Fig. 4.8C-C'), as well as in the R4 region of males (Fig. 4.8C''), upon *CG17192* knock-down in adult ECs. Neither the anterior (R2) female nor the posterior (R4) male midgut showed any variation in the number of LDs (Fig. 4.8C, C''). However, *mex1^{ts}>CG17192RNAi* females had lower LDs levels in the R4 region (Fig. 4.8C').

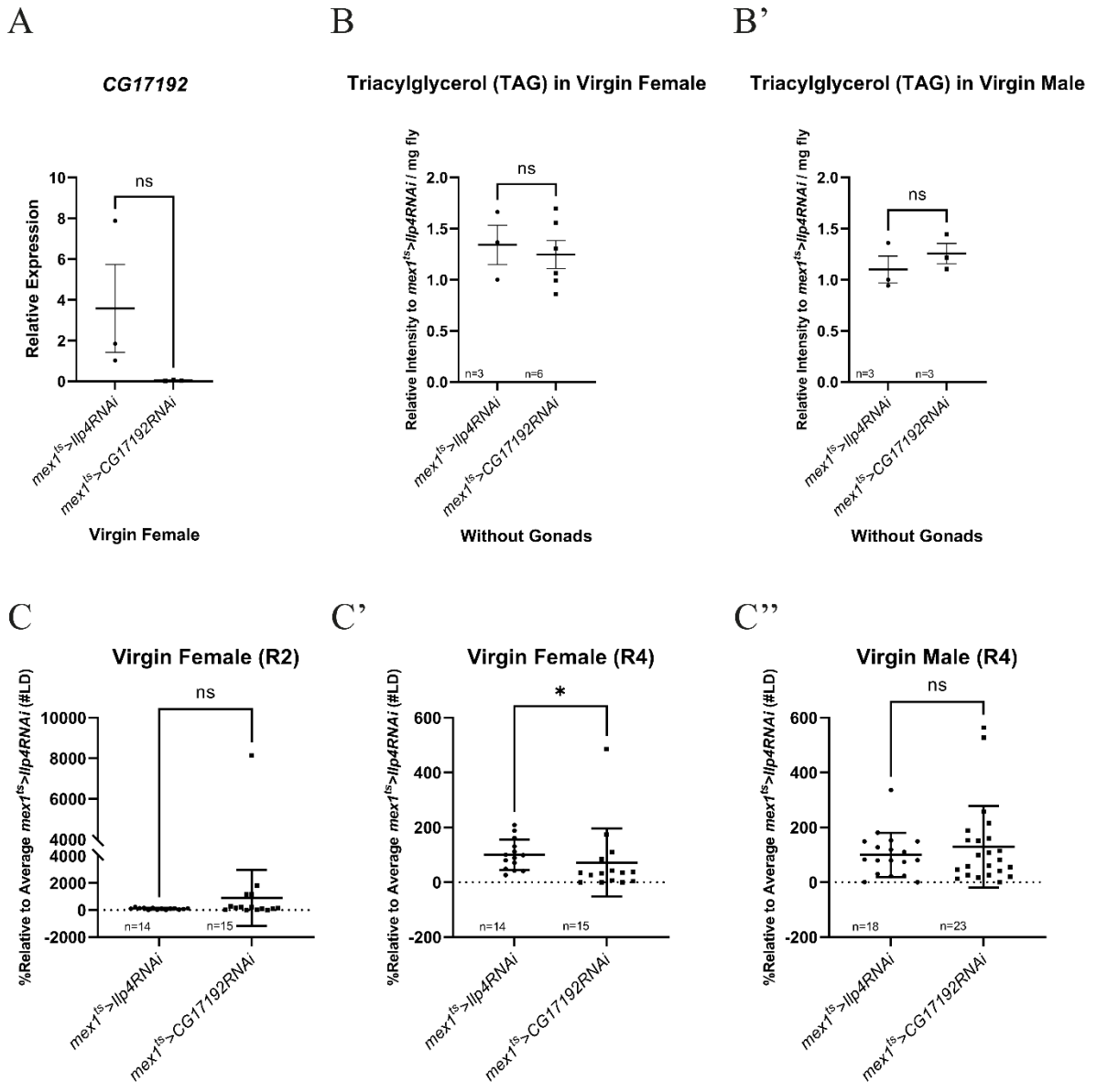

Figure 4.8: Changes in whole-fly TAG and midgut LDs in virgin female and male upon *CG17192* downregulation in adult ECs

(A) Midguts of *mex1^{ts}>CG17192RNAi* virgin females show a non-statistically significant decrease of *CG17192*. N=3, normalised to *Vha100-4* and relative to one sample control. Quantification of *mex1^{ts}>CG17192RNAi* virgin females (B) and males (B') without gonads. In the X axis, the genotypes. In the Y axis, the relative intensity to control *mex1^{ts}>Ilp4RNAi* flies normalised by the weigh. Number of samples in the graph shows the number of replicates (n=3-6), which consists of 4 females or 5 males. Quantification of LDs in the midgut epithelium in the R2 (C) and in the R4 (C') of virgin females, as well as in the R4 (C'') of virgin males upon *CG17192* knock-down in adult ECs. Number of midguts quantified per condition is stated in each graph (n=14-23). Values are plotted

relative to the average of LDs particles of the *mex1^{ts}>Ilp4RNAi* control per each experimental day. In all the graphs (A-C''), results are shown as mean ±SEM. P-value < 0.05 with Mann-Whitney test.

Third, I examined the amount of fat in *mex1^{ts}>CG17192RNAi* virgin females (Fig. 4.8B) and males (Fig. 4.8B'), both in the midgut and in whole-body (by conducting TLC of flies with gonads removed). Flies which had the gonads previously removed showed no statistically significant changes in TAG upon *CG17192* downregulation in adult ECs. If anything, there seems to be a minor female-specific downregulation of TAG levels, and an upregulation in males.

From these results, together with the established regionality of lipid homeostasis in the midgut (see Introduction), I hypothesise that CG17192 is secreted in the R2 region to break down ingested lipids which are further absorbed (and possibly retained) in the R4 region. Because *CG17192* is higher in females, it might explain why the R4 reduction in LDs is female-specific. Consistent with this hypothesis, I would have expected a decrease in whole-body fat of *mex1^{ts}>CG17192RNAi* females, as a consequence of the decreased intestinal digestion and absorption. Nevertheless, I did not observe statistically significant differences in whole-body fat upon *CG17192* knock-down in adult ECs. This might be due to the sensitivity of the technique, the variation within replicates and/or the low number of replicates in some conditions. Interestingly, the above-mentioned recent study showed reduction of whole-body TAG in *mex>CG17192RNAi* flies (Praggastis, Lam et al. 2021). The authors quantified TAG by a previously described colorimetric assay (Tennessen, Barry et al. 2014) and *CG17192* knock-down was not adult-specific (but throughout development). These differences could explain why in *mex1^{ts}>CG17192RNAi* flies I only observe a very mild trend of TAG reduction by TLC.

4.3 Conclusion & Discussion

Collectively, my data indicates that, although Dsx affects both intestinal and peripheral TAG accumulation, it does so in a region-specific manner and may affect different aspects of how lipids are handled by the intestine.

In wild-type flies, I observed sexual dimorphism of the LDs in the midgut of virgin adult flies: females have LDs in the R2 and R4 region, whereas males only in the R4 (Fig. 4.1). This regionality seems to be under the control of Dsx in ECs. Overexpression of *dsxF* "feminised" the lipid profile in virgin males by the gain of LDs in R2. Overexpression of *dsxM* "masculinised" the lipid profile in virgin females by the loss of LDs in R2 (and through the

whole gut) (Fig. 4.5). Knock-down of *dsx* reduced the amount of lipids in the R4 region of virgin males (Fig. 4.2), which was also observed in a cell-autonomous manner by downregulation of *dsx* in a mosaic pattern (Fig. 4.3). Even though there were effects of *dsxRNAi* at the cellular and organ level, there were no changes in peripheral/whole-body TAG (Fig. 4.6). Instead, males with "feminised" ECs showed a reduction of peripheral TAG (with midgut removed) (Fig. 4.6B') and females with "masculinised" ECs had more peripheral TAG (excluding the midgut) (Fig. 4.6C'). These findings suggest that Dsx might be regulating lipid homeostasis in a sex- and region-specific manner and might influence distinct processes of intestinal lipid metabolism.

Lipid homeostasis is the result of a fine equilibrium between a complex network of different pathways: ingestion from the diet, digestion in the midgut lumen, absorption, synthesis, breakdown, systemic transport and storage. This vast network complicates the elucidation of which processes might be affected upon *dsx* manipulation in the ECs. In *mex1^{ts}>dsxF* males, high LDs numbers and low peripheral TAGs (with midgut removed) (Fig. 4.5, 4.6) could be caused by a Dsx-dependent increased lipid ingestion, impaired lipid transport to other organs, increased lipid synthesis and/or reduction of lipolysis. In *mex^{ts}>dsxM* females, low LDs numbers and high peripheral TAG (excluding midgut) (Fig. 4.5, 4.6) might be indicative of Dsx putatively regulating an increase in lipid transport from the midgut to other organs. Furthermore, even though an individual mechanism may be impaired under *dsx* regulation, other metabolic pathways could be compensating and masking the *dsx*-dependent phenotype. For example, I observed the same phenotypes (LD reduction and unchanged TAG levels) in *mex1^{ts}>dsxRNAi* and *mex1^{ts}>dsxM* virgin males (although further research is required, 26 out of the 33 midguts analysed showed lack of LDs upon *dsxM* overexpression) (Fig. 4.2, 4.3, 4.5, 4.6). This indicates that, although the snapshot of LDs is the same between the two conditions, distinct pathways are likely independently capable of generating this phenotype.

With this in mind, I complemented my data by analysing the food intake in *mex1^{ts}>Ilp4RNAi, mex1^{ts}>dsxRNAi, mex1^{ts}>dsxF* and *mex1^{ts}>dsxM* virgin females (Fig. 4.9A) and virgin males (Fig. 4.9A'). I hypothesised that an increase in food intake might result in higher LDs particles in the midgut, whilst a decrease in food intake might correlate with fewer LDs. In females, there were no statistically significant differences between experimental and control flies, suggesting that food intake is not impaired by *dsx* downregulation/upregulation in the ECs and does not contribute to *dsx*-dependent lipid homeostasis (Fig. 4.9A). In males, there was no food intake variation upon *dsx* downregulation in the ECs. Furthermore, this observation was

corroborated by using FlyPAD to quantify the number of sips, which showed similarity between the number of sips of the *mex1^{ts}>GFP* control and *mex1^{ts}>dsxRNAi* virgin males (Fig. 4.9B). Therefore, the reduction of LDs observed in male midguts with *dsx* knock-down cannot be explained by change in food intake. Nevertheless, in *mex1^{ts}>dsxF* and *mex1^{ts}>dsxM* virgin males there was an increase in food intake (Fig. 4.9A'), which could help us comprehend the lipid phenotype observed in the midgut upon *dsx* manipulations in ECs. Upon *dsxF* overexpression, there is a lipid retention in the midgut, possibly caused by an increase in food intake in males. Upon *dsxM* overexpression, there seems to be a lipid reduction in the midgut, possibly nutritionally overcompensated by increasing the food intake in males.

Another putative explanation for the reduction in LDs but unchanged TAG levels could be the frequency and/or number of excreta. In *Drosophila*, a dedicated protocol and software tool are used for the analysis of faecal outputs (Wayland, Defaye et al. 2014). I hypothesise that flies with low amounts of fat in the midgut are unable to breakdown and absorb fat correctly, thus increasing the number/frequency of excreta (showing fast lipid transit along the midgut). Additionally, we could also expect that those flies, given the fast intestinal transit, would eat more (or more frequently) to maintain their nutritional state. This could be the case for *mex1^{ts}>dsxM* males.

All these phenotypical observations lead to the following essential questions: how is Dsx regulating (in a sex-specific manner) lipid homeostasis? Which are the molecular targets involved? What metabolic pathways are impaired?

My RNA-seq experiment demonstrates that many multi-pathway lipid metabolism genes are differentially expressed upon *dsx* downregulation (Fig. 3.8). For example, there are changes in the expression of lipid transport genes, which might indicate that *dsx* is regulating fat mobilization from the gut to the periphery. *Lsd-1* (*Lipid storage droplet-1* or *plin1*), which facilitates lipid mobilization, fission and fusion, is upregulated in males upon *dsx* downregulation (and, interestingly, is sexually dimorphic with higher expression in control females). Also, *Fabp* (*Fatty acid binding protein*), which transports fatty acids to organelles (Kis, Barti et al. 2015), is upregulated in *mex1^{ts}>dsxRNAi*. Additionally, *Npc1b* (*Niemann-Pick type C1*), gene involved in sterol absorption, is also upregulated by *dsxRNAi* in ECs (and higher in control females than males). To better comprehend how Dsx establishes the sexual dimorphism of fat homeostasis, the Dsx-dependent regulation of these molecular targets, as well as their physiological contribution, require further examination.

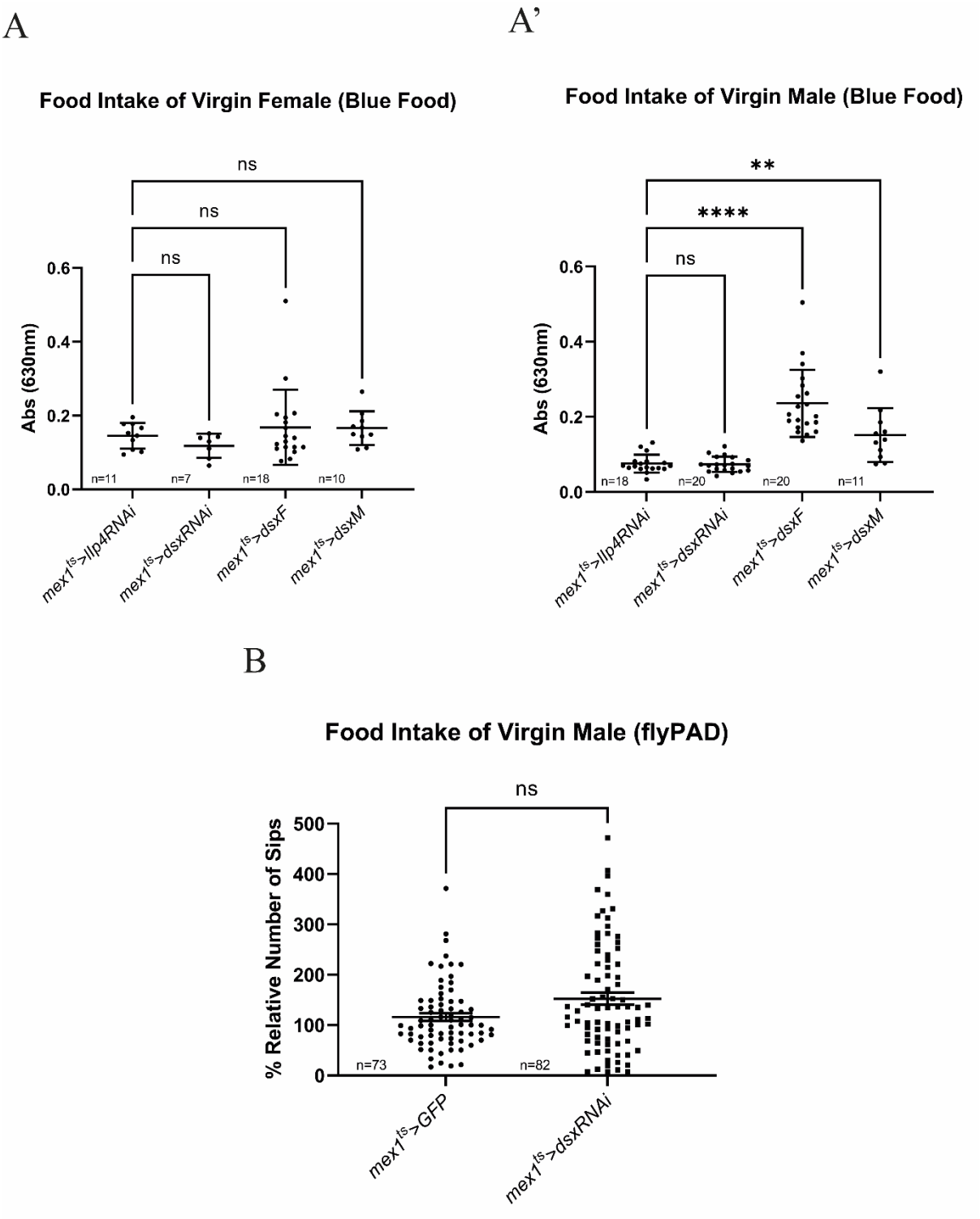

Figure 4.9: Food intake in virgin female and male upon *dsx* manipulations in ECs

Intake of blue food ingestion in virgin females (A) and males (A') of *mex1^{ts}>Ilp4RNAi, mex1^{ts}>dsxRNAi, mex1^{ts}>dsxF* and *mex1^{ts}>dsxM*. Absorbance of blue food (630nm) is shown on the Y axis. Number of replicates are stated in the graphs. Each replicate is a group of 3 flies. Results are shown as mean ±SEM. P-value < 0.05 with Kruskal-Wallis test. (B) Food intake of *mex1^{ts}>GFP* and *mex1^{ts}>dsxRNAi* virgin males, quantified via the number of sips in the FlyPAD. Number of overall flies are n=73 and n=82 across four independent experiments. Values are plotted relative to the control per each experimental day, in percentages. Results are shown as mean ±SEM. P-value < 0.05 with Mann-Whitney test.

In this chapter, I started to study the role of the CG17192 lipase as a Dsx target to regulate lipid homeostasis in a sex-biased (and region-specific) manner. *CG17192* levels are higher in females (RNA-seq from this study and from Hudry, Khadayate et al. 2016), in the anterior region of the midgut (trend from qPCR in Fig. 4.7 and in the single-cell RNA-seq from Hung, Hu et al. 2020), and in ECs (qPCR trend in Fig. 4.8). Because of the LDs reduction in the female R4 region of the midgut, I hypothesise that CG17192 is secreted in the anterior midgut, thus breaking down the dietary lipids and allowing the subsequent absorption of fatty acids at the R4 region. The sexual dimorphism of *CG17192* expression levels might contribute to females having higher amounts of fat than males. Additionally, the sexual dimorphism of Dsx might participate in establishing *CG17192* differences between males and females, and thus establishing in a Dsx-dependent manner the amount of lipids (in the midgut and whole-body). In *mex1^{ts}>dsxM* (females and possibly males), there were fewer LDs in the posterior (R4) midgut (Fig. 4.5) and a non-statistically significant reduction of *CG17192* levels (Fig. 4.7), which aligns with the LDs phenotype observed in *mex1^{ts}>CG17192RNAi* (in the R4 region of females) (Fig. 4.8). Males with *dsx* downregulation in ECs exhibited increased transcription of *CG17192*, which was consistent with "masculinised" female ECs (by *tra* knock-down) with a descending trend of *CG17192* levels (Fig. 4.7).

Recently, Praggastis et al. have also begun characterizing CG17192 lipase. Their study shows that CG17192 is required in the intestine to maintain systemic lipids levels: knock-down reduces TAG by ~30% (Praggastis, Lam et al. 2021). Additionally, they prove that the E78A nuclear receptor regulates *CG17192* expression and lipid digestion (Praggastis, Lam et al. 2021). The role of nuclear receptors in controlling systemic lipid levels is also described for the Hormone receptor-like in 96 (Hr96) nuclear receptor and the lipase *magro*: under low cholesterol conditions, Hr96 is upregulated and activates the expression of *magro* (Sieber and Thummel 2009, Sieber and Thummel 2012). Despite Praggastis et al. primarily using male flies in their study, and even though E78A is neither sexually dimorphic in my RNA-seq data nor changing upon *dsx* downregulation in ECs, it would be interesting to further characterise a putative sexual dimorphism of CG17192 (either *dsx*-dependent or *dsx*-independent).

All this physiological data suggests that in males, the presence of Dsx in the ECs is downregulating, in a sex-specific manner, the levels of *CG17192*, which might be regulating lipid homeostasis in a sexually dimorphic manner. However, there is an inconsistency: in *mex1^{ts}>dsxRNAi* males, in which the levels of *CG17192* are upregulated, one would expect to see an increase in fat. Yet there is a reduction of LDs in the midgut. Given the complexity of

lipid homeostasis, and the many putative targets of *dsx* in fat metabolism, *dsx* could regulate lipid metabolism in a sexually dimorphic manner through other molecular pathways. For instance, an interesting Dsx target which requires further investigation is *fu12* (also known as *Agpat2*). This gene is predicted to have a role in lipid storage/transport because it is involved in *de novo* synthesis of TAG and glycerophospholipids (Yamashita, Hayashi et al. 2014). Furthermore, from the single-cell RNA-seq of the gut published recently by Perrimon and colleagues (Hung, Hu et al. 2020), *fu12* is higher in the posterior ECs, where fatty acids are re-absorbed in the midgut (see Introduction). Interestingly, *fu12* expression is regulated by *dsx* (upregulated in *mex1^{ts}>dsxRNAi*) and sexually dimorphic (higher in females). Thus, I speculate that *mex1^{ts}>dsxF* males have higher LDs because *fu12* might be upregulated. On the contrary, *mex1^{ts}>dsxM* males could have lower LDs because *fu12* mRNA might be reduced.

Finally, at the beginning of this chapter I validated the genetic tools of *dsx* overexpression in adult ECs. I have shown that both *dsxF* and *dsxM* overexpression in the ECs increase *dsx* mRNA levels in virgin females and males. The highest (and statistically significant) *dsx* upregulation was observed in consonance with the sex of the midgut: *dsxF* is higher in *mex1^{ts}>dsxF* females than males, and *dsxM* is higher in *mex1^{ts}>dsxM* males than females. Since I limited this analysis to transcriptomic data, it should be noted that these findings may not extrapolate to protein abundance. However, at least at the transcript level, the sex of the isoform and the sex of the midgut seem to matter to achieve optimal mRNA levels. These observations contribute to the hypothesis of a putative sex-specific post-transcriptional regulation of *dsx* in the ECs. However, one should be cautious in interpreting those results because the landing site of the UAS construct can affect the transcriptional efficiency. And in these two lines (BL#44223 and BL#44224) the landing sites are in two different chromosomes. From the published papers which generated the constructs by insertion of *dsx* CDS (An, Cho et al. 1996, Lee, Hall et al. 2002), I understand that the 5'UTR of *dsx* transcript is not inserted. However, it is less clear for the 3'UTR. After having sequenced both constructs, I confirmed that the 5'UTR is absent, but there is a residual truncated 3'UTR. Whether the remaining 3'UTR sequence plays a role in the sex-specific post-transcriptional regulation of the construct requires further clarification. Additionally, for the phenotypical characterization, one should consider that the overexpression of a protein is far from being a wild-type situation, resulting sometimes in undesired phenotypical changes.

The RNA-seq produced putative *dsx* targets involved in lipid metabolism (see Results I). In this chapter, I have taken a physiological approach and quantified the amount of fat in the

midgut and whole-body upon *dsx* knock-down (and overexpression) in adult ECs. I also began to decipher the molecular mechanisms through which *dsx* might be regulating (directly or indirectly) lipid content in a sexually dimorphic manner. In the next chapter, I study the role of another candidate Dsx target, Myc, and its potential roles in modulating lipid homeostasis.

CHAPTER 5

Results (III)

MYC CONTRIBUTES TO THE SEX DIFFERENCES IN LIPID METABOLISM

5.1 Introduction

In the previous chapters, I have explored the role of Dsx in regulating fat metabolism in a sexually dimorphic manner and shown that *CG17192* lipase is affected by Dsx. However, from the RNA-seq, there were many other Dsx-dependent molecular mechanisms that could be controlling the balance between fat catabolism and anabolism, as well as regulating digestion, absorption and transport.

In this chapter, I focus on studying the role of Myc (as a Dsx-dependent target) in the adult midgut and its contribution to the sexually dimorphic fat metabolism.

Myc is an interesting candidate to study because of several reasons. Firstly, its expression in the midgut is sexually dimorphic: in the female midgut it is higher than in the male (RNA-seq in this study and in Hudry, Khadayate et al. 2016, and trend from qPCR in Fig. 5.1A). Secondly, *Myc* is controlled by Dsx in the adult midgut: in *mex1^{ts}>dsxRNAi* males there is an upregulation of Myc (from the RNA-seq). Thus, in a "feminised" male midgut (by *dsx* knock-down), the levels of *Myc* increase to mimic the female midgut. Also, no significant changes were observed in *mex1^{ts}>dsxRNAi* females. Thirdly, a DamID-seq in the adult fat body of males and females suggests that *Myc* is a putative binding site for Dsx transcription factor (Clough, Jimenez et al. 2014). Whether this is also the case in the midgut is currently unknown.

Here I aim to investigate the relationship between Dsx and Myc at the transcript and protein level. I first characterise the wild-type Myc expression in the adult midgut under normal and dietary challenges. By quantifying intestinal proliferation, I explore the link of Dsx and Myc from the ECs to the ISCs in terms of cell-communication.

Myc is also an attractive candidate because of its functions in lipid metabolism (see Introduction). In *Drosophila melanogaster*, Parisi et al. investigated the roles of Myc in the larval fat body (Parisi, Riccardo et al. 2013). When *Myc* was downregulated in the fat body (by the driver *collagen type 4*), TAG levels decreased, as well as the size of the fat cells. Additionally, genes involved in lipid metabolism such as *ACC* and *FAS* downregulated their transcription. Conversely, when *Myc* was upregulated, TAG, cell size, *ACC* and *FAS* were increased. Intriguingly, LD size was diminished in *cg>Myc* and increased in *cg>MycRNAi* (Parisi, Riccardo et al. 2013). Beyond flies, links between Myc and lipid metabolism have been recently established in mice: Myc (together with SREBP1) controls lipogenesis, which in turn, promotes tumorigenesis. Thus, in Myc-induced tumours, there is a benefit when inhibiting

lipogenesis (Gouw, Margulis et al. 2019). Genes such as *FASN* and *AGPAT1* (*Drosophila* orthologues *FAS* and *Agpat1*) were upregulated under *Myc* overexpression (Gouw, Margulis et al. 2019). Excitingly, this year, a study has demonstrated intestinal Myc contribution to fat systemic metabolism in humans (Luo, Yang et al. 2021). In obese individuals (both mice and humans), Myc expression was increased in the ileum. In mice, *Myc* downregulation specifically in the intestine improved high-fat-diet-induced obesity and insulin resistance, promoting glucagon-like peptide (GLP-1) production and secretion. The authors showed beneficial effects on high-fat-diet-induced obesity upon Myc inhibitor and put forward the idea that Myc could become a drug target to treat human metabolic diseases (Luo, Yang et al. 2021).

To summarise, Myc has an evolutionary conserved function in lipid metabolism of flies, mice and humans, but neither its roles in the fly intestine nor possible sexual dimorphisms in its expression and/or functions (in any organism) had been investigated. Since *Myc* is sexually dimorphic and its transcription regulated by Dsx, I hypothesised that Myc regulates lipid metabolism in a (Dsx-dependent) sexually dimorphic manner.

5.2 Results

5.2.1 Myc in the adult midgut

At the transcript level, I first validated by qPCR the sexual dimorphism of *Myc* in the adult midgut. Even though the results are non-statistically significant most likely due to the low number of replicates, I observed an increasing trend of *Myc* mRNA levels in the adult midgut of wild-type females (Fig. 5.1A).

Next, I sought to explore the expression of Myc in the adult midgut of female and male flies. Firstly, I tried several anti-Myc antibodies, mostly publicly available but also the guinea pig anti-Myc antibody, kindly provided by Prof. Gines Morata. Although these antibodies are broadly used in the field (generally in the wing disc of the flies, but also in the adult midgut (Cordero, Stefanatos et al. 2012)), I was unable to detect midgut expression in either males or females, despite being able to visualise it in the larval brain (Fig. 5.1B, B''). Fortunately, I was able to use an endogenous reporter line as an alternative. The lab of Jean-Paul Vincent shared the Myc::eGFP transgenic line, which I used to investigate intestinal Myc expression.

5.2.1.1 Myc::eGFP reporter line

Jean-Paul Vincent and Cyrille Alexandre recently generated the Myc::eGFP reporter line by using CRISPR to insert eGFP before the Myc stop codon (see Materials & Methods, Poernbacher, Crossman et al. 2019). They validated the line molecularly, but also phenotypically by GFP immunostaining in the wing disc.

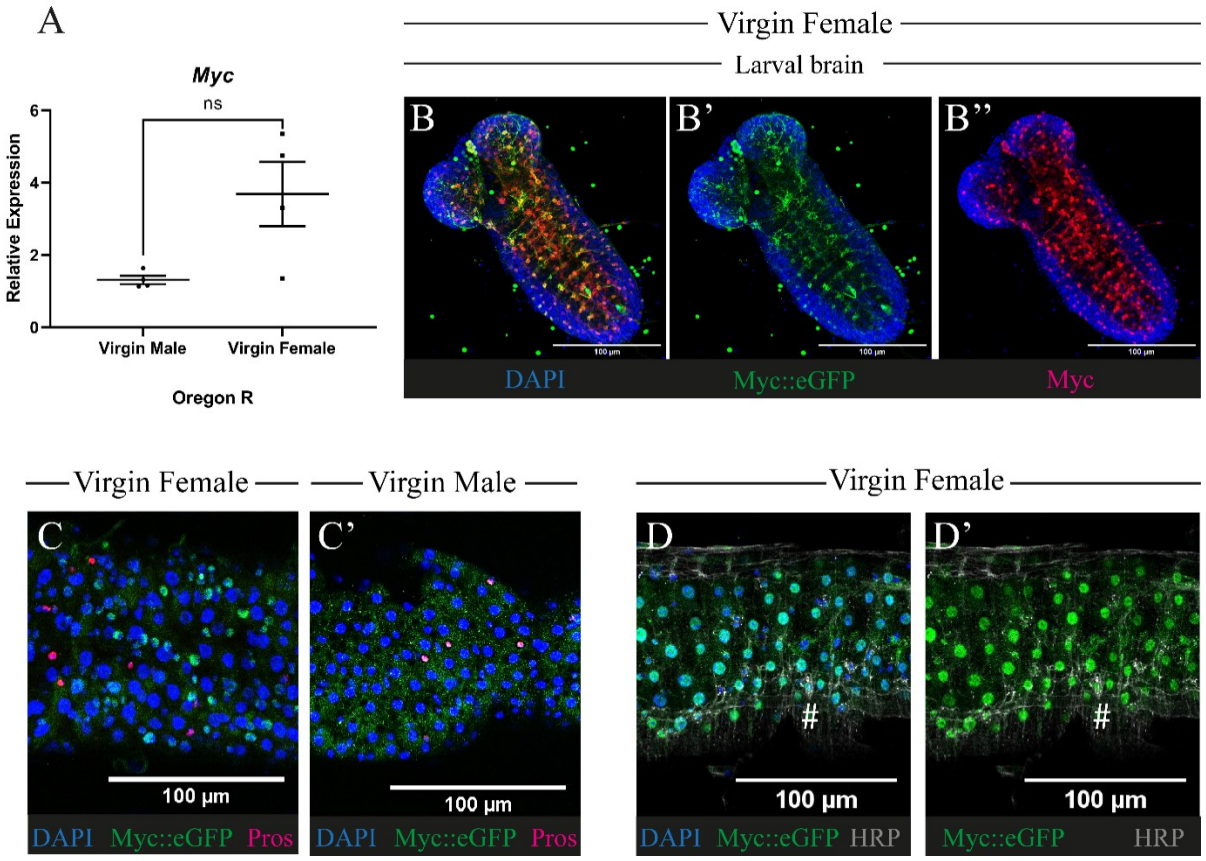

Figure 5.1: Myc expression in the male and female adult midgut

(A) *Myc* transcript levels in adult midguts show an increasing trend in virgin females, assessed by qPCR. N=4, normalised to *Vha100-4* and relative to one sample control. Results are shown as mean ±SEM. P-value < 0.05 with Mann-Whitney test. Larval brain of a Myc::eGFP female shows GFP (B') and anti-Myc expression (B'') colocalizing (B). (C) Expression of Myc::eGFP is absent from the Pros-positive EECs of the female midgut. (C') No Myc::eGFP expression is apparent in male midguts. (D) Myc::eGFP virgin female: GFP expression is apparent in in polynucleated ECs and progenitor cells (HRP^+ cells, # depicts one example). In blue, DAPI; in green, GFP; in red, either guinea pig anti-Myc or Prospero; in grey, HRP. Scale bars are shown in each panel.

To complement their validations, I first assessed Myc::eGFP expression in the larval brain. I saw overlap of GFP and anti-Myc signals (Fig. 5.1B-B''), suggesting that insertion of GFP in the Myc locus had not disrupted its endogenous expression.

Second, I examined Myc::eGFP in the adult midgut of females (Fig. 5.1C) and males (Fig. 5.1C'). In males, GFP signal was absent, whereas in females GFP was detected in several cell types (Fig. 5.1C-C'). Myc was not expressed in the EECs, since the GFP^+ cells were $Pros^-$ (Fig.

5.1C). Myc was in progenitor cells (HRP^+) (i.e. ISCs and EBs) and ECs (polyploid cells) (Fig. 5.1D-D').

This finding was suggestive of a Myc-sexual dimorphism in the adult midgut. However, one needs to consider the genetics of the reporter line. In Myc::eGFP flies, the GFP is inserted into the Myc endogenous locus on the X chromosome. Thus, in XX females flies, there are two copies of the transgene (homozygous), and in XY males, only one (hemizygous). In male flies, there are well-studied compensatory mechanisms of X overactivation to achieve the same transcription of X genes than in the females. Therefore, one would have expected the same amount of Myc::eGFP in the two sexes. Since it is not the case, this might suggest an escape of dosage compensation and/or post-transcriptional regulation of Myc. Additionally, in heterozygous females (reporter line crossed with a wild-type fly, resulting in one copy of the transgene) there was no GFP (data not shown). This indicated that expression of GFP was only achieved when the gene copy levels were above a threshold. Despite being able to explain the cause of the sex-biased Myc::eGFP expression, the sex differences at the protein level are consistent with the sexual dimorphism at the transcript level.

5.2.1.2 Myc::eGFP in the adult midgut upon different diets

While characterizing Myc::eGFP expression, I encountered variability of GFP according to the cell-type: GFP signal in ECs and ISCs appeared to be inversely correlated (i.e. midguts with higher Myc::eGFP in ISCs seemed to have less signal in ECs, and vice versa). The role of Myc as a transcription factor has been studied in ISCs in midguts under challenging conditions (see Introduction) but less is known about its functions in ECs. Here, I began to explore whether Myc levels in one cell type (ISCs) negatively regulate Myc levels in the other cell type (ECs) by performing dietary manipulations that impact ISC proliferation.

To this end, I used the Myc::eGFP reporter line to quantify the levels of GFP expression under high yeast, DSS, sucrose and H_2O (starvation) diets; and compared the changes of Myc expression between progenitor cells (HRP^+) and ECs (HRP^- and polyploid) (Fig. 5.2). Myc expression was higher in ECs in virgin females in sucrose and H_2O, and there was an increasing trend in high yeast (Fig. 5.2A-B'). On the opposite, under DSS treatment, the levels of Myc were dramatically increased in the progenitor cells (Fig. 5.2C-C'). These suggest that, although Myc is more abundant in the ECs upon several dietary conditions (high yeast, sucrose and starvation), once the midgut epithelium is challenged by DSS, the progenitor cells increase Myc abruptly (Fig. 5.2A, C-C').

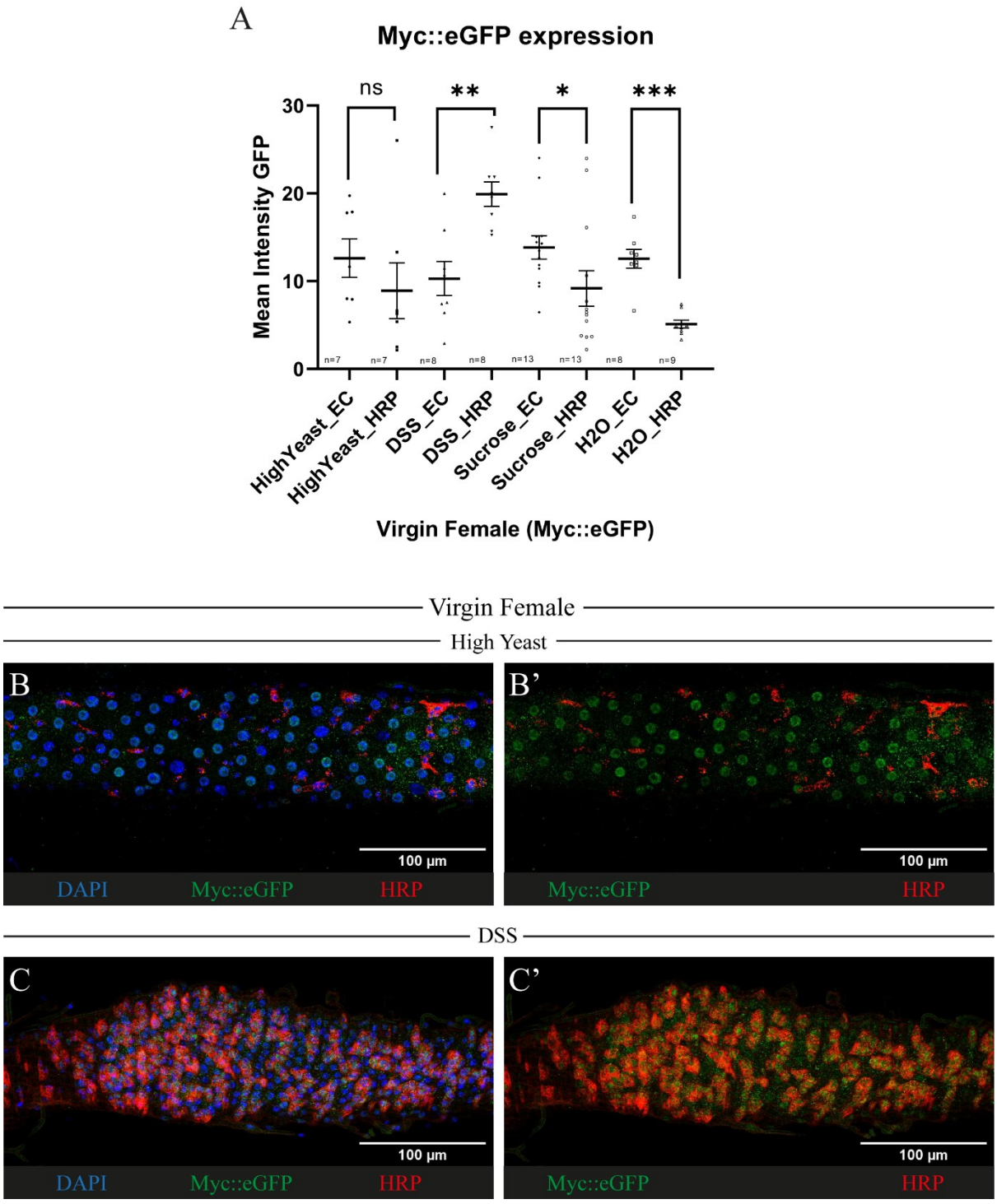

Figure 5.2: Expression of Myc::eGFP in ECs and progenitor cells under different dietary conditions

(A) Quantification of GFP intensity in ECs *vs* HRP cells the R4 region of virgin female flies fed high yeast, DSS, sucrose and H_2O. Replicates (n=7-13 midguts) are shown in the graph. The mean intensity per each midgut analysed is plotted in the Y axis. Results are shown as mean ±SEM. P-value < 0.05 with Mann-Whitney test. Expression of Myc::eGFP in the R4 region of females fed with high yeast (B-B') or DSS (C-C'). In blue, DAPI; in green, GFP; in red, HRP. Scale bars (100µm) are shown in each panel.

5.2.2 Epistasis between *Dsx* and *Myc*

Previously, I have shown that *Myc* is sexually dimorphic in the adult midgut of flies (RNA-seq and trend from the qPCR in Fig. 5.1A), and that the transcript levels are upregulated in *mex1^{ts}>dsxRNAi* male midguts (RNA-seq from this study). In this section, I aim to further explore Myc changes upon *dsx* manipulations in adult ECs, both at the transcript and protein level.

First, I wondered whether in "masculinised" female flies, *Myc* expression would be downregulated to match the *Myc* levels of wild-type males. To do so, I "masculinised" female ECs by the knock-down of *tra* and assessed mRNA levels by qPCR. Despite the increasing trend of *dsx* (suggestive of *tra* knock-down) (Fig. 5.3A), the levels of *Myc* seemed to remain unchanged or little upregulated (barely 0.5x increase) (Fig. 5.3A'). This finding is contradictory to the RNA-seq results from Hudry, Khadayate et al. 2016, in which *Myc* mRNA was downregulated in *tra* mutants. Even though further research needs to be done to understand the conflicting results, one possible explanation could be the different sensitivity of the techniques and/or cell-type specificity (i.e. *tra* mutants showed lack of *tra* in all cell types, whereas *tra* was only downregulated in adult enterocytes).

Second, I confirmed by qPCR that in male midguts, when the ECs were "feminised" by the knock-down of *dsx*, there was an increasing trend of *Myc* (Fig. 5.3B). Third, I quantified the changes in *Myc* mRNA upon *dsx* overexpression in adult male ECs by qPCR (Fig. 5.3B). There were no changes observed in *mex1^{ts}>dsxF* males. However, and unexpectedly, *dsxM* overexpression in ECs increased *Myc* levels non-statistically significant (further replicates are needed to validate these results with statistical significance). Although this seems contradictory, one should keep in mind that Myc is a master regulator in many biological processes, thus the increase in *Myc* could be either direct or indirect by Dsx. Furthermore, since I observed Myc::eGFP expression increase in ISCs under DSS treatment, it will be important to contextualise this finding by addressing the changes in proliferation in *mex1^{ts}>dsxM* males (Fig. 5.5).

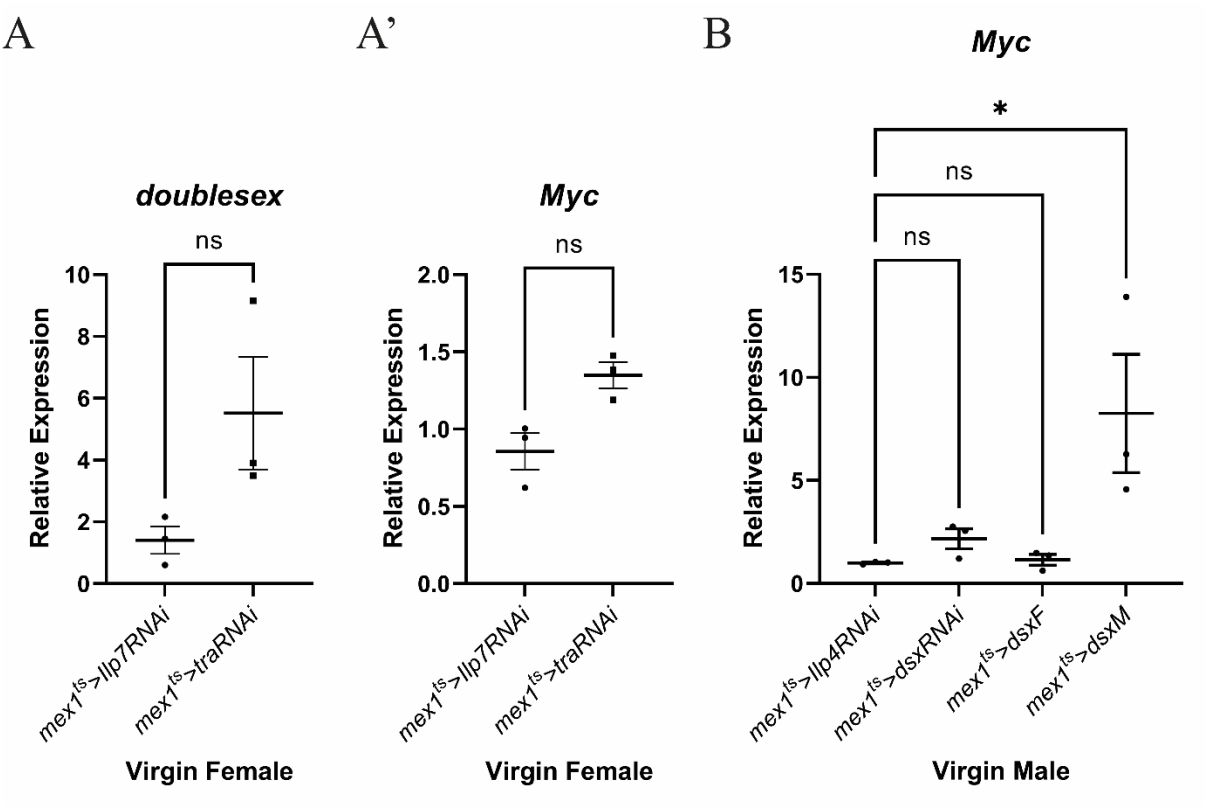

Figure 5.3: *Myc* transcriptional changes upon *dsx* manipulations in adult ECs

Dsx (A) and *Myc* (A') transcript levels in *mex1^{ts}>Ilp7RNAi* control and *mex1^{ts}>traRNAi* virgin females. (B) Relative expression of *Myc* in *mex1^{ts}>Ilp4RNAi* control virgin males *vs mex1^{ts}>dsxRNAi, mex1^{ts}>dsxF* and *mex1^{ts}>dsxM* virgin males. Sample (n=3) normalised to the housekeeping *Vha100-4*. Relative expression values are calculated against one sample control as reference. Results are shown as mean ±SEM. P-value < 0.05 with Mann-Whitney (A, A') or Kruskal-Wallis test (B).

Finally, I aimed to observe whether these findings translate at the protein level. Are *dsx* downregulation and/or *dsxM* overexpression in virgin male ECs also affecting Myc::eGFP protein levels?

Firstly, I downregulated *dsx* in ECs in two different ways: constitutively since embryogenesis (Gal4 system), or by confining downregulation to the adult stage (Gal4Gal80^{ts} system). Most of the midguts analysed did not show Myc::eGFP: only 4 out of the 14 midguts examined showed GFP signal (not ubiquitous throughout the gut). The very few GFP^{+} midguts had very low signal and exclusively in ECs (despite one of them which had Myc::eGFP exclusively in small-nucleated cells) (Fig. 7.4A-B'). These observations suggest that the upregulation of *Myc* transcript observed upon *dsx* knock-down could sometimes result in increased Myc protein in ECs. However, as previously discussed, Myc::eGFP flies with one copy of the construct (either hemizygous males or heterozygous females) lack GFP signal. Thus, the fact that the increase

in mRNA level is not observed at the protein level should be corroborated by the usage of anti-Myc antibody.

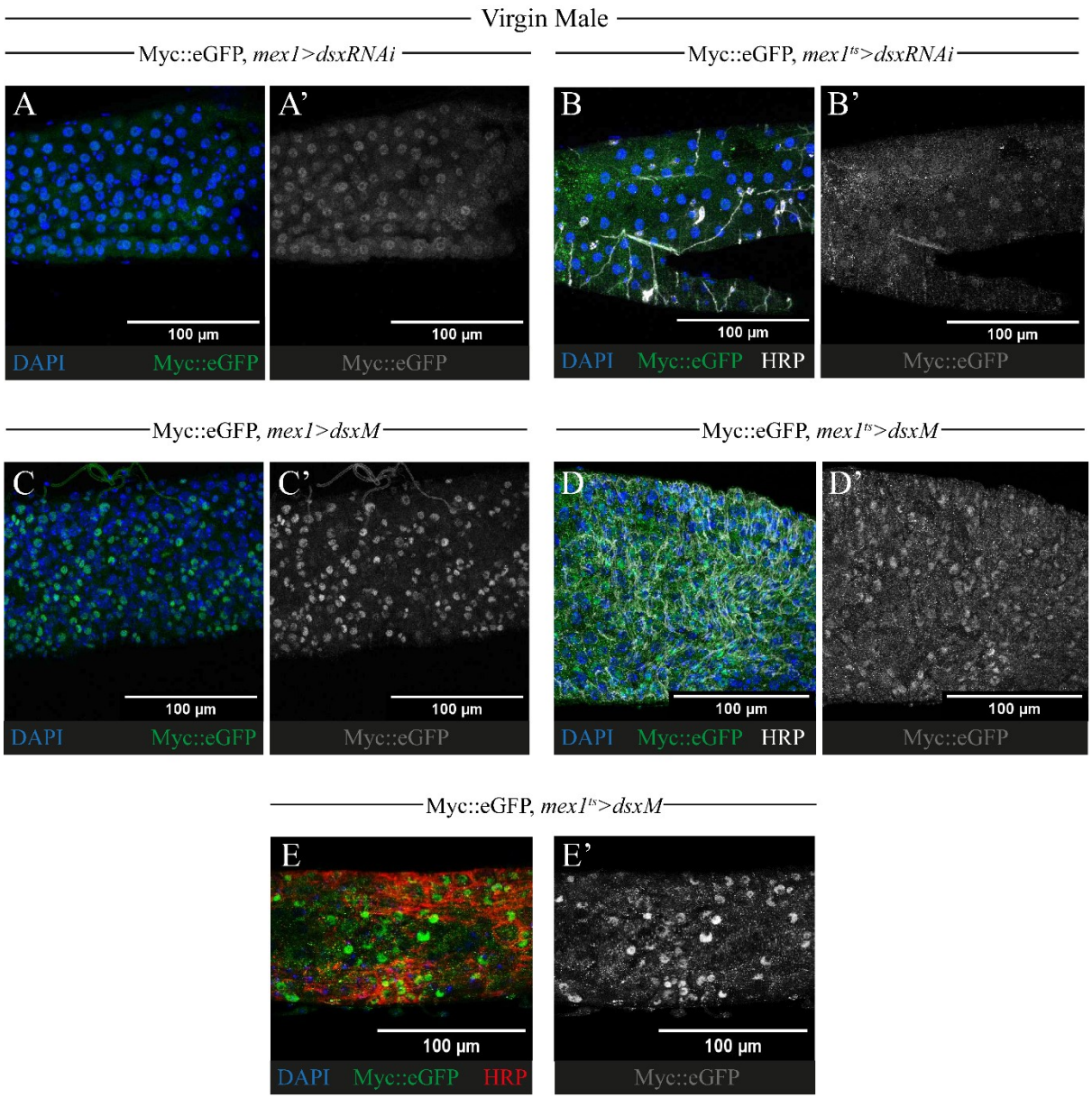

Figure 5.4: Myc::eGFP protein changes upon *dsx* manipulations in ECs

(A, A') Myc::eGFP in enterocytes of *mex1>dsxRNAi* virgin males. (B, B') Myc::eGFP in enterocytes of *mex1^{ts}>dsxRNAi* virgin males. (C, C') Myc::eGFP in small-nucleated cells of *mex1>dsxM* virgin males. (D, D') Myc::eGFP in small-nucleated cells of *mex1^{ts}>dsxM* virgin males. (E, E') Myc::eGFP mostly in HRP^{+} cells of *mex1^{ts}>dsxM* virgin males. In blue, DAPI; in green or grey, Myc::eGFP; in white or red, HRP. Scale bars in each panel.

Secondly, I overexpressed *dsxM* in ECs by the two aforementioned ways (constitutively *vs* adult-specific). In both scenarios, Myc::eGFP was observed in most of all the midguts, and generally in small-nucleated cells (Fig. 5.4C-D'). Although there were ECs expressing Myc::eGFP, the majority of the GFP signal was in progenitor cells (HRP^{+}) (Fig. 5.4E-E'). The

GFP signal in progenitor cells, together with the drastic increase in Myc mRNA, is suggestive of an increase in proliferation in *mex1^{ts}>dsxM* males (Fig. 5.5). Since the pattern of Myc::eGFP staining was similar to the one observed upon DSS treatment (Fig. 5.2C-C'), I wondered whether *dsxM* overexpression might induce epithelium proliferation.

5.2.3 ISC proliferation under *dsx* and *Myc* manipulations in adult ECs

In this section, I started exploring the effects of Dsx and Myc in the EC on ISCs division. I characterised the changes in proliferation by using pH3^{+} cells as a readout upon *dsx* and *Myc* manipulations.

First, I quantified the pH3^{+} cells in virgin male (Fig. 5.5A) and female (Fig. 5.5A') *mex1^{ts}>dsxRNAi*, *mex1^{ts}>dsxF* and *mex1^{ts}>dsxM* compared with *mex1^{ts}>Ilp4RNAi* control. Upon *dsxF* and *dsxM* overexpression, there was an increase in proliferation in both sexes, although much higher in *mex1^{ts}>dsxM*.

In *mex1^{ts}>dsxRNAi* flies, the number of proliferative ISCs did not vary (Fig. 5.5A-A'). Since the levels of basal proliferation, especially in the males, were low, I decided to challenge the midguts by DSS. Therefore, I tested whether there was an effect of *dsx* in highly proliferative conditions. Although DSS treatment increased pH3^{+} cells in control virgin males (non-statistically significant) and in virgin females (statistically significant), *dsx* knock-down in adult ECs did not vary ISCs proliferation (Fig. 5.5B-B').

In short, *dsx* downregulation did not affect proliferation in female/male adult midguts. Overexpression of *dsxM*, and *dsxF* in lower amounts, generated an increase of pH3^{+} cells. This finding shows a cell-communication between ECs and ISCs: changes in the sexual dimorphism of ECs had an effect in the progenitor cells. However, one should be cautious in interpreting those results, as massive overexpression of a protein might have deleterious effects on ECs unrelated to the role of the protein of interest, which might promote ISC proliferation to regenerate the intestinal epithelium.

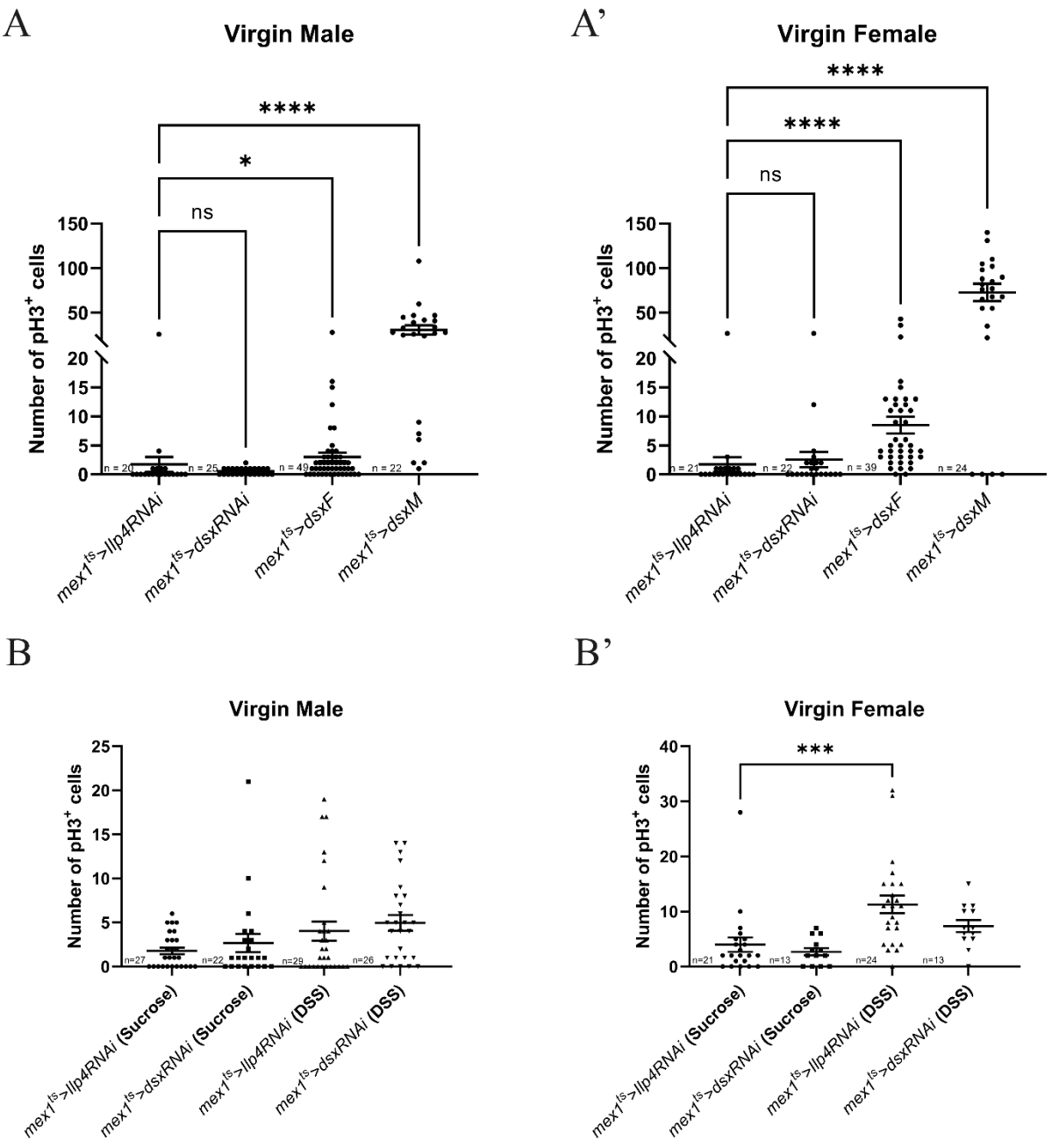

Figure 5.5: Proliferation changes upon *dsx* downregulation/overexpression in the ECs of adult males and females

Changes in number of pH3^{+} cells in virgin males (A) and virgin females (A') in *mex1^{ts}>Ilp4RNAi*, *mex1^{ts}>dsxRNAi*, *mex1^{ts}>dsxF* and *mex1^{ts}>dsxM*. There is an increase in proliferation upon *dsxF* and *dsxM* overexpression in adult ECs in both sexes. Quantification of proliferation upon DSS *vs* sucrose treatment in *mex1^{ts}>Ilp4RNAi* and *mex1^{ts}>dsxRNAi* virgin males (B) and females (B'). There are no changes in proliferation upon *dsx* knock-down in both sexes. Number of midguts quantified are plotted in the graphs. Results are shown as mean ±SEM. P-value < 0.05 with Kruskal-Wallis test.

Second, given the changes of Myc::eGFP expression in cell-type upon DSS treatment (Fig. 5.2), I wondered whether the Myc in ECs could influence Myc levels in ISCs and thus their proliferative capacity. Therefore, I quantified the amount of proliferation upon *Myc*

manipulations. In *mex1^{ts}>MycRNAi* female and male flies, the number of pH3^{+} cells were increased (Fig. 5.6 A-A'). Thus, when flies had lower levels of *Myc* in the ECs, the progenitor cells were proliferating more. On the contrary, overexpression of *Myc* in the ECs did not change the pH3^{+} cells in females or males (Fig. 5.6 B-B'). In females, there was an increase of proliferation when compared with the driver control line (*mex1^{ts}>+*), which was lost in the UAS-*Myc* control line (Fig. 5.6 B). Since the two controls give inconsistent results, one cannot conclude that *mex1^{ts}>Myc* increased proliferation in females.

To summarise, *mex1^{ts}>dsxM* and *mex1^{ts}>MycRNAi* increased proliferation in both male and female adult midgut.

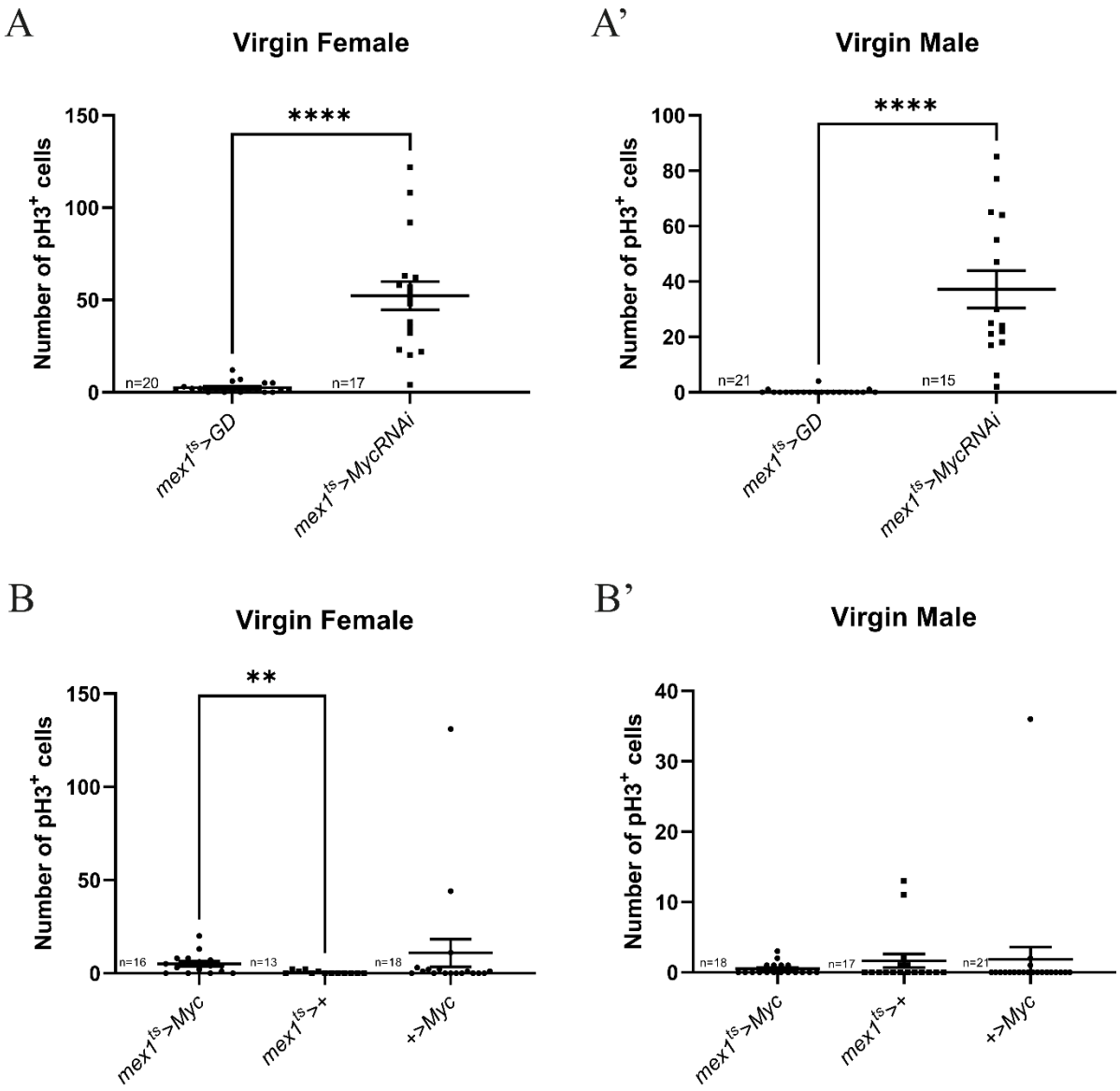

Figure 5.6: Proliferation changes upon *Myc* downregulation/overexpression in the ECs of adult males and females

Quantification of pH3^{+} cells in virgin females (A) and virgin males (A') in *mex1^{ts}>GD* control *vs* *mex1^{ts}>MycRNAi*. There is higher proliferation upon *Myc* knock-down in both sexes. Changes in ISC proliferation upon *Myc* overexpression in the female (B) and male (B') adult ECs when compared with the two controls *mex1^{ts}>+* and *+>Myc*. In females, proliferation is only increased when compared with the driver control. In males, there are no changes in proliferative cells. Number of midguts quantified are plotted in the graphs (n=13-21). Results are shown as mean ±SEM. P-value < 0.05 with Mann-Whitney test (A-A') or Kruskal-Wallis test (B-B').

5.2.4 Myc in ECs regulates LDs in the midgut and whole-fly TAG

In this section I investigate whether lipid metabolism is regulated by Myc in adult ECs. Given the possible epistasis between Myc and Dsx, and the previously studied role of Myc in controlling fat homeostasis in the fat body of flies (Parisi, Riccardo et al. 2013), as well as in mice (Gouw, Margulis et al. 2019, Luo, Yang et al. 2021) and human intestines (Luo, Yang et al. 2021), I hypothesise that Dsx in males represses Myc which establishes the sexual dimorphism in fat.

I begin this section by establishing the most appropriate experimental set-up and genetic tools for Myc downregulation in the adult ECs. Subsequently, I investigate whether lipid metabolism genes are regulated by Myc in adult ECs, as well as its effects on intestinal and whole-fly lipid content.

5.2.4.1 Effects of Myc on lipid metabolism gene expression

I made use of publicly available RNAi lines to downregulate *Myc* in the adult ECs from *mex1^{ts}* and assessed the degree of *Myc* downregulation using four different RNAi lines (Fig. 5.7A). Given the sexual dimorphism of *Myc*, I tested only virgin females. While non-statistically significant (possibly because of the low number of replicates), out of the four lines, only *MycRNAi* from VDRC (#2947) had a strong reduction of *Myc* transcript, as well as little variation across experiments.

Next, I started to elucidate the putative contribution of Myc to lipid metabolism by examining the changes in transcription of *CG17192*, *fu12*, *CG2772*, *bmm* and *Lsd-1*, all involved in fat homeostasis, in *mex1^{ts}>MycRNAi* females (Fig. 5.7B-B'''''). Encouragingly, *CG17192* was downregulated upon *Myc* knock-down in adult enterocytes. Thus, virgin females with a *Myc* "male-like" signature in the ECs display reduced expression of *CG17192*, akin to control males. Because *CG17192* is a lipase, it could provide a link between Myc and lipid catabolism in the midgut.

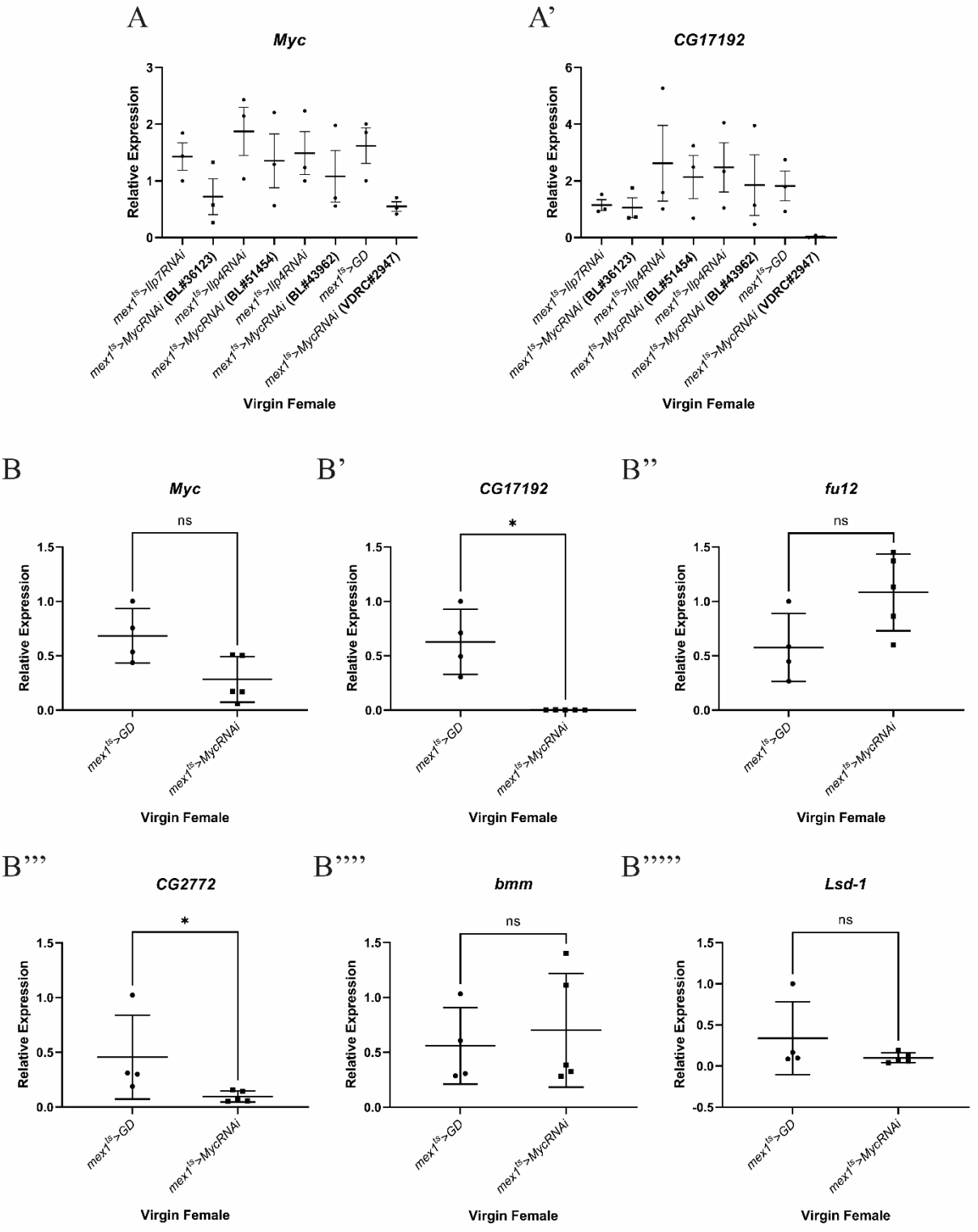

Figure 5.7: Validation of *Myc* knock-down in adult ECs and its effects on lipid metabolism gene expression

Levels of *Myc* (A) and *CG17192* (A') in virgin females comparing control *vs* experimental *MycRNAi* lines: *mex1^{ts}>Ilp7RNAi vs mex1^{ts}>MycRNAi* (BL#36123), *mex1^{ts}>Ilp4RNAi vs mex1^{ts}>MycRNAi* (BL#51454), *mex1^{ts}>Ilp4RNAi vs mex1^{ts}>MycRNAi* (BL#43962) and *mex1^{ts}>GD vs mex1^{ts}>MycRNAi* (VDRC#2947). Using the VDRC line to downregulate *Myc* in adult ECs, the levels of *Myc* (B) as well as the lipid metabolism genes *CG17192* (B'), *fu12* (B''), *CG2772* (B'''), *bmm* (C'''') and *Lsd-1* (C''''') are displayed. N=3 (A-A') or N=4-5

(C-C’’’’’) normalised to *Vha100-4* and relative to one sample control. In all the graphs, results are shown as mean ±SEM. P-value < 0.05 with Mann-Whitney test in B-B’’’’’.

Furthermore, to further validate the choice of VDRC *MycRNAi* line, I quantified the *CG17192* mRNA in all the four previously tested experimental lines. While non-statistically significant, only the line with the highest *Myc* downregulation showed the most dramatic *CG17192* decrease (Fig. 5.7A’).

Since both Dsx and Myc affect the transcription levels of *CG17192*, this suggests the following hypothesis: Dsx negatively regulates Myc in males, which normally sustains *CG17192* expression; consequently, in females, lack of Dsx results in high *Myc* and *CG17192* expression, whereas in males Dsx represses *Myc* expression, generating low *CG17192* transcription. Therefore, partially explained by the control of *CG17192* lipase, I wanted to further elucidate the role of Myc in regulating lipid metabolism by examining the phenotypical effects on LDs and TAG following Myc downregulation in adult ECs.

5.2.4.2 *Myc* knock-down in adult ECs reduces intestinal LDs and whole-body TAG

In *mex1^{ts}>MycRNAi* virgin females, the number of LDs was reduced in both the R2 and R4 regions of the midgut (Fig. 5.8A-A’). In the R4 region of virgin males, there were fewer LDs upon *Myc* downregulation in the ECs (Fig. 5.8A’’). Therefore, this suggests that in both sexes, Myc in the ECs controls lipid homeostasis in the midgut.

At the level of the whole-fly (without gonads) fat, *mex1^{ts}>MycRNAi* virgin females (Fig. 5.8B, B’’) and males (Fig. 5.8B’) had lower TAG.

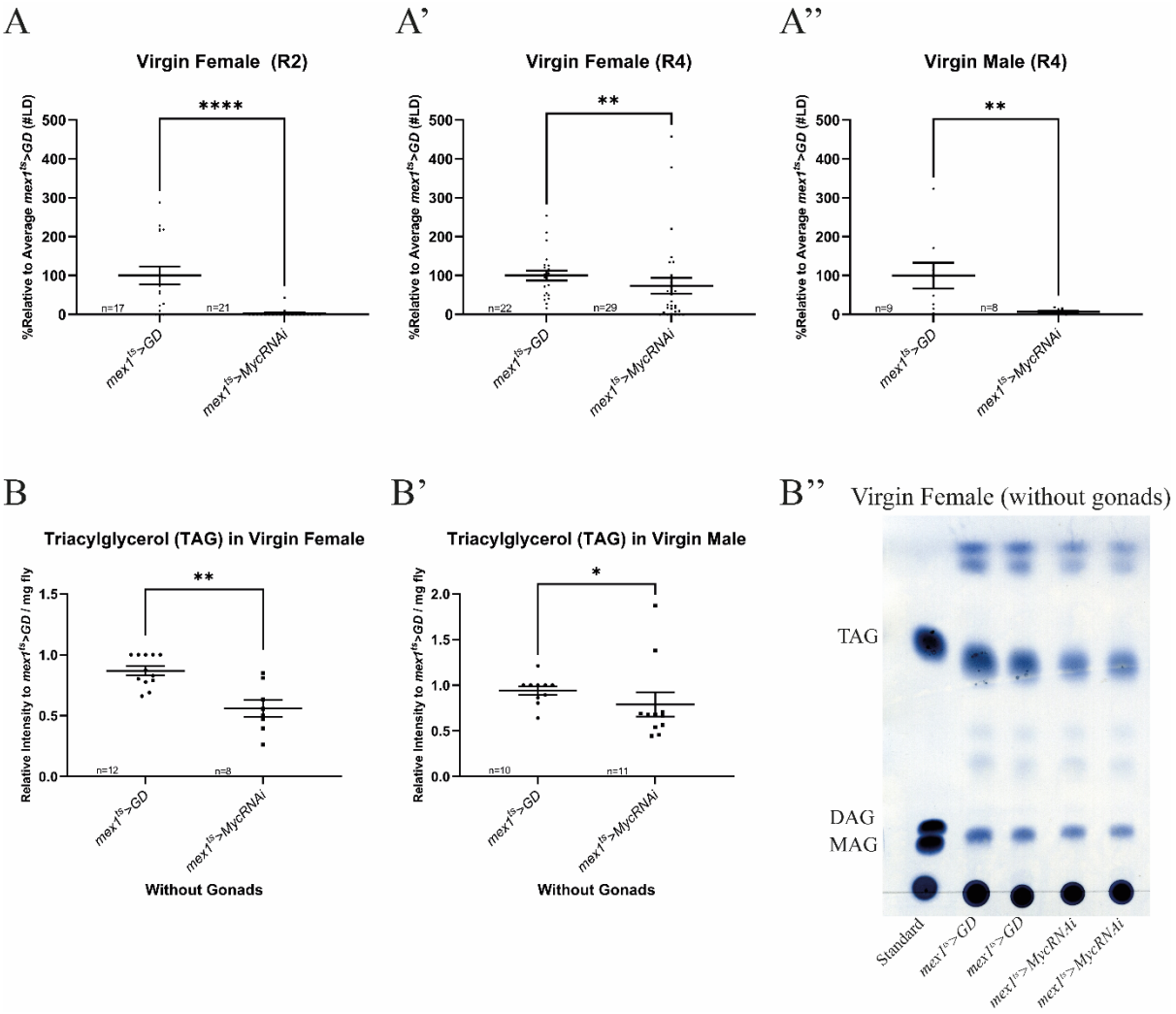

Figure 5.8: *Myc* downregulation in ECs decreases LDs and TAG

The number of LDs is reduced in *mex1^{ts}>MycRNAi* in the R2 region of virgin females (A), the R4 region of virgin females (A') and the R4 region of virgin males (A''). The number of quantified midguts is stated in each graph (n=8-29). Values are plotted relative to the average of LDs particles of the *mex1^{ts}>GD* control per each experimental day. Quantity of TAG in virgin females (B) and virgin males (B') without gonads is lower in *mex1^{ts}>MycRNAi*. In the X axis, the genotypes. In the Y axis, the relative intensity to control *mex1^{ts}>GD* flies normalised by the weigh. Number of samples in the graph shows the number of replicates (n=8-12), which consists of 4 females or 5 males. (B'') Example of a representative TLC plate with extracts from females without gonads: the left column shows migration of the standard, which contains TAG, DAG and MAG. The second and third columns, correspond to two control samples (*mex1^{ts}>GD*), whereas the fourth and fifth contain two experimental samples (*mex1^{ts}>MycRNAi*). Results are shown as mean ±SEM. P-value < 0.05 with Mann-Whitney test.

5.3 Conclusion & Discussion

In this chapter I have shown that *Myc* expression in the adult midgut is sexually dimorphic, higher in females than males (RNA-seq and trend from qPCR in Fig. 5.1). Myc in the ECs of flies seems to regulate TAG levels both in the midgut and whole body (Fig. 5.8). In *Drosophila*,

the role of Myc has been characterised in the ISC, but little is known about its function in the ECs. The effects on lipids from Myc expressed in the fly ECs are novel, and is well aligned with recent findings in humans, mice and in the fat body of flies (Parisi, Riccardo et al. 2013, Gouw, Margulis et al. 2019, Luo, Yang et al. 2021).

Knock-down of *Myc* in adult ECs modified the mRNA amount of several lipid metabolism genes: in particular, *CG17192* expression was reduced in *mex1^{ts}>MycRNAi* females (Fig. 5.7). *CG17192* is sexually dimorphic and seems to be negatively regulated by Dsx in males and positively regulated by Myc in females. Because of the sexually dimorphic expression of Myc and Dsx, and its effects on *CG17192* lipase, I postulate the following working model: in males, Dsx expression results in lower Myc expression, which normally promotes *CG17192* transcription; in females, the absence of Dsx results in higher levels of Myc and *CG17192*. Hence, Dsx function to sculpt sex differences in the intestinal lipid metabolism by restraining expression of Myc and its lipase target in males, resulting in lower LDs and TAGs.

In this chapter, I have explored the current model by analysing the epistasis between Dsx and Myc at the transcript and protein level (Fig. 5.3 and 5.4). Although *mex1^{ts}>dsxRNAi* virgin males increased *Myc* mRNA, Myc::eGFP was barely detected in ECs. In *mex1^{ts}>dsxM* virgin males, transcript levels of *Myc* were drastically upregulated, and Myc::eGFP was mostly in progenitor HRP^{+} cells, resembling DSS conditions (Fig. 5.2) and correlated with an increase in pH3^{+} cells (Fig. 5.5).

To confidently assess the increase in Myc protein upon *dsx* manipulations, as well as the sexual dimorphism at the protein level, the use of an anti-Myc antibody becomes crucial. The reporter Myc::eGFP was only visualised in flies with two copies of the transgene: neither hemizygous males (X,Myc::eGFP/Y) nor heterozygous females (X,Myc::eGFP/X) showed GFP^{+} cells. Strangely, because of X-dosage compensation in males, one would have expected similar Myc::eGFP levels in males and females. Expression from the single X chromosome in males should be twice as high than in the 2X chromosomes of females, so comparable Myc levels in males and females should have been observed (both at the transcript and protein level). In *Drosophila* and mammals, contrary to the expanded theoretical view, the dose compensatory mechanisms appear to be facultative for few genes (Valsecchi, Basilicata et al. 2018), and even absent in the primordial germ cells of the fly embryos (Ota, Hayashi et al. 2021). In males, the lack of Sxl allows *msl-2* translation, and MSL complex increases transcription of X-linked genes for dosage compensation (reviewed in Lucchesi and Kuroda 2015). Interestingly,

Mathews et al. described how Myc escapes dosage compensation in males and sets the smaller body size (Mathews, Cavegn et al. 2017). Also, in females, Myc is a weak XSE helping to establish sustained expression of Sxl in early zygotic females (Erickson and Quintero 2007, Kappes, Deshpande et al. 2011, Mathews, Cavegn et al. 2017). In this chapter I started to elucidate a putative Dsx-dependent *Myc* regulation at the mRNA and protein level. The transcription factor Dsx has recently been shown to control *fruitless* expression in the gonad stem cell niche (Zhou, Whitworth et al. 2021). Therefore, we speculate whether Myc escaping dosage compensation has to do with Dsx being sexually dimorphic: in males, is Dsx, via *msl-2* transcriptional control, allowing *Myc* to evade dosage compensation?

Myc protein half-life is affected by phosphorylation of specific sites which results in ubiquitination and protein degradation (Moberg, Mukherjee et al. 2004, Galletti, Riccardo et al. 2009 and reviewed in Bellosta and Gallant 2010). The mammalian Myc is subject to post-transcriptional modifications which regulate its stabilization, its interaction with partners and its function (Vervoorts, Lüscher-Firzlaff et al. 2006). Myc post-transcriptional modifications were also suggested in the fly midgut (Ren, Shi et al. 2013). Also, diverse signalling pathways control Myc stability, particularly insulin increases its stability (unpublished in Bellosta and Gallant 2010). Thus, it will be important to corroborate the findings from this thesis at the Myc protein level.

In the midgut, there are many cell-communication mechanisms, few of them promoting ISC division (Pasco, Loudhaief et al. 2015). Many cell-types communicate to ISC (in addition to the epithelial cells, also visceral muscle and tracheal cells, as well as haemolymph and basal membrane) to regulate proliferation. For example, ECs and EBs, via Keren and Spitz ligands, signal to ISCs to activate the EGFR pathway which stimulates proliferation. In turn, the EGFR cascade is known to phosphorylate Myc. Interestingly, those ligands change expression in *mex1^{ts}>dsxRNAi* virgin males. Upon *dsx* knock-down in ECs, there is a reduction of *spitz* and *karen* (as well as *rolled*, the orthologue of *MAPK*) transcript. Thus, I hypothesise that under *dsxM* overexpression, those ligands might be upregulated. In *mex1^{ts}>dsxM* virgin males, there is an increase in *Myc*, Myc::eGFP in progenitor cells, and pH3 numbers. Therefore, I propose that, upon *dsxM* overexpression, there is upregulation of Spitz/Karen from the ECs, which signal through EGFR pathway to increase Myc (and Rolled) in the ISCs and consequently, promote cell division in ISCs. This mechanism should be *dsxM* specific, since *dsxF* in the ECs did not have such an increase in *Myc* expression or proliferation. Further experiments and research need to be done to confirm this hypothesis.

However, overexpression of a protein by the Gal4 system could have unspecific secondary effects, thus, having pH3 as a phenotypical read-out could be misleading. Because both female and male flies upon *dsxF* and *dsxM* overexpression had high levels of proliferation (Fig. 5.5), this could hint towards indirect toxic effects. However, there are few other things that should be considered arguing against it: a) *Myc* levels were increased upon *dsxM* overexpression in adult ECs, and not upon *dsxF*, suggestive of a Myc-specific proliferative phenotype (Fig. 5.3); b) *dsxM* overexpression showed higher pH3 numbers than *dsxF* (both in males and females) (Fig. 5.5). Also, the effect seems to be unspecific to the amount of *dsx* transcript, since females had higher $pH3^+$ cells upon *dsxM* overexpression, but *dsx* transcript was higher in $mex1^{ts}>dsxF$ than $mex1^{ts}>dsxM$ females (Fig. 5.5 and Fig. 4.4).

In this chapter I have focussed on exploring the role of Myc::eGFP in adult ECs. Given the changes in the expression pattern according to the dietary challenge (i.e. DSS treatment) and the characterised function of ISCs Myc in cellular division, I characterised levels of proliferation in midguts upon *Myc* manipulations in adult ECs (Fig. 5.6).

Myc in ECs controls both lipid metabolism and proliferation. In the future, it would be interesting to study whether Myc sexual dimorphism is also establishing other physiological traits, such as sex differences in food intake or food preferences. Moreover, given the role in lipid homeostasis (partially by CG17192 lipase), Myc in females could influence survival upon starvation or induce high fertility.

As in mammals, *Drosophila* has a Myc/Max/Mnt network. The C-terminus of Myc mediates Myc:Max heterodimerization. Mnt forms heterodimers with Max, and binds to the same E-boxes (CACGTG sequences) as Myc:Max, therefore Mnt antagonises Myc function (reviewed in Bellosta and Gallant 2010, Gallant 2013, Grifoni and Bellosta 2015). Since the absence of Max results in weaker phenotypes than the lack of Myc, Myc can function independently of Max or Mnt (Steiger, Furrer et al. 2008, Gallant and Steiger 2009). In this thesis I have focused on the Max-independent Myc effects on lipid metabolism. Interestingly, Mondo-Max-like protein family (Mlx) controls glucose and glutamine metabolism; in flies, *Mondo* (or *Mio*) and *bigmax* are the orthologues (O'Shea and Ayer 2013). In my RNA-seq control, *Max* is sexually dimorphic. Curiously, *bigmax* is highly expressed in female midguts, suggestive of a sex-specific regulation of glucose and glutamine via the Mlx pathway. Aside from the carbohydrate metabolism implications, Mondo/Mlx have been shown to control lipid metabolism genes such as *ACC* and *FASN1* (involved in FAs synthesis) upon sugar feeding via *sugarbabe,* but also

others such as *Desat1* and *Lsd1* (Mattila, Havula et al. 2015). Furthermore, Mattila et al. observed sugar-induced repression of several gut-specific lipases (*CG6283* and *CG6277*) under the control of Mlx (Mattila, Havula et al. 2015). These observations, together with my findings, suggest a possible synergy between Myc and the Mondo/Mlx network in regulating fat homeostasis.

CHAPTER 6

Conclusions & Outlook

6.1 General Discussion

Throughout this thesis I have focused on the main question: what is the role of Doublesex in the adult enterocytes? Other investigations arose from this, with the common interest of deciphering sexual differences in the adult intestine.

After verifying the sex- and the cell-specificity of Dsx in male ECs, I took a transcriptomic approach to start elucidating the role of this transcription factor. From the numerous changes observed in the RNA-seq, it is clear that Dsx is involved in many biological functions. The previous fly studies describing a sexual dimorphism in fat levels and metabolism (Schwasinger-Schmidt, Kachman et al. 2012, Sieber and Spradling 2015, Jehrke, Stewart et al. 2018, Wat, Chao et al. 2020) prompted me to investigate the contributions of Dsx within the intestine and to whole-body lipid metabolism. In wild-type flies, I have characterised sex differences in the regionality of LDs in the midgut and shown that this signature is lost upon *dsx* manipulations in ECs. These findings, together with the LD reduction in *mex1^{ts}>dsxRNAi* guts (and clones), suggest a role of Dsx in regulating lipid metabolism. Its function as a transcription factor could be either direct, by affecting the expression of genes involved in fat homeostasis, or indirect, by changing the transcription of genes which subsequently impact other genes or proteins from several lipid processes.

One strong candidate that seems to establish the sexual dimorphism in lipid homeostasis is the oncogene Myc. Previous studies have described in the fat body the effect of Myc in lipid metabolism (Parisi, Riccardo et al. 2013, Paiardi, Mirzoyan et al. 2017). In mice, Myc (together with SREBP1) is accentuating lipogenesis, which is beneficial for tumorigenesis (Gouw, Margulis et al. 2019). Excitingly, and very relevant for this project, a new study in humans shows that Myc levels in the intestine positively correlates with obesity (Luo, Yang et al. 2021). The authors prove that mice with an intestinal-specific reduction in Myc have lower levels of obesity on high fat diet, suggesting Myc as a putative target against metabolic diseases (Luo, Yang et al. 2021). Their study is in consonance with my findings of TAG and LDs reduction in the midgut upon *Myc* knock-down in adult flies, indicating that the mechanism might be conserved among species.

In the adult midgut, *Myc* is highly expressed in females. The male-specific *Myc* signature is lost upon *dsx* knock-down in ECs, and the lack of Dsx in females correlates with elevated *Myc* levels. Hence, I speculate that *Myc* is downregulated by Dsx. Since both *Myc* expression and

fat homeostasis are sexually dimorphic, I suggest that in females, Myc inactivates lipolytic processes or promotes lipogenic processes. Therefore, the current working model is the following: Dsx in males represses a female Myc-driven lipogenic programme, which controls midgut and whole-body adiposity, as well as ISC proliferation.

I propose that, at least partly, Myc establishes the sexual dimorphism in lipid metabolism by the adult midgut-specific CG17192 lipase. Like *Myc*, *CG17192* is higher in female midguts. Also, this TAG lipase seems to be under Dsx and Myc regulation: mRNA levels increase in *mex1^{ts}>dsxRNAi* (males) and are reduced in *mex1^{ts}>dsxM* (males, non-statistically significant), *mex1^{ts}>traRNAi* (females, non-statistically significant) and *mex1^{ts}>MycRNAi* (females). Thus, in the *Drosophila* female midgut, Myc could be boosting *CG17192* expression in the R2 to increase lipid digestion for subsequent fat absorption and storage. It would be interesting to discover whether Myc directly binds to the regulatory regions of *CG17192*.

Furthermore, the transcription factor Myc could regulate lipid homeostasis by controlling the expression of other metabolic targets. In the fat cells, a critical enzyme in the FA synthesis pathway named *Desat1*, is an indirect target of Myc (Paiardi, Mirzoyan et al. 2017). *Desat1* is also expressed in the midgut (its expression does not statistically differ upon *dsx* downregulation). In their proteomic analysis, Paiardi et al. showed that other targets, in addition to Desat1, were upregulated in Myc overexpressing cells from larvae (Paiardi, Mirzoyan et al. 2017). Interestingly, these include Lsd1/Plin1, the transcription of which is strongly upregulated in *mex1^{ts}>dsxRNAi* males. Plin1 is localised at the surface of LDs and allows access lipases such as Bmm at the LD surface (Beller, Bulankina et al. 2010, Bi, Xiang et al. 2012). Therefore, *Plin1* could be a Dsx target, either directly or indirectly through Myc. In the control RNA-seq, *Plin1* is not sexually dimorphic in the midgut, thus it might not be sufficient to establish the sexually dimorphic midgut lipid signature. In mice, Myc regulates lipogenesis via several pathways, but one of the targets is AGPAT1, which is *fu12* fly orthologue. Since *fu12* is sexually dimorphic in the midgut (RNA-seq from this study) and involved in the *de novo* synthesis of TAG, Myc could also be directing the female-specific lipid accumulation via *fu12*. This process could be Dsx-dependent, since *Myc* (and also *fu12*) are Dsx-targets, both of them upregulated in *mex1^{ts}>dsxRNAi* (RNA-seq from this study).

In the current working model, I hypothesise that Dsx in males represses *Myc* expression. However, *mex1^{ts}>dsxM* males show *Myc* upregulation and Myc::eGFP in the midgut, arguing against Dsx inactivating Myc. Because Myc is a transcription factor with broad biological

functions and transcriptional regulation, *Myc* upregulation in *mex1^{ts}>dsxM* could be Dsx-independent. The increased levels of proliferation in *mex1^{ts}>dsxM* could indicate levels of toxicity from the UAS overexpression of sex determination members (Miguel-Aliaga, personal communication). At the end of the PhD, I begun to study the effects of *dsx* manipulations in the ECs on fly survival under starvation conditions, to explore a possible link to lipid storage (data not shown). *mex1^{ts}>dsxM* males in starvation seemed to have a shorter life, which could be caused by a) lack of lipids in the midguts, b) specific DsxM functions or c) toxicity of UAS-*dsxM* overexpression. Notably, despite *mex1^{ts}>dsxF* males having higher proliferation, the starvation period did not have a significant impact on survival, arguing against a generalised UAS toxicity. Furthermore, the increased DsxM-dependent proliferation could be explained by the gain of *spi* and *krn* mRNA (*mex1^{ts}>dsxRNAi* show less *spi* and *krn*) which, via EGFR signalling and Myc, would result in ISC proliferation (reviewed in Pasco, Loudhaief et al. 2015).

Among other functions, Myc controls ISCs proliferation and sustains tumour progression (Ren, Shi et al. 2013, Pasco, Loudhaief et al. 2015, Jiang, Tian et al. 2016). However, less is known about Myc in the adult ECs. In normal high yeast diet, Myc::eGFP is higher in ECs, whilst once the gut is challenged by DSS, Myc levels in ISCs are dramatically increased. This suggests that Myc levels rise in ISCs during proliferation, while basal Myc in ECs might have metabolic functions such as in lipid metabolism. Levels of Myc in ECs impact ISC division because *mex1^{ts}>MycRNAi* shows increased pH3^{+} cells. In *mex1^{ts}>MycRNAi* flies there is a reduction in fat and increased cellular proliferation. Recently, a positive feedback loop between Myc and glycolysis was described to sustain tumorigenesis (Wong, Liao et al. 2019), and overproliferation could also be sustained by fat (Sasamura, Matsuno et al. 2013, Lian, Wu et al. 2018, von Frieling, Faisal et al. 2020). In flies, I have confirmed high levels of LDs in the R4 region, which is known to be a region prone to mitosis (Marianes and Spradling 2013). Therefore, these could be suggestive of an interconnected network between Dsx, Myc, fat levels and cellular division.

Open to discussion is the lack of correlation between the female *dsx* transcript and the Dsx protein. This finding seems to be midgut-specific, since I observed Dsx in other female tissues such as the brain, the VNC or the fat body. In "masculinised clones" of a wild-type female intestine (mosaic cells upon *tra* knock-down) there was expression of Dsx::eGFP, which is suggestive of a cell-intrinsic and Tra-dependent *dsx* regulation (Fig. 3.9). Additionally, in mated females there is an upregulation of *dsx* mRNA (Jake Jacobson, unpublished) which does

not result in Dsx protein. Altogether, these suggest that *dsx* transcript itself might have a role beyond making Dsx protein. Although subject to study, I am inclined to speculate that putatively, the *dsx* non-coding intronic sequences might have a functional significance, as observed by the role of non-coding RNAs (Graveley, Brooks et al. 2011, Brown, Boley et al. 2014).

Deciphering the *dsx* female-specific significance and post-transcriptional regulation requires further investigation. Experimentally, I would start by performing FISH with *dsxF* and *dsxM* individually labelled probes. The exclusive localization of *dsxF* mRNA in female ECs nucleus would explain its absence of translation. Recently, the sexual dimorphism of nuclear pore proteins has been described in the brain: *Nup54* knock-down in dsx^{+} neurons has effects on sexual differentiation and male X-chromosome dosage compensation (Nallasivan, Haussmann et al. 2020). Whether the sexual dimorphism of Nup54 applies in the midgut and whether it is involved in Dsx regulation needs to be elucidated. Additionally, during development, but also in adult flies, the location of mRNA often plays a biological purpose. For example, the position of specific mRNA directs neural stem cell differentiation, or is involved in establishing epithelial cell polarity (reviewed in Hughes and Simmonds 2019). Thus, by FISH staining, I could identify whether there is a pattern of *dsxF* localization within each cell. Alternatively, to test the contribution of the sex-specific UTRs in post-transcriptional regulation, one could use the fly lines from the FlyORF stock collection. These fly lines have the coding sequence linked to the 3'UTR of the *tubulin alpha 1* sequence, thus eliminating 3'UTR transcript differences and putative post-transcriptional regulation. Furthermore, it would be interesting to create a *dsx* construct with swapped UTRs: male *dsxM* with female-specific UTRs and female *dsxF* with male-specific UTRs. Finally, I questioned whether the Myc sexual dimorphism could promote the post-transcriptional regulation. However, I did not observe anti-Dsx staining in $mex1^{ts}$*>MycRNAi* females (data not shown).

In this thesis I have used the *Drosophila melanogaster* adult midgut as a model to study the role of the sex determination transcription factor Dsx. In summary, Dsx appears to regulate the sexual dimorphism of fat homeostasis, furthering our understanding of the metabolic differences between males and females. Despite its female-specific post-transcriptional regulation being unknown, Dsx might control fat levels via the CG17192 lipase and/or the well-known oncogene Myc. In this study, I have also shown a sexual dimorphism and a metabolic role of Myc in the enterocytes in establishing lipid levels.

6.2 Limitations

Fat homeostasis in the midgut is a complex process which involves lipid digestion, absorption, transport, storage, lipolysis and lipogenesis. In this thesis, I have assessed whole-body TAG levels (upon removal of either gonads or gut) and quantified the numbers of LDs in the epithelium of the midgut. Nevertheless, these two techniques fail to capture the full repertoire of lipid-related processes. Therefore, it would be of great relevance to complement these findings by conducting lipidomics of midguts, whole flies and excreta, and to use stable isotope labelling to directly assess the turnover of lipids (Schlame, Xu et al. 2020). Furthermore, O_2/CO_2 consumption could be assessed to estimate the metabolic consumption (Berrigan and Partridge 1997).

One of the methodological concerns of this thesis is the usage of *mex1^{ts}>GFP* flies as a control for the RNA-seq experiment. Although this line is recommended by the TRiP collection and used extensively in many studies, we cannot exclude the possibility of indirect effects from the GFP overexpression on gene expression (Paola Cognigni reported lethality of *mex>GFP* flies in the lab; Miguel-Aliaga, personal communication). Ideally, the RNA-seq should have been performed with the *mex1^{ts}>Ilp4RNAi* control, consistent with the subsequent experiments.

Moreover, to avoid any putative effects resulting from the high expression driven by UAS, and to validate the results of *dsx* knock-down, I could make use of the *dsx*$^{\Delta}$ null mutant (Cande, Stern et al. 2014) or *dsx* deficiency line (BL# 66710) (Chatterjee, Uppendahl et al. 2011, Mellert, Robinett et al. 2012), despite them not being adult-specific. Also, crossing these lines to the alleles *dsx^{D}* (BL# 67749) (Chan Fung and Gowen 1957) and *dsx^{11}* (BL#1865) (Baker, Hoff et al. 1991) generates, respectively, only *dsxM* and *dsxF*, which could complement the adult-specific UAS-*dsxM* and UAS-*dsxF* experiments.

Notably, is important to consider that mRNA levels do not always correlate with protein levels (reviewed in Biggin and Tjian 2001, de Sousa Abreu, Penalva et al. 2009, Liu, Beyer et al. 2016). Therefore, it would be crucial to investigate whether the changes of the *CG17192* transcript are translated at the protein level, as well as the location of the protein. The secreted TAG lipase could travel from the anterior to posterior gut, where other lipases like *magro* are active (Buchon, Osman et al. 2013). In this thesis, I was limited by the lack of expression of the previously generated CG17192 fosmid. Hence, the region- and cellular-specific expression

should be verified by a *CG17192*-Gal4 line or by a fluorescence *in situ* hybridization (FISH) probe, and the protein localization by a CG17192::GFP line or an anti-CG17192 antibody.

Among many uncharacterised *Drosophila* lipases and lipid genes, this study is limited to CG17192 lipase. Several other fat metabolism targets were affected in the midgut upon *dsx* knock-down in the ECs (RNA-seq from this study). Thus, I would expand the knowledge of how *dsx* controls lipid genes, by further unravelling its transcriptional control of the lipase *CG2772* (up in *mex1^{ts}>dsxRNAi* and higher in females than males, also downregulated in *mex1^{ts}>MycRNAi* females), the lipase *magro* (up upon *dsx* knock-down but not sexually dimorphic in my RNA-seq *mex1^{ts}>GFP* control), the DGAT2 member *CG1941* (down in *mex1^{ts}>dsxRNAi* and higher in males than females) and/or the lipocalin *neural lazarillo* (up in *mex1^{ts}>dsxRNAi* and higher in females). Interestingly, in the adult head and CNS, Dsx controls expression of *CG4979* (a novel target gene predicted at the time to be a sex-specific lipid metabolism enzyme): DsxF represses this lipase in females, whilst DsxM activates *CG4979* in males (Goldman and Arbeitman 2007).

The vast majority of experiments in this thesis are done in flies reared in control diet. Experiments under high sugar (or high fat) diet might exacerbate the differences between males and females and provide a clear understanding of *dsx*-dependent lipid function. Along these lines, a recent study showed that females change more than males their lipid transcriptional profile after a week on high fat diet (Stobdan, Sahoo et al. 2019).

6.3 Future work

In addition to the above-mentioned experiments, the work in this thesis opens the door to further exciting avenues for the future, a few of these being discussed here.

The current working model is that Dsx in males suppresses a female Myc-driven lipogenic programme, at least partly mediated by CG17192 lipase. Other experiments could be done to further corroborate this. Since both Myc and Dsx have an impact on *CG17192* levels, another possibility is that these two transcription factors are independently controlling *CG17192* transcription. To answer this question of epistasis, a double mutant fly line (*mex1^{ts}>dsxRNAi,MycRNAi*) is essential. If Dsx regulates *CG17192* via Myc, in the adult guts of *mex1^{ts}>dsxRNAi,MycRNAi* the lipase mRNA levels would be as low as in the single mutant *mex1^{ts}>MycRNAi* but lower than in *mex1^{ts}>dsxRNAi*. An intermediate mRNA expression of the double mutant compared to the single mutants would indicate that *CG17192* is regulated

by Dsx and Myc independently. Furthermore, to confirm that Dsx in males is repressing Myc, I would "feminise" male midguts by overexpressing *traF* in the enterocytes and check Myc expression.

Moreover, I suggest that the female-specific lipogenic programme controls physiological traits such as ISC proliferation and adiposity (whole-body and midgut fat). I would perform additional experiments assessing the effects on food intake, starvation resistance, female fecundity and/or male fertility; specially in *mex1^{ts}>MycRNAi* and *mex1^{ts}>CG17192* adult flies.

Finally, to investigate whether the functions of Dsx in lipid metabolism are adult midgut-specific, it would be relevant to characterise its role in the fat body (which also expresses Dsx) and/or at the developmental stages.

The generation of the RNA-seq dataset as a transcriptional approach gives global information of all the molecular pathways affected in the adult midgut upon *dsx* downregulation. I have chosen to focus on the lipid metabolic effects for the reasons stated throughout the thesis. However, many other interesting and biologically relevant targets are good candidates to follow-up. Here I state (not by priority order) a few of them which I find relevant and interesting.

Firstly, I would focus on genes from the cholesterol homeostasis pathway since there is an interconnected network between lipids and cholesterol. For example, *Npc1b* is required for cholesterol absorption in the midgut (Voght, Fluegel et al. 2007), is sexually dimorphic (higher in females) and upregulated in *mex1^{ts}>dsxRNAi* males. Interestingly, *Npc1b* is localised at the X chromosome, and mutants show abnormal sterol accumulation and failure in spermatogenesis (Wang, Ma et al. 2011). Particularly, given that the fluorometric assay to quantify free cholesterol is available in flies (reviewed in Tennessen, Barry et al. 2014) it would be relevant to assess the phenotypic changes upon *dsx* knock-down. The study of cholesterol homeostasis is remarkably significant because it is the building block of crucial fly-hormones such as ecdysone (Lavrynenko, Rodenfels et al. 2015).

Secondly, and following-up with the cholesterol changes, I would focus on the *dsx*-dependent effects on fly hormones. Surprisingly, although at very low levels (thus I cannot exclude an artefact from the technique), *ecdysone oxidase* (*eo*), which generates merely a hormone inactivation product, is upregulated in *mex1^{ts}>dsxRNAi* males and sexually dimorphic (higher in females) (Takeuchi, Rigden et al. 2005). On the contrary, *shade* (*shd*) which converts ecdysone to the active 20E, is also upregulated in *mex1^{ts}>dsxRNAi* and is sexually dimorphic

(Petryk, Warren et al. 2003). Among many physiological roles, such as being a moulting hormone in development (reviewed in Yamanaka, Rewitz et al. 2013), Ec has a role in adult flies (reviewed in Schwedes and Carney 2012). Particularly, it has been shown that EcR is located in the midgut (Schwedes, Tulsiani et al. 2011), and systemic 20E from ovaries and haemolymph stimulates local ISCs differentiation into ECs to ensure epithelial growth (Ahmed, Maldera et al. 2020, Zipper, Jassmann et al. 2020). Therefore, I speculate that *dsx* might be involved in the sexually dimorphic Ec regulation in the adult midgut. Following-up with the hormonal contribution, and because JH regulates lipid metabolism and gut remodelling after mating (Reiff, Jacobson et al. 2015), I would further investigate the role of *dsx* in regulating the JH receptor called *germ cell-expressed bHLH-PAS* (*gce*). It is sexually dimorphic in the midgut (higher in females) and its expression is upregulated in *mex1^{ts}>dsxRNAi*.

Thirdly, I would study genes linked to the peroxisomes (reviewed in Faust, Verma et al. 2012, Pridie, Ueda et al. 2020). Of note, in the KEGG analysis, peroxisome related genes were one of the categories upregulated more highly after *dsx* knock-down in male ECs. For example, the members *Pex16* and *Pex19*, involved in membrane assembly and spermatogenesis, increase their transcription in *mex1^{ts}>dsxRNAi*, although they are not sexually dimorphic. LDs distribute lipids to various membrane-bound organelles, such as peroxisomes (as well as endosomes, mitochondria and endoplasmic reticulum) (Zehmer, Huang et al. 2009), suggesting a tight network between lipids and peroxisomes.

Finally, I found *Allatostatin A* (*AstA*) a pertinent candidate. *AstA* is a neurotransmitter and appears to be elevated in male midguts, as well as downregulated once the male midgut is "feminised" by *dsx* knock-down. Thus, the high levels of *AstA* seem to be a male-specific signature activated by Dsx. This is of particular interest because *AstA* mutants accumulate high lipid levels (Hentze, Carlsson et al. 2015). Also, AstA balances food intake according to metabolic nutritious needs (Hentze, Carlsson et al. 2015). Therefore, it would be interesting to investigate whether the sexually dimorphic Dsx signature, via *AstA*, is regulating food intake and lipid metabolism.

6.4 Overall significance

This thesis delineates previously undefined roles of Dsx and Myc in the adult fly enterocytes in regulating fat homeostasis. The sexually dimorphic expression of these two transcription factors might contribute to the sexual dimorphic lipid profile. In mammals, the role of Dmrt family members (Dsx homologues) in the intestine remains uncharacterised, yet the intestinal Myc correlates with obesity. Further studies will be required to continue interrogating the nature of the fat dimorphism, the direct implications of Myc and Dsx, and its intrinsic interactions.

Taking into account the impact of the sexual dimorphism of Dsx and Myc on the intestine and on the whole-body metabolism will be key in understanding the consequences for reproduction and intestine growth. Both transcription factors showed an effect on lipids and proliferation, which might have repercussions on reproductive success as well as tumorigenesis.

In addition to the systemic and hormonal regulation, the sex of the cell should be considered as an interplay between physiology and inherited information. Thus, future research would benefit from controlling for sex as an experimental variable.

Finally, the realisation that there is a sex-specific incidence of certain diseases, opens up the possibility that the cellular sexual signature might come with a cost. It is worth considering the possible trade-offs of any effects sex determinants may have on physiology: for example, in *Drosophila*, the female fate of stem cells allows them to resize the gut during reproduction, but also renders them more vulnerable to tumours. It will therefore be of interest to investigate the effects of Dsx and Myc not only on normal physiology (e.g. reproduction, lipid homeostasis) but also its dysregulation in the context of obesity or tumorigenesis.

Bibliography

Adams, M. D., et al. (2000). "The genome sequence of Drosophila melanogaster." Science **287**(5461): 2185-2195.

Agarwal, V., et al. (2018). "Predicting microRNA targeting efficacy in Drosophila." Genome Biol **19**(1): 152.

Ahmed, S. M. H., et al. (2020). "Fitness trade-offs incurred by ovary-to-gut steroid signalling in Drosophila." Nature **584**(7821): 415-419.

Amcheslavsky, A., et al. (2009). "Tissue Damage-Induced Intestinal Stem Cell Division in Drosophila." Cell Stem Cell **4**(1): 49-61.

Amcheslavsky, A., et al. (2014). "Enteroendocrine Cells Support Intestinal Stem-Cell-Mediated Homeostasis in Drosophila." Cell Rep **9**(1): 32-39.

Amrein, H., et al. (1988). "The sex-determining gene tra-2 of Drosophila encodes a putative RNA binding protein." Cell **55**(6): 1025-1035.

An, W., et al. (1996). "Sex-specific and non-sex-specific oligomerization domains in both of the doublesex transcription factors from Drosophila melanogaster." Mol Cell Biol **16**(6): 3106-3111.

An, W. and P. C. Wensink (1995). "Integrating sex- and tissue-specific regulation within a single Drosophila enhancer." Genes Dev **9**(2): 256-266.

An, W. and P. C. Wensink (1995). "Three protein binding sites form an enhancer that regulates sex- and fat body-specific transcription of Drosophila yolk protein genes." Embo j **14**(6): 1221-1230.

Arbeitman, M. N., et al. (2004). "A genomic analysis of Drosophila somatic sexual differentiation and its regulation." **131**(9): 2007-2021.

Arbeitman, M. N., et al. (2016). "Sex Differences in Drosophila Somatic Gene Expression: Variation and Regulation by doublesex." G3 (Bethesda) **6**(7): 1799-1808.

Bachtrog, D., et al. (2014). "Sex Determination: Why So Many Ways of Doing It?" PLoS Biol **12**(7): e1001899.

Baker, B. S., et al. (1991). "The doublesex locus of Drosophila melanogaster and its flanking regions: a cytogenetic analysis." Genetics **127**(1): 125.

Baker, B. S. and M. F. Wolfner (1988). "A molecular analysis of doublesex, a bifunctional gene that controls both male and female sexual differentiation in Drosophila melanogaster." Genes Dev **2**(4): 477-489.

Bashaw, G. J. and B. S. Baker (1997). "The regulation of the Drosophila msl-2 gene reveals a function for Sex-lethal in translational control." Cell **89**(5): 789-798.

Bayer, E. A., et al. (2020). "Ubiquitin-dependent regulation of a conserved DMRT protein controls sexually dimorphic synaptic connectivity and behavior." Elife **9**: e59614.

Beller, M., et al. (2010). "PERILIPIN-dependent control of lipid droplet structure and fat storage in Drosophila." Cell Metab **12**(5): 521-532.

Bellosta, P. and P. Gallant (2010). "Myc Function in Drosophila." Genes & Cancer **1**(6): 542-546.

Berrigan, D. and L. Partridge (1997). "Influence of temperature and activity on the metabolic rate of adult Drosophila melanogaster." Comparative Biochemistry and Physiology Part A: Physiology **118**(4): 1301-1307.

Bi, J., et al. (2012). "Opposite and redundant roles of the two Drosophila perilipins in lipid mobilization." **125**(15): 3568-3577.

Bier, E. (2005). "Drosophila, the golden bug, emerges as a tool for human genetics." Nat Rev Genet **6**(1): 9-23.

Biggin, M. D. and R. Tjian (2001). "Transcriptional regulation in Drosophila: the post-genome challenge." Funct Integr Genomics **1**(4): 223-234.

Boggs, R. T., et al. (1987). "Regulation of sexual differentiation in D. melanogaster via alternative splicing of RNA from the transformer gene." Cell **50**(5): 739-747.

Bopp, D., et al. (1991). "Developmental distribution of female-specific Sex-lethal proteins in Drosophila melanogaster." Genes Dev **5**(3): 403-415.

Brand, A. H. and N. Perrimon (1993). "Targeted gene expression as a means of altering cell fates and generating dominant phenotypes." Development **118**(2): 401-415.

Bridges, C. B. (1921). "Triploid intersexes in Drosophila melanogaster." Science **54**(1394): 252-254.

Brown, J. B., et al. (2014). "Diversity and dynamics of the Drosophila transcriptome." Nature **512**(7515): 393-399.

Buchon, N., et al. (2013). "Morphological and molecular characterization of adult midgut compartmentalization in Drosophila." Cell Rep **3**(5): 1725-1738.

Burtis, K. C. (1993). "The regulation of sex determination and sexually dimorphic differentiation in Drosophila." Curr Opin Cell Biol **5**(6): 1006-1014.

Burtis, K. C. and B. S. Baker (1989). "Drosophila doublesex gene controls somatic sexual differentiation by producing alternatively spliced mRNAs encoding related sex-specific polypeptides." Cell **56**(6): 997-1010.

Burtis, K. C., et al. (1991). "The doublesex proteins of Drosophila melanogaster bind directly to a sex-specific yolk protein gene enhancer." Embo j **10**(9): 2577-2582.

Camara, N., et al. (2019). "Doublesex controls specification and maintenance of the gonad stem cell niches in Drosophila." Development **146**(11): dev170001.

Camara, N., et al. (2008). Chapter 3 The Creation of Sexual Dimorphism in the Drosophila Soma. Current Topics in Developmental Biology, Academic Press. **83:** 65-107.

Cande, J., et al. (2014). "Looking Under the Lamp Post: Neither fruitless nor doublesex Has Evolved to Generate Divergent Male Courtship in Drosophila." Cell Rep **8**(2): 363-370.

Chan Fung, S. T. and J. W. Gowen (1957). "The developmental effect of a sex-limited gene in Drosophila melanogaster." J Exp Zool **134**(3): 515-532.

Chandegra, B., et al. (2017). "Sexually dimorphic effects of dietary sugar on lifespan, feeding and starvation resistance in Drosophila." Aging (Albany NY) **9**(12): 2521-2528.

Chang, T. H., et al. (2013). "An enhanced computational platform for investigating the roles of regulatory RNA and for identifying functional RNA motifs." BMC Bioinformatics **14 Suppl 2**(Suppl 2): S4.

Chatterjee, D., et al. (2014). "Control of metabolic adaptation to fasting by dILP6-induced insulin signaling in Drosophila oenocytes." Proceedings of the National Academy of Sciences **111**(50): 17959.

Chatterjee, N. and N. Perrimon (2021). "What fuels the fly: Energy metabolism in Drosophila and its application to the study of obesity and diabetes." Sci Adv **7**(24).

Chatterjee, S. S., et al. (2011). "The female-specific doublesex isoform regulates pleiotropic transcription factors to pattern genital development in Drosophila." Development **138**(6): 1099-1109.

Chintapalli, V. R., et al. (2007). "Using FlyAtlas to identify better Drosophila melanogaster models of human disease." Nat Genet **39**(6): 715-720.

Cho, S. and P. C. Wensink (1997). "DNA binding by the male and female doublesex proteins of Drosophila melanogaster." J Biol Chem **272**(6): 3185-3189.

Cho, S. and P. C. Wensink (1998). "Linkage between oligomerization and DNA binding in Drosophila doublesex proteins." Biochemistry **37**(32): 11301-11308.

Christiansen, A. E., et al. (2002). "Sex comes in from the cold: the integration of sex and pattern." Trends Genet **18**(10): 510-516.

Clegg, D. J. and F. Mauvais-Jarvis (2018). "An integrated view of sex differences in metabolic physiology and disease." Molecular metabolism **15**: 1-2.

Clough, E., et al. (2014). "Sex- and Tissue-Specific Functions of Drosophila Doublesex Transcription Factor Target Genes." Developmental Cell **31**(6): 761-773.

Cook, M. B., et al. (2009). "Sex disparities in cancer incidence by period and age." Cancer Epidemiol Biomarkers Prev **18**(4): 1174-1182.

Cordero, J. B., et al. (2012). "Non-autonomous crosstalk between the Jak/Stat and Egfr pathways mediates Apc1-driven intestinal stem cell hyperplasia in the Drosophila adult midgut." Development **139**(24): 4524-4535.

Cordero, J. B., et al. (2012). "Inducible progenitor-derived Wingless regulates adult midgut regeneration in Drosophila." Embo j **31**(19): 3901-3917.

Coschigano, K. T. and P. C. Wensink (1993). "Sex-specific transcriptional regulation by the male and female doublesex proteins of Drosophila." Genes Dev **7**(1): 42-54.

D'Souza, L. (2019). Profiling Doublesex-DNA interactions with targeted DamID in Drosophila melanogaster, University of Oxford.

de Beco, S., et al. (2012). "New frontiers in cell competition." Dev Dyn **241**(5): 831-841.

de la Cova, C., et al. (2004). "Drosophila myc regulates organ size by inducing cell competition." Cell **117**(1): 107-116.

de la Cova, C. and L. A. Johnston (2006). "Myc in model organisms: a view from the flyroom." Semin Cancer Biol **16**(4): 303-312.

de Sousa Abreu, R., et al. (2009). "Global signatures of protein and mRNA expression levels." Molecular bioSystems **5**(12): 1512-1526.

Diao, F., et al. (2015). "Plug-and-Play Genetic Access to Drosophila Cell Types using Exchangeable Exon Cassettes." Cell Rep **10**(8): 1410-1421.

Dietzl, G., et al. (2007). "A genome-wide transgenic RNAi library for conditional gene inactivation in Drosophila." Nature **448**(7150): 151-156.

Doane, W. W. (1960). "Developmental physiology of the mutant female sterile(2)adipose of Drosophila melanogaster. I. Adult morphology, longevity, egg production, and egg lethality." J Exp Zool **145**: 1-21.

Duneau, D. F., et al. (2017). "The Toll pathway underlies host sexual dimorphism in resistance to both Gram-negative and Gram-positive bacteria in mated Drosophila." BMC Biol **15**(1): 124.

Erdman, S. E. and K. C. Burtis (1993). "The Drosophila doublesex proteins share a novel zinc finger related DNA binding domain." Embo j **12**(2): 527-535.

Erdman, S. E., et al. (1996). "Functional and genetic characterization of the oligomerization and DNA binding properties of the Drosophila doublesex proteins." Genetics **144**(4): 1639-1652.

Erickson, J. W. and J. J. Quintero (2007). "Indirect effects of ploidy suggest X chromosome dose, not the X:A ratio, signals sex in Drosophila." PLoS Biol **5**(12): e332.

Fairbairn, D. J. (1997). "Allometry for Sexual Size Dimorphism: Pattern and Process in the Coevolution of Body Size in Males and Females." Annual Review of Ecology and Systematics **28**(1): 659-687.

Faust, J. E., et al. (2012). "An Inventory of Peroxisomal Proteins and Pathways in Drosophila melanogaster." Traffic **13**(10): 1378-1392.

Franks, A., et al. (2017). "Post-transcriptional regulation across human tissues." PLOS Computational Biology **13**(5): e1005535.

Fujii, S. and H. Amrein (2002). "Genes expressed in the Drosophila head reveal a role for fat cells in sex-specific physiology." Embo j **21**(20): 5353-5363.

Galikova, M., et al. (2015). "Energy Homeostasis Control in Drosophila Adipokinetic Hormone Mutants." Genetics **201**(2): 665-683.

Gallant, P. (2013). "Myc function in Drosophila." Cold Spring Harb Perspect Med **3**(10): a014324.

Gallant, P. and D. Steiger (2009). "Myc's secret life without Max." Cell Cycle **8**(23): 3848-3853.

Galletti, M., et al. (2009). "Identification of domains responsible for ubiquitin-dependent degradation of dMyc by glycogen synthase kinase 3beta and casein kinase 1 kinases." Mol Cell Biol **29**(12): 3424-3434.

Gamble, T. and D. Zarkower (2012). "Sex determination." Current Biology **22**(8): R257-R262.

Garrett-Engele, C. M., et al. (2002). "intersex, a gene required for female sexual development in Drosophila, is expressed in both sexes and functions together with doublesex to regulate terminal differentiation." Development **129**(20): 4661-4675.

Germani, F., et al. (2018). "Mosaic Analysis in Drosophila." Genetics **208**(2): 473-490.

Gervais, L. and A. J. Bardin (2017). "Tissue homeostasis and aging: new insight from the fly intestine." Curr Opin Cell Biol **48**: 97-105.

Ghosh, N., et al. (2019). "The Hox gene Abdominal-B uses Doublesex(F) as a cofactor to promote neuroblast apoptosis in the Drosophila central nervous system." Development **146**(16).

Gilbert, S. F. (2000). "Chromosomal Sex Determination in Mammals." Developmental Biology. 6th edition. Sunderland (MA): Sinauer Associates.

Goldman, T. D. and M. N. Arbeitman (2007). "Genomic and Functional Studies of Drosophila Sex Hierarchy Regulated Gene Expression in Adult Head and Nervous System Tissues." PLoS Genet **3**(11): e216.

Golic, K. G. and S. Lindquist (1989). "The FLP recombinase of yeast catalyzes site-specific recombination in the Drosophila genome." Cell **59**(3): 499-509.

Goralski, T. J., et al. (1989). "The sex determination locus transformer-2 of Drosophila encodes a polypeptide with similarity to RNA binding proteins." Cell **56**(6): 1011-1018.

Gorman, M. and B. S. Baker (1994). "How flies make one equal two: dosage compensation in Drosophila." Trends Genet **10**(10): 376-380.

Gouw, A. M., et al. (2019). "The MYC Oncogene Cooperates with Sterol-Regulated Element-Binding Protein to Regulate Lipogenesis Essential for Neoplastic Growth." Cell Metabolism **30**(3): 556-572.e555.

Graveley, B. R., et al. (2011). "The developmental transcriptome of Drosophila melanogaster." Nature **471**(7339): 473-479.

Grifoni, D. and P. Bellosta (2015). "Drosophila Myc: A master regulator of cellular performance." Biochim Biophys Acta **1849**(5): 570-581.

Gronke, S., et al. (2005). "Brummer lipase is an evolutionary conserved fat storage regulator in Drosophila." Cell Metab **1**(5): 323-330.

Gronke, S., et al. (2007). "Dual lipolytic control of body fat storage and mobilization in Drosophila." PLoS Biol **5**(6): e137.

Gutierrez, E., et al. (2007). "Specialized hepatocyte-like cells regulate Drosophila lipid metabolism." Nature **445**(7125): 275-280.

Hales, K. G., et al. (2015). "Genetics on the Fly: A Primer on the Drosophila Model System." Genetics **201**(3): 815-842.

Heier, C., et al. (2021). "The Drosophila model to interrogate triacylglycerol biology." Biochim Biophys Acta Mol Cell Biol Lipids **1866**(6): 158924.

Heier, C. and R. P. Kühnlein (2018). "Triacylglycerol Metabolism in Drosophila melanogaster." Genetics **210**(4): 1163-1184.

Heinrichs, V., et al. (1998). "Regulation of sex-specific selection of fruitless 5' splice sites by transformer and transformer-2." Mol Cell Biol **18**(1): 450-458.

Hempel, L. U. and B. Oliver (2007). "Sex-specific DoublesexM expression in subsets of Drosophila somatic gonad cells." BMC Dev Biol **7**: 113.

Hentze, J. L., et al. (2015). "The Neuropeptide Allatostatin A Regulates Metabolism and Feeding Decisions in Drosophila." Scientific Reports **5**(1): 11680.

Herboso, L., et al. (2011). "Expression of the Scavenger Receptor Class B type I (SR-BI) family in Drosophila melanogaster." The International journal of developmental biology **55**(6): 603-611.

Herpin, A. and M. Schartl (2011). "Dmrt1 genes at the crossroads: a widespread and central class of sexual development factors in fish." The FEBS Journal **278**(7): 1010-1019.

Hildreth, P. E. (1965). "Doublesex, recessive gene that transforms both males and females of Drosophila into intersexes." Genetics **51**(4): 659-678.

Holtof, M., et al. (2019). "Extracellular nutrient digestion and absorption in the insect gut." Cell Tissue Res **377**(3): 397-414.

Hong, C.-S., et al. (2007). "The function of Dmrt genes in vertebrate development: It is not just about sex." Dev Biol **310**(1): 1-9.

Hopkins, B. R. and A. Kopp (2021). "Evolution of sexual development and sexual dimorphism in insects." Current Opinion in Genetics & Development **69**: 129-139.

Horne, I., et al. (2009). "Comparative and functional genomics of lipases in holometabolous insects." Insect Biochem Mol Biol **39**(8): 547-567.

Hoshijima, K., et al. (1991). "Control of doublesex alternative splicing by transformer and transformer-2 in Drosophila." Science **252**(5007): 833-836.

Hoy, M. A. (2019). Chapter 4 - Genetic Systems, Genome Evolution, and Genetic Control of Embryonic Development in Insects. Insect Molecular Genetics (Fourth Edition). M. A. Hoy, Academic Press**:** 103-175.

Huang, X., et al. (2007). "Drosophila Niemann-Pick Type C-2 genes control sterol homeostasis and steroid biosynthesis: a model of human neurodegenerative disease." Development **134**(20): 3733-3742.

Hudry, B., et al. (2019). "Sex Differences in Intestinal Carbohydrate Metabolism Promote Food Intake and Sperm Maturation." Cell **178**(4): 901-918.e916.

Hudry, B., et al. (2016). "The sexual identity of adult intestinal stem cells controls organ size and plasticity." Nature **530**(7590): 344-348.

Hughes, S. C. and A. J. Simmonds (2019). "Drosophila mRNA Localization During Later Development: Past, Present, and Future." Front Genet **10**(135).

Hung, R.-J., et al. (2020). "A cell atlas of the adult Drosophila midgut." Proceedings of the National Academy of Sciences **117**(3): 1514.

Ida, T., et al. (2011). "Identification of the novel bioactive peptides dRYamide-1 and dRYamide-2, ligands for a neuropeptide Y-like receptor in Drosophila." Biochem Biophys Res Commun **410**(4): 872-877.

Inoue, K., et al. (1992). "Binding of the Drosophila transformer and transformer-2 proteins to the regulatory elements of doublesex primary transcript for sex-specific RNA processing." Proc Natl Acad Sci U S A **89**(17): 8092-8096.

Inoue, K., et al. (1990). "Binding of the Drosophila sex-lethal gene product to the alternative splice site of transformer primary transcript." Nature **344**(6265): 461-463.

Ito, H., et al. (1996). "Sexual orientation in Drosophila is altered by the satori mutation in the sex-determination gene fruitless that encodes a zinc finger protein with a BTB domain." Proc Natl Acad Sci U S A **93**(18): 9687-9692.

Ito, K., et al. (1997). "The Drosophila mushroom body is a quadruple structure of clonal units each of which contains a virtually identical set of neurones and glial cells." Development **124**(4): 761-771.

Itskov, P. M., et al. (2014). "Automated monitoring and quantitative analysis of feeding behaviour in Drosophila." Nat Commun **5**(1): 4560.

Jackson, A. S., et al. (2002). "The effect of sex, age and race on estimating percentage body fat from body mass index: The Heritage Family Study." Int J Obes Relat Metab Disord **26**(6): 789-796.

Jallon, J.-M., et al. (1988). "Female pheromones in Drosophila melanogaster are controlled by the doublesex locus." Genetical Research **51**(1): 17-22.

Jehrke, L., et al. (2018). "The impact of genome variation and diet on the metabolic phenotype and microbiome composition of Drosophila melanogaster." Scientific Reports **8**(1): 6215.

Jiang, H. and B. A. Edgar (2011). "Intestinal stem cells in the adult Drosophila midgut." Experimental Cell Research **317**(19): 2780-2788.

Jiang, H., et al. (2016). "Intestinal stem cell response to injury: lessons from Drosophila." Cellular and molecular life sciences : CMLS **73**(17): 3337-3349.

Johnston, L. A. (2009). "Competitive interactions between cells: death, growth, and geography." Science **324**(5935): 1679-1682.

Johnston, L. A. (2014). "Socializing with MYC: cell competition in development and as a model for premalignant cancer." Cold Spring Harb Perspect Med **4**(4): a014274.

Johnston, L. A. and P. Gallant (2002). "Control of growth and organ size in Drosophila." Bioessays **24**(1): 54-64.

Johnston, L. A., et al. (1999). "Drosophila myc regulates cellular growth during development." Cell **98**(6): 779-790.

Kappes, G., et al. (2011). "The Drosophila Myc gene, diminutive, is a positive regulator of the Sex-lethal establishment promoter, Sxl-Pe." Proc Natl Acad Sci U S A **108**(4): 1543-1548.

Karp, N. A., et al. (2017). "Prevalence of sexual dimorphism in mammalian phenotypic traits." Nat Commun **8**(1): 15475.

Kelley, R. L., et al. (1997). "Sex lethal controls dosage compensation in Drosophila by a non-splicing mechanism." Nature **387**(6629): 195-199.

Kim, D., et al. (2013). "TopHat2: accurate alignment of transcriptomes in the presence of insertions, deletions and gene fusions." Genome Biology **14**(4): R36.

King, D. G. (1988). "Cellular organization and peritrophic membrane formation in the cardia (proventriculus) of Drosophila melanogaster." J Morphol **196**(3): 253-282.

Kis, V., et al. (2015). "Specialized Cortex Glial Cells Accumulate Lipid Droplets in Drosophila melanogaster." PloS one **10**(7): e0131250.

Klowden, M. J. (2013). Physiological systems in insects. Amsterdam; Boston; Heidelberg [etc.], Elsevier.

Kopp, A. (2011). "Drosophila sex combs as a model of evolutionary innovations." Evolution & Development **13**(6): 504-522.

Kopp, A. (2012). "Dmrt genes in the development and evolution of sexual dimorphism." Trends in Genetics **28**(4): 175-184.

Kuhnlein, R. P. (2011). "The contribution of the Drosophila model to lipid droplet research." Prog Lipid Res **50**(4): 348-356.

Kuhnlein, R. P. (2012). "Thematic review series: Lipid droplet synthesis and metabolism: from yeast to man. Lipid droplet-based storage fat metabolism in Drosophila." J Lipid Res **53**(8): 1430-1436.

Lavrynenko, O., et al. (2015). "The ecdysteroidome of Drosophila: influence of diet and development." Development **142**(21): 3758-3768.

Lease, H. M. and B. O. Wolf (2011). "Lipid content of terrestrial arthropods in relation to body size, phylogeny, ontogeny and sex." Physiological Entomology **36**(1): 29-38.

Lee, G., et al. (2002). "Doublesex gene expression in the central nervous system of Drosophila melanogaster." J Neurogenet **16**(4): 229-248.

Lemaitre, B. and I. Miguel-Aliaga (2013). "The Digestive Tract of Drosophila melanogaster." Annu Rev Genet. **47**(1): 377-404.

Li, H. and B. S. Baker (1998). "hermaphrodite and doublesex function both dependently and independently to control various aspects of sexual differentiation in Drosophila." Development **125**(14): 2641-2651.

Lian, T., et al. (2018). "Drosophila Gut—A Nexus Between Dietary Restriction and Lifespan." International Journal of Molecular Sciences **19**(12).

Liao, Y., et al. (2014). "featureCounts: an efficient general purpose program for assigning sequence reads to genomic features." Bioinformatics **30**(7): 923-930.

Lilián E Canavoso, et al. (2001). "Fat Metabolism in Insects." Annu Rev Nutr. **21**(1): 23-46.

Liu, Y., et al. (2016). "On the Dependency of Cellular Protein Levels on mRNA Abundance." Cell **165**(3): 535-550.

Love, M. I., et al. (2014). "Moderated estimation of fold change and dispersion for RNA-seq data with DESeq2." Genome Biology **15**(12): 550.

Lucchesi, J. C. and M. I. Kuroda (2015). "Dosage compensation in Drosophila." Cold Spring Harb Perspect Biol **7**(5).

Lucchetta, E. M. and B. Ohlstein (2017). "Amitosis of Polyploid Cells Regenerates Functional Stem Cells in the Drosophila Intestine." Cell Stem Cell **20**(5): 609-620.e606.

Lue, N. F., et al. (1987). "Interaction of GAL4 and GAL80 gene regulatory proteins in vitro." Mol Cell Biol **7**(10): 3446-3451.

Luo, S. D. and B. S. Baker (2015). "Constraints on the evolution of a doublesex target gene arising from doublesex's pleiotropic deployment." Proc Natl Acad Sci U S A **112**(8): E852-E861.

Luo, S. D., et al. (2011). "Direct targets of the D. melanogaster DSXF protein and the evolution of sexual development." Development **138**(13): 2761-2771.

Luo, Y., et al. (2021). "Intestinal MYC modulates obesity-related metabolic dysfunction." Nat Metab **3**(7): 923-939.

Manolakou, P., et al. (2006). "Molecular patterns of sex determination in the animal kingdom: a comparative study of the biology of reproduction." Reproductive Biology and Endocrinology **4**(1): 59.

Marianes, A. and A. C. Spradling (2013). "Physiological and stem cell compartmentalization within the Drosophila midgut." Elife **2**: e00886.

Mathews, K. W., et al. (2017). "Sexual Dimorphism of Body Size Is Controlled by Dosage of the Chromosomal Gene Myc and by the Sex-Determining Gene tra in Drosophila." Genetics **205**(3): 1215-1228.

Mathews, K. W., et al. (2017). "Sexual Dimorphism of Body Size Is Controlled by Dosage of the X-Chromosomal Gene Myc and by the Sex-Determining Gene tra in Drosophila." Genetics **205**(3): 1215-1228.

Matson, C. K. and D. Zarkower (2012). "Sex and the singular DM domain: insights into sexual regulation, evolution and plasticity." Nature Reviews Genetics **13**(3): 163-174.

Mattila, J., et al. (2015). "Mondo-Mlx Mediates Organismal Sugar Sensing through the Gli-Similar Transcription Factor Sugarbabe." Cell Rep **13**(2): 350-364.

Mattox, W., et al. (1990). "Alternative splicing of the sex determination gene transformer-2 is sex-specific in the germ line but not in the soma." Genes Dev **4**(5): 789-805.

Mauvais-Jarvis, F. (2015). "Sex differences in metabolic homeostasis, diabetes, and obesity." Biology of Sex Differences **6**(1): 14.

Mayr, C. (2017). "Regulation by 3′-Untranslated Regions." Annual Review of Genetics **51**(1): 171-194.

McGuire, S. E., et al. (2003). "Spatiotemporal rescue of memory dysfunction in Drosophila." Science **302**(5651): 1765-1768.

McLeod, C. J., et al. (2010). "Stem Cell Dynamics in Response to Nutrient Availability." Current Biology **20**(23): 2100-2105.

Medenbach, J., et al. (2011). "Translational Control via Protein-Regulated Upstream Open Reading Frames." Cell **145**(6): 902-913.

Mellert, D. J., et al. (2012). "doublesex Functions Early and Late in Gustatory Sense Organ Development." PloS one **7**(12): e51489.

Micchelli, C. A. and N. Perrimon (2006). "Evidence that stem cells reside in the adult Drosophila midgut epithelium." Nature **439**(7075): 475-479.

Miguel-Aliaga, I., et al. (2018). "Anatomy and Physiology of the Digestive Tract of Drosophila melanogaster." Genetics **210**(2): 357-396.

Miguel-Aliaga, I., et al. (2008). "Postmitotic Specification of Drosophila Insulinergic Neurons from Pioneer Neurons." PLoS Biol **6**(3): e58.

Mikoluk, C., et al. (2018). "The splicing factor transformer2 (tra2) functions in the Drosophila fat body to regulate lipid storage." Biochem Biophys Res Commun **495**(1): 1528-1533.

Millington, J. W., et al. (2021). "Genetic manipulation of insulin/insulin-like growth factor signaling pathway activity has sex-biased effects on Drosophila body size." G3 (Bethesda) **11**(3).

Millington, J. W., et al. (2021). "Female-biased upregulation of insulin pathway activity mediates the sex difference in Drosophila body size plasticity." Elife **10**: e58341.

Moberg, K. H., et al. (2004). "The Drosophila F box protein archipelago regulates dMyc protein levels in vivo." Curr Biol **14**(11): 965-974.

Mohr, S. E., et al. (2014). "Resources for functional genomics studies in Drosophila melanogaster." Genetics **197**(1): 1-18.

Mori, E., et al. (2017). Sexual Dimorphism. Encyclopedia of Animal Cognition and Behavior. J. Vonk and T. Shackelford. Cham, Springer International Publishing**:** 1-7.

Murphy, M. W., et al. (2007). "Vertebrate DM domain proteins bind similar DNA sequences and can heterodimerize on DNA." BMC Molecular Biology **8**(1): 58.

Musselman, L. P. and R. P. Kuhnlein (2018). "Drosophila as a model to study obesity and metabolic disease." J Exp Biol **221**(Pt Suppl 1).

Nagoshi, R. N. and B. S. Baker (1990). "Regulation of sex-specific RNA splicing at the Drosophila doublesex gene: cis-acting mutations in exon sequences alter sex-specific RNA splicing patterns." Genes Dev **4**(1): 89-97.

Nagoshi, R. N., et al. (1988). "The control of alternative splicing at genes regulating sexual differentiation in D. melanogaster." Cell **53**(2): 229-236.

Nallasivan, M. P., et al. (2020). "Channel nuclear pore protein 54 directs sexual differentiation and neuronal wiring required for female reproductive behaviors in Drosophila." bioRxiv(806380): 806380.

Narendra, U., et al. (2002). "Sex-specific gene regulation. The Doublesex DM motif is a bipartite DNA-binding domain." J Biol Chem **277**(45): 43463-43473.

O'Brien, L. E., et al. (2011). "Altered modes of stem cell division drive adaptive intestinal growth." Cell **147**(3): 603-614.

O'Shea, J. M. and D. E. Ayer (2013). "Coordination of nutrient availability and utilization by MAX- and MLX-centered transcription networks." Cold Spring Harb Perspect Med **3**(9): a014258.

Obniski, R., et al. (2018). "Dietary Lipids Modulate Notch Signaling and Influence Adult Intestinal Development and Metabolism in Drosophila." Developmental Cell **47**(1): 98-111.e115.

Ohlstein, B. and A. Spradling (2006). "The adult Drosophila posterior midgut is maintained by pluripotent stem cells." Nature **439**(7075): 470-474.

Ohsaki, Y., et al. (2014). "Open Questions in Lipid Droplet Biology." Chemistry & Biology **21**(1): 86-96.

Ota, R., et al. (2021). "Absence of X-chromosome dosage compensation in the primordial germ cells of Drosophila embryos." Scientific Reports **11**(1): 4890.

Paiardi, C., et al. (2017). "The Stearoyl-CoA Desaturase-1 (Desat1) in Drosophila cooperated with Myc to Induce Autophagy and Growth, a Potential New Link to Tumor Survival." Genes (Basel) **8**(5).

Palanker, L., et al. (2009). "Drosophila HNF4 regulates lipid mobilization and beta-oxidation." Cell Metab **9**(3): 228-239.

Palm, W., et al. (2012). "Lipoproteins in Drosophila melanogaster--assembly, function, and influence on tissue lipid composition." PLoS Genet **8**(7): e1002828.

Pandey, U. B. and C. D. Nichols (2011). "Human disease models in Drosophila melanogaster and the role of the fly in therapeutic drug discovery." Pharmacol Rev **63**(2): 411-436.

Parisi, F., et al. (2013). "dMyc expression in the fat body affects DILP2 release and increases the expression of the fat desaturase Desat1 resulting in organismal growth." Dev Biol **379**(1): 64-75.

Parisi, M., et al. (2011). "Lipid profiles of female and male Drosophila." BMC Research Notes **4**(1): 198.

Pasco, M. Y., et al. (2015). "The cellular homeostasis of the gut: what the Drosophila model points out." Histol Histopathol **30**(3): 277-292.

Pavlou, H. J., et al. (2016). "Neural circuitry coordinating male copulation." Elife **5**.

Perkins, L. A., et al. (2015). "The Transgenic RNAi Project at Harvard Medical School: Resources and Validation." Genetics **201**(3): 843-852.

Petryk, A., et al. (2003). "Shade is the Drosophila P450 enzyme that mediates the hydroxylation of ecdysone to the steroid insect molting hormone 20-hydroxyecdysone." Proceedings of the National Academy of Sciences **100**(24): 13773.

Phillips, M. D. and G. H. Thomas (2006). "Brush border spectrin is required for early endosome recycling in Drosophila." Journal of Cell Science **119**(7): 1361-1370.

Poernbacher, I., et al. (2019). "Lessons in genome engineering: opportunities, tools and pitfalls." bioRxiv(710871): 710871.

Praggastis, S. A., et al. (2021). "The Drosophila E78 nuclear receptor regulates dietary triglyceride uptake and systemic lipid levels." Developmental Dynamics **250**(5): 640-651.

Pridie, C., et al. (2020). "Rosy Beginnings: Studying Peroxisomes in Drosophila." Front Cell Dev Biol. **8**(835).

Raymond, C. S., et al. (1998). "Evidence for evolutionary conservation of sex-determining genes." Nature **391**(6668): 691-695.

Regan, J. C., et al. (2016). "Sex difference in pathology of the ageing gut mediates the greater response of female lifespan to dietary restriction." Elife **5**: e10956.

Reiff, T., et al. (2015). "Endocrine remodelling of the adult intestine sustains reproduction in Drosophila." Elife **4**: e06930.

Reiter, L. T., et al. (2001). "A systematic analysis of human disease-associated gene sequences in Drosophila melanogaster." Genome Res **11**(6): 1114-1125.

Ren, F., et al. (2013). "Drosophila Myc integrates multiple signaling pathways to regulate intestinal stem cell proliferation during midgut regeneration." Cell Research **23**(9): 1133-1146.

Rezaval, C., et al. (2016). "Activation of Latent Courtship Circuitry in the Brain of Drosophila Females Induces Male-like Behaviors." Curr Biol **26**(18): 2508-2515.

Riddiford, L. M., et al. (2000). Ecdysone receptors and their biological actions. Vitamins & Hormones, Academic Press. **60:** 1-73.

Rideout, E. J., et al. (2007). "The sex-determination genes fruitless and doublesex specify a neural substrate required for courtship song." Curr Biol **17**(17): 1473-1478.

Rideout, E. J., et al. (2010). "Control of sexual differentiation and behavior by the doublesex gene in Drosophila melanogaster." Nat Neurosci **13**(4): 458-466.

Rideout, E. J., et al. (2015). "The Sex Determination Gene transformer Regulates Male-Female Differences in Drosophila Body Size." PLoS Genet **11**(12): e1005683.

Robinett, C. C., et al. (2010). "Sex and the single cell. II. There is a time and place for sex." PLoS Biol **8**(5): e1000365.

Rommelaere, S., et al. (2019). "The Exchangeable Apolipoprotein Nplp2 Sustains Lipid Flow and Heat Acclimation in Drosophila." Cell Rep **27**(3): 886-899.e886.

Ryner, L. C., et al. (1996). "Control of male sexual behavior and sexual orientation in Drosophila by the fruitless gene." Cell **87**(6): 1079-1089.

Salz, H. K. and J. W. Erickson (2010). "Sex determination in Drosophila: The view from the top." Fly (Austin) **4**(1): 60-70.

Sanders, L. and M. Arbeitman (2008). "Doublesex establishes sexual dimorphism in the Drosophila central nervous system in an isoform-dependent manner by directing cell number." Dev Biol **320**: 378-390.

Sarov, M., et al. (2016). "A genome-wide resource for the analysis of protein localisation in Drosophila." Elife **5**: e12068.

Sasamura, T., et al. (2013). "Disruption of Drosophila melanogaster Lipid Metabolism Genes Causes Tissue Overgrowth Associated with Altered Developmental Signaling." PLoS Genet **9**(11): e1003917.

Sato, K., et al. (2019). "Sex Mysteries of the Fly Courtship Master Regulator Fruitless." Frontiers in behavioral neuroscience **13**: 245-245.

Sawala, A. and A. P. Gould (2017). "The sex of specific neurons controls female body growth in Drosophila." PLoS Biol **15**(10): e2002252.

Sawala, A. and A. P. Gould (2018). "Sex-lethal in neurons controls female body growth in Drosophila." Fly (Austin) **12**(2): 133-141.

Schindelin, J., et al. (2012). "Fiji: an open-source platform for biological-image analysis." Nature Methods **9**(7): 676-682.

Schlame, M., et al. (2020). "Lipidome-wide 13C flux analysis: a novel tool to estimate the turnover of lipids in organisms and cultures." J Lipid Res **61**(1): 95-104.

Schlegel, A. and D. Y. Stainier (2007). "Lessons from "lower" organisms: what worms, flies, and zebrafish can teach us about human energy metabolism." PLoS Genet **3**(11): e199.

Schneider, C. A., et al. (2012). "NIH Image to ImageJ: 25 years of image analysis." Nature Methods **9**(7): 671-675.

Schwasinger-Schmidt, T. E., et al. (2012). "Evolution of starvation resistance in Drosophila melanogaster: measurement of direct and correlated responses to artificial selection." J Evol Biol **25**(2): 378-387.

Schwedes, C., et al. (2011). "Ecdysone receptor expression and activity in adult Drosophila melanogaster." J Insect Physiol **57**(7): 899-907.

Schwedes, C. C. and G. E. Carney (2012). "Ecdysone signaling in adult Drosophila melanogaster." J Insect Physiol **58**(3): 293-302.

She, Z. Y. and W. X. Yang (2014). "Molecular mechanisms involved in mammalian primary sex determination." J Mol Endocrinol **53**(1): R21-37.

Shen, M. M. and J. Hodgkin (1988). "mab-3, a gene required for sex-specific yolk protein expression and a male-specific lineage in C. elegans." Cell **54**(7): 1019-1031.

Shim, J., et al. (2013). "Nutritional regulation of stem and progenitor cells in Drosophila." Development **140**(23): 4647-4656.

Shirangi, T. R., et al. (2009). "Rapid evolution of sex pheromone-producing enzyme expression in Drosophila." PLoS Biol **7**(8): e1000168.

Sieber, M. H. and A. C. Spradling (2015). "Steroid Signaling Establishes a Female Metabolic State and Regulates SREBP to Control Oocyte Lipid Accumulation." Curr Biol **25**(8): 993-1004.

Sieber, M. H. and C. S. Thummel (2009). "The DHR96 Nuclear Receptor Controls Triacylglycerol Homeostasis in Drosophila." Cell Metabolism **10**(6): 481-490.

Sieber, Matthew H. and Carl S. Thummel (2012). "Coordination of Triacylglycerol and Cholesterol Homeostasis by DHR96 and the Drosophila LipA Homolog magro." Cell Metabolism **15**(1): 122-127.

Singh, S. R., et al. (2016). "The lipolysis pathway sustains normal and transformed stem cells in adult Drosophila." Nature **538**(7623): 109-113.

Song, W., et al. (2014). "Control of Lipid Metabolism by Tachykinin in Drosophila." Cell Rep **9**(1): 40-47.

Sosnowski, B. A., et al. (1989). "Sex-specific alternative splicing of RNA from the transformer gene results from sequence-dependent splice site blockage." Cell **58**(3): 449-459.

Southall, T. D., et al. (2008). "The GAL4 System: A Versatile Toolkit for Gene Expression in Drosophila." CSH Protoc **2008**: pdb.top49.

Steiger, D., et al. (2008). "Max-independent functions of Myc in Drosophila melanogaster." Nat Genet **40**(9): 1084-1091.

Stobdan, T., et al. (2019) High fat diet induces sex-specific differential gene expression in Drosophila melanogaster. PloS one **14**, e0213474.

Stoffolano, J. G. and A. T. Haselton (2013). "The Adult Dipteran Crop: A Unique and Overlooked Organ." Annual Review of Entomology **58**(1): 205-225.

Strilbytska, O. M., et al. (2017). "Activation of the Tor/Myc signaling axis in intestinal stem and progenitor cells affects longevity, stress resistance and metabolism in drosophila." Comparative Biochemistry and Physiology Part B: Biochemistry and Molecular Biology **203**: 92-99.

Suijkerbuijk, S. J. E., et al. (2016). "Cell Competition Drives the Growth of Intestinal Adenomas in Drosophila." Current Biology **26**(4): 428-438.

Szostak, E. and F. Gebauer (2013). "Translational control by 3'-UTR-binding proteins." Briefings in functional genomics **12**(1): 58-65.

Takeuchi, H., et al. (2005). "Regulation of ecdysteroid signalling during Drosophila development: identification, characterization and modelling of ecdysone oxidase, an enzyme involved in control of ligand concentration." Biochemical Journal **389**(3): 637-645.

Tanaka, K., et al. (2011). "Evolution of sex-specific traits through changes in HOX-dependent doublesex expression." PLoS Biol **9**(8): e1001131.

Taylor, B. J. and J. W. Truman (1992). "Commitment of abdominal neuroblasts in Drosophila to a male or female fate is dependent on genes of the sex-determining hierarchy." Development **114**(3): 625-642.

Tennessen, J. M., et al. (2014). "Methods for studying metabolism in Drosophila." Methods (San Diego, Calif.) **68**(1): 105-115.

Toprak, U., et al. (2020). "A journey into the world of insect lipid metabolism." Arch Insect Biochem Physiol. **104**(2): e21682.

Tschapalda, K., et al. (2016). "A Class of Diacylglycerol Acyltransferase 1 Inhibitors Identified by a Combination of Phenotypic High-throughput Screening, Genomics, and Genetics." EBioMedicine **8**: 49-59.

Ugrankar, R., et al. (2011). "Lipin Is a Central Regulator of Adipose Tissue Development and Function in Drosophila melanogaster." Mol Cell Biol. **31**(8): 1646-1656.

Valsecchi, C. I. K., et al. (2018). "Facultative dosage compensation of developmental genes on autosomes in Drosophila and mouse embryonic stem cells." Nat Commun **9**(1): 3626.

Verhulst, E. C. and L. van de Zande (2015). "Double nexus--Doublesex is the connecting element in sex determination." Briefings in functional genomics **14**(6): 396-406.

Vervoorts, J., et al. (2006). "The ins and outs of MYC regulation by posttranslational mechanisms." J Biol Chem **281**(46): 34725-34729.

Voght, S. P., et al. (2007). "Drosophila NPC1b promotes an early step in sterol absorption from the midgut epithelium." Cell Metab **5**(3): 195-205.

von Frieling, J., et al. (2020). "A high-fat diet induces a microbiota-dependent increase in stem cell activity in the Drosophila intestine." PLoS Genet **16**(5): e1008789.

Wang, C., et al. (2011). "The cholesterol trafficking protein NPC1 is required for Drosophila spermatogenesis." Dev Biol **351**(1): 146-155.

Wat, L. W., et al. (2020). "A role for triglyceride lipase brummer in the regulation of sex differences in Drosophila fat storage and breakdown." PLoS Biol **18**(1): e3000595.

Wat, L. W., et al. (2021). "Sex determination gene transformer regulates the male-female difference in Drosophila fat storage via the Adipokinetic hormone pathway." bioRxiv: 2021.2007.2020.453098.

Waterbury, J. A., et al. (1999). "Analysis of the doublesex female protein in Drosophila melanogaster: role on sexual differentiation and behavior and dependence on intersex." Genetics **152**(4): 1653-1667.

Wayland, M. T., et al. (2014). "Spotting the differences: probing host/microbiota interactions with a dedicated software tool for the analysis of faecal outputs in Drosophila." J Insect Physiol **69**: 126-135.

Wessels, H.-H., et al. (2019). "Global identification of functional microRNA-mRNA interactions in Drosophila." Nat Commun **10**(1): 1626.

Wicker-Thomas, C., et al. (2015). "Flexible origin of hydrocarbon/pheromone precursors in Drosophila melanogaster." J Lipid Res **56**(11): 2094-2101.

Williams, T. M., et al. (2008). "The regulation and evolution of a genetic switch controlling sexually dimorphic traits in Drosophila." Cell **134**(4): 610-623.

Wisidagama, D. R. and C. S. Thummel (2019). "Regulation of Drosophila Intestinal Stem Cell Proliferation by Enterocyte Mitochondrial Pyruvate Metabolism." G3 (Bethesda) **9**(11): 3623-3630.

Wong, K. K. L., et al. (2019). "A positive feedback loop between Myc and aerobic glycolysis sustains tumor growth in a Drosophila tumor model." Elife **8**.

Wu, D. C. and L. A. Johnston (2010). "Control of wing size and proportions by Drosophila myc." Genetics **184**(1): 199-211.

Yamanaka, N., et al. (2013). "Ecdysone Control of Developmental Transitions: Lessons from Drosophila Research." Annual Review of Entomology **58**(1): 497-516.

Yamashita, A., et al. (2014). "Glycerophosphate/Acylglycerophosphate acyltransferases." Biology (Basel) **3**(4): 801-830.

Yang, Y., et al. (2008). "Doublesex and the regulation of sexual dimorphism in Drosophila melanogaster: structure, function, and mutagenesis of a female-specific domain." J Biol Chem **283**(11): 7280-7292.

Young, M. D., et al. (2010). "Gene ontology analysis for RNA-seq: accounting for selection bias." Genome Biology **11**(2): R14.

Zehmer, J. K., et al. (2009). "A role for lipid droplets in inter-membrane lipid traffic." Proteomics **9**(4): 914-921.

Zhao, X. and J. Karpac (2020). "The Drosophila midgut and the systemic coordination of lipid-dependent energy homeostasis." Current Opinion in Insect Science **41**: 100-105.

Zhou, C., et al. (2014). "Central Brain Neurons Expressing doublesex Regulate Female Receptivity in Drosophila." Neuron **83**(1): 149-163.

Zhou, H., et al. (2021). "Doublesex regulates fruitless expression to promote sexual dimorphism of the gonad stem cell niche." PLoS Genet **17**(3): e1009468.

Zhou, X., et al. (2020). "Physiological and Pathological Regulation of Peripheral Metabolism by Gut-Peptide Hormones in Drosophila." Front Physiol. **11**(1241).

Zipper, L., et al. (2020). "Ecdysone steroid hormone remote controls intestinal stem cell fate decisions via the PPARγ-homolog Eip75B in Drosophila." Elife **9**: e55795.

Appendix

Supplementary Figures

A

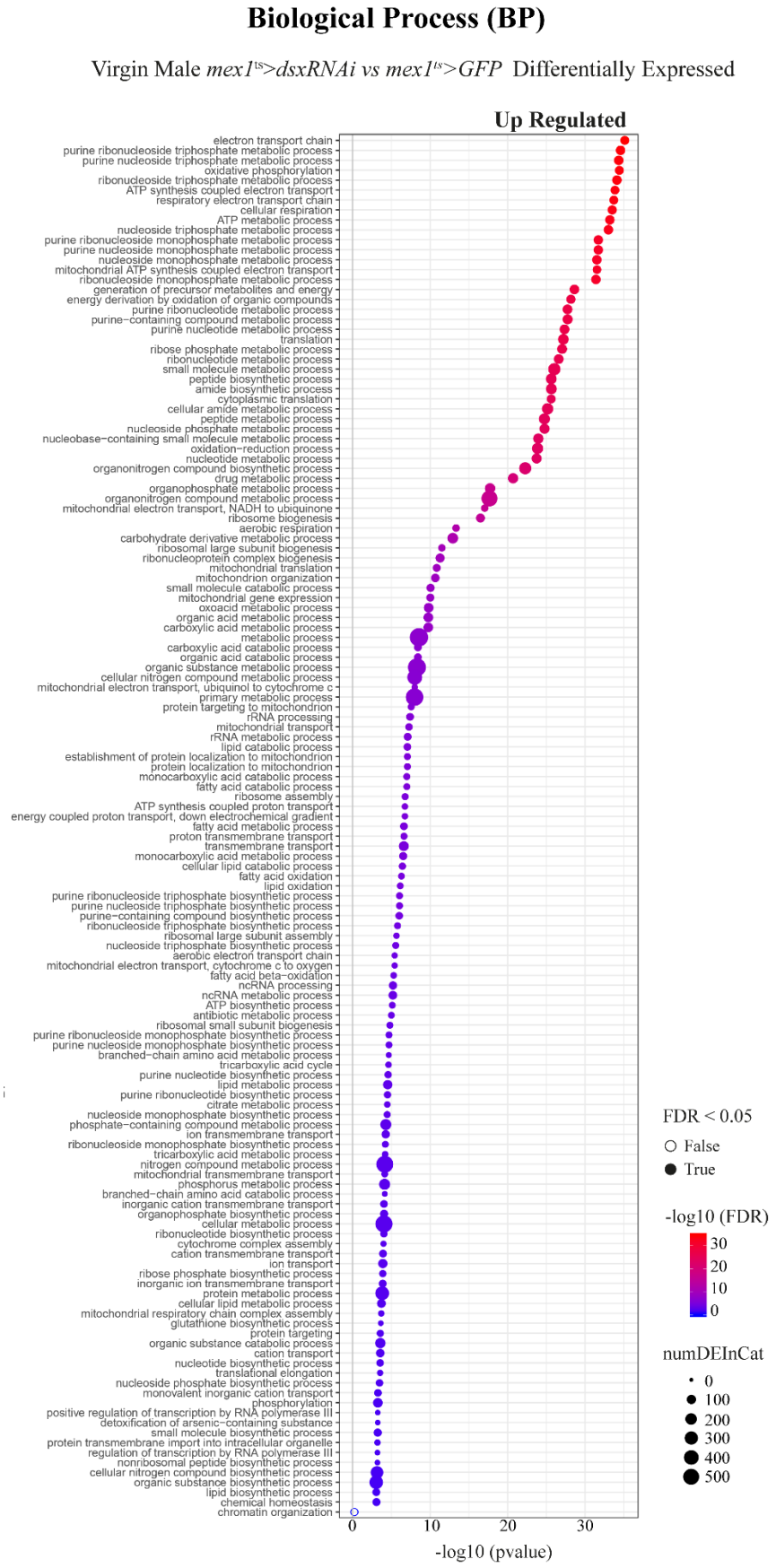

A’

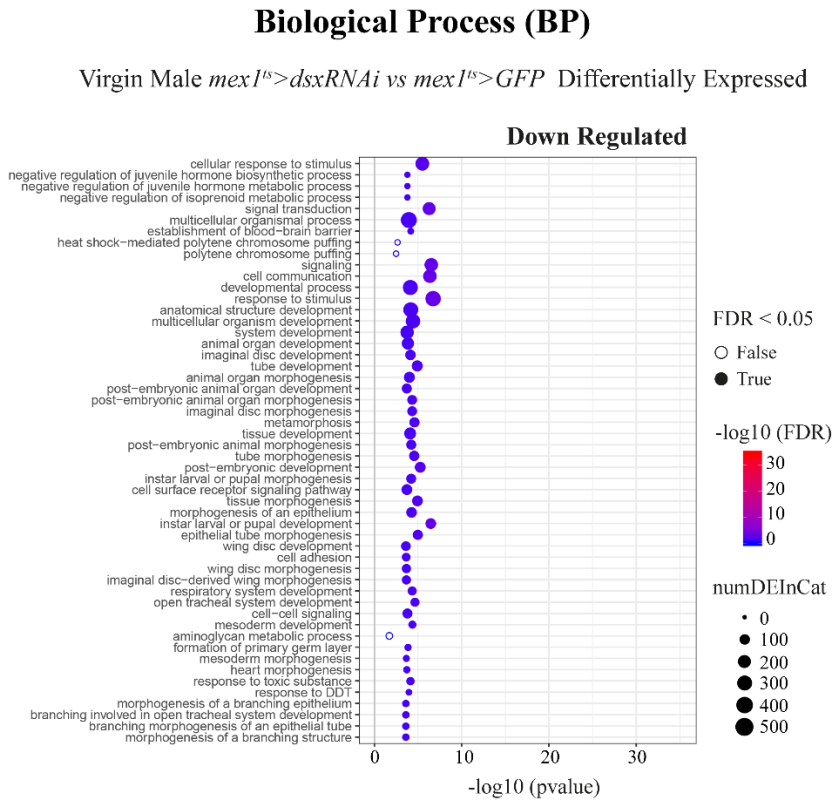

Supplementary Figure 1: Gene Ontology terms for the upregulated and downregulated genes in biological processes

Changes at the level of differentially expressed genes from experimental (*mex1^{ts}>dsxRNAi*) *vs* control (*mex1^{ts}>GFP*) virgin male. Listed BP categories of upregulated (A) and downregulated (A’) genes in the Y axis. Value of -log10(p-value) in the X axis. Size of the circular points in the graph shows the number of differentially expressed genes in each category (from small to big, 0 to 500 genes). Colour of the circle corresponds to the -log10 of False Discovery Rate (FDR), which corrects for multiple comparisons. The lower the -log10(p-value) correlates with lower -log10(FDR). Empty circles represent genes in which the FDR has a p-value higher than 0.05. Full circles show true FDR<0.05.

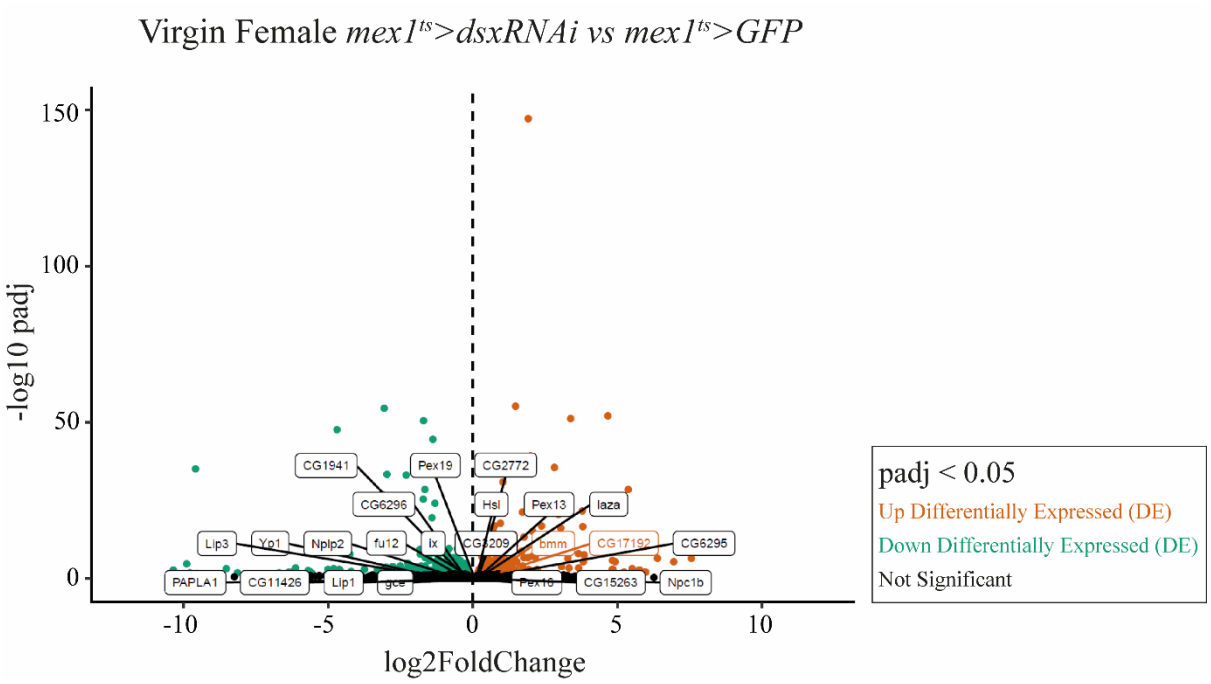

Supplementary Figure 2: Changes in lipid metabolism genes in the midgut of virgin adult females upon *dsx* downregulation in the ECs

Volcano plot of transcriptional changes of lipid metabolism genes in experimental (*mex1^{ts}>dsxRNAi*) *vs* control (*mex1^{ts}>GFP*) virgin female. Y axis is -log10(p-adjusted), X axis is log2(fold change). Black dots and genes written in black show no difference of expression. Orange dots and gene names are the ones which upregulate expression upon *dsx* downregulation. Turquoise dots and gene names, the ones with lowered expression in *dsx* knock-down. P-adjusted of less than 0.05 are counted as statistically significant changes.

Genotype list

Figure 3.1 (A) Oregon R

Figure 3.1 (C-F") *y[1]w[*];+/+;Dsx::eGFP/Dsx::eGFP*

Figure 3.2 (A-D') *y[1]w[*];+/+;Dsx::eGFP/Dsx::eGFP*

Figure 3.3 (B) *w[*]/Y;tubGal4UAS-dsxRNAi;+/+*

w[*]/ y[1]sc[*]v[1]sev[1];tubGal4UAS-dsxRNAi;+/+

Figure 3.3 (C) *y[1]sc[*]v[1]sev[21]/Y;mex1Gal4/UAS-dsxRNAi;tubGal80^{ts}/+*

y[1]v[1]/Y;mex1Gal4/+;tubGal80^{ts}/UAS-GFP

Figure 3.4 - 3.8

y[1]sc[*]v[1]sev[21]/Y;mex1Gal4/UAS-dsxRNAi;tubGal80^{ts}/+

y[1]v[1]/Y;mex1Gal4/+;tubGal80^{ts}/UAS-GFP

y[1]sc[*]v[1]sev[21]/w[*];mex1Gal4/UAS-dsxRNAi;tubGal80^{ts}/+

y[1]v[1]/[w];mex1Gal4/+;tubGal80^{ts}/UAS-GFP*

Figure 3.9 *yw,hs-flp/y[1]w[*];Act>y>Gal4UAS-lacZ/+;UAS-traRNAi/Dsx::eGFP*

Figure 4.1 (A) Oregon R

Figure 4.1 (A') *y[1]sc[*]v[1]sev[21]/w[*];mex1Gal4/UAS-Ilp4RNAi;tubGal80^{ts}/+*

y[1]sc[*]v[1]sev[21]/Y;mex1Gal4/UAS-Ilp4RNAi;tubGal80^{ts}/+

Figure 4.2 (A) *y[1]v[1]/Y;mex1Gal4/+;tubGal80^{ts}/UAS-GFP*

Figure 4.2 (A') *y[1]sc[*]v[1]sev[21]/Y;mex1Gal4/UAS-dsxRNAi;tubGal80^{ts}/+*

Figure 4.2 (B-C') *y[1]v[1]/Y;mex1Gal4/+;tubGal80^{ts}/UAS-GFP*

y[1]sc[*]v[1]sev[21]/Y;mex1Gal4/UAS-dsxRNAi;tubGal80^{ts}/+

y[1]sc[*]v[1]sev[21]/Y;mex1Gal4/UAS-Ilp4RNAi;tubGal80^{ts}/+

Figure 4.3 (A-B') *yw,hs-flp/Y;UAS-dsxRNAi/Act>y>Gal4UAS-RFP;(MKRS)/(TM6B)*

yw,hs-flp/Y;Act>y>Gal4UAS-RFP/CyO;(MKRS)/(TM6B)

Figure 4.4 - 4.6

y[1]sc[*]v[1]sev[21]/w[*];mex1Gal4/UAS-Ilp4RNAi;tubGal80^{ts}/+

y[1]sc[*]v[1]sev[21]/w[*];mex1Gal4/UAS-dsxRNAi;tubGal80^{ts}/+

y[1]w[*]/w[*];mex1Gal4/+;tubGal80^{ts}/UAS-dsxF

y[1]w[*]/w[*];mex1Gal4/UAS-dsxM;tubGal80^{ts}/+

y[1]sc[*]v[1]sev[21]/Y;mex1Gal4/UAS-Ilp4RNAi;tubGal80^{ts}/+

y[1]sc[*]v[1]sev[21]/Y;mex1Gal4/UAS-dsxRNAi;tubGal80^{ts}/+

y[1]w[*]/Y;mex1Gal4/+;tubGal80^{ts}/UAS-dsxF

y[1]w[*]/Y;mex1Gal4/UAS-dsxM;tubGal80^{ts}/+

Figure 4.7 (A-B') Oregon R

Figure 4.7 (C) *y[1]sc[*]v[1]sev[21]/Y;mex1Gal4/UAS-Ilp4RNAi;tubGal80^{ts}/+*

y[1]sc[*]v[1]sev[21]/Y;mex1Gal4/UAS-dsxRNAi;tubGal80^{ts}/+

y[1]w[*]/Y;mex1Gal4/+;tubGal80^{ts}/UAS-dsxF

y[1]w[*]/Y;mex1Gal4/UAS-dsxM;tubGal80^{ts}/+

Figure 4.7 (C'-C'') *y[1]sc[*]v[1]sev[21]/w[*];mex1Gal4/UAS-Ilp4RNAi;tubGal80^{ts}/+*

y[1]w[*]/w[*];mex1Gal4/+;tubGal80^{ts}/UAS-dsxF

y[1]w[*]/w[*];mex1Gal4/UAS-dsxM;tubGal80^{ts}/+

Figure 4.7 (D-D') *y[1]sc[*]v[1]sev[21]/w[*];mex1Gal4/+;tubGal80^{ts}/UAS-Ilp7RNAi*

w[*]UAS-Dcr2/w[*];mex1Gal4/+;tubGal80^{ts}/UAS-traRNAi

Figure 4.8 *y[1]sc[*]v[1]sev[21]/w[*];mex1Gal4/UAS-CG17192RNAi;tubGal80^{ts}/+*

y[1]sc[*]v[1]sev[21]/w[*];mex1Gal4/UAS-Ilp4RNAi;tubGal80^{ts}/+

w[*]/Y;mex1Gal4/UAS-CG17192RNAi;tubGal80^{ts}/+

w[*]/Y;mex1Gal4/UAS-Ilp4RNAi;tubGal80^{ts}/+

Figure 4.9 (A-A') *y[1]sc[*]v[1]sev[21]/w[*];mex1Gal4/UAS-Ilp4RNAi;tubGal80^{ts}/+*

y[1]sc[*]v[1]sev[21]/w[*];mex1Gal4/UAS-dsxRNAi;tubGal80^{ts}/+

y[1]w[*]/w[*];mex1Gal4/+;tubGal80^{ts}/UAS-dsxF

y[1]w[*]/w[*];mex1Gal4/UAS-dsxM;tubGal80^{ts}/+

y[1]sc[*]v[1]sev[21]/Y;mex1Gal4/UAS-Ilp4RNAi;tubGal80^{ts}/+

y[1]sc[*]v[1]sev[21]/Y;mex1Gal4/UAS-dsxRNAi;tubGal80^{ts}/+

y[1]w[*]/Y;mex1Gal4/+;tubGal80^{ts}/UAS-dsxF

y[1]w[*]/Y;mex1Gal4/UAS-dsxM;tubGal80^{ts}/+

Figure 4.9 (B) *y[1]v[1]/Y;mex1Gal4/+;tubGal80^{ts}/UAS-GFP*

y[1]sc[*]v[1]sev[21]/Y;mex1Gal4/UAS-dsxRNAi;tubGal80^{ts}/+

Figure 5.1 (A) Oregon R

Figure 5.1 - 5.2

w,Myc::eGFP/w,Myc::eGFP;+/+;+/+

w,Myc::eGFP/Y;+/+;+/+

Figure 5.3 (A-A') *y[1]sc[*]v[1]sev[21]/w[*];mex1Gal4/+;tubGal80^{ts}/UAS-Ilp7RNAi*

w[*]UAS-Dcr2/w[*];mex1Gal4/+;tubGal80^{ts}/UAS-traRNAi

Figure 5.3 (B) *y[1]sc[*]v[1]sev[21]/Y;mex1Gal4/UAS-Ilp4RNAi;tubGal80^{ts}/+*

y[1]sc[*]v[1]sev[21]/Y;mex1Gal4/UAS-dsxRNAi;tubGal80^{ts}/+

y[1]w[*]/Y;mex1Gal4/+;tubGal80^{ts}/UAS-dsxF

y[1]w[*]/Y;mex1Gal4/UAS-dsxM;tubGal80^{ts}/+

Figure 5.4 (A-A') *Myc::eGFP/Y;mexGal4/UAS-dsxRNAi;+/+*

Figure 5.4 (B-B') *Myc::eGFP/Y;mexGal4/UAS-dsxRNAi;tubGal80^{ts}/+*

Figure 5.4 (C-C') *Myc::eGFP/Y;mexGal4/UAS-dsxM;+/+*

Figure 5.4 (D-E') *Myc::eGFP/Y;mexGal4/UAS-dsxM;tubGal80^{ts}/+*

Figure 5.5 (A) *y[1]sc[*]v[1]sev[21]/Y;mex1Gal4/UAS-Ilp4RNAi;tubGal80^{ts}/+*

y[1]sc[*]v[1]sev[21]/Y;mex1Gal4/UAS-dsxRNAi;tubGal80^{ts}/+

y[1]w[*]/Y;mex1Gal4/+;tubGal80^{ts}/UAS-dsxF

y[1]w[*]/Y;mex1Gal4/UAS-dsxM;tubGal80^{ts}/+

Figure 5.5 (A') *y[1]sc[*]v[1]sev[21]/w[*];mex1Gal4/UAS-Ilp4RNAi;tubGal80^{ts}/+*

y[1]sc[*]v[1]sev[21]/w[*];mex1Gal4/UAS-dsxRNAi;tubGal80^{ts}/+

y[1]w[*]/w[*];mex1Gal4/+;tubGal80^{ts}/UAS-dsxF

y[1]w[*]/w[*];mex1Gal4/UAS-dsxM;tubGal80^{ts}/+

Figure 5.5 (B) *y[1]sc[*]v[1]sev[21]/Y;mex1Gal4/UAS-Ilp4RNAi;tubGal80^{ts}/+*

y[1]sc[*]v[1]sev[21]/Y;mex1Gal4/UAS-dsxRNAi;tubGal80^{ts}/+

Figure 5.5 (B') *y[1]sc[*]v[1]sev[21]/w[*];mex1Gal4/UAS-Ilp4RNAi;tubGal80^{ts}/+*

y[1]sc[*]v[1]sev[21]/w[*];mex1Gal4/UAS-dsxRNAi;tubGal80^{ts}/+

Figure 5.6 (A-A') *[w1118]/w[*];mex1Gal4/+;tubGal80^{ts}/+*

[w1118]/w[*];mex1Gal4/UAS-MycRNAi;tubGal80^{ts}/+

w[*]/Y;mex1Gal4/+;tubGal80^{ts}/+

w[*]/Y;mex1Gal4/UAS-MycRNAi;tubGal80^{ts}/+

Figure 5.6 (B) *w[*]/w[1118];mex1Gal4/UAS-Myc;tubGal80^{ts}/+*

w[*]/w[1118];mex1Gal4/+;tubGal80^{ts}/+

w[*]/w[1118];+/UAS-Myc;+/+

Figure 5.6 (B') *w[*]/Y;mex1Gal4/UAS-Myc;tubGal80^{ts}/+*

w[*]/Y;mex1Gal4/+;tubGal80^{ts}/+

w[1118]/Y;+/UAS-Myc;+/+

Figure 5.7 (A-A') *y[1]sc[*]v[1]sev[21]/w[*];mex1Gal4/+;tubGal80^{ts}/UAS-Ilp7RNAi*

y[1]sc[*]v[1]sev[21]/w[*];mex1Gal4/+;tubGal80^{ts}/UAS-MycRNAi

y[1]sc[*]v[1]sev[21]/w[*];mex1Gal4/UAS-Ilp4RNAi;tubGal80^{ts}/+

y[1]v[1]/w[*];mex1Gal4/UAS-MycRNAi;tubGal80^{ts}/+

y[1]sc[*]v[1]sev[21]/w[*];mex1Gal4/UAS-MycRNAi;tubGal80^{ts}/+

[w1118]/w[*];mex1Gal4/+;tubGal80^{ts}/+

[w1118]/w[*];mex1Gal4/UAS-MycRNAi;tubGal80^{ts}/+

Figure 5.7 (B-B’’’’’) *[w1118]/w[*];mex1Gal4/+;tubGal80^{ts}/+*

[w1118]/w[*];mex1Gal4/UAS-MycRNAi;tubGal80^{ts}/+

Figure 5.8 *[w1118]/w[*];mex1Gal4/+;tubGal80^{ts}/+*

[w1118]/w[*];mex1Gal4/UAS-MycRNAi;tubGal80^{ts}/+

w[*]/Y;mex1Gal4/+;tubGal80^{ts}/+

w[*]/Y;mex1Gal4/UAS-MycRNAi;tubGal80^{ts}/+